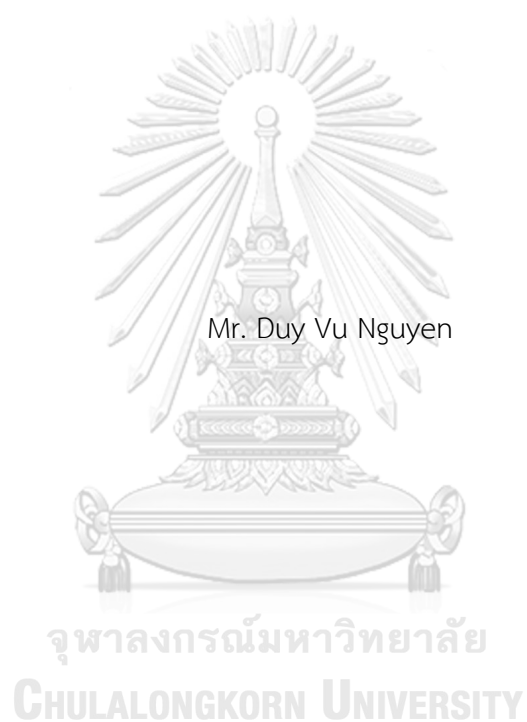


SYNTHESIS OF CHALCONE DERIVATIVES AS AMPK ACTIVATORS



A Thesis Submitted in Partial Fulfillment of the Requirements
for the Degree of Master of Science in Chemistry

Department of Chemistry

Faculty of Science

Chulalongkorn University

Academic Year 2019

Copyright of Chulalongkorn University

การสังเคราะห์อนุพันธ์แคลโคนเพื่อเป็นตัวยาระดับเอเอ็มพีเค



นายดุย วุฒิจำน

วิทยานิพนธ์นี้เป็นส่วนหนึ่งของการศึกษาตามหลักสูตรปริญญาวิทยาศาสตรมหาบัณฑิต
สาขาวิชาเคมี ภาควิชาเคมี
คณะวิทยาศาสตร์ จุฬาลงกรณ์มหาวิทยาลัย
ปีการศึกษา 2562
ลิขสิทธิ์ของจุฬาลงกรณ์มหาวิทยาลัย

Thesis Title	SYNTHESIS OF CHALCONE DERIVATIVES AS AMPK ACTIVATORS
By	Mr. Duy Vu Nguyen
Field of Study	Chemistry
Thesis Advisor	Assistant Professor WARINTHORN CHAVASIRI, Ph.D.

Accepted by the Faculty of Science, Chulalongkorn University in Partial Fulfillment of the Requirement for the Master of Science

..... Dean of the Faculty of Science
(Professor POLKIT SANGVANICH, Ph.D.)

THESIS COMMITTEE

..... Chairman
(Associate Professor VUDHICHAJ PARASUK, Ph.D.)

..... Thesis Advisor
(Assistant Professor WARINTHORN CHAVASIRI, Ph.D.)

..... Examiner
(Assistant Professor NAWAPORN VINAYAVEKHIN, Ph.D.)

..... External Examiner
(Dr. Titawat Sungkaworn)

ดุษฎี เวียง : การสังเคราะห์อนุพันธ์แคลโคนเพื่อเป็นตัวกระตุ้นเอเอ็มพีเค. (SYNTHESIS OF CHALCONE DERIVATIVES AS AMPK ACTIVATORS) อ.ที่ปรึกษา
 หลัก : ผศ. ดร.วรินทร์ ชวศิริ

เบาหวานและโรคไตที่เกิดจากเบาหวานเป็นความผิดปกติที่พบมากในปัจจุบัน แคลโคนเป็นตัวแทนของกลุ่มสารที่ดี เนื่องจากสามารถกระตุ้น AMPK ที่เกี่ยวข้องกับโรคทั้งสอง ได้สังเคราะห์แคลโคนที่วงเอ มีหมู่แทนที่เป็น 2'-hydroxy หรือ 3',4',5'-trimethoxy หรือหมู่แทนที่อื่น และวงบีมีหมู่แทนที่หนึ่ง สองหรือสามหมู่ด้วยปฏิกิริยา Claisen-Schmidt, อีเทอร์ฟิเคชันและไฮโดรจิเนชัน ได้ผลิตในปริมาณปานกลางถึงสูง สำหรับหมู่แทนที่หมู่เดียวบนวงบี หมู่เมทอกซีที่ตำแหน่งที่ 3 แสดงฤทธิ์ที่ดีที่สุด หมู่แทนที่ 3,4-dimethoxy และ 3,4-methylenedioxy บนวงบี (63 และ 65) ส่งผลให้ฤทธิ์เพิ่มขึ้น ซึ่งบอกเป็นนัยถึงความสำคัญของหมู่แทนที่ที่ตำแหน่ง 3,4- นี้ หมู่แทนที่ 3',4',5'-trimethoxy แสดงฤทธิ์น้อยกว่า 2'-hydroxy ไดไฮโดรแคลโคนสองตัว (121 และ 122) แสดงฤทธิ์ที่ดีเท่ากับ 63 ได้เลือกแคลโคนสี่ตัว (63, 65, 121 และ 122) เพื่อศึกษาความสัมพันธ์ระหว่างความเข้มข้นและการตอบสนอง และ EC_{50} พบว่าแคลโคน 121 เป็นสารที่มีศักยภาพสูงสุดที่มีค่า EC_{50} และค่าความเป็นพิษต่อเซลล์ต่ำที่สุดและควรจะศึกษาต่อไป

จุฬาลงกรณ์มหาวิทยาลัย
 CHULALONGKORN UNIVERSITY

สาขาวิชา เคมี
 ปีการศึกษา 2562

ลายมือชื่อนิสิต
 ลายมือชื่อ อ.ที่ปรึกษาหลัก

6072200723 : MAJOR CHEMISTRY

KEYWORD: Chalcone, AMPK activator, Diabetic nephropathy

Duy Vu Nguyen : SYNTHESIS OF CHALCONE DERIVATIVES AS AMPK
ACTIVATORS. Advisor: Asst. Prof. WARINTHORN CHAVASIRI, Ph.D.

Diabetes and diabetic nephropathy are two noticeable disorders in modern life. Chalcones are considered as a feasible candidate for these medication disorders due to the capability to activate AMPK relating to these two diseases. A series of chalcones with A-ring possessing 2'-hydroxy-, 3',4',5'-trimethoxyacetophenones or other types and B-ring decorated with mono-, di-, trisubstitution were accomplished by Claisen-Schmidt, etherification and hydrogenation reactions in almost moderate to high yield. 3-Methoxy group was found to be the best substituent for the activity in case of monosubstitution on B-ring. 3,4-Dimethoxy and 3,4-methylenedioxy groups on B-ring (63 and 65) enhanced the activity of disubstituted chalcones significantly, implying the important role of 3,4-disubstitution on B-ring for the activity. A-ring with 3',4',5'-trimethoxy group made chalcones less active than that with 2'-hydroxy group. Two dihydrochalcones (121 and 122) exhibited comparable potency to 63. Four chalcones (63, 65, 121 and 122) were selected to determine the concentration-response relationship and EC_{50} values. The chalcone 121, considered as the most potent candidate with the lowest EC_{50} and cytotoxicity, should be used for further studies.

Field of Study: Chemistry

Student's Signature

Academic Year: 2019

Advisor's Signature

ACKNOWLEDGEMENTS

The author would like to show his sincere gratitude, appreciation, and respect for his advisor Assistant Professor Dr. Warinthorn Chavasiri who always encourages and takes care of the author in every difficult situation. Thanks to his advisor, the author can keep the faith to do the research work and believe that “Nothing is impossible if you try your best”.

The author wants to express his gratitude and respect to Associate Professor Dr. Chatchai Muanprasat who helps the author for biological activity testing. Thanks to him, the author can learn many new practical lessons about physiology. This knowledge definitely supports the author a lot in future research work.

The author is very much obliged to Associate Professor Dr. Vudhichai Parasuk, Assistant Professor Dr. Nawaporn Vinayaveknin, and Dr. Titiwat Sungkaworn for attending the author’s thesis defense. I am most grateful to receive their advice and comments in order to complete the thesis thoroughly in the best way.

The author also wants to show his sincere thankfulness to all of the sponsors of ASEAN scholarship who support the author's tuition fee, and scholarship money during the time the author studied a Master's degree at Chulalongkorn University.

Moreover, the author would like to thank all of WC lab members especially Ph.D students Kieu Van Nguyen, Ade Danova and other students who always stand by the author and support him a lot. Especially, the author would like to express his appreciation to Suchada Kaewin who helps the author with biological experiments and explains the results to the author.

Finally, the author wants to show his sincere gratitude to his family. Thanks to them, the author can stay strong to proceed with his master's work abroad. No words can describe their sacrifices for the success of the author today.

Duy Vu Nguyen

TABLE OF CONTENTS

	Page
ABSTRACT (THAI).....	iii
ABSTRACT (ENGLISH).....	iv
ACKNOWLEDGEMENTS	v
TABLE OF CONTENTS.....	vi
LIST OF TABLES.....	ix
LIST OF FIGURES	xii
LIST OF ABBREVIATIONS	xxi
CHAPTER I INTRODUCTION.....	1
1.1 Chalcone.....	1
1.1.1 Natural chalcones.....	2
1.1.2 Synthetic chalcones.....	4
1.2 Diabetic nephropathy disease (DN) and AMPK.....	7
1.2.1 Diabetic nephropathy disease (DN).....	8
1.2.2 Glomerulus and podocyte	10
1.2.3 AMPK – drug target for diabetic nephropathy treatment.....	13
1.3 Reported chalcones as AMPK activation agents	16
1.4 The aim of this research.....	19
CHAPTER II EXPERIMENTAL	21
2.1 Instruments	21
2.2 General.....	21
2.3 Preparation of chalcones with monosubstitution on B-ring.....	21

2.4 Preparation of chalcones with disubstitution (OH, OCH ₃ and OCH ₂ O) on B-ring	24
2.5 Preparation of chalcones with disubstitution with 4-OH group on B-ring	28
2.5.1 Preparation of chloromethyl methyl ether (MOMCl)	28
2.5.2 Preparation of benzaldehydes bearing protecting groups	29
2.5.3 Preparation of chalcones bearing protecting groups and removal of protecting groups from chalcones	30
2.6 Preparation of chalcones with 3,4-disubstitution on B-ring	31
2.6.1 Preparation of benzaldehydes with 3,4-disubstitution	31
2.6.2 Preparation of chalcones with 3,4-disubstitution on B-ring	34
2.7 Preparation of chalcones with 2,4,5-trisubstitution on B-ring	38
2.7.1 Preparation of 2'-hydroxychalcones with 2,4,5-trisubstitution on B-ring	38
2.7.2 Preparation of chalcones with 2,4,5-trimethoxy substituents on B-ring	40
2.8 Preparation of dihydrochalcones	45
2.9 AMPK activation activity assessment	46
2.9.1 Potency and EC ₅₀	47
2.9.2 Assessment procedure	47
CHAPTER III RESULTS AND DISCUSSION	49
3.1 Synthesis and evaluation of chalcones with monosubstitution on B-ring	49
3.1.1 Synthesis and structural elucidation	49
3.1.2 Biological activity evaluation	51
3.2 Synthesis and evaluation of chalcones with disubstitution (OH, OCH ₃ and OCH ₂ O) on B-ring	57
3.2.1 Synthesis and structural elucidation	57
3.2.2 Biological activity evaluation	64

3.3 Synthesis of chalcones with 3,4-disubstitution on B-ring.....	67
3.3.1 Synthesis and structural elucidation	67
3.3.2 Biological activity evaluation.....	68
3.4 Synthesis of chalcones with 2,4,5-trisubstitution on B-ring.....	78
3.4.1 Synthesis and structural elucidation	78
3.4.2 Biological activity evaluation.....	82
3.5 Synthesis of dihydrochalcones	90
3.5.1 Synthesis and structural elucidation	90
3.5.2 Biological activity evaluation.....	91
3.6 Concentration-response relationship and EC ₅₀ calculation.....	93
CHAPTER 4 CONCLUSIONS.....	97
APPENDIX.....	99
REFERENCES	182
VITA.....	190

LIST OF TABLES

Table 1.1 Clinical stages of diabetic nephropathy (DN).	10
Table 3.1 Yields and characteristics of chalcones (25, 49-56).....	51
Table 3.2 Tentative NMR chemical shift assignment of chalcones 49-51.....	52
Table 3.3 Tentative NMR chemical shift assignment of chalcones 52-54.....	53
Table 3.4 Tentative NMR chemical shift assignment of chalcones 25, 55 and 56.....	54
Table 3.5 Theory about the crucial function of the 3-methoxy group for AMPK activation activity of chalcone derivatives.	56
Table 3.6 Yields and characteristics of chalcones 57-68.	Error! Bookmark not defined.
Table 3.7 Tentative NMR chemical shift assignment of chalcones 57-59.....	59
Table 3.8 Tentative NMR chemical shift assignment of chalcones 60-62 and 66.....	60
Table 3.9 Tentative NMR chemical shift assignment of chalcones 63-65.....	61
Table 3.10 Tentative NMR chemical shift assignment of chalcones 67 and 68.	62
Table 3.11 The yields and characteristics of products 69, 70, 72-74.	63
Table 3.12 Tentative NMR chemical shift assignment of chalcones 69, 70, 72-74.....	65
Table 3.13 Yields, characteristics and HR-MS (ESI) outcomes of products 82-105.	69
Table 3.14 NMR chemical shift assignment of benzaldehydes and chalcones 76, 77, 88 and 89.....	70
Table 3.15 NMR chemical shift assignment of benzaldehydes and chalcones 85, 86, 97 and 98.....	71
Table 3.16 NMR chemical shift assignment of benzaldehydes and chalcones 78, 79, 90 and 91.....	72

Table 3.17 NMR chemical shift assignment of benzaldehydes and chalcones 84, 87, 96 and 99	73
Table 3.18 NMR chemical shift assignment of benzaldehydes and chalcones 82, 83, 94 and 95	74
Table 3.19 NMR chemical shift assignment of chalcones 92 and 93	75
Table 3.20 Relationship between the ratio of a number of carbon and oxygen atoms of substituents and compound potency.....	78
Table 3.21 Yields and characteristics of products 106-109	79
Table 3.22 NMR chemical shift assignment of benzaldehydes and chalcones 100-103	80
Table 3.23 Yields and characteristics of products 48, 104-120	82
Table 3.24 NMR chemical shift assignment of chalcones 48, 104 and 105	83
Table 3.25 NMR chemical shift assignment of chalcones 106, 108-110	84
Table 3.26 NMR chemical shift assignment of chalcones 111, 112 and 118	85
Table 3.27 NMR chemical shift assignment of chalcones 113, 114 and 119	85
Table 3.28 NMR chemical shift assignment of chalcones 115-117	86
Table 3.29 NMR chemical shift assignment of chalcone 120	87
Table 3.30 Yields, characteristics and HR-MS (ESI) results of products 48, 121-124 . .	91
Table 3.31 NMR chemical shift assignment of chalcones 127-130	91



จุฬาลงกรณ์มหาวิทยาลัย
CHULALONGKORN UNIVERSITY

LIST OF FIGURES

Figure 1.1 Core structure of chalcone.....	2
Figure 1.2 Chalcone cyclization.....	2
Figure 1.3 Natural chalcones 1, 5-13	3
Figure 1.4 Prenylated chalcones 14-16 from <i>Psoralea corylifolia</i> (L.).....	4
Figure 1.5 Geranyl chalcone derivatives isolated from the leaves of <i>Artocarpus communis</i>	4
Figure 1.6 Some potent chalcones for anticancer activity 22-29	5
Figure 1.7 Some dominant molecules for anti-diabetic activity.....	6
Figure 1.8 Procedure for synthesizing heterocycles-linked chalcone hybrid.....	7
Figure 1.9 Two candidates as cytotoxic agents and tubulin polymerization inhibitors.....	7
Figure 1.10 Renal glomerulus components.....	12
Figure 1.11 Licochalcone A (LA) structure.....	17
Figure 1.12 Chemical structures of 21, 45-47	18
Figure 1.13 Chemical structure of 48	19
Figure 2.1 The structures of chalcones with monosubstitution on B-ring.....	22
Figure 2.2 The structures of chalcones with hydroxyl, methoxy, and methylenedioxy on B-ring.....	25
Figure 2.3 Chalcones with hydroxy substituents at position 2 or 4 on B-ring.	28
Figure 2.4 Two benzaldehydes bearing protecting groups.	29
Figure 2.5 Two chalcones bearing protecting groups and two deprotected chalcones.	30
Figure 2.6 Benzaldehydes with 3,4-disubstitution.	32
Figure 2.7 Chalcones with 3,4-disubstitution on B-ring.....	34

Figure 2.8 Benzaldehydes with 2,4,5-trisubstitution.....	39
Figure 2.9 2'-Hydroxychalcones with 2,4,5-trisubstitution on B-ring.....	39
Figure 2.10 Chalcones with 2,4,5-trimethoxy on B-ring.....	41
Figure 2.11 Hydrogenated chalcones.....	45
Figure 2.12 General procedure for AMPK phosphorylation activity assessment of chalcone compounds.....	48
Figure 3.1 Synthesis of chalcones with monosubstitution on B-ring.....	50
Figure 3.2 Resonance system of α,β -unsaturated ketone.....	50
Figure 3.3 Biological evaluation of chalcones with monosubstitution on B-ring.....	55
Figure 3.4 Synthesis of chalcones with disubstitution including hydroxy, methoxy and methylenedioxy on B-ring.....	57
Figure 3.5 Synthesis of disubstituted chalcones with 4-OH on B-ring.....	63
Figure 3.6 Biological evaluation of disubstituted chalcones with OH, OCH ₃ and methylenedioxy on B-ring.....	66
Figure 3.7 Synthesis of di-substituted benzaldehydes and chalcones with 3,4-disubstitution on B-ring.....	68
Figure 3.8 Biological evaluation of chalcones with 3,4-disubstitution on B-ring.....	76
Figure 3.9 Synthesis of tri-substituted benzaldehydes and 2'-hydroxychalcones with 2,4,5-trisubstitution on B-ring.....	79
Figure 3.10 Synthesis of chalcones with 2,4,5-trimethoxy on B-ring.....	81
Figure 3.11 Biological evaluation of chalcones with 2,4,5-trisubstitution on B-ring.....	89
Figure 3.12 Synthesis of dihydrochalcones.....	91
Figure 3.13 Biological evaluation of hydrogenated chalcones.....	93
Figure 3.14 Biological activity results of active compounds.....	94
Figure 3.15 Structure of active compounds.....	94

Figure 3.16 Concentration – response relationship and EC ₅₀ calculation.....	95
Figure A.1 The ¹ H NMR spectrum (acetone-d ₆ , 400 MHz) of 49	100
Figure A.2 The ¹³ C NMR spectrum (acetone-d ₆ , 100 MHz) of 49	100
Figure A.3 The ¹ H NMR spectrum (CDCl ₃ , 400 MHz) of 50	101
Figure A.4 The ¹³ C NMR spectrum (CDCl ₃ , 100 MHz) of 50	101
Figure A.5 The ¹ H NMR spectrum (acetone-d ₆ , 400 MHz) of 51	102
Figure A.6 The ¹³ C NMR spectrum (acetone-d ₆ , 100 MHz) of 51	102
Figure A.7 The ¹ H NMR spectrum (CDCl ₃ , 400 MHz) of 52	103
Figure A.8 The ¹³ C NMR spectrum (CDCl ₃ , 100 MHz) of 52	103
Figure A.9 The ¹ H NMR spectrum (CDCl ₃ , 400 MHz) of 53	104
Figure A.10 The ¹³ C NMR spectrum (CDCl ₃ , 100 MHz) of 53	104
Figure A.11 The ¹ H NMR spectrum (CDCl ₃ , 400 MHz) of 54	105
Figure A.12 The ¹³ C NMR spectrum (CDCl ₃ , 100 MHz) of 54	105
Figure A.13 The ¹ H NMR spectrum (CDCl ₃ , 400 MHz) of 55	106
Figure A.14 The ¹³ C NMR spectrum (CDCl ₃ , 100 MHz) of 55	106
Figure A.15 The ¹ H NMR spectrum (DMSO-d ₆ , 400 MHz) of 25	107
Figure A.16 The ¹³ C NMR spectrum (DMSO-d ₆ , 100 MHz) of 25	107
Figure A.17 The ¹ H NMR spectrum (DMSO-d ₆ , 400 MHz) of 56	108
Figure A.18 The ¹³ C NMR spectrum (DMSO-d ₆ , 100 MHz) of 56	108
Figure A.19 The ¹ H NMR spectrum (CDCl ₃ , 400 MHz) of 57	109
Figure A.20 The ¹³ C NMR spectrum (CDCl ₃ , 100 MHz) of 57	109
Figure A.21 The ¹ H NMR spectrum (CDCl ₃ , 400 MHz) of 58	110
Figure A.22 The ¹³ C NMR spectrum (CDCl ₃ , 100 MHz) of 58	110

Figure A.23	The ^1H NMR spectrum (CDCl_3 , 400 MHz) of 59	111
Figure A.24	The ^{13}C NMR spectrum (CDCl_3 , 100 MHz) of 59	111
Figure A.25	The ^1H NMR spectrum (CDCl_3 , 400 MHz) of 60	112
Figure A.26	The ^{13}C NMR spectrum (CDCl_3 , 100 MHz) of 60	112
Figure A.27	The ^1H NMR spectrum (CDCl_3 , 400 MHz) of 61	113
Figure A.28	The ^{13}C NMR spectrum (CDCl_3 , 100 MHz) of 61	113
Figure A.29	The ^1H NMR spectrum (CDCl_3 , 400 MHz) of 62	114
Figure A.30	The ^{13}C NMR spectrum (CDCl_3 , 100 MHz) of 62	114
Figure A.31	The ^1H NMR spectrum (CDCl_3 , 400 MHz) of 63	115
Figure A.32	The ^{13}C NMR spectrum (CDCl_3 , 100 MHz) of 63	115
Figure A.33	The ^1H NMR spectrum (CDCl_3 , 400 MHz) of 64	116
Figure A.34	The ^{13}C NMR spectrum (CDCl_3 , 100 MHz) of 64	116
Figure A.35	The ^1H NMR spectrum (CDCl_3 , 400 MHz) of 65	117
Figure A.36	The ^{13}C NMR spectrum (CDCl_3 , 100 MHz) of 65	117
Figure A.37	The ^1H NMR spectrum (CDCl_3 , 400 MHz) of 66	118
Figure A.38	The ^{13}C NMR spectrum (CDCl_3 , 100 MHz) of 66	118
Figure A.39	The ^1H NMR spectrum (CDCl_3 , 400 MHz) of 67	119
Figure A.40	The ^{13}C NMR spectrum (CDCl_3 , 100 MHz) of 67	119
Figure A.41	The ^1H NMR spectrum (CDCl_3 , 400 MHz) of 68	120
Figure A.42	The ^{13}C NMR spectrum (CDCl_3 , 100 MHz) of 68	120
Figure A.43	The ^1H NMR spectrum (CDCl_3 , 400 MHz) of 69	121
Figure A.44	The ^{13}C NMR spectrum (CDCl_3 , 100 MHz) of 69	121
Figure A.45	The ^1H NMR spectrum (acetone- d_6 , 400 MHz) of 70	122
Figure A.46	The ^{13}C NMR spectrum (acetone- d_6 , 100 MHz) of 70	122

Figure A.47	The ^1H NMR spectrum (CDCl_3 , 400 MHz) of 72	123
Figure A.48	The ^{13}C NMR spectrum (CDCl_3 , 100 MHz) of 72	123
Figure A.49	The ^1H NMR spectrum (CDCl_3 , 400 MHz) of 73	124
Figure A.50	The ^{13}C NMR spectrum (CDCl_3 , 100 MHz) of 73	124
Figure A.51	The ^1H NMR spectrum (CDCl_3 , 400 MHz) of 74	125
Figure A.52	The ^{13}C NMR spectrum (CDCl_3 , 100 MHz) of 74	125
Figure A.53	The ^1H NMR spectrum (CDCl_3 , 400 MHz) of 76	126
Figure A.54	The ^{13}C NMR spectrum (CDCl_3 , 100 MHz) of 76	126
Figure A.55	The ^1H NMR spectrum (CDCl_3 , 400 MHz) of 77	127
Figure A.56	The ^{13}C NMR spectrum (CDCl_3 , 100 MHz) of 77	127
Figure A.57	The ^1H NMR spectrum (CDCl_3 , 400 MHz) of 78	128
Figure A.58	The ^{13}C NMR spectrum (CDCl_3 , 100 MHz) of 78	128
Figure A.59	The ^1H NMR spectrum (CDCl_3 , 400 MHz) of 79	129
Figure A.60	The ^{13}C NMR spectrum (CDCl_3 , 100 MHz) of 79	129
Figure A.61	The ^1H NMR spectrum (acetone- d_6 , 400 MHz) of 82	130
Figure A.62	The ^{13}C NMR spectrum (acetone- d_6 , 100 MHz) of 82	130
Figure A.63	The ^1H NMR spectrum (acetone- d_6 , 400 MHz) of 83	131
Figure A.64	The ^{13}C NMR spectrum (acetone- d_6 , 100 MHz) of 83	131
Figure A.65	The ^1H NMR spectrum (CDCl_3 , 400 MHz) of 84	132
Figure A.66	The ^{13}C NMR spectrum (CDCl_3 , 100 MHz) of 84	132
Figure A.67	The ^1H NMR spectrum (CDCl_3 , 400 MHz) of 85	133
Figure A.68	The ^{13}C NMR spectrum (CDCl_3 , 100 MHz) of 85	133
Figure A.69	The ^1H NMR spectrum (CDCl_3 , 400 MHz) of 86	134
Figure A.70	The ^{13}C NMR spectrum (CDCl_3 , 100 MHz) of 86	134

Figure A.71	The ^1H NMR spectrum (CDCl_3 , 400 MHz) of 87	135
Figure A.72	The ^{13}C NMR spectrum (CDCl_3 , 100 MHz) of 87	135
Figure A.73	The ^1H NMR spectrum (CDCl_3 , 400 MHz) of 88	136
Figure A.74	The ^{13}C NMR spectrum (CDCl_3 , 100 MHz) of 88	136
Figure A.75	The ^1H NMR spectrum (CDCl_3 , 400 MHz) of 89	137
Figure A.76	The ^{13}C NMR spectrum (CDCl_3 , 100 MHz) of 89	137
Figure A.77	The ^1H NMR spectrum (CDCl_3 , 400 MHz) of 90	138
Figure A.78	The ^{13}C NMR spectrum (CDCl_3 , 100 MHz) of 90	138
Figure A.79	The ^1H NMR spectrum (CDCl_3 , 400 MHz) of 91	139
Figure A.80	The ^{13}C NMR spectrum (CDCl_3 , 100 MHz) of 91	139
Figure A.81	The ^1H NMR spectrum (CDCl_3 , 400 MHz) of 92	140
Figure A.82	The ^{13}C NMR spectrum (CDCl_3 , 100 MHz) of 92	140
Figure A.83	The ^1H NMR spectrum (CDCl_3 , 400 MHz) of 93	141
Figure A.84	The ^{13}C NMR spectrum (CDCl_3 , 100 MHz) of 93	141
Figure A.85	The ^1H NMR spectrum (CDCl_3 , 400 MHz) of 94	142
Figure A.86	The ^{13}C NMR spectrum (CDCl_3 , 100 MHz) of 94	142
Figure A.87	The ^1H NMR spectrum (CDCl_3 , 400 MHz) of 95	143
Figure A.88	The ^{13}C NMR spectrum (CDCl_3 , 100 MHz) of 95	143
Figure A.89	The ^1H NMR spectrum (CDCl_3 , 400 MHz) of 96	144
Figure A.90	The ^{13}C NMR spectrum (CDCl_3 , 100 MHz) of 96	144
Figure A.91	The ^1H NMR spectrum (CDCl_3 , 400 MHz) of 97	145
Figure A.92	The ^{13}C NMR spectrum (CDCl_3 , 100 MHz) of 97	145
Figure A.93	The ^1H NMR spectrum (CDCl_3 , 400 MHz) of 98	146
Figure A.94	The ^{13}C NMR spectrum (CDCl_3 , 100 MHz) of 98	146

Figure A.95	The ^1H NMR spectrum (CDCl_3 , 400 MHz) of 99	147
Figure A.96	The ^{13}C NMR spectrum (CDCl_3 , 100 MHz) of 99	147
Figure A.97	The ^1H NMR spectrum (CDCl_3 , 400 MHz) of 100	148
Figure A.98	The ^{13}C NMR spectrum (CDCl_3 , 100 MHz) of 100	148
Figure A.99	The ^1H NMR spectrum (CDCl_3 , 400 MHz) of 101	149
Figure A.100	The ^{13}C NMR spectrum (CDCl_3 , 100 MHz) of 101	149
Figure A.101	The ^1H NMR spectrum (CDCl_3 , 400 MHz) of 102	150
Figure A.102	The ^{13}C NMR spectrum (CDCl_3 , 100 MHz) of 102	150
Figure A.103	The ^1H NMR spectrum (DMSO-d_6 , 400 MHz) of 103	151
Figure A.104	The ^{13}C NMR spectrum (DMSO-d_6 , 100 MHz) of 103	151
Figure A.105	The ^1H NMR spectrum (CDCl_3 , 400 MHz) of 48	152
Figure A.106	The ^{13}C NMR spectrum (CDCl_3 , 100 MHz) of 48	152
Figure A.107	The ^1H NMR spectrum (acetone- d_6 , 400 MHz) of 104	153
Figure A.108	The ^{13}C NMR spectrum (acetone- d_6 , 100 MHz) of 104	153
Figure A.109	The ^1H NMR spectrum (acetone- d_6 , 400 MHz) of 105	154
Figure A.110	The ^{13}C NMR spectrum (acetone- d_6 , 100 MHz) of 105	154
Figure A.111	The ^1H NMR spectrum (CDCl_3 , 400 MHz) of 106	155
Figure A.112	The ^{13}C NMR spectrum (CDCl_3 , 100 MHz) of 106	155
Figure A.113	The ^1H NMR spectrum (CDCl_3 , 400 MHz) of 108	156
Figure A.114	The ^{13}C NMR spectrum (CDCl_3 , 100 MHz) of 108	156
Figure A.115	The ^1H NMR spectrum (acetone- d_6 , 400 MHz) of 109	157
Figure A.116	The ^{13}C NMR spectrum (acetone- d_6 , 100 MHz) of 109	157
Figure A.117	The ^1H NMR spectrum (CDCl_3 , 400 MHz) of 110	158
Figure A.118	The ^{13}C NMR spectrum (CDCl_3 , 100 MHz) of 110	158

Figure A.119	The ^1H NMR spectrum (CDCl_3 , 400 MHz) of 111 .	159
Figure A.120	The ^{13}C NMR spectrum (CDCl_3 , 100 MHz) of 111 .	159
Figure A.121	The ^1H NMR spectrum (CDCl_3 , 400 MHz) of 112 .	160
Figure A.122	The ^{13}C NMR spectrum (CDCl_3 , 100 MHz) of 112 .	160
Figure A.123	The ^1H NMR spectrum (CDCl_3 , 400 MHz) of 113 .	161
Figure A.124	The ^{13}C NMR spectrum (CDCl_3 , 100 MHz) of 113 .	161
Figure A.125	The ^1H NMR spectrum (CDCl_3 , 400 MHz) of 114 .	162
Figure A.126	The ^{13}C NMR spectrum (CDCl_3 , 100 MHz) of 114 .	162
Figure A.127	The ^1H NMR spectrum (CDCl_3 , 400 MHz) of 115 .	163
Figure A.128	The ^{13}C NMR spectrum (CDCl_3 , 100 MHz) of 115 .	163
Figure A.129	The ^1H NMR spectrum (CDCl_3 , 400 MHz) of 116 .	164
Figure A.130	The ^{13}C NMR spectrum (CDCl_3 , 100 MHz) of 116 .	164
Figure A.131	The ^1H NMR spectrum (CDCl_3 , 400 MHz) of 117 .	165
Figure A.132	The ^{13}C NMR spectrum (CDCl_3 , 100 MHz) of 117 .	165
Figure A.133	The ^1H NMR spectrum (CDCl_3 , 400 MHz) of 118 .	166
Figure A.134	The ^{13}C NMR spectrum (CDCl_3 , 100 MHz) of 118 .	166
Figure A.135	The ^1H NMR spectrum (acetone- d_6 , 400 MHz) of 119 .	167
Figure A.136	The ^{13}C NMR spectrum (acetone- d_6 , 100 MHz) of 119 .	167
Figure A.137	The ^1H NMR spectrum (acetone- d_6 , 400 MHz) of 120 .	168
Figure A.138	The ^{13}C NMR spectrum (acetone- d_6 , 100 MHz) of 120 .	168
Figure A.139	The ^1H NMR spectrum (CDCl_3 , 400 MHz) of 121 .	169
Figure A.140	The ^{13}C NMR spectrum (CDCl_3 , 100 MHz) of 121 .	169
Figure A.141	The ^1H NMR spectrum (CDCl_3 , 400 MHz) of 122 .	170
Figure A.142	The ^{13}C NMR spectrum (CDCl_3 , 100 MHz) of 122 .	170

Figure A.143	The ^1H NMR spectrum (DMSO- d_6 , 400 MHz) of 123	171
Figure A.144	The ^{13}C NMR spectrum (DMSO- d_6 , 100 MHz) of 123	171
Figure A.145	The ^1H NMR spectrum (DMSO- d_6 , 400 MHz) of 124	172
Figure A.146	The ^{13}C NMR spectrum (DMSO- d_6 , 100 MHz) of 124	172
Figure A.147	The HR-ESI-MS of 59	173
Figure A.148	The HR-ESI-MS of 74	173
Figure A.149	The HR-ESI-MS of 89	174
Figure A.150	The HR-ESI-MS of 92	174
Figure A.151	The HR-ESI-MS of 93	175
Figure A.152	The HR-ESI-MS of 94	175
Figure A.153	The HR-ESI-MS of 95	176
Figure A.154	The HR-ESI-MS of 98	176
Figure A.155	The HR-ESI-MS of 99	177
Figure A.156	The HR-ESI-MS of 102	177
Figure A.157	The HR-ESI-MS of 103	178
Figure A.158	The HR-ESI-MS of 113	178
Figure A.159	The HR-ESI-MS of 114	179
Figure A.160	The HR-ESI-MS of 119	179
Figure A.161	The HR-ESI-MS of 121	180
Figure A.162	The HR-ESI-MS of 122	180
Figure A.163	The HR-ESI-MS of 123	181

LIST OF ABBREVIATIONS

calcd	calculated
concd	concentrated
d	doublet (NMR)
dd	doublet of doublets (NMR)
DMSO	dimethyl sulfoxide
EC	Effective concentration
equiv.	equivalent
EtOAc	Ethyl acetate
g	gram (s)
HR-ESI-MS	High resolution-electrospray ionization mass
m	multiplet (NMR)
MHz	Mega Hertz
mL	milliliter (s)
mm	millimeter (s)
mmol	millimole (s)
NMR	Nuclear Magnetic Resonance
p	pentet

ppm part per million

q quartet (NMR)

sext sextet (NMR)

s singlet (NMR)

t triplet (NMR)

rt room temperature

TLC Thin layer chromatography

$[M+Na]^+$ pseudomolecular ion

α alpha

β beta

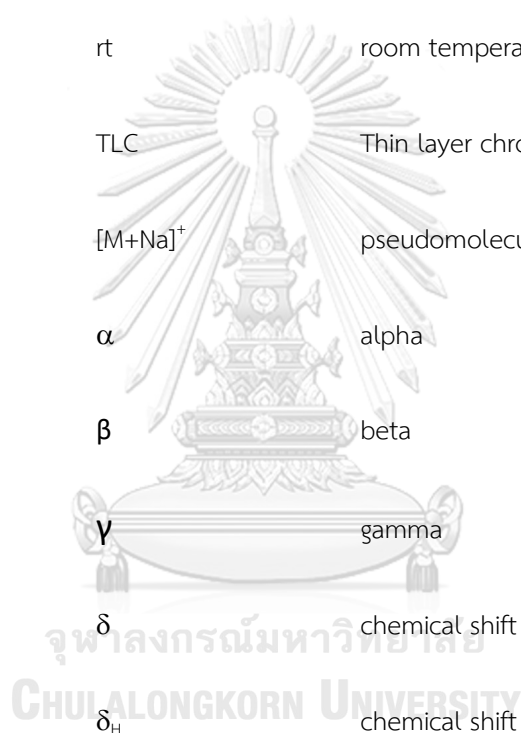
γ gamma

δ chemical shift

δ_H chemical shift of proton

μL microliter (s)

μM micromolar (s)



CHAPTER I

INTRODUCTION

In modern life, human has to confront with many disease morbidities resulting from the unhealthy lifestyles such as having a high-fat diet, consuming a lot of sugary foods, no time for exercise, drinking too much alcohol and so on. Type 2 diabetes is one of the most popular disorders in developed countries and the number of patients with diabetes tends to increase in developing countries these years. Notably, most diabetic patients have been diagnosed to have diabetic nephropathy (DN) concurrently. A victim with chronic DN will suffer end-stage renal disease requiring renal replacement therapy containing hemodialysis and renal transplantation. Therefore, it is imperative to find suitable medication for diabetes and diabetic nephropathy diseases. In addition, adenosine monophosphate-activated protein kinase or AMPK was found to regulate many kinds of cellular processes in the cells and AMPK activation seems to protect podocyte, the most injured part in DN patients, from impairment and stable insulin activity. Thus, AMPK activation was considered as a potent target for drug design for diabetes and DN treatment. Besides, it was reported that chalcone is a feasible structure possessing a diverse variety of biological activity including anti-diabetic and AMPK activation activity. As a result, the preparation of chalcone derivatives as AMPK activators would be an attractive direction for finding a new therapy for diabetes and diabetic nephropathy disorder.

1.1 Chalcone

Chalcone (1,3-diphenyl-2-propen-1-one) is an organic compound with a resonance system comprising two phenyl rings connecting to each other by an enone component (**Figure 1.1**). In the chalcone skeleton, two aromatic rings possibly possess various substituents such as hydroxy, methoxy and prenyl. It belongs to flavonoid classification and usually expresses the yellow pigmentation in plants. Chalcone is the original intermediate taking part in the biosynthetic pathways of various flavonoids.

Theoretically, chalcones carrying 2'-hydroxy, especially those additionally bearing another one at 6'-position can easily transform into a racemic mixture of (2*S*)- and (2*R*)-flavanones by Michael addition on α,β -double bond. In fact, (2*S*)-flavanones are predominant products due to the catalysis of chalcone isomerase (CHI) (**Figure 1.2**). Therefore, only (2*S*)-flavanones can be chosen as intermediates for constructing further flavonoid diversity.¹ The chalcone-based skeleton has appealed intensive scientific studies throughout the world since its derivatives demonstrate a variety of promising biological activity such as anti-inflammatory^{2, 3}, NF- κ B inhibition⁴⁻⁶, HDAC inhibition⁷, anticancer^{3, 4, 8}, anti-oxidant⁹ and anti-diabetic¹⁰. Besides, in addition to chalcone-based compounds available widely in natural resources, the ease of synthesis allows chalcone derivatives to be prepared diversely.

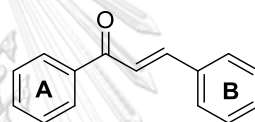


Figure 1.1 Core structure of chalcone.

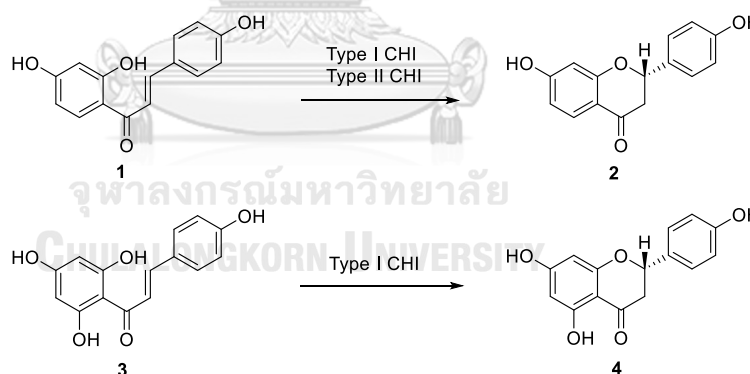


Figure 1.2 Chalcone cyclization.

1.1.1 Natural chalcones

Chalcones are prevalent in the natural resources but they do not accumulate to an appreciable degree in most plants. The largest number of natural chalcones has been isolated from species of the Leguminosae, Asteraceae and Moraceae families.¹¹ In 2012, Orlikova *et al.* utilized a series of natural chalcones to evaluate for HDAC

inhibition and TNF α -induced NF- κ B inhibition activity because the nuclear factor NF- κ B is controlled by histone deacetylase enzyme.⁷ The results showed that only four compounds such as isoliquiritigenin (**1**), butein (**9**), homobutein (**11**) and glycoside marein (**13**) demonstrated noticeable HDAC activity with IC₅₀ ranging from 60 to 190 μ M (Figure 1.3). Besides, with IC₅₀ values of 8 and 11 μ M, flavokawain C (**10**) and calomelanone (**8**) were the most feasible NF- κ B inhibitors respectively. In addition, the other chalcones **1**, **5-7**, **9**, **11** and **12** also exhibited good potential with IC₅₀ values fluctuating between 24-41 μ M.

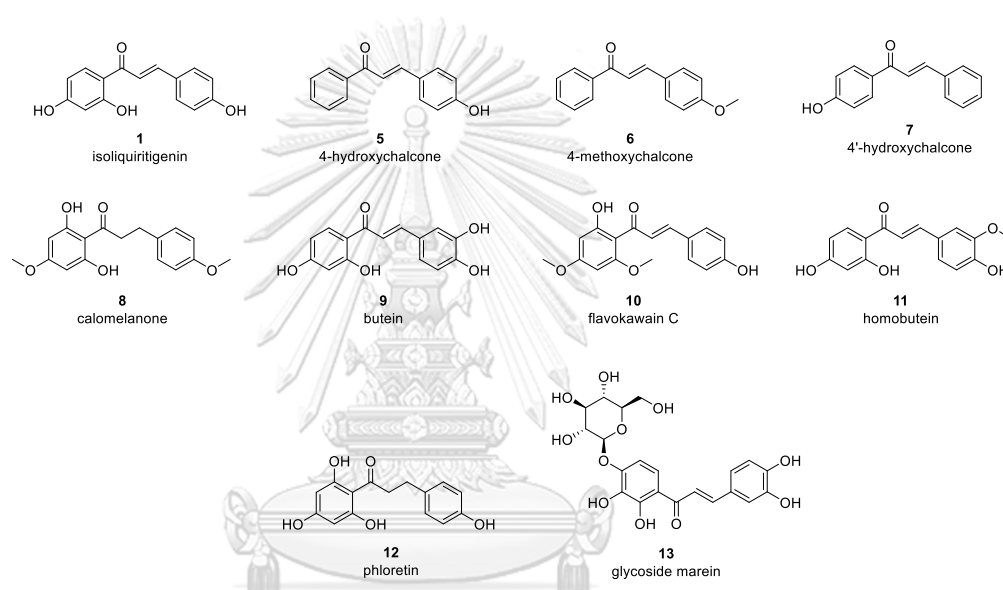


Figure 1.3 Natural chalcones **1**, **5-13**.

In addition, three prenylated chalcones **14-16** isolated from *Psoralea corylifolia* (L.) were reported to possess potent concentration-dependent inhibitory effects on NO and PGE₂ production in lipopolysaccharide (LPS)-activated microglia for the treatment of neuro-inflammatory diseases by Kim *et al.* in 2018 (Figure 1.4).⁶ The signal of protein and mRNA of inducible nitric oxide synthase (iNOS) and cyclooxygenase-2 (COX-2) were decreased in LPS-activated microglia. Since NF- κ B governed the expression of pro-inflammatory enzymes such as iNOS and COX-2, the effect of compounds **1-3** on nuclear factor κ B (NF- κ B) were assessed. Then, the reduction of the degradation of I- κ B α and nuclear level of NF- κ B in LPS-stimulated BV-2 microglia were obtained by the treatment of these prenylated chalcones at 5 μ M.

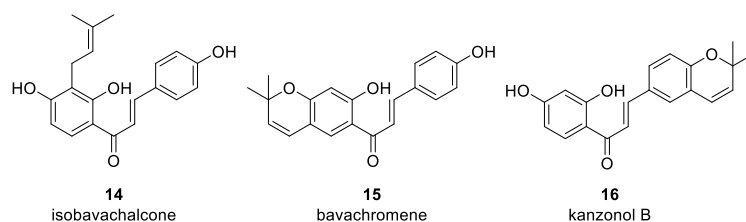


Figure 1.4 Prenylated chalcones **14-16** from *Psoralea corylifolia* (L.).

In 2008, five geranyl chalcone derivatives containing isolespeol (**17**), 5'-geranyl-2',4',4'-trihydroxychalcone (**18**), lespeol (**19**), 3,4,2',4'-tetrahydroxy-3'-geranyldihydrochalcone (**20**) and xanthoangelol (**21**) were isolated from the leaves of Breadfruit (*Artocarpus communis* Moraceae) – a tropical and subtropical medicinal plant by Fang *et al.* (**Figure 1.5**).¹² They were used to examine the *in vitro* anticancer activity on a wide range of tumor cells. The outcome indicated that isolespeol (**18**) presented the strongest inhibitory activity ($IC_{50} = 3.8 \mu\text{M}$) in SW 872 human liposarcoma cells. Furthermore, the disruption of mitochondrial membrane potential was observed when SW 872 human liposarcoma cells were treated with isolespeol (**17**). By some further testings, they concluded that solespeol (**17**) caused apoptosis in SW 872 cells through Fas- and mitochondria-induced pathways.

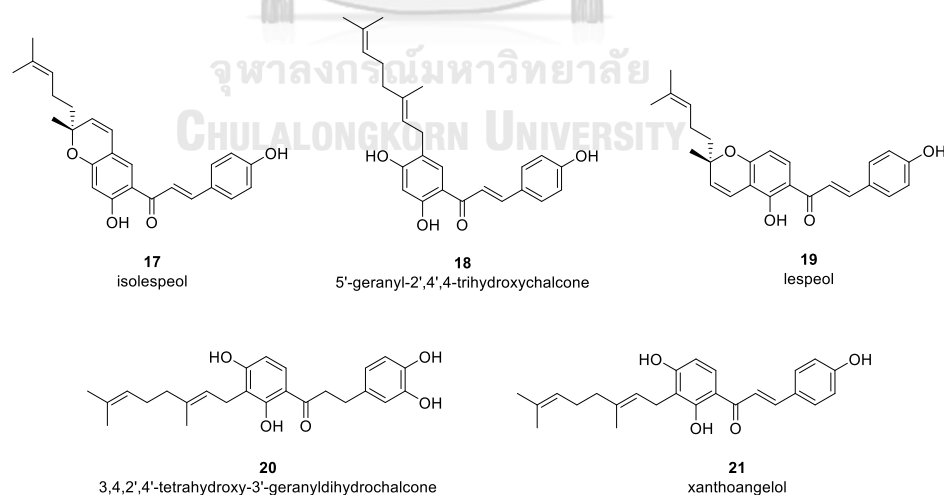


Figure 1.5 Geranyl chalcone derivatives isolated from the leaves of *Artocarpus communis*.

1.1.2 Synthetic chalcones

Many chalcone derivatives have also been prepared because of their convenient synthesis by Claisen-Schmidt reaction. In 2009, Srinivasan *et al.* prepared a series of chalcone-based compounds with different substituents on both rings such as halogen, methyl and trifluoromethyl, where several chalcones with only hydroxy and methoxy substituents on both rings demonstrated good activity with low IC₅₀ values, some of them are displayed in **Figure 1.6**.⁴ The A-ring with 3',4',5'-trimethoxy substitution was the best component for increasing NF-κB inhibitory activity. Furthermore, the alteration of **22** to **28** and **29** resulted in relatively unchanged IC₅₀ values, thereby creating a new direction to improve the activity of chalcone-based compounds.

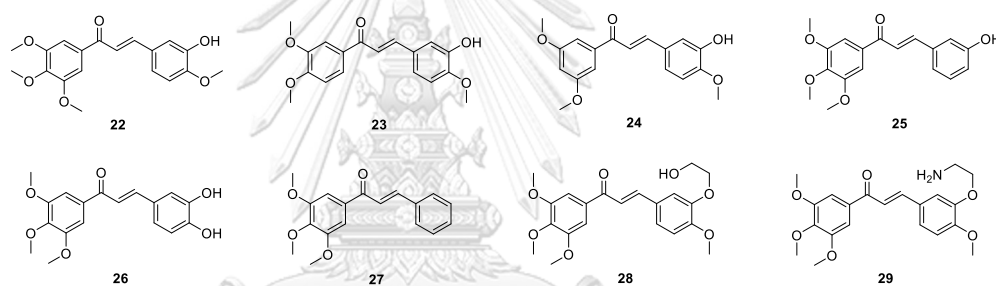


Figure 1.6 Some potent chalcones for anticancer activity **22-29**.

Chalcone derivatives were also exploited to evaluate antidiabetic activity by Hsieh *et al.* in 2012.¹⁰ A series of chalcones bearing electron donating or electron withdrawing substitutions by a one-step protocol were synthesized and assessed for glucose uptake activity. The potent chalcone candidates with halogen except fluoro or hydroxy group at 2'-position on A-ring showed a feasible activity with glucose medium concentration from 210 to 236 mg/dL compared to pioglitazone and rosiglitazone (230 and 263 mg/dL, respectively). Moreover, chalcones bearing iodo substituent at 3-position on A-ring exhibited considerable activity with glucose medium concentration lower than 239 mg/dL. Some potent compounds are illustrated in **Figure 1.7**.

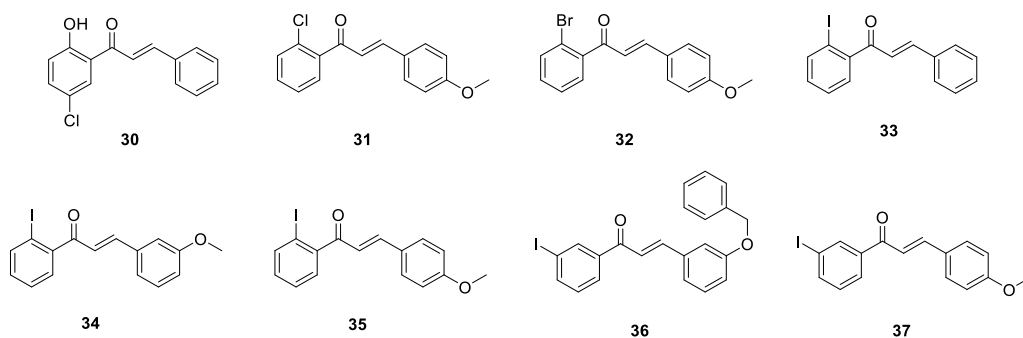


Figure 1.7 Some dominant molecules for anti-diabetic activity.

In addition, some kind of chalcone-based derivatives were prepared to test diverse biological activity due to their privilege structure. In 2017, Shankaraiah *et al.* synthesized a series of heterocycles-linked chalcone conjugated by various saturated carbon chains and utilized for examining cytotoxic and tubulin polymerization inhibitory activity.¹³ Firstly, the etherification of vanillin compounds (**38**) with dibromo alkane linkages of alternating carbon numbers ($n = 2, 3, 4$), in the existence of K_2CO_3 as the base to produce the intermediate **39** was performed. Next, the other bromide atom was replaced by different kinds of nitrogen containing heterocycles under refluxing in acetonitrile in the presence of K_2CO_3 , to obtain vanillin derivatives **40** in quantitative yields. Finally, different aldehydes **40** were used to combine with several substituted acetophenones by aldol condensation reaction under the base catalyst as $Ba(OH)_2$ to afford the chalcone derivatives **41** in good yields. Regarding biological evaluation, by many different methods, chalcone **42** demonstrated a strong anticancer activity on NCI-H460 (lung cancer) cells with IC_{50} of $1.48 \pm 0.19 \mu M$. This molecule also caused apoptosis in NCI-H460 cells and arrested these lung cancer cells in the G2/M phase of the cell cycle. For tubulin polymerization inhibitory activity, it was found that tubulin polymerization and the formation of microtubules were suppressed considerably by **42** ($IC_{50} = 9.66 \pm 0.06 \mu M$). In addition, the possible interaction manner between the most potent candidates (**42** and **43**) and the colchicine site of the tubulin was observed by molecular docking investigates.

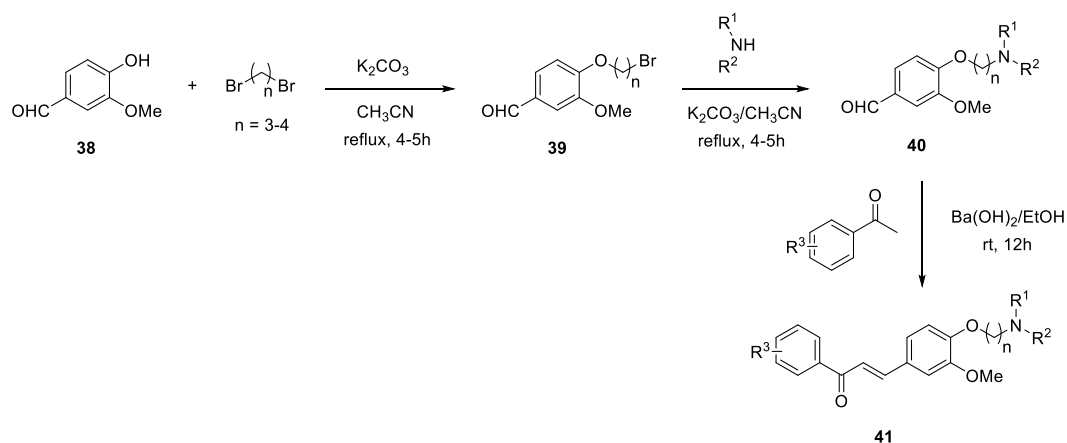


Figure 1.8 Procedure for synthesizing heterocycles-linked chalcone hybrid.

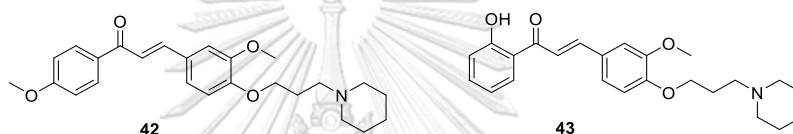


Figure 1.9 Two candidates as cytotoxic agents and tubulin polymerization inhibitors.

1.2 Diabetic nephropathy disease (DN) and AMPK

Diabetes has been spreading as morbid epidemic all over the world in the 21st century. This consequence is derived from many reasons such as aging population, abundant nutrition and sedentary lifestyle. With respect to WHO statistics, between 1980 and 2014, there is significant growth from 108 million to 422 million in the number of people with diabetes. In addition, the global pervasiveness of diabetes among people over 18 years of age has increased rapidly from 4.7% in 1980 to 8.5% in 2014. Notably, diabetes prevalence has been raising more swiftly in middle- and low-income countries. Diabetes is the main cause of many kinds of chronic diseases such as blindness, kidney failure, heart attacks, stroke and lower limb amputation. It is reported that approximately 1.6 million deaths were directly ensued from diabetes in 2016 and another 2.2 million deaths were resulted from high blood glucose in 2012. Ultimately, WHO assesses that diabetes was the seventh leading cause of death in 2016.

Type 2 diabetes (formerly called non-insulin-dependent, or adult-onset) includes the majority of people with diabetes around the world and is mostly the consequence of obesity and physical inactivity. Type 2 diabetes results from the body's ineffective use of insulin. In the United States, 40% of 29 million citizens diagnosed to have type 2 diabetes also suffer from diabetic nephropathy (DN). Similarly, around 45% of 3,795 diabetic patients have been struggling with DN in Thailand. The prolonging DN will result in end-stage renal disease (ESRD) requiring renal replacement therapy containing hemodialysis and renal transplantation.

1.2.1 Diabetic nephropathy disease (DN)

In the Industrial Revolution 4.0, population around the world have to face many new pressures such as many blue-collar jobs have been gradually deserved for high-technology robots and most of human will become white-collar workers in the future. Therefore, the sedentary lifestyle has been a hallmark of office job so far, which would mediate many chronic disorders to the people such as cardiovascular diseases, obesity, stroke and heart attacks. Diabetes mellitus (DM) or diabetes is also one of the outcomes, it is a group of metabolic disorders characterized by hyperglycemia derived from impairments in insulin secretion, insulin action or all together. The number of global citizens over 18 years of age diagnosed to have diabetes is about 415 million and this number is estimated to approach 592 million in 2035.¹⁴ Diabetes also take responsibility for almost half of new cases suffering kidney failure. As a result, kidney defects induced by diabetes should be a deserved global public health concern to fulfill the urgent medical requirement.¹⁵

Diabetic nephropathy (DN), being one of the primary microvascular complications of DM, emerges in 20–40% of patients with Type 2 DM and over 40% of new cases of end-stage renal disease (ESRD).^{16, 17} DN is specialized by immoderate depletion of protein mostly albumin in the urine (albuminuria), attenuates renal function and damage property of kidney filtration. These alterations lead to clinical

proteinuria (>300 mg per day). Therefore, kidney can not eliminate waste or abundant secretion from the body leading to excrement accumulation in the body and fluid retention. At this period, victim must have their kidney function support by dialysis and eventually may require a kidney transplant.^{18, 19}

There are five different clinical stages of DN disorder distinguished by the values of the glomerular filtration rate (GFR), urinary albumin excretion (UAE) and systemic arterial blood pressure (**Table 1.1**). Patients suffer more serious conditions in higher stages. In stage I, the urine is still free of albumin protein and normal blood pressure is measured. In all diabetic patients, the glomeruli are found to be hypertrophied leading to an increase in filtration area. In addition, glomerular perfusion and the transglomerular hydraulic pressure alterations are evaluated to increase. These structural defects along with hemodynamic factors cause a rise in the GFR exceeding normal rate of 20 to 40%. Then, patients have to confront microalbuminuria which is defined as a UAE of 30-300 mg/day in stage II. Structure of the glomerular and tubular basement membranes continues to thicken and some degree of podocyte loss are measured. Moreover, mesangial matrix expansion and diffuse glomerulosclerosis are manifest. In stage III, diffuse and/or nodular glomerulosclerosis, as well as podocyte loss increase significantly and macroalbuminuria, takes place with UAE exceeding 300 mg/day. In the last stages IV and V, proteinuria is approached. The GFR attenuates progressively at a low rate in stage IV and patients are required renal replacement therapy in ESRD stage (stage V).

The current therapies for curing DN disorder comprises two approaches such as glucose-lowering control and blood pressure control through blockade of the renin-angiotensin system involving angiotensin-converting enzyme (ACE) inhibitor and angiotensin receptor blocker. Nevertheless, the profound glucose-lowering control seems to be useless after onset of complexity or prolonging diabetes have been undergone. Moreover, some drug regulating glucose concentration and blood pressure can cause some serious side effects such as bone disorder, bladder cancer,

hyperkalemia, and cardiovascular diseases if they are utilized for long time.¹⁹ Although some sort of treatments were applied to tackle DN morbidity, they might not be effective due to the complication of pathogenic mechanisms. As a result, the imperative need is discovering the drug-target and the pathogenic mechanism of DN so as to ameliorate renal function of DN patients.

Table 1.1 Clinical stages of diabetic nephropathy (DN).

Stage	GFR	UAE	Blood Pressure
1. Hyperfiltration	Supernormal	Less than 30 mg/day	Normal
2. Microalbuminuria	High normal-normal	30-300 mg/day	Rising
3. Overt proteinuria	Normal-decreasing	More than 300 mg/day	Elevated
4. Progressive nephropathy	Decreasing	Increasing	Elevated
5. ESRD	Less than 15 mL/min	Massive	Elevated

1.2.2 Glomerulus and podocyte

Under usual physiological conditions, the kidneys take a crucial responsibility in filtration, collection, and stabilization of body homeostasis. Filtration and collection mean the kidneys or smaller functional units called nephron transport the blood from artery including important nutrients such as Na⁺ ion, amino acids, protein, as well as oxygen passing the filter and return them into vein while the abundant salts, exceeding water and urea are collected to transfer them into urine. Normally, these processes occur at glomerulus part of nephron and filtrate can pass across glomerular filtration barrier. This glomerular filtration barrier contains three main layers i.e., fenestrated capillary endothelium, glomerular basement membrane, and podocyte (**Figure 1.10**). These three layers form gates that are size and charge selective to make sure relatively protein-free urine formation. The rate of filtration and composition of the urine were determined by the transportation of the filtrate and solutes through glomerular

filtration system. In DN patients, the composition of kidneys relating to renal filtration bearing structural defects and functional disorder, which leads to albumin protein passing through filter system to approach into urine (albuminuria). Some physiological manners observed in glomerulus of DN patients comprise the early hypertrophy of glomerular and tubular parts, subsequent thickening of basement membrane in glomeruli and tubules, gradual accumulation of extracellular matrix proteins in the glomerular mesangium, loss of podocyte and urine including protein (proteinuria) as well.

Podocytes are the principal component of the renal glomerulus, are terminally differentiated epithelial cells. It has long cytoplasmic extensions called foot processes that prolong from the cell body. Podocyte foot processes, controlled by intact structure called actin cytoskeleton, are formed on the urinary side of the glomerular basement membrane, and foot processes from the neighboring cells are interdigitated. Foot processes wrap around the glomerular capillaries and interlace with one another, leaving narrow filtration slits, a gap between slit diaphragms that plays a key role as size, shape, and charge selective barrier to the passage of macromolecules such as albumin from underlying capillary network to the extravascular urinary space.¹⁵ Therefore, the integrity of podocyte is very significant for hindering macromolecule such as protein in entering the urine.²⁰

In addition, insulin action is proposed to be very predominant in regulating podocyte in order to stable glomerular filtration barrier by glucose uptake stimulation, cytoskeletal reorganization. However, in the body of DN patients, podocyte fails to respond correctly with insulin signals leading to the formation of improper structure of podocyte and then the destruction of podocyte cytoskeleton ensues.²¹ Albuminuria occurs due to the disappearance of filtering barrier. Besides, podocyte network is also vulnerable in response to hyperglycemia disorder, causing apoptosis and disturbance

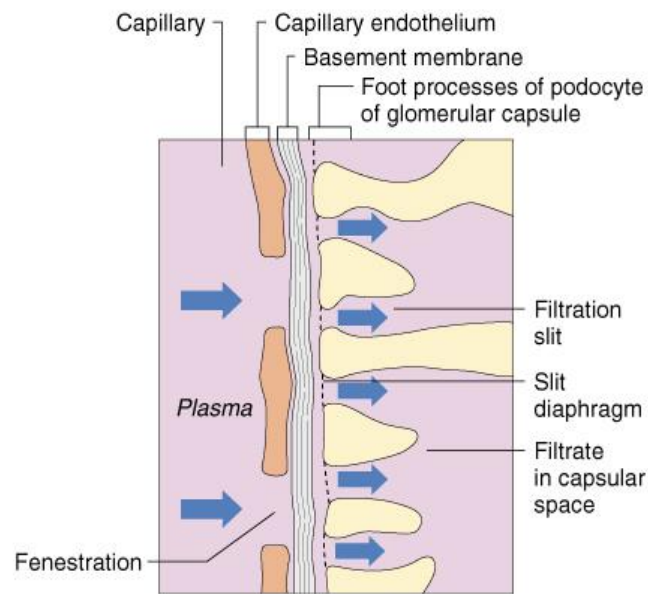


Figure 1.10 Renal glomerulus components.

in skeletal integrity.²² For instance, it was reported that immortalized podocyte cell line was killed via apoptosis under high-glucose conditions which was monitored by DAPI fluorescent staining to approach chromatin condensation and segregation.²³ In contrast, podocyte loss is considered as the sign of diabetes-induced glomerular diseases as well which can deteriorate to reach tubular damage and thorough nephron loss. As podocyte are terminally differentiated and have a restricted capability for amelioration or regeneration, the foot process effacement in podocyte phenotypes resulting in kidney disorders usually happen at early stages and subsequently podocyte depletion synchronizes with progression of glomerular disease.²³ Experimental animal models showed that a loss of 20% of podocyte leads to transient proteinuria and further injury can process to progressive proteinuria, glomerulosclerosis and finally end up with loss of renal function.²⁴ Thus, the potential therapies for DN treatment should be addressing insulin resistance and impeding podocyte loss or impairment.

Insulin is a vital hormone involved in the regulation of glucose and lipid metabolism. Its biological activity is activated when binding of insulin to insulin receptor occurs. Activation form of insulin receptor causes initiation and

autophosphorylation of the receptor tyrosine kinase and different cascades of phosphorylation processes. However, the cellular response to insulin in insulin-resistant state is diminished leading to higher requirement of insulin concentration for insulin-mediated cellular events. Some noticeable donors causing insulin resistance are hyperinsulinemia, hyperglycemia, inflammation, lipid excess, mitochondrial dysfunction, and endoplasmic reticulum (ER) stress.²⁵ Podocyte is an insulin-responsive cell which expresses all the elements of the insulin-signaling cascade such as functional IRS1 and insulin receptor, it also regulates to develop glucose absorption by glucose transporter, representatively glucose transporter type 4 (GLUT4) under insulin stimulation. The relationship among insulin signaling, podocyte, and DN pathogenesis was found in the experiment that podocyte collected from diabetic *db/db* mice can not manage to phosphorylate AKT as well as transfer GLUT4 to the plasma membrane under insulin regulation resulting to vulnerability to cell death. Therefore, the number of podocytes was declined to pave the way for albuminuria seen in the early stage of DN disorder.²¹ Moreover, the mice with insulin receptor gene removed suffer from albuminuria hypertrophy coinciding with podocyte foot processes effacement, apoptosis, thickening of the glomerular basement membrane and enlarging glomerulosclerosis which are all the pathological hallmarks of DN disease.²² These findings propose that proper-operation of insulin signaling pathway is crucial for maintaining podocyte foot processes and hindering albuminuria event

1.2.3 AMPK – drug target for diabetic nephropathy treatment

Adenosine monophosphate-activated protein kinase or AMPK is a heterotrimeric complex containing three subunits: an α subunit harboring a protein kinase catalytic domain and non-catalytic β and γ (PRKAG) regulatory subunits. There are two isoforms of α and β subunits and three isoforms of γ subunit resulting in twelve possible combinations of the heterotrimeric $\alpha\beta\gamma$ AMPK complex. In addition, the amino-terminal region of α subunit possesses a typical serine/threonine kinase

domain which comprises a region called the activation loop, or T-loop conserved by many protein kinases and taking prominent responsibility in their regulation. It is believed that AMPK is stimulated effectively when phosphorylation process of Thr172 (pThr172) within the activation loop occur.^{26, 27}

There are two upstream kinases controlling the physiological phosphorylation of Thr172 such as liver kinase B1 (LKB1)²⁷⁻²⁹ and calcium/calmodulin-dependent protein kinase kinase 2 (CAMKK2 or CAMKK β).³⁰⁻³² These two factors affect AMPK's activity through metabolic stresses that increase ADP: ATP and/or AMP: ATP ratios. There is some evidence proved that the sensitivity between AMPK and cellular stresses sees a decrease during the aging process so it would cause disorders in downstream signaling, the stability of cellular energy balance as well as the stress resistance. Nevertheless, it was recognized that AMPK defect can induce several diseases to young people. For example, dysfunctions in AMPK signaling cause a decline in mitochondrial biogenesis, rise in cellular stresses and inflammatory accumulation which are some typical processes in aged people and they have a close connection to several pathological movements.³³⁻³⁵ It can be seen AMPK regulate a variety of cellular process in cells; therefore, AMPK-activating treatment seems to a promising therapy for healing different relating impairments.^{33, 36}

AMPK expresses in many types of tissues in the body such as kidney, skeletal muscle, adipose tissue, liver, heart, and hypothalamus of the brain. Nonetheless, renal cells containing mesangial cells, glomerular endothelial cells and podocytes see a high expression of AMPK. It was found that the decrease in AMPK activity is associated with a metabolic syndrome phenotype such as central adiposity, dyslipidemia, and a predisposition to type 2 diabetes, atherosclerotic cardiovascular disease.³⁷ In muscle-specific transgenic mice possessing an inactive form of AMPK, insulin-stimulated glucose transport declined and insulin resistance was aggravated in high-fat feeding condition.³⁸ From these two examples, a connection among AMPK dysfunction, metabolic syndrome disorders, escalation of insulin resistance and type 2 diabetes diseases was observed.³⁷ Several studies indicated that metformin, a popular drug used for type 2 diabetes patients to boost insulin sensitivity was realized to be an AMPK activation agent.³⁹

The relationship between diabetic nephropathy disorder and AMPK activity was also researched, for instance, immunofluorescence staining presented that the intraglomerular intensity of AMPK phosphorylation was diminished in the kidney biopsy of DN patients.⁴⁰ In addition, the hindrance of AMPK action was measured in immortalized mouse podocytes cultured in glucose circumstance and this suppression was considered as an upstream pathway via LKB1 kinase.⁴¹ Moreover, metformin, which is used as the first-line drug prescribed for type 2 diabetes because of their positive pharmacological effect on AMPK, was recognized to reduce permeability of glomerular filtration barrier as well as improve glucose absorption into rat podocytes cultured in high glucose condition (25 mM).⁴² On the other hand, activation of AMPK by metformin was realized to impede the generation of superoxide anion, an oxidative stress responsible for initiating and handling DN disorder, via down-regulation of the Nox4/NaD(P)H oxidase subunit in cultured mouse podocytes under both normoglycemic and hyperglycemic conditions.⁴³ Therefore, AMPK seem to have protective activity by inhibiting of oxidative stress. Furthermore, much research suggested a connection among DN disorder, disturbed lipid metabolism and renal accumulation of lipids. In the animal models, it can be seen that mice fed with high-fat diet (HFD) are not only susceptible to suffer glomerular fibrosis, inflammatory cytokines and urinary albumin secretion which deteriorate kidneys but they are also confronted with renal AMPK suppression. Nevertheless, under metformin administration, inflammatory cytokines and renal impairment were reduced.⁴⁴ In the streptozotocin-induced diabetic rat, AMPK activity was impeded due to fatty acid oxidation forming toxic free fatty acid.⁴⁵ It is believed that excessive fatty acids can injure podocytes, proximal tubular epithelial cells, and the tubulointerstitial tissue through different mechanisms; particularly, by initiating the production of reactive oxygen species (ROS) and lipid peroxidation, inducing mitochondrial impairment and tissue inflammation, which ensue in glomerular and tubular injuries.⁴⁶ AMPK also has a close linkage to mitochondria which is known as energy production plant of the cell and metabolic syndromes have been considered as the results from mitochondrial defects. For instance, some research indicated that glomerular disease and podocyte injury are attributed to mitochondrial dysfunction, hyperglycemia and insulin resistance

in diabetes.⁴⁷ Therefore, AICAR was applied to activating AMPK to stimulate mitochondrial biogenesis via peroxisome proliferator-activated receptor gamma coactivator 1-alpha (PGC-1 α) promotion in the glomeruli and podocyte of streptozotocin-induced diabetic mice.⁴⁸ Notably, the association between insulin signaling and AMPK activation activity was encouraged by insulin-sensitive podocyte cells. For example, the abatement of AMPK phosphorylation and insulin-dependent glucose uptake as well as the apparent insulin resistance were monitored in primary rat podocytes growth in high glucose circumstances.⁴⁹ While it was found that metformin can promote AMPK activity and disrupt high glucose-mediated impairment of glucose absorption into podocytes leading to maintenance of podocyte function.⁴² As a result, AMPK activation pathway is considered an appealing direction of drug discovery for DN remedy.

1.3 Reported chalcones as AMPK activation agents

Licochalcone A (**44**), isolated from the *Glycyrrhiza* plant as a major phenolic compound, was found to display a wide range of pharmacological applications including the impact on hepatic lipid metabolism by Quan *et al.* in 2013 (**Figure 1.11**).⁵⁰ **44** was suggested to impede the hepatic triglyceride accumulation in HepG2 cells and ICR mice fed on a high-fat diet (HFD). Particularly, **44** showed upstream regulation of gene expression of proteins such as peroxisome proliferator-activated receptor α (PPAR α) and fatty acid transporter (FAT/CD36), which are accountable for lipolysis and fatty acid transport, respectively. In addition, the mechanism of these effects were attributed to AMPK activation and they were abolished if HepG2 cells were consumed with an AMPK inhibitor, compound C. Subsequently, oxygen consumption rate, and ATP levels were measured in HepG2 cells to discover how **44** is able to stimulate AMPK and the results presented that mitochondrial respiration and ATP levels dropped meaning that indirect AMPK activation occurred. Eventually, *in vivo* outcomes also matched with available results that triglyceride levels were realized to reduce considerably in six-week-old mice orally administered with **44** (5 and 10 mg/kg) once

a day for three weeks; furthermore, AMPK was found to intensify in the liver of ICR mice fed on an HFD.

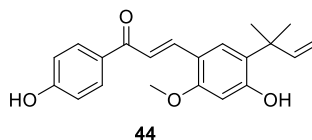


Figure 1.11 Licochalcone A (LA) structure.

In 2014, Zhang *et al.* carried out the research relating to attenuation of excessive lipid accumulation causing various severe diseases containing hyperlipidemia, diabetes and fatty liver disorder by chalcones.⁵¹ There are four compounds chosen such as 4-hydroxyderricin (**45**), xanthoangelol (**21**), cardamonin (**46**) and flavokawain B (**47**) which were reported to possess feasible biological activity against obesity, inflammation, and diabetes (**Figure 1.12**). Hepatocyte cells (HepG2) were firstly treated with a mixture of fatty acids (palmitic acid: oleic acid = 1: 2 ratio), then lipid level in cells develops markedly. Under the same protocol, addition of 5 μ M chalcone compound reduced the concentration of lipid accumulation in hepatocyte cells. In addition, the results displayed that the decline of SREBP-1 expression and the growth of PPAR α activity were obtained in HepG2 cells under chalcone treatment, they are also essentially responsible for lipogenesis and fatty acid oxidation, respectively. Furthermore, phosphorylation of AMPK and LKB1 which up-regulate SREBP-1 and PPAR α were considered to occur. Thereafter, compound C, an AMPK inhibitor, was utilized and it was realized that SREBP-1 and PPAR α expression were abolished in HepG2 cells consuming chalcones. As a result, **21**, **45-47** were proved to decrease lipid accumulation through activation of the LKB1/AMPK signaling pathway in HepG2 cells.

Two chalcones **21** and **45** isolated from n-hexane/EtOAc (5:1) extract of the yellow-colored stem juice of *Angelica keiskei* as major products were also investigated about the mechanism in rising glucose transporter 4 (GLUT4)-dependent glucose uptake in 3T3-L1 adipocytes by Ohta *et al.* in 2015 (**Figure 1.12**).⁵² They were found

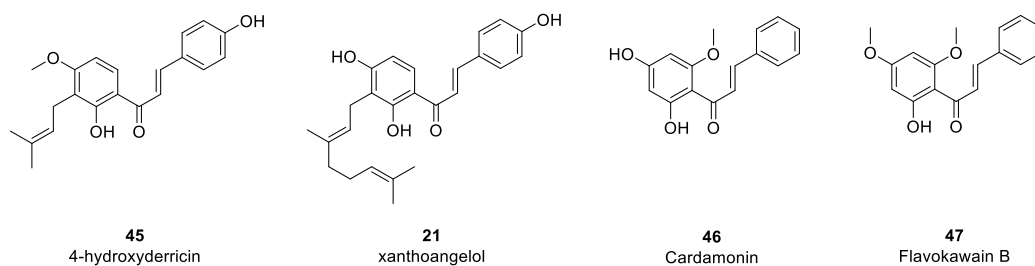


Figure 1.12 Chemical structures of **21**, **45-47**.

to increase glucose uptake and GLUT4 translocation to the plasma membrane. Moreover, both chalcones also activated the phosphorylation of AMPK, liver kinase B1 (LKB1), which acts upstream of AMPK and AMPK's downstream target acetyl-CoA carboxylase. Thus, these outcomes showed that two compounds **21** and **45** are able to develop GLUT4-dependent glucose uptake via the LKB1/AMPK signaling pathway in 3T3-L1 adipocytes.

Some chalcones can affect the digestive system via AMPK activation pathway. For instance, Yibcharoenporn *et al.* used a series of synthetic chalcone derivatives for biological testing of antidiarrheal activity through CFTR Cl⁻ inhibition pathway in 2019.⁵³ After screening 27 compounds, **48** with A-ring as 2'-hydroxyacetophenone and B-ring bearing 2,4,5-trimethoxy groups was the most potent candidate that reversibly inhibited CFTR Cl⁻ channel secretion in T84 cells with IC₅₀ of approximately 1.5 μM (**Figure 1.13**). After that, electrophysiological and biochemical analyses were performed to explore how **48** was able to suppress the operation of CFTR Cl⁻ channel and AMPK activation pathway was the answer. Thereafter, it was found that **48** bound at the allosteric site of an upstream kinase calcium-calmodulin kinase kinase β (CaMKKβ) to activate AMPK which was measured by western blot analyses and molecular dynamics (MD). Therefore, **48** is considered as a persuasive model to further investigate structure-activity relationship of synthetic chalcone derivatives for AMPK activation activity.

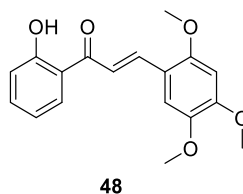


Figure 1.13 Chemical structure of **48**.

In this research, 2'-hydroxyacetophenone was used to combine with diverse benzaldehydes possessing different substituents on B-ring to prepare a series of chalcone derivatives for AMPK activation activity testing. From literature reviews, most chalcones as AMPK activator bearing 2'-hydroxy group on A-ring; for instance, **21**, **45-48** having 2'-hydroxy group along with other groups on A-ring demonstrated impressive activity to activate AMPK. It is thus believed that 2'-hydroxy group may be responsible for AMPK activation activity. In addition, chalcone with A-ring as 3',4',5'-trimethoxyacetophenone was reported to exhibit strong cytotoxicity and anti-inflammatory but there have been no literature reviews about AMPK activation activity of chalcones possessing this kind of A-ring; as a result, it was chosen for screening for the first time. Furthermore, other types of A-ring were also synthesized to compare their activity with 2'-hydroxy- and 3',4',5'-trimethoxychalcones. The substituents on B-ring can alter among mono-, di-, and trisubstitutions with various types of substituents such as hydroxyl, methoxy and so on. These chalcones were prepared to evaluate biological activity compared to chalcone **48** which was reported as AMPK activator.

1.4 The aim of this research

Chalcone is a privileged structure that expresses a broad variety of biological activities such as antidiabetic, anticancer, anti-inflammatory and so on. Thus, this core skeleton was selected to manipulate a series of products to evaluate AMPK activation activity. Chalcones bear two aromatic rings (A- and B-rings) with various substituents linked to each other by α,β -unsaturated ketone component.

A series of chalcone derivatives with A-ring bearing 2'-hydroxy-, 3',4',5'-trimethoxyacetophenones or other types was synthesized. The substituents on B-ring can be mono-, di- or trisubstitutions. The synthesized and characterized chalcones were submitted to evaluate for biological activity screening to analyse structure-activity relationship. Thereafter, the most potent compounds were selected for concentration-response relationship and EC_{50} values calculation. Compounds with the highest potency, lowest EC_{50} and cytotoxicity should be utilized for further study.



CHAPTER II

EXPERIMENTAL

A series of chalcones were mainly synthesized by Claisen-Schmidt reaction using acetophenones and benzaldehydes as two components. Many kinds of benzaldehydes and acetophenones with different substituents at various positions (mono/di/tri-substitution) on phenyl ring were reacted to form a wide range of products. In addition, etherification was performed between benzaldehydes with some hydroxy groups and alkyl bromides to obtain a number of benzaldehyde derivatives. Moreover, hydrogenation was conducted to achieve some dihydrochalcones. Totally 60 chalcones and related compounds were attained for biological testing.

2.1 Instruments

^1H and ^{13}C NMR spectra were performed in CDCl_3 , acetone- d_6 or DMSO- d_6 or otherwise stated and were recorded by using a Bruker Ultrashield 400 Plus NMR spectrometer or a Varian Mercury NMR spectrometer with an Oxford YH400 magnet operating at 400 MHz for ^1H and 100 MHz for ^{13}C . High-resolution mass spectra (HRMS) were recorded on a Bruker Daltonics microTOF using electron spray ionization (ESI).

2.2 General

All solvents used in this research were distilled prior to use except those which were reagent grades. Thin-layer chromatography (TLC) was performed on aluminum sheets precoated with silica gel (Merk Kieselgel 60 PF₂₅₄). Silica gel (No. 7734 and 9385, Merck) was used as stationary phase on open column chromatography.

2.3 Preparation of chalcones with monosubstitution on B-ring

The chalcone derivatives were prepared by Claisen-Schmidt reaction as previously reported with some modification.⁴ The corresponding acetophenone (1 equiv) and NaOH (3 equiv) in EtOH (3 mL for 1 mmol of acetophenone) were stirred at

room temperature for 10 min. Then the corresponding aldehyde (1 equiv) was added. The reaction mixture was proceeded at room temperature and monitored by TLC (usually 12-18 h). After that, HCl (10%) was added until pH 5 was obtained. In the situation that chalcones precipitated, they were collected by filtration and crystallization from MeOH. In other situations, the products were purified by utilizing silica gel chromatography. Nine chalcones (**25** and **49-56**) with mono-substitution on B-ring are described in **Figure 2.1**.

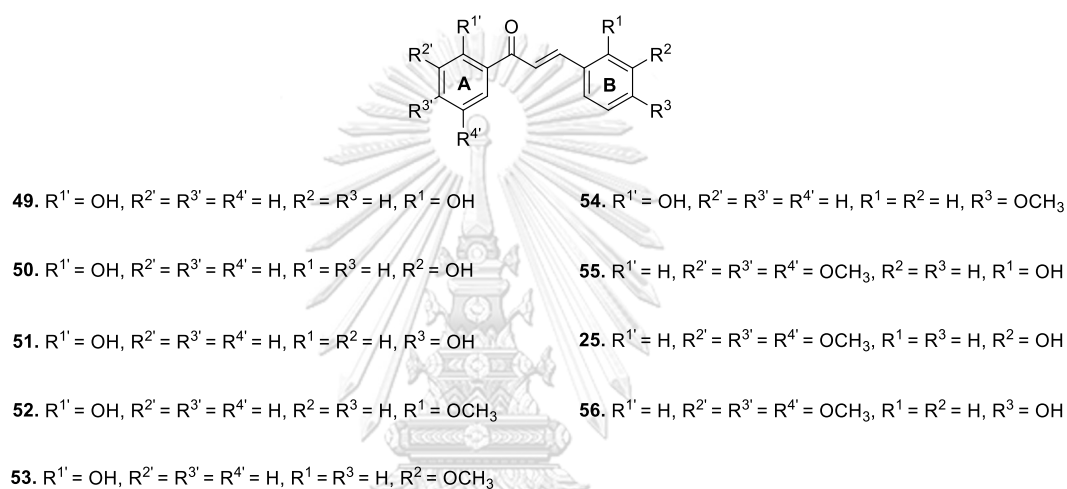


Figure 2.1 The structures of chalcones with monosubstitution on B-ring.

49 ((*E*)-1,3-bis(2-hydroxyphenyl)prop-2-en-1-one). ¹H NMR (acetone-*d*₆, 400 MHz): δ (ppm) 13.03 (s, 1H), 9.51 (s, 1H), 8.33 (d, *J* = 15.6 Hz, 1H), 8.19 (dd, *J* = 8.0, 1.2 Hz, 1H), 8.07 (d, *J* = 15.6 Hz, 1H), 7.85 (dd, *J* = 7.6, 1.2 Hz, 1H), 7.55 (td, *J* = 8.4, 1.6 Hz, 1H), 7.31 (td, *J* = 8.4, 1.6 Hz, 1H), 7.03 (d, *J* = 8.0 Hz, 1H), 6.99 (t, *J* = 7.2 Hz, 1H), 6.97 (t, *J* = 6.4 Hz, 1H), 6.92 (d, *J* = 7.2 Hz, 1H). ¹³C NMR (acetone-*d*₆, 100 MHz): δ (ppm) 195.1, 164.2, 158.2, 141.8, 136.9, 133.0, 130.9, 130.1, 122.5, 120.8, 120.7, 120.5, 119.5, 118.7, 117.0.

50 ((*E*)-1-(2-hydroxyphenyl)-3-(3-hydroxyphenyl)prop-2-en-1-one). ¹H NMR (CDCl₃, 400 MHz): δ (ppm) 12.79 (s, 1H), 7.92 (d, *J* = 8.0 Hz, 1H), 7.86 (d, *J* = 15.6 Hz, 1H), 7.63 (d, *J* = 15.6 Hz, 1H), 7.51 (t, *J* = 8.0 Hz, 1H), 7.31 (t, *J* = 7.6 Hz, 1H), 7.24 (d, *J* = 7.6 Hz, 1H), 7.14 (s, 1H), 7.04 (d, *J* = 8.0 Hz, 1H), 6.95 (t, *J* = 7.6 Hz, 1H), 6.92 (d, *J* =

7.6 Hz, 1H). ^{13}C NMR (CDCl_3 , 100 MHz): δ (ppm) 193.9, 163.7, 156.2, 145.2, 136.6, 136.4, 130.4, 129.8, 121.7, 120.8, 120.2, 119.1, 118.8, 118.2, 115.0.

51 ((*E*)-1-(2-hydroxyphenyl)-3-(4-hydroxyphenyl)prop-2-en-1-one). ^1H NMR (acetone- d_6 , 400 MHz): δ (ppm) 13.08 (s, 1H), 9.27 (s, 1H), 8.23 (dd, $J = 8.4, 1.6$ Hz, 1H), 7.91 (d, $J = 15.6$, 1H), 7.85 (d, $J = 15.2$ Hz, 1H), 7.77 (d, $J = 8.8$ Hz, 2H), 7.54 (td, $J = 8.4, 1.6$ Hz, 1H), 6.96 (m, 4H). ^{13}C NMR (acetone- d_6 , 100 MHz): δ (ppm) 194.7, 164.3, 161.3, 146.5, 136.8, 131.9, 130.9, 127.1, 120.8, 119.5, 118.7, 117.8, 116.7.

52 ((*E*)-1-(2-hydroxyphenyl)-3-(2-methoxyphenyl)prop-2-en-1-one). ^1H NMR (CDCl_3 , 400 MHz): δ (ppm) 12.95 (s, 1H), 8.23 (d, $J = 15.6$ Hz, 1H), 7.92 (dd, $J = 8.0, 1.2$ Hz, 1H), 7.78 (d, $J = 15.6$ Hz, 1H), 7.65 (dd, $J = 7.6, 0.8$ Hz, 1H), 7.49 (td, $J = 8.4, 1.2$ Hz, 1H), 7.40 (td, $J = 8.4, 1.2$ Hz, 1H), 7.03 (d, $J = 8.4$ Hz, 1H), 7.02 (t, $J = 8.0$ Hz, 1H), 6.96 (d, $J = 8.0$ Hz, 1H), 6.94 (t, $J = 7.6$ Hz, 1H), 3.94 (s, 3H). ^{13}C NMR (CDCl_3 , 100 MHz): δ (ppm) 194.5, 163.7, 159.2, 141.3, 136.2, 132.3, 129.8, 129.7, 123.8, 121.0, 120.9, 120.4, 118.9, 118.7, 111.5, 55.7.

53 ((*E*)-1-(2-hydroxyphenyl)-3-(3-methoxyphenyl)prop-2-en-1-one). ^1H NMR (CDCl_3 , 400 MHz): δ (ppm) 12.83 (s, 1H), 7.94 (d, $J = 8.4$ Hz, 1H), 7.91 (d, $J = 16.0$ Hz, 1H), 7.66 (d, $J = 15.6$ Hz, 1H), 7.53 (td, $J = 8.0, 1.2$ Hz, 1H), 7.38 (t, $J = 7.6$ Hz, 1H), 7.29 (d, $J = 7.2$ Hz, 1H), 7.19 (s, 1H), 7.06 (d, $J = 8.4$ Hz, 1H), 7.01 (dd, $J = 8.4, 2.0$ Hz, 1H), 6.97 (t, $J = 7.6$ Hz, 1H), 3.89 (s, 3H). ^{13}C NMR (CDCl_3 , 100 MHz): δ (ppm) 193.7, 163.6, 160.0, 145.4, 136.4, 136.0, 130.0, 129.7, 121.3, 120.5, 120.0, 118.8, 118.6, 116.6, 113.8, 55.4.

54 ((*E*)-1-(2-hydroxyphenyl)-3-(4-methoxyphenyl)prop-2-en-1-one). ^1H NMR (CDCl_3 , 400 MHz): δ (ppm) 12.95 (s, 1H), 7.91 (dd, $J = 8.0, 1.2$ Hz, 1H), 7.90 (d, $J = 15.6$ Hz, 1H), 7.62 (d, $J = 8.0$ Hz, 2H), 7.53 (d, $J = 15.2$ Hz, 1H), 7.48 (td, $J = 8.4, 1.6$ Hz, 1H), 7.02 (d, $J = 8.4$ Hz, 1H), 6.95 (d, $J = 8.8$ Hz, 2H), 6.94 (t, $J = 7.6$ Hz, 1H), 3.86 (s, 3H). ^{13}C NMR (CDCl_3 , 100 MHz): δ (ppm) 193.8, 163.7, 162.2, 145.5, 136.2, 130.6, 129.6, 127.5, 120.3, 118.9, 118.7, 117.8, 114.6, 55.6.

55 ((*E*)-3-(2-hydroxyphenyl)-1-(3,4,5-trimethoxyphenyl)prop-2-en-1-one). ^1H NMR (CDCl_3 , 400 MHz): δ (ppm) 8.20 (d, $J = 16.0$ Hz, 1H), 7.72 (s, 1H), 7.64 (d, $J = 16.0$ Hz, 1H), 7.58 (dd, $J = 8.0, 1.2$ Hz, 1H), 7.29 (s, 2H), 7.25 (t, $J = 8.0, 1.6$ Hz, 1H), 6.96 (d, $J = 8.4$ Hz, 1H), 6.92 (t, $J = 8.0$ Hz, 1H), 3.93 (s, 3H), 3.91 (s, 6H). ^{13}C NMR (CDCl_3 , 100 MHz): δ (ppm) 191.3, 156.5, 153.2, 142.6, 141.6, 133.7, 132.0, 129.5, 122.5, 122.3, 120.7, 116.8, 106.6, 61.1, 56.5.

25 ((*E*)-3-(3-hydroxyphenyl)-1-(3,4,5-trimethoxyphenyl)prop-2-en-1-one). ^1H NMR ($\text{DMSO}-d_6$, 400 MHz): δ (ppm) 9.64 (s, 1H), 7.85 (d, $J = 15.6$ Hz, 1H), 7.65 (d, $J = 15.2$ Hz, 1H), 7.42 (s, 2H), 7.32 (d, $J = 7.6$ Hz, 1H), 7.26 (m, 2H), 6.88 (dd, $J = 7.6, 1.6$ Hz, 1H), 3.90 (s, 6H), 3.76 (s, 3H). ^{13}C NMR ($\text{DMSO}-d_6$, 100 MHz): δ (ppm) 187.9, 157.7, 152.9, 144.1, 142.0, 136.0, 133.0, 129.8, 121.8, 120.0, 117.7, 115.3, 106.2, 60.1, 56.2.

56 ((*E*)-3-(4-hydroxyphenyl)-1-(3,4,5-trimethoxyphenyl)prop-2-en-1-one). ^1H NMR ($\text{DMSO}-d_6$, 400 MHz): δ (ppm) 10.10 (s, 1H), 7.75 (d, $J = 8.4$ Hz, 2H), 7.73 (d, $J = 14.8$ Hz, 1H), 7.68 (d, $J = 15.2$ Hz, 1H), 7.39 (s, 2H), 6.84 (d, $J = 8.4$ Hz, 2H), 3.89 (s, 6H), 3.76 (s, 3H). ^{13}C NMR ($\text{DMSO}-d_6$, 100 MHz): δ (ppm) 187.8, 160.1, 152.9, 144.3, 141.8, 133.4, 131.1, 125.9, 118.4, 115.8, 106.0, 60.2, 56.2.

2.4 Preparation of chalcones with disubstitution (OH, OCH_3 and OCH_2O) on B-ring

Following the procedure described in part **2.3**, twelve chalcones with one hydroxy along with one methoxy, dimethoxy, and methylenedioxy at various positions on B-ring (**57-68**) were prepared (**Figure 2.2**). Among the products, **59** is a new compound with HR-MS data shown below.

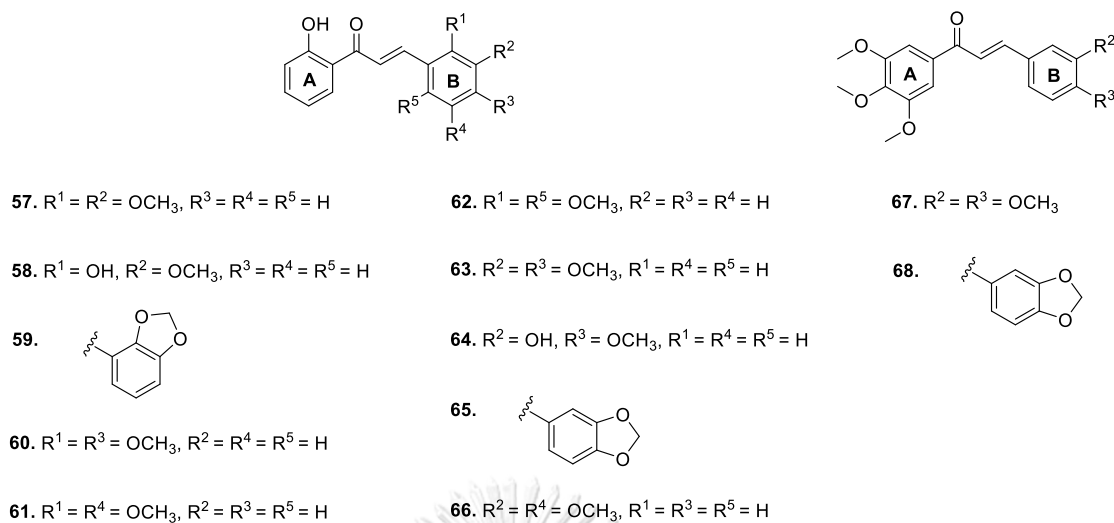


Figure 2.2 The structures of chalcones with hydroxyl, methoxy, and methylenedioxy on B-ring.

57 ((*E*)-3-(2,3-dimethoxyphenyl)-1-(2-hydroxyphenyl)prop-2-en-1-one). ^1H NMR (CDCl_3 , 400 MHz): δ (ppm) 12.88 (s, 1H), 8.20 (d, $J = 15.6$ Hz, 1H), 7.90 (d, $J = 8.0$ Hz, 1H), 7.73 (d, $J = 15.6$ Hz, 1H), 7.48 (t, $J = 8.0$ Hz, 1H), 7.27 (d, $J = 7.6$ Hz, 1H), 7.09 (t, $J = 8.0$ Hz, 1H), 7.01 (d, $J = 8.4$ Hz, 1H), 6.97 (d, $J = 8.0$ Hz, 1H), 6.92 (t, $J = 8.0$ Hz, 1H), 3.90 (s, 3H), 3.88 (s, 3H). ^{13}C NMR (CDCl_3 , 100 MHz): δ (ppm) 194.2, 163.7, 153.3, 149.3, 140.5, 136.3, 129.8, 128.8, 124.3, 121.7, 120.2, 120.0, 118.9, 118.6, 114.8, 61.4, 56.0.

58 ((*E*)-3-(2-hydroxy-3-methoxyphenyl)-1-(2-hydroxyphenyl)prop-2-en-1-one). ^1H NMR (CDCl_3 , 400 MHz): δ (ppm) 12.94 (s, 1H), 8.14 (d, $J = 15.6$ Hz, 1H), 7.94 (d, $J = 7.6$ Hz, 1H), 7.92 (d, $J = 15.2$ Hz, 1H), 7.49 (t, $J = 7.6$ Hz, 1H), 7.20 (dd, $J = 6.8$, 1.6 Hz, 1H), 7.02 (d, $J = 8.4$ Hz, 1H), 6.94 (t, $J = 7.6$ Hz, 1H), 6.91 (t, $J = 8.0$ Hz, 1H), 6.90 (d, $J = 8.0$ Hz, 1H), 6.40 (s, 1H), 3.94 (s, 3H). ^{13}C NMR (CDCl_3 , 100 MHz): δ (ppm) 194.6, 163.7, 147.1, 146.3, 141.0, 136.3, 130.0, 129.7, 122.4, 121.8, 120.0, 119.9, 118.9, 118.7, 112.5, 56.4.

59 ((*E*)-3-(benzo[d][1,3]dioxol-4-yl)-1-(2-hydroxyphenyl)prop-2-en-1-one). ^1H NMR (CDCl_3 , 400 MHz): δ (ppm) 12.86 (s, 1H), 7.90 (dd, $J = 6.8$, 1.6 Hz, 1H), 7.89 (d, $J = 16.0$ Hz, 1H), 7.81 (d, $J = 15.2$ Hz, 1H), 7.49 (td, $J = 7.2$, 1.2 Hz, 1H), 7.01 (m, 2H), 6.94 (t,

$J = 7.6, 0.8$ Hz, 1H), 6.88 (d, $J = 4.4$ Hz, 2H), 6.14 (s, 2H). ^{13}C NMR (CDCl_3 , 100 MHz): δ (ppm) 194.2, 163.8, 148.2, 147.0, 140.1, 136.5, 129.9, 123.8, 123.1, 122.2, 120.2, 119.0, 118.7, 117.9, 110.5, 101.8. HR-MS (ESI) for $\text{C}_{16}\text{H}_{12}\text{O}_4\text{Na}$ $[\text{M}+\text{Na}]^+$ requires 291.06333 found 291.06270.

60 ((*E*)-3-(2,4-dimethoxyphenyl)-1-(2-hydroxyphenyl)prop-2-en-1-one). ^1H NMR (CDCl_3 , 400 MHz): δ (ppm) 13.11 (s, 1H), 8.16 (d, $J = 15.6$ Hz, 1H), 7.90 (d, $J = 8.0$ Hz, 1H), 7.67 (d, $J = 15.2$ Hz, 1H), 7.56 (d, $J = 8.8$ Hz, 1H), 7.46 (t, $J = 8.4$ Hz, 1H), 7.00 (d, $J = 8.4$ Hz, 1H), 6.91 (t, $J = 8.0$ Hz, 1H), 6.53 (dd, $J = 8.4, 2.0$ Hz, 1H), 6.46 (d, $J = 2.0$ Hz, 1H), 3.90 (s, 3H), 3.84 (s, 3H). ^{13}C NMR (CDCl_3 , 100 MHz): δ (ppm) 194.3, 163.7, 163.6, 160.8, 141.4, 135.9, 131.5, 129.7, 120.4, 118.7, 118.5, 118.2, 117.0, 105.8, 98.6, 55.7, 55.6.

61 ((*E*)-3-(2,5-dimethoxyphenyl)-1-(2-hydroxyphenyl)prop-2-en-1-one). ^1H NMR (CDCl_3 , 400 MHz): δ (ppm) 12.92 (s, 1H), 8.19 (d, $J = 15.6$ Hz, 1H), 7.92 (d, $J = 8.0$ Hz, 1H), 7.74 (d, $J = 15.6$ Hz, 1H), 7.49 (t, $J = 8.0$ Hz, 1H), 7.17 (s, 1H), 7.02 (d, $J = 8.4$ Hz, 1H), 6.96 (m, 2H), 6.90 (t, $J = 8.0$ Hz, 1H), 3.89 (s, 3H), 3.83 (s, 3H). ^{13}C NMR (CDCl_3 , 100 MHz): δ (ppm) 194.4, 163.7, 153.8, 153.7, 141.0, 136.3, 129.8, 124.4, 121.2, 120.3, 118.9, 118.7, 117.8, 114.4, 112.7, 56.3, 56.0.

62 ((*E*)-3-(2,6-dimethoxyphenyl)-1-(2-hydroxyphenyl)prop-2-en-1-one). ^1H NMR (CDCl_3 , 400 MHz): δ (ppm) 13.12 (s, 1H), 8.40 (d, $J = 15.6$ Hz, 1H), 8.15 (d, $J = 15.6$ Hz, 1H), 7.91 (dd, $J = 8.0, 1.2$ Hz, 1H), 7.47 (td, $J = 8.4, 1.6$ Hz, 1H), 7.32 (t, $J = 8.4$ Hz, 1H), 7.01 (dd, $J = 8.4, 0.8$ Hz, 1H), 6.93 (td, $J = 8.4, 1.2$ Hz, 1H), 6.60 (d, $J = 8.4$ Hz, 2H), 3.94 (s, 6H). ^{13}C NMR (CDCl_3 , 100 MHz): δ (ppm) 195.6, 163.7, 160.8, 136.6, 135.9, 132.2, 129.9, 122.9, 120.7, 118.7, 118.6, 112.9, 104.0, 56.1.

63 ((*E*)-3-(3,4-dimethoxyphenyl)-1-(2-hydroxyphenyl)prop-2-en-1-one). ^1H NMR (CDCl_3 , 400 MHz): δ (ppm) 12.92 (s, 1H), 7.92 (dd, $J = 8.0, 0.8$ Hz, 1H), 7.87 (d, $J = 15.6$ Hz, 1H), 7.51 (d, $J = 15.2$ Hz, 1H), 7.48 (td, $J = 7.2, 1.6$ Hz, 1H), 7.26 (dd, $J = 8.4, 1.6$ Hz, 1H), 7.16 (d, $J = 1.6$ Hz, 1H), 7.01 (d, $J = 8.4$ Hz, 1H), 6.94 (dd, $J = 7.2, 0.8$ Hz, 1H), 6.91 (t, $J = 8.4$ Hz, 1H), 3.96 (s, 3H), 3.93 (s, 3H). ^{13}C NMR (CDCl_3 , 100 MHz): δ (ppm) 193.7,

163.7, 152.0, 149.5, 145.8, 136.3, 129.6, 127.8, 123.7, 120.2, 118.8, 118.7, 118.0, 111.4, 110.6, 56.2.

64 ((*E*)-3-(3-hydroxy-4-methoxyphenyl)-1-(2-hydroxyphenyl)prop-2-en-1-one). ^1H NMR (CDCl_3 , 400 MHz): δ (ppm) 12.93 (s, 1H), 7.92 (d, $J = 8.0$ Hz, 1H), 7.87 (d, $J = 15.2$ Hz, 1H), 7.50 (d, $J = 15.2$ Hz, 1H), 7.48 (td, $J = 7.8, 1.6$ Hz, 1H), 7.25 (dd, $J = 8.0, 1.2$ Hz, 1H), 7.14 (s, 1H), 7.02 (d, $J = 8.4$ Hz, 1H), 6.97 (d, $J = 8.4$ Hz, 1H), 6.93 (t, $J = 7.2$ Hz, 1H), 6.04 (s, 1H), 3.97 (s, 3H). ^{13}C NMR (CDCl_3 , 100 MHz): δ (ppm) 193.8, 163.7, 148.9, 147.0, 146.0, 136.3, 129.7, 127.4, 123.8, 120.3, 118.9, 118.7, 117.7, 115.2, 110.5, 56.2.

65 ((*E*)-3-(benzo[d][1,3]dioxol-5-yl)-1-(2-hydroxyphenyl)prop-2-en-1-one). ^1H NMR (CDCl_3 , 400 MHz): δ (ppm) 12.92 (s, 1H), 7.91 (dd, $J = 8.0, 0.8$ Hz, 1H), 7.86 (d, $J = 15.2$ Hz, 1H), 7.51 (td, $J = 8.0, 1.6$ Hz, 1H), 7.50 (d, $J = 15.2$ Hz, 1H), 7.19 (d, $J = 1.2$ Hz, 1H), 7.16 (d, $J = 8.0$ Hz, 1H), 7.04 (d, $J = 8.0$ Hz, 1H), 6.95 (t, $J = 8.0$ Hz, 1H), 6.87 (d, $J = 8.0$ Hz, 1H), 6.05 (s, 2H). ^{13}C NMR (CDCl_3 , 100 MHz): δ (ppm) 193.6, 163.6, 150.3, 148.5, 145.3, 136.2, 129.5, 129.1, 125.7, 120.1, 118.8, 118.6, 118.0, 108.8, 106.8, 101.8.

66 ((*E*)-3-(3,5-dimethoxyphenyl)-1-(2-hydroxyphenyl)prop-2-en-1-one). ^1H NMR (CDCl_3 , 400 MHz): δ (ppm) 12.81 (s, 1H), 7.88 (d, $J = 7.6$ Hz, 1H), 7.79 (d, $J = 15.6$ Hz, 1H), 7.56 (d, $J = 15.2$ Hz, 1H), 7.47 (t, $J = 8.0$ Hz, 1H), 7.01 (d, $J = 8.4$ Hz, 1H), 6.92 (t, $J = 7.6$ Hz, 1H), 6.76 (s, 2H), 6.52 (s, 1H), 3.82 (s, 6H). ^{13}C NMR (CDCl_3 , 100 MHz): δ (ppm) 193.7, 163.6, 161.2, 145.5, 136.5, 136.4, 129.7, 120.6, 120.0, 118.9, 118.6, 106.7, 103.1, 55.5.

67 ((*E*)-3-(3,4-dimethoxyphenyl)-1-(3,4,5-trimethoxyphenyl)prop-2-en-1-one). ^1H NMR (CDCl_3 , 400 MHz): δ (ppm) 7.74 (d, $J = 15.6$ Hz, 1H), 7.31 (d, $J = 15.6$ Hz, 1H), 7.25 (s, 2H), 7.24 (dd, $J = 7.2, 1.6$ Hz, 1H), 7.13 (d, $J = 1.6$ Hz, 1H), 6.89 (d, $J = 8.0$ Hz, 1H), 3.93 (s, 9H), 3.92 (s, 6H). ^{13}C NMR (CDCl_3 , 100 MHz): δ (ppm) 189.5, 153.2, 151.6, 149.4, 145.0, 142.6, 133.9, 128.0, 123.0, 120.0, 111.3, 110.7, 106.3, 61.0, 56.6, 56.2, 56.1.

68 ((*E*)-3-(benzo[d][1,3]dioxol-5-yl)-1-(3,4,5-trimethoxyphenyl)prop-2-en-1-one). ^1H NMR (CDCl_3 , 400 MHz): δ (ppm) 7.74 (d, $J = 15.6$ Hz, 1H), 7.32 (d, $J = 15.6$ Hz, 1H),

7.26 (s, 2H), 7.17 (d, $J = 0.8$ Hz, 1H), 7.13 (dd, $J = 8.0, 1.2$ Hz, 1H), 6.85 (d, $J = 8.0$ Hz, 1H), 6.03 (s, 2H), 3.95 (s, 6H), 3.93 (s, 3H). ^{13}C NMR (CDCl_3 , 100 MHz): δ (ppm) 189.2, 153.3, 150.0, 148.6, 144.7, 142.6, 133.8, 129.5, 125.3, 119.9, 108.8, 106.8, 106.2, 101.8, 61.1, 56.5.

2.5 Preparation of chalcones with disubstitution with 4-OH group on B-ring

2.5.1 Preparation of chloromethyl methyl ether (MOMCl)

In the synthesizing process, it can be seen that chalcones bearing hydroxy group at position 2 or 4 on B-ring (**58**, **69** and **70**) were usually achieved in low yield, prolonging reaction time or even no product was observed (**Figure 2.3**). Therefore, in these cases, protecting groups such as MOM was used to inactivate the hydroxy group. The compounds with protecting groups were generally obtained in high yield so they could be utilized as compounds for biological testing or deprotection was performed to collect the first target chalcones in considerable yield.

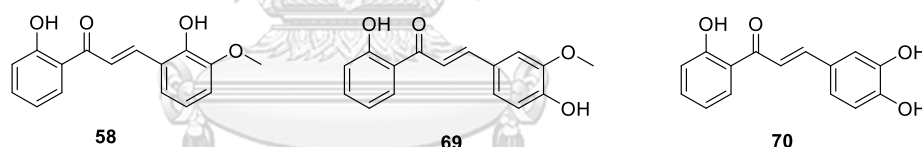


Figure 2.3 Chalcones with hydroxy substituents at position 2 or 4 on B-ring.

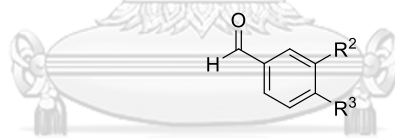
CHULALONGKORN UNIVERSITY

The first step is the preparation of protecting agent as MOM-Cl (**71**) using the method of Reggelin *et al.*⁵⁴ Because of the severe toxicity and tumorigenicity of **71**, the reaction must be carried out in a well-ventilated hood. A 1000 mL, two-necked, round-bottomed flask was charged with 140.6 g (1.0 mol, 1 equiv) benzoyl chloride, 76.1 g (1.0 mol, 1 equiv) dimethoxymethane and 5.0 g (51.0 mmol) conc H_2SO_4 . An Ar balloon was connected to the condenser and the flask was flushed with Ar briefly and then covered by a glass stopper. The mixture was stirred and refluxed in an oil bath at 60–65°C. After 64 h the reaction mixture was allowed to cool to room temperature. The reflux condenser was replaced by a distillation bridge equipped with a thermometer

and a balloon filled with Ar. After flushing with Ar again, the solution was heated stepwise up to 130°C to accumulate the product **71** in high yield (74%).

2.5.2 Preparation of benzaldehydes bearing protecting groups

The procedure for the synthesis of MOM-protected benzaldehydes was consulted from Kim *et al.*⁵⁵ A solution of 3,4-dihydroxybenzaldehyde (21.71 mmol) and K₂CO₃ (217.20 mmol) in acetone (100 mL) was cooled to 0°C under Ar atmosphere, and then MOM-Cl (93.65 mmol) was added dropwise. The resulting mixture was stirred at room temperature for 6-10 h. Then, the reaction mixture was diluted with water (100 mL) and extracted with EtOAc (50 mL × 3). After that, the combined organic layer was washed with water and brine, dried over anhydrous MgSO₄ and evaporated to dryness to yield crude MOM-protected benzaldehyde which was purified by silica gel column chromatography to give pure compounds **72** and **73** (Figure 2.4). For the case of aldehyde as vanillin, the amount of K₂CO₃, MOM-Cl were divided in half when the amount of vanillin was kept the same as 3,4-dihydroxybenzaldehyde since the vanillin molecule has only one hydroxy group.



72. R² = OCH₃, R³ = OCH₂OCH₃

73. R² = R³ = OCH₂OCH₃

Figure 2.4 Two benzaldehydes bearing protecting groups.

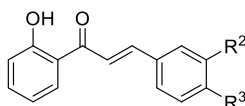
72 (3-methoxy-4-(methoxymethoxy)benzaldehyde). ¹H NMR (CDCl₃, 400 MHz): δ (ppm) 9.54 (s, 1H), 7.12 (s, 1H), 7.11 (d, *J* = 8.8 Hz, 1H), 6.93 (d, *J* = 8.8 Hz, 1H), 5.01 (s, 2H), 3.61 (s, 3H), 3.21 (s, 3H). ¹³C NMR (CDCl₃, 100 MHz): δ (ppm) 190.2, 151.4, 149.6, 130.6, 125.3, 114.4, 109.3, 94.4, 55.7, 55.2.

73 (3,4-bis(methoxymethoxy)benzaldehyde). ¹H NMR (CDCl₃, 400 MHz): δ (ppm) 9.80 (s, 1H), 7.62 (s, 1H), 7.45 (d, *J* = 8.0 Hz, 1H), 7.23 (d, *J* = 8.4 Hz, 1H), 5.27 (s, 2H),

5.24 (s, 2H), 3.47 (s, 6H). ^{13}C NMR (CDCl_3 , 100 MHz): δ (ppm) 190.8, 152.7, 147.5, 131.2, 126.3, 116.0, 115.5, 95.4, 95.0, 56.4, 56.3.

2.5.3 Preparation of chalcones bearing protecting groups and removal of protecting groups from chalcones

Also following the methodology from Kim *et al.*, two MOM-protected chalcones **74** and **75** and two deprotected chalcones **69** and **70** were prepared (Figure 2.5).⁵⁵ 2'-hydroxyacetophenone (1 mmol) and 5% sodium aqueous NaOH (1.1 mmol, 0.5 mL) in EtOH (10 mL) were stirred at room temperature for 10 min. Then the appropriate MOM-protected benzaldehyde (0.9 mmol) (**72** and **73**) was added. The reaction mixture was stirred at room temperature for 1 - 2 h. After checking the completion of the condensation reaction, HCl (10%) was added until pH 5 was obtained. If the target products are MOM-protected chalcones **74** and **75**, the reaction mixture should be filtered and crystallized from MeOH in case of precipitation of chalcones emerging or utilizing silica gel chromatography to purify the compounds. On the other hand, 10% HCl (1 mL) was added more and the mixture was further stirred for further 30 min at 60 °C to deprotect the MOM groups. And then the whole mixture was diluted with water (20 mL) and its pH was adjusted to 5 with 1N aqueous NaOH solution. After that, purifications were performed to achieve pure products **69** and **70**. Unfortunately, **75** could not be isolated because of its fast decomposition to **70**. Moreover, **74** is a new compound with the HR-MS data shown below.



69. $\text{R}^2 = \text{OCH}_3$, $\text{R}^3 = \text{OH}$ **74.** $\text{R}^2 = \text{OCH}_3$, $\text{R}^3 = \text{OCH}_2\text{OCH}_3$
70. $\text{R}^2 = \text{R}^3 = \text{OH}$ **75.** $\text{R}^2 = \text{R}^3 = \text{OCH}_2\text{OCH}_3$

Figure 2.5 Two chalcones bearing protecting groups and two deprotected chalcones.

69 ((*E*)-3-(4-hydroxy-3-methoxyphenyl)-1-(2-hydroxyphenyl)prop-2-en-1-one).

^1H NMR (CDCl_3 , 400 MHz): δ (ppm) 12.94 (s, 1H), 7.92 (d, $J = 7.6$ Hz, 1H), 7.87 (d, $J =$

15.2 Hz, 1H), 7.50 (d, $J = 14.4$ Hz, 1H), 7.48 (t, $J = 8.0$ Hz, 1H), 7.25 (d, $J = 8.0$ Hz, 1H), 7.14 (s, 1H), 7.02 (d, $J = 8.4$ Hz, 1H), 6.97 (d, $J = 8.4$ Hz, 1H), 6.94 (t, $J = 7.6$ Hz, 1H), 6.06 (s, 1H), 3.97 (s, 3H). ^{13}C NMR (CDCl_3 , 100 MHz): δ (ppm) 193.8, 163.7, 148.9, 147.0, 146.0, 136.3, 129.6, 127.4, 123.8, 120.3, 118.9, 118.7, 117.7, 115.1, 110.5, 56.2.

70 ((*E*)-3-(3,4-dihydroxyphenyl)-1-(2-hydroxyphenyl)prop-2-en-1-one). ^1H NMR (acetone- d_6 , 400 MHz): δ (ppm) 13.08 (s, 1H), 8.43 (s, 2H), 8.22 (dd, $J = 8.4, 1.6$ Hz, 1H), 7.85 (d, $J = 15.2$ Hz, 1H), 7.79 (d, $J = 15.2$ Hz, 1H), 7.53 (td, $J = 8.4, 1.6$ Hz, 1H), 7.40 (d, $J = 2.0$ Hz, 1H), 7.27 (dd, $J = 8.0, 2.0$ Hz, 1H), 6.97 (td, $J = 8.4, 1.2$ Hz, 1H), 6.96 (dd, $J = 8.4, 1.2$ Hz, 1H), 6.93 (d, $J = 8.0$ Hz, 1H). ^{13}C NMR (Acetone- d_6 , 100 MHz): δ (ppm) 194.8, 164.4, 149.6, 147.0, 146.4, 137.0, 131.1, 128.1, 123.9, 121.0, 119.7, 118.9, 118.1, 116.5, 116.2.

74 ((*E*)-1-(2-hydroxyphenyl)-3-(3-methoxy-4-(methoxymethoxy)phenyl)prop-2-en-1-one). ^1H NMR (CDCl_3 , 400 MHz): δ (ppm) 12.91 (s, 1H), 7.93 (dd, $J = 8.0, 1.2$ Hz, 1H), 7.87 (d, $J = 15.6$ Hz, 1H), 7.51 (d, $J = 15.2$ Hz, 1H), 7.49 (td, $J = 7.8, 1.6$ Hz, 1H), 7.50 (s, 1H), 7.32 (dd, $J = 8.4, 2.0$ Hz, 1H), 7.02 (dd, $J = 8.0, 0.4$ Hz, 1H), 6.95 (td, $J = 8.0, 0.8$ Hz, 1H), 6.94 (d, $J = 8.4$ Hz, 1H), 5.30 (s, 2H), 3.94 (s, 3H), 3.56 (s, 3H). ^{13}C NMR (CDCl_3 , 100 MHz): δ (ppm) 193.8, 163.7, 152.6, 147.1, 145.6, 136.3, 129.8, 128.0, 125.0, 120.3, 118.9, 118.7, 118.3, 115.8, 111.9, 95.8, 56.5, 56.2. HR-MS (ESI) for $\text{C}_{18}\text{H}_{18}\text{O}_5\text{Na}$ $[\text{M}+\text{Na}]^+$ requires 337.10519 found 337.10480.

2.6 Preparation of chalcones with 3,4-disubstitution on B-ring

2.6.1 Preparation of benzaldehydes with 3,4-disubstitution

The synthesis of benzaldehyde derivatives was performed following the Matsuda *et al.* method.⁵⁶ The stirred mixture of phenolic compounds (1 equiv) and excess K_2CO_3 in acetone (2.5 mL for 1 mmol of acetophenone) was added slowly by alkyl chloride (1.5 equiv for 1 hydroxy group). The reaction mixture was stirred at 80 °C for 24 h and then diluted with water and extracted with EtOAc. The organic layer

was washed with brine, dried over Na_2SO_4 and concentrated by rotary evaporator. The residue was purified by silica gel column chromatography to give the target compound. Lastly, twelve benzaldehydes **76–87** with different substitutions at positions 3 and 4 are described below (Figure 2.6).

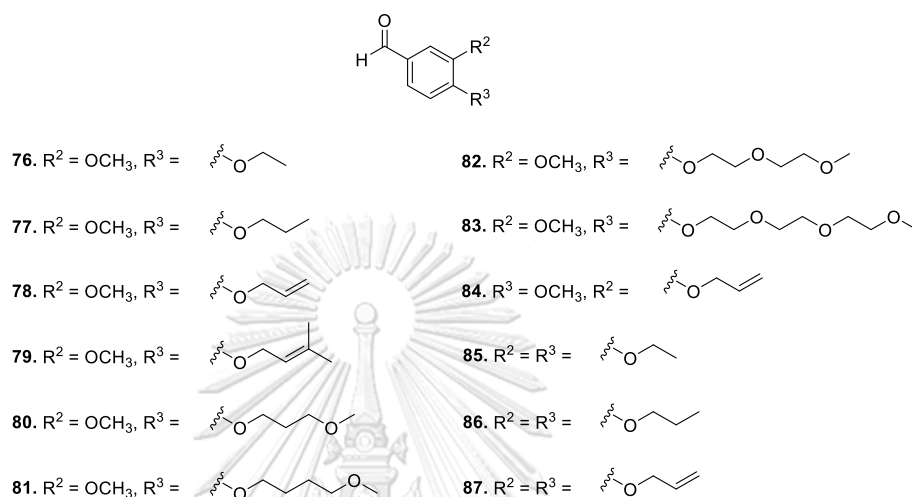


Figure 2.6 Benzaldehydes with 3,4-disubstitution.

76 (4-ethoxy-3-methoxybenzaldehyde). ^1H NMR (CDCl_3 , 400 MHz): δ (ppm) 9.75 (s, 1H), 7.34 (d, $J = 8.4$ Hz, 1H), 7.32 (s, 1H), 6.88 (d, $J = 8.0$ Hz, 1H), 4.10 (tetra, $J = 6.4$ Hz, 2H), 3.84 (s, 3H) 1.42 (t, $J = 7.2$ Hz, 3H). ^{13}C NMR (CDCl_3 , 100 MHz): δ (ppm) 190.7, 153.9, 149.7, 129.9, 126.6, 111.3, 109.2, 64.5, 55.9, 14.5.

77 (3-methoxy-4-propoxybenzaldehyde). ^1H NMR (CDCl_3 , 400 MHz): δ (ppm) 9.84 (s, 1H), 7.43 (dd, $J = 8.0, 2.0$ Hz, 1H), 7.40 (d, $J = 1.6$ Hz, 1H), 6.96 (d, $J = 8.4$ Hz, 1H), 4.06 (t, $J = 6.8$ Hz, 2H), 3.92 (s, 3H), 1.90 (sextet, $J = 7.2$ Hz, 2H) 1.06 (t, $J = 7.6$ Hz, 3H). ^{13}C NMR (CDCl_3 , 100 MHz): δ (ppm) 191.0, 154.4, 150.1, 130.1, 126.9, 111.6, 109.6, 70.8, 56.2, 22.4, 10.5.

78 (4-allyloxy)-3-methoxybenzaldehyde). ^1H NMR (CDCl_3 , 400 MHz): δ (ppm) 9.85 (s, 1H), 7.43 (d, $J = 6.4$ Hz, 1H), 7.42 (s, 1H), 6.98 (d, $J = 8.8$ Hz, 1H), 6.08 (ddt, $J = 16.4, 10.8, 5.2$ Hz, 1H), 5.44 (d, $J = 17.2$ Hz, 1H), 5.34 (d, $J = 10.4$ Hz, 1H), 4.71 (d, $J = 5.6$

Hz, 2H) 3.94 (s, 3H). ^{13}C NMR (CDCl_3 , 100 MHz): δ (ppm) 191.0, 153.7, 132.4, 130.4, 126.7, 124.4, 118.9, 112.2, 109.6, 70.0, 56.2.

79 (3-methoxy-4-((3-methylbut-2-en-1-yl)oxy)benzaldehyde). ^1H NMR (CDCl_3 , 400 MHz): δ (ppm) 9.80 (s, 1H), 7.39 (dd, $J = 8.4, 2.0$ Hz, 1H), 7.36 (d, $J = 1.6$ Hz, 1H), 6.93 (d, $J = 8.4$ Hz, 1H), 5.47 (tt, $J = 6.8, 1.2$ Hz, 1H), 4.63 (d, $J = 6.8$ Hz, 2H), 3.88 (s, 3H), 1.75 (s, 3H), 1.72 (s, 3H). ^{13}C NMR (CDCl_3 , 100 MHz): δ (ppm) 190.9, 154.0, 150.0, 138.7, 130.0, 126.7, 119.0, 111.8, 109.3, 66.0, 56.0, 25.8, 18.3.

82 (3-methoxy-4-(2-(2-methoxyethoxy)ethoxy)benzaldehyde). ^1H NMR (acetone- d_6 , 400 MHz): δ (ppm) 9.81 (s, 1H), 7.47 (d, $J = 7.6$ Hz, 1H), 7.38 (s, 1H), 7.08 (d, $J = 8.0$ Hz, 1H), 4.21 (t, $J = 4.6$ Hz, 2H), 3.86 (s, 3H), 3.84 (t, $J = 5.2$ Hz, 2H), 3.64 (t, $J = 4.4$ Hz, 2H), 3.48 (t, $J = 4.8$ Hz, 2H), 3.28 (s, 3H). ^{13}C NMR (acetone- d_6 , 100 MHz): δ (ppm) 190.2, 153.2, 149.0, 129.5, 125.2, 111.3, 109.0, 70.9, 69.5, 68.3, 67.7, 57.2, 54.6.

83 (3-methoxy-4-(2-(2-(2-methoxyethoxy)ethoxy)ethoxy)benzaldehyde). ^1H NMR (acetone- d_6 , 400 MHz): δ (ppm) 9.83 (s, 1H), 7.48 (dd, $J = 8.0, 1.2$ Hz, 1H), 7.39 (d, $J = 1.6$ Hz, 1H), 7.10 (d, $J = 8.0$ Hz, 1H), 4.22 (t, $J = 4.4$ Hz, 2H), 3.87 (s, 3H), 3.85 (t, $J = 4.8$ Hz, 2H), 3.66 (t, $J = 4.8$ Hz, 2H), 3.58 (t, $J = 4.8$ Hz, 2H), 3.56 (t, $J = 5.0$ Hz, 2H), 3.45 (t, $J = 4.6$ Hz, 2H), 3.26 (s, 3H). ^{13}C NMR (acetone- d_6 , 100 MHz): δ (ppm) 190.9, 154.2, 150.1, 130.6, 126.1, 112.4, 110.1, 72.0, 70.8, 70.5, 70.4, 69.4, 68.7, 58.2, 55.4.

84 (3-(allyloxy)-4-methoxybenzaldehyde). ^1H NMR (CDCl_3 , 400 MHz): δ (ppm) 9.63 (s, 1H), 7.25 (dd, $J = 8.4, 1.6$ Hz, 1H), 7.20 (s, 1H), 6.78 (d, $J = 8.4$ Hz, 1H), 5.90 (ddt, $J = 16.0, 10.4, 5.2$ Hz, 1H), 5.26 (d, $J = 17.2$ Hz, 1H), 5.12 (d, $J = 10.4$ Hz, 1H), 4.44 (d, $J = 4.8$ Hz, 2H) 3.73 (s, 3H). ^{13}C NMR (CDCl_3 , 100 MHz): δ (ppm) 190.3, 154.5, 148.1, 132.3, 129.6, 126.2, 117.8, 110.7, 110.4, 69.2, 55.6.

85 (3,4-diethoxybenzaldehyde). ^1H NMR (CDCl_3 , 400 MHz): δ (ppm) 9.80 (s, 1H), 7.39 (d, $J = 8.0$ Hz, 1H), 7.38 (s, 1H), 6.93 (d, $J = 8.4$ Hz, 1H), 4.16 (tetra, $J = 6.8$ Hz, 2H), 4.13 (tetra, $J = 6.8$ Hz, 2H), 1.47 (t, $J = 7.2$ Hz, 3H), 1.45 (t, $J = 7.2$ Hz, 3H). ^{13}C NMR

(CDCl₃, 100 MHz): δ (ppm) 191.0, 154.4, 149.2, 130.0, 126.6, 111.8, 111.0, 64.7, 64.6, 14.7, 14.6.

86 (3,4-dipropoxybenzaldehyde). ¹H NMR (CDCl₃, 400 MHz): δ (ppm) 9.81 (s, 1H), 7.40 (dd, J = 8.8, 1.6 Hz, 1H), 7.39 (s, 1H), 6.94 (d, J = 8.0 Hz, 1H), 4.03 (t, J = 6.8 Hz, 2H), 4.01 (t, J = 6.8 Hz, 2H), 1.87 (sextet, J = 7.2 Hz, 2H), 1.85 (sextet, J = 7.2 Hz, 2H), 1.05 (t, J = 7.2 Hz, 3H), 1.04 (t, J = 7.2 Hz, 3H). ¹³C NMR (CDCl₃, 100 MHz): δ (ppm) 191.1, 154.8, 149.6, 130.0, 126.6, 112.0, 111.4, 70.7, 22.6, 10.5.

87 (3,4-bis(allyloxy)benzaldehyde). ¹H NMR (CDCl₃, 400 MHz): δ (ppm) 9.60 (s, 1H), 7.19 (d, J = 8.0 Hz, 1H), 7.18 (s, 1H), 6.74 (d, J = 8.0 Hz, 1H), 5.85 (ddt, J = 16.0, 10.4, 5.2 Hz, 2H), 5.25 (d, J = 17.2 Hz, 2H), 5.09 (d, J = 9.6 Hz, 2H), 4.41 (d, J = 4.8 Hz, 4H). ¹³C NMR (CDCl₃, 100 MHz): δ (ppm) 190.1, 153.4, 148.3, 132.4, 132.1, 129.7, 125.8, 117.4, 117.2, 112.0, 111.2, 69.1, 69.0.

2.6.2 Preparation of chalcones with 3,4-disubstitution on B-ring

Also following the procedure described in part 2.3, twelve aldehydes **76–87** above were performed aldol condensation with 2'-hydroxyacetophenone to achieve twelve chalcones with 3,4-disubstitution on B-ring **88–99** (Figure 2.7). There are seven no-reported compounds and their HR-MS results are presented below.

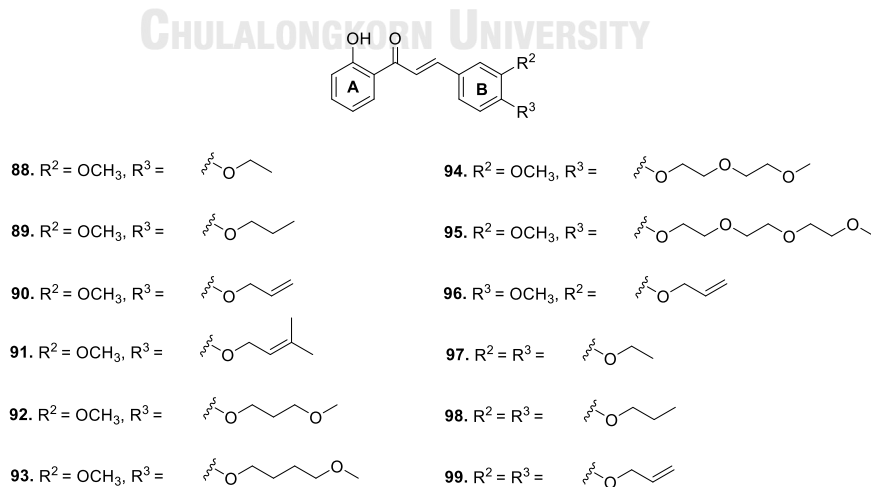


Figure 2.7 Chalcones with 3,4-disubstitution on B-ring.

88 ((*E*)-3-(4-ethoxy-3-methoxyphenyl)-1-(2-hydroxyphenyl)prop-2-en-1-one). ^1H NMR (CDCl_3 , 400 MHz): δ (ppm) 12.92 (s, 1H), 7.93 (dd, $J = 8.0, 1.6$ Hz, 1H), 7.89 (d, $J = 15.2$ Hz, 1H), 7.52 (d, $J = 15.6$ Hz, 1H), 7.49 (td, $J = 8.8, 1.6$ Hz, 1H), 7.25 (dd, $J = 8.4, 2.0$ Hz, 1H), 7.18 (d, $J = 1.6$ Hz, 1H), 7.03 (d, $J = 8.0$ Hz, 1H), 6.94 (td, $J = 8.0, 0.8$ Hz, 1H), 6.91 (d, $J = 8.4$ Hz, 1H), 4.17 (tetra, $J = 7.2$ Hz, 2H), 3.96 (s, 3H), 1.50 (t, $J = 7.2$ Hz, 3H). ^{13}C NMR (CDCl_3 , 100 MHz): δ (ppm) 193.8, 163.7, 151.5, 149.7, 145.9, 136.3, 129.7, 127.6, 123.7, 120.3, 118.9, 118.8, 117.9, 112.5, 111.0, 64.6, 56.3, 14.8.

89 ((*E*)-1-(2-hydroxyphenyl)-3-(3-methoxy-4-propoxyphenyl)prop-2-en-1-one). ^1H NMR (CDCl_3 , 400 MHz): δ (ppm) 12.96 (s, 1H), 7.91 (dd, $J = 8.4, 1.6$ Hz, 1H), 7.85 (d, $J = 15.2$ Hz, 1H), 7.49 (d, $J = 15.2$ Hz, 1H), 7.45 (td, $J = 8.4, 1.6$ Hz, 1H), 7.21 (dd, $J = 8.4, 2.0$ Hz, 1H), 7.15 (d, $J = 2.0$ Hz, 1H), 7.00 (dd, $J = 8.4, 0.8$ Hz, 1H), 6.90 (td, $J = 8.0, 0.8$ Hz, 1H), 6.87 (d, $J = 8.4$ Hz, 1H), 4.00 (t, $J = 6.8$ Hz, 2H), 3.92 (s, 3H), 1.88 (sextet, $J = 7.6$ Hz, 2H), 1.04 (t, $J = 7.6$ Hz, 3H). ^{13}C NMR (CDCl_3 , 100 MHz): δ (ppm) 193.6, 163.6, 151.6, 149.7, 145.8, 136.1, 129.6, 127.4, 123.6, 120.1, 118.7, 118.6, 117.6, 112.5, 111.0, 70.5, 56.2, 22.4, 10.4. HR-MS (ESI) for $\text{C}_{19}\text{H}_{20}\text{O}_4\text{Na}$ $[\text{M}+\text{Na}]^+$ requires 335.12593 found 335.12410.

90 ((*E*)-3-(4-(allyloxy)-3-methoxyphenyl)-1-(2-hydroxyphenyl)prop-2-en-1-one). ^1H NMR (CDCl_3 , 400 MHz): δ (ppm) 12.93 (s, 1H), 7.91 (d, $J = 8.0$ Hz, 1H), 7.85 (d, $J = 15.6$ Hz, 1H), 7.50 (d, $J = 15.2$ Hz, 1H), 7.47 (t, $J = 8.0$ Hz, 1H), 7.21 (d, $J = 8.4$ Hz, 1H), 7.16 (s, 1H), 7.00 (d, $J = 8.4$ Hz, 1H), 6.93 (d, $J = 8.0$ Hz, 1H), 6.90 (t, $J = 8.0$ Hz, 1H), 6.08 (ddt, $J = 16, 10.8, 5.6$ Hz, 1H), 5.42 (d, $J = 16.8$ Hz, 1H), 5.32 (d, $J = 10.4$ Hz, 1H), 4.65 (d, $J = 5.6$ Hz, 1H), 3.94 (s, 3H). ^{13}C NMR (CDCl_3 , 100 MHz): δ (ppm) 193.6, 163.6, 151.0, 149.8, 145.7, 136.2, 132.8, 129.6, 127.9, 123.4, 120.2, 118.8, 118.6, 118.5, 118.0, 113.1, 111.0, 69.8, 56.2.

91 ((*E*)-1-(2-hydroxyphenyl)-3-(3-methoxy-4-((3-methylbut-2-en-1-yl)oxy)phenyl)prop-2-en-1-one). ^1H NMR (CDCl_3 , 400 MHz): δ (ppm) 12.93 (s, 1H), 7.93 (d, $J = 8.0$ Hz, 1H), 7.88 (d, $J = 15.2$ Hz, 1H), 7.51 (d, $J = 15.6$ Hz, 1H), 7.48 (t, $J = 7.2$ Hz,

1H), 7.24 (dd, $J = 8.4, 1.6$ Hz, 1H), 7.17 (s, 1H), 7.02 (d, $J = 8.4$ Hz, 1H), 6.94 (t, $J = 8.0$ Hz, 1H), 6.92 (d, $J = 8.4$ Hz, 1H), 5.52 (t, $J = 6$ Hz, 1H), 4.65 (d, $J = 6.4$ Hz, 2H), 3.95 (s, 3H), 1.79 (s, 3H), 1.76 (s, 3H). ^{13}C NMR (CDCl_3 , 100 MHz): δ (ppm) 193.8, 163.7, 151.4, 149.9, 145.9, 138.4, 136.2, 129.7, 127.6, 123.6, 120.3, 119.5, 118.8, 118.7, 117.8, 112.9, 110.8, 66.0, 56.2, 25.9, 18.4.

92 ((*E*)-1-(2-hydroxyphenyl)-3-(3-methoxy-4-(3-methoxypropoxy)phenyl)prop-2-en-1-one). ^1H NMR (CDCl_3 , 400 MHz): δ (ppm) 12.95 (s, 1H), 7.90 (d, $J = 7.6$ Hz, 1H), 7.84 (d, $J = 15.2$ Hz, 1H), 7.48 (d, $J = 15.2$ Hz, 1H), 7.44 (t, $J = 7.2$ Hz, 1H), 7.21 (d, $J = 8.0$ Hz, 1H), 7.14 (s, 1H), 6.98 (d, $J = 8.4$ Hz, 1H), 6.90 (d, $J = 8.0$ Hz, 1H), 6.89 (t, $J = 6.8$ Hz, 1H), 4.14 (t, $J = 6.4$ Hz, 2H), 3.91 (s, 3H), 3.55 (t, $J = 6.0$ Hz, 2H), 3.34 (s, 3H), 2.10 (p, $J = 6.0$ Hz, 2H). ^{13}C NMR (CDCl_3 , 100 MHz): δ (ppm) 193.6, 163.6, 151.5, 149.7, 145.7, 136.1, 129.6, 127.6, 123.6, 120.2, 118.7, 118.6, 117.7, 112.7, 111.1, 69.1, 66.1, 58.7, 56.1, 29.5. HR-MS (ESI) for $\text{C}_{20}\text{H}_{22}\text{O}_5\text{Na}$ [$\text{M}+\text{Na}$] $^+$ requires 365.13649 found 365.13620.

93 ((*E*)-1-(2-hydroxyphenyl)-3-(3-methoxy-4-(4-methoxybutoxy)phenyl)prop-2-en-1-one). ^1H NMR (CDCl_3 , 400 MHz): δ (ppm) 12.93 (s, 1H), 7.92 (d, $J = 7.6$ Hz, 1H), 7.86 (d, $J = 15.2$ Hz, 1H), 7.50 (d, $J = 15.6$ Hz, 1H), 7.47 (t, $J = 7.6$ Hz, 1H), 7.23 (dd, $J = 8.0, 1.6$ Hz, 1H), 7.16 (s, 1H), 7.01 (d, $J = 8.4$ Hz, 1H), 6.92 (t, $J = 7.2$ Hz, 1H), 6.89 (d, $J = 8.4$ Hz, 1H), 4.09 (t, $J = 6.4$ Hz, 2H), 3.92 (s, 3H), 3.45 (t, $J = 6.0$ Hz, 2H), 3.34 (s, 3H), 1.93 (pentet, $J = 6.8$ Hz, 2H), 1.76 (pentet, $J = 6.4$ Hz, 2H). ^{13}C NMR (CDCl_3 , 100 MHz): δ (ppm) 193.7, 163.6, 151.6, 149.8, 145.8, 136.2, 129.6, 127.6, 123.7, 120.2, 118.8, 118.7, 117.8, 112.7, 111.2, 72.4, 68.9, 58.6, 56.2, 26.2, 26.0. HR-MS (ESI) for $\text{C}_{21}\text{H}_{24}\text{O}_5\text{Na}$ [$\text{M}+\text{Na}$] $^+$ requires 379.15214 found 379.15150.

94 ((*E*)-1-(2-hydroxyphenyl)-3-(3-methoxy-4-(2-(2-methoxyethoxy)ethoxy)phenyl)prop-2-en-1-one). ^1H NMR (CDCl_3 , 400 MHz): δ (ppm) 12.91 (s, 1H), 7.93 (d, $J = 8.0$ Hz, 1H), 7.87 (d, $J = 15.6$ Hz, 1H), 7.51 (d, $J = 15.6$ Hz, 1H), 7.49 (t, $J = 8.8$ Hz, 1H), 7.24 (d, $J = 8.4$ Hz, 1H), 7.16 (s, 1H), 7.02 (d, $J = 8.4$ Hz, 1H), 6.95 (d, $J = 8.0$ Hz, 1H), 6.94 (t, $J = 7.2$ Hz, 1H), 4.25 (t, $J = 4.8$ Hz, 2H), 3.93 (s, 3H), 3.92 (t, J

= 4.4 Hz, 2H), 3.73 (t, J = 4.4 Hz, 2H), 3.57 (t, J = 4.8 Hz, 2H), 3.39 (s, 3H). ^{13}C NMR (CDCl_3 , 100 MHz): δ (ppm) 193.7, 163.7, 151.4, 149.9, 145.7, 136.3, 129.7, 128.1, 123.5, 120.3, 118.8, 118.7, 118.1, 113.4, 111.4, 72.1, 71.0, 69.7, 68.6, 59.2, 56.3. HR-MS (ESI) for $\text{C}_{21}\text{H}_{24}\text{O}_6\text{Na}$ $[\text{M}+\text{Na}]^+$ requires 395.14706 found 395.14650.

95

((*E*)-1-(2-hydroxyphenyl)-3-(3-methoxy-4-(2-(2-(2-methoxyethoxy)ethoxy)ethoxy)ethoxy) phenyl)prop-2-en-1-one).

^1H NMR (CDCl_3 , 400 MHz): δ (ppm) 12.91 (s, 1H), 7.91 (d, J = 8.0 Hz, 1H), 7.84 (d, J = 15.2 Hz, 1H), 7.49 (d, J = 14.8 Hz, 1H), 7.46 (t, J = 7.6 Hz, 1H), 7.21 (d, J = 8.4 Hz, 1H), 7.14 (s, 1H), 6.99 (d, J = 8.0 Hz, 1H), 6.92 (d, J = 8.0 Hz, 1H), 6.91 (t, J = 7.6 Hz, 1H), 4.22 (t, J = 4.6 Hz, 2H), 3.91 (s, 3H), 3.89 (t, J = 4.8 Hz, 2H), 3.72 (t, J = 4.4 Hz, 2H), 3.66 (t, J = 4.8 Hz, 2H), 3.63 (t, J = 4.8 Hz, 2H), 3.52 (t, J = 4.8 Hz, 2H), 3.35 (s, 3H). ^{13}C NMR (CDCl_3 , 100 MHz): δ (ppm) 193.6, 163.6, 151.3, 149.8, 145.7, 136.2, 129.6, 128.0, 123.4, 120.2, 118.8, 118.6, 118.0, 113.2, 111.2, 72.0, 70.9, 70.7, 70.6, 69.5, 68.5, 59.0, 56.1. HR-MS (ESI) for $\text{C}_{23}\text{H}_{28}\text{O}_7\text{Na}$ $[\text{M}+\text{Na}]^+$ requires 439.17327 found 439.17360.

96 ((*E*)-3-(3-(allyloxy)-4-methoxyphenyl)-1-(2-hydroxyphenyl)prop-2-en-1-one).

^1H NMR (CDCl_3 , 400 MHz): δ (ppm) 12.92 (s, 1H), 7.91 (dd, J = 8.0, 1.6 Hz, 1H), 7.86 (d, J = 15.2 Hz, 1H), 7.49 (d, J = 15.2 Hz, 1H), 7.48 (t, J = 8.8 Hz, 1H), 7.27 (dd, J = 8.0, 1.6 Hz, 1H), 7.19 (s, 1H), 7.02 (d, J = 8.4 Hz, 1H), 6.93 (t, J = 7.6 Hz, 1H), 6.91 (d, J = 8.0 Hz, 1H), 6.10 (m, 1H), 5.46 (d, J = 17.2 Hz, 1H), 5.34 (d, J = 10.4 Hz, 1H), 4.68 (d, J = 5.6 Hz, 1H), 3.92 (s, 3H). ^{13}C NMR (CDCl_3 , 100 MHz): δ (ppm) 193.7, 163.7, 152.5, 148.4, 145.7, 136.2, 133.1, 129.6, 127.7, 123.8, 120.2, 118.8, 118.7, 118.4, 118.0, 113.1, 111.7, 70.2, 56.2.

97 ((*E*)-3-(3,4-diethoxyphenyl)-1-(2-hydroxyphenyl)prop-2-en-1-one).

^1H NMR (CDCl_3 , 400 MHz): δ (ppm) 12.93 (s, 1H), 7.93 (d, J = 8.0 Hz, 1H), 7.88 (d, J = 15.2 Hz, 1H), 7.50 (d, J = 15.2 Hz, 1H), 7.49 (t, J = 8.0 Hz, 1H), 7.25 (m, 1H), 7.20 (s, 1H), 7.03 (d, J = 8.4 Hz, 1H), 6.94 (t, J = 7.6 Hz, 1H), 6.89 (d, J = 8.4 Hz, 1H), 4.17 (q, J = 6.8 Hz, 2H), 4.16 (q, J = 6.8 Hz, 2H), 1.50 (t, J = 6.8 Hz, 3H), 1.49 (t, J = 7.2 Hz, 3H). ^{13}C NMR (CDCl_3 ,

100 MHz): δ (ppm) 193.8, 163.7, 154.4, 152.0, 146.0, 136.3, 129.7, 127.7, 123.8, 120.4, 118.9, 118.8, 117.8, 113.1, 113.0, 65.1, 64.7, 15.0, 14.8.

98 ((*E*)-3-(3,4-dipropoxyphenyl)-1-(2-hydroxyphenyl)prop-2-en-1-one). ^1H NMR (CDCl_3 , 400 MHz): δ (ppm) 12.97 (s, 1H), 7.92 (dd, $J = 8.0, 1.2$ Hz, 1H), 7.86 (d, $J = 15.2$ Hz, 1H), 7.49 (d, $J = 15.2$ Hz, 1H), 7.47 (t, $J = 8.4$ Hz, 1H), 7.22 (dd, $J = 8.0, 1.2$ Hz, 1H), 7.19 (s, 1H), 7.01 (d, $J = 8.4$ Hz, 1H), 6.93 (t, $J = 7.6$ Hz, 1H), 6.89 (d, $J = 8.0$ Hz, 1H), 4.03 (t, $J = 6.8$ Hz, 2H), 4.01 (t, $J = 6.8$ Hz, 2H), 1.88 (sextet, $J = 7.0$ Hz, 2H), 1.87 (sextet, $J = 7.2$ Hz, 2H), 1.08 (t, $J = 7.6$ Hz, 3H), 1.06 (t, $J = 7.6$ Hz, 3H). ^{13}C NMR (CDCl_3 , 100 MHz): δ (ppm) 193.7, 163.6, 152.3, 149.4, 145.9, 136.1, 129.6, 127.6, 123.8, 120.2, 118.8, 118.6, 117.7, 113.4, 113.2, 71.1, 70.6, 22.8, 22.6, 10.6, 10.5. HR-MS (ESI) for $\text{C}_{21}\text{H}_{24}\text{O}_4\text{Na}$ [$\text{M}+\text{Na}$] $^+$ requires 363.15723 found 363.15710.

99 ((*E*)-3-(3,4-bis(allyloxy)phenyl)-1-(2-hydroxyphenyl)prop-2-en-1-one). ^1H NMR (CDCl_3 , 400 MHz): δ (ppm) 12.91 (s, 1H), 7.91 (d, $J = 8.0$ Hz, 1H), 7.86 (d, $J = 15.2$ Hz, 1H), 7.49 (d, $J = 15.6$ Hz, 1H), 7.48 (t, $J = 8.8$ Hz, 1H), 7.25 (dd, $J = 9.2, 2.4$ Hz, 1H), 7.21 (s, 1H), 7.02 (d, $J = 8.4$ Hz, 1H), 6.94 (t, $J = 8.4$ Hz, 1H), 6.92 (d, $J = 8.4$ Hz, 1H), 6.10 (m, 2H), 5.47 (d, $J = 17.2$ Hz, 1H), 5.45 (d, $J = 17.2$ Hz, 1H), 5.33 (d, $J = 10.8$ Hz, 1H), 5.32 (d, $J = 10.4$ Hz, 1H), 4.68 (d, $J = 4.4$ Hz, 2H), 4.67 (d, $J = 5.2$ Hz, 2H). ^{13}C NMR (CDCl_3 , 100 MHz): δ (ppm) 193.7, 163.7, 151.6, 148.8, 145.7, 136.3, 133.3, 132.9, 129.6, 128.0, 123.8, 120.3, 118.9, 118.8, 118.2, 118.1, 118.0, 113.8, 113.7, 70.4, 69.9. HR-MS (ESI) for $\text{C}_{21}\text{H}_{20}\text{O}_4\text{Na}$ [$\text{M}+\text{Na}$] $^+$ requires 359.12593 found 359.12590.

2.7 Preparation of chalcones with 2,4,5-trisubstitution on B-ring

2.7.1 Preparation of 2'-hydroxychalcones with 2,4,5-trisubstitution on B-ring

Following the procedure illustrated in part 2.5.1, two benzaldehyde derivatives bearing 2,4,5-trisubstitution were attained (**100** and **101**) (Figure 2.8).

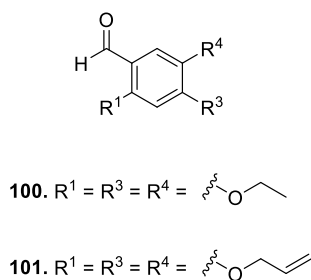


Figure 2.8 Benzaldehydes with 2,4,5-trisubstitution.

100 (2,4,5-triethoxybenzaldehyde). ^1H NMR (CDCl_3 , 400 MHz): δ (ppm) 10.32 (s, 1H), 7.32 (s, 1H), 6.47 (s, 1H), 4.15 (q, $J = 7.2$ Hz, 2H), 4.11 (q, $J = 6.8$ Hz, 2H), 4.08 (q, $J = 6.8$ Hz, 2H), 1.50 (t, $J = 7.2$ Hz, 3H), 1.45 (t, $J = 6.8$ Hz, 3H), 1.42 (t, $J = 7.2$ Hz, 3H). ^{13}C NMR (CDCl_3 , 100 MHz): δ (ppm) 188.4, 158.0, 153.2, 138.9, 111.3, 110.0, 98.5, 65.2, 65.1, 64.9, 14.9, 14.7.

101 (2,4,5-tris(allyloxy)benzaldehyde). ^1H NMR (CDCl_3 , 400 MHz): δ (ppm) 10.30 (s, 1H), 7.30 (s, 1H), 6.48 (s, 1H), 6.02 (m, 3H), 5.41 (dd, $J = 17.2, 1.2$ Hz, 1H), 5.39 (dd, $J = 17.2, 1.2$ Hz, 1H), 5.38 (dd, $J = 17.2, 1.2$ Hz, 1H), 5.30 (dd, $J = 10.4, 1.2$ Hz, 1H), 5.29 (dd, $J = 10.4, 1.2$ Hz, 1H), 5.24 (dd, $J = 10.4, 1.2$ Hz, 1H), 4.63 (d, $J = 5.2$ Hz, 2H), 4.56 (d, $J = 5.2$ Hz, 2H), 4.53 (d, $J = 5.2$ Hz, 2H). ^{13}C NMR (CDCl_3 , 100 MHz): δ (ppm) 187.9, 157.6, 155.3, 143.0, 133.1, 132.6, 132.4, 118.3, 118.2, 118.1, 117.9, 112.0, 99.5, 70.3, 70.2, 69.9.

Thereafter following the procedure described in part **2.3**, two benzaldehydes **100** and **101** were carried out Claisen-Schmidt reaction with 2'-hydroxyacetophenone to achieve two chalcones with 2,4,5-trisubstitution on B-ring **102** and **103** (**Figure 2.9**). Both chalcones are new compounds with the HR-MS results below.

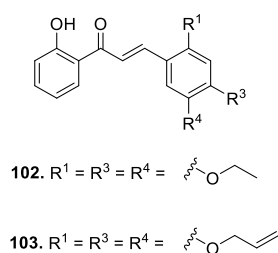


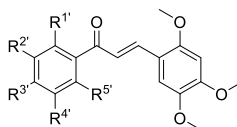
Figure 2.9 2'-Hydroxychalcones with 2,4,5-trisubstitution on B-ring.

102 ((*E*)-1-(2-hydroxyphenyl)-3-(2,4,5-triethoxyphenyl)prop-2-en-1-one). ^1H NMR (CDCl_3 , 400 MHz): δ (ppm) 13.10 (s, 1H), 8.16 (d, $J = 15.6$ Hz, 1H), 7.91 (d, $J = 8.0$ Hz, 1H), 7.70 (d, $J = 15.6$ Hz, 1H), 7.47 (td, $J = 7.6, 1.2$ Hz, 1H), 7.16 (s, 1H), 7.02 (d, $J = 8.4$ Hz, 1H), 6.93 (t, $J = 7.6$ Hz, 1H), 6.51 (s, 1H), 4.13 (m, 6H), 1.53 (t, $J = 7.2$ Hz, 3H), 1.49 (t, $J = 7.2$ Hz, 3H), 1.45 (t, $J = 7.2$ Hz, 3H). ^{13}C NMR (CDCl_3 , 100 MHz): δ (ppm) 194.4, 163.7, 155.0, 151.4, 141.5, 138.6, 135.9, 129.6, 120.2, 118.8, 118.7, 118.3, 116.0, 109.4, 99.4, 66.1, 65.1, 64.9, 15.2, 15.1, 14.9. HR-MS (ESI) for $\text{C}_{21}\text{H}_{24}\text{O}_5\text{Na}$ $[\text{M}+\text{Na}]^+$ requires 379.15214 found 379.1529.

103 ((*E*)-1-(2-hydroxyphenyl)-3-(2,4,5-tris(allyloxy)phenyl)prop-2-en-1-one). ^1H NMR ($\text{DMSO}-d_6$, 400 MHz): δ (ppm) 12.87 (s, 1H), 8.24 (d, $J = 8.0$ Hz, 1H), 8.20 (d, $J = 15.6$ Hz, 1H), 7.87 (d, $J = 15.2$ Hz, 1H), 7.61 (s, 1H), 7.55 (t, $J = 8.0$ Hz, 1H), 7.00 (t, $J = 7.6$ Hz, 1H), 6.98 (d, $J = 8.4$ Hz, 1H), 6.78 (s, 1H), 6.09 (m, 3H), 5.44 (d, $J = 17.2$ Hz, 3H), 5.32 (d, $J = 10.4$ Hz, 1H), 5.30 (d, $J = 11.2$ Hz, 1H), 5.27 (d, $J = 10.8$ Hz, 1H), 4.68 (d, $J = 4.8$ Hz, 4H), 4.62 (d, $J = 5.2$ Hz, 2H). ^{13}C NMR ($\text{DMSO}-d_6$, 100 MHz): δ (ppm) 193.6, 162.2, 153.6, 152.6, 142.2, 139.5, 136.0, 134.0, 133.4, 133.2, 130.5, 120.5, 118.9, 118.1, 118.0, 117.8, 117.7, 117.4, 114.9, 113.7, 100.2, 70.0, 69.6, 69.1. HR-MS (ESI) for $\text{C}_{24}\text{H}_{24}\text{O}_5\text{Na}$ $[\text{M}+\text{Na}]^+$ requires 415.15214 found 415.14970.

2.7.2 Preparation of chalcones with 2,4,5-trimethoxy substituents on B-ring

The procedure displayed in part 2.3 continues to apply for preparing eighteen chalcones **48**, **104-120** with 2,4,5-trimethoxybenzaldehydes (**Figure 2.10**). The ^1H and ^{13}C -NMR spectra of compound **107** have not received so this information is not shown. There are three new compounds prepared such as **113**, **114** and **119** with the HR-MS results below.



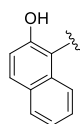
48. $R^1 = \text{OH}, R^2 = R^3 = R^4 = R^5 = \text{H}$ 110. $R^1 = \text{CF}_3, R^2 = R^3 = R^4 = R^5 = \text{H}$ 117. $R^1 = R^5 = \text{OCH}_3, R^2 = R^3 = R^4 = \text{H}$
104. $R^2 = \text{OH}, R^1 = R^3 = R^4 = R^5 = \text{H}$ 111. $R^1 = \text{OH}, R^3 = \text{OCH}_3, R^2 = R^3 = R^4 = \text{H}$ 118. $R^1 = \text{OH}, R^3 = R^5 = \text{OCH}_3, R^2 = R^4 = \text{H}$
105. $R^3 = \text{OH}, R^1 = R^2 = R^4 = R^5 = \text{H}$ 112. $R^1 = \text{OH}, R^5 = \text{OCH}_3, R^2 = R^3 = R^4 = \text{H}$ 119. $R^1 = \text{OH}, R^2 = R^4 = \text{Br}, R^3 = R^5 = \text{H}$
106. $R^1 = \text{OCH}_3, R^2 = R^3 = R^4 = R^5 = \text{H}$ 113. $R^1 = \text{OH}, R^3 = \text{Br}, R^2 = R^4 = R^5 = \text{H}$ 120. 
107. $R^2 = \text{OCH}_3, R^1 = R^3 = R^4 = R^5 = \text{H}$ 114. $R^1 = \text{OH}, R^4 = \text{Br}, R^2 = R^3 = R^5 = \text{H}$
108. $R^3 = \text{OCH}_3, R^1 = R^2 = R^4 = R^5 = \text{H}$ 115. $R^1 = R^3 = \text{OCH}_3, R^2 = R^4 = R^5 = \text{H}$

Figure 2.10 Chalcones with 2,4,5-trimethoxy on B-ring.

48 ((*E*)-1-(2-hydroxyphenyl)-3-(2,4,5-trimethoxyphenyl)prop-2-en-1-one). ^1H NMR (CDCl_3 , 400 MHz): δ (ppm) 13.07 (s, 1H), 8.20 (d, $J = 15.6$ Hz, 1H), 7.92 (dd, $J = 8.0, 1.2$ Hz, 1H), 7.61 (d, $J = 15.2$ Hz, 1H), 7.46 (td, $J = 8.4, 1.2$ Hz, 1H), 7.12 (s, 1H), 7.00 (dd, $J = 8.0, 0.8$ Hz, 1H), 6.92 (t, $J = 8.0, 0.8$ Hz, 1H), 6.52 (s, 1H), 3.95 (s, 3H), 3.92 (s, 3H), 3.91 (s, 3H). ^{13}C NMR (CDCl_3 , 100 MHz): δ (ppm) 194.2, 163.6, 155.3, 153.2, 143.5, 141.0, 136.0, 129.7, 120.4, 118.7, 118.6, 118.0, 115.4, 112.1, 97.0, 56.8, 56.5, 56.2.

104 ((*E*)-1-(3-hydroxyphenyl)-3-(2,4,5-trimethoxyphenyl)prop-2-en-1-one). ^1H NMR ($\text{acetone-}d_6$, 400 MHz): δ (ppm) 8.66 (s, 1H), 8.14 (d, $J = 15.6$ Hz, 1H), 7.66 (d, $J = 15.6$ Hz, 1H), 7.58 (d, $J = 7.6$ Hz, 1H), 7.52 (t, $J = 2.0$ Hz, 1H), 7.46 (s, 1H), 7.36 (t, $J = 7.6$ Hz, 1H), 7.08 (dd, $J = 8.0, 2.4$ Hz, 1H), 6.78 (s, 1H), 3.94 (s, 3H), 3.92 (s, 3H), 3.85 (s, 3H). ^{13}C NMR ($\text{acetone-}d_6$, 100 MHz): δ (ppm) 190.1, 158.7, 155.8, 154.4, 144.8, 141.4, 139.8, 130.6, 120.6, 120.4, 120.3, 116.2, 115.7, 112.8, 98.5, 57.1, 56.9, 56.4.

105 ((*E*)-1-(4-hydroxyphenyl)-3-(2,4,5-trimethoxyphenyl)prop-2-en-1-one). ^1H NMR ($\text{acetone-}d_6$, 400 MHz): δ (ppm) 9.37 (s, 1H), 8.11 (d, $J = 15.6$ Hz, 1H), 8.03 (d, $J = 8.8$ Hz, 2H), 7.72 (d, $J = 15.6$ Hz, 1H), 7.45 (s, 1H), 6.94 (d, $J = 8.8$ Hz, 2H), 6.78 (s, 1H), 3.94 (s, 3H), 3.91 (s, 3H), 3.84 (s, 3H). ^{13}C NMR ($\text{acetone-}d_6$, 100 MHz): δ (ppm) 188.3,

162.4, 155.4, 154.0, 144.6, 142.7, 138.6, 131.5, 120.0, 116.2, 116.0, 112.6, 98.4, 57.0, 56.7, 56.2.

106 ((*E*)-1-(2-methoxyphenyl)-3-(2,4,5-trimethoxyphenyl)prop-2-en-1-one). ^1H NMR (CDCl_3 , 400 MHz): δ (ppm) 7.86 (d, $J = 16.0$ Hz, 1H), 7.51 (d, $J = 7.6$ Hz, 1H), 7.37 (t, $J = 7.6$ Hz, 1H), 7.20 (d, $J = 16.0$ Hz, 1H), 7.03 (s, 1H), 6.96 (t, $J = 7.2$ Hz, 1H), 6.92 (d, $J = 8.8$ Hz, 1H), 6.44 (s, 1H), 3.85 (s, 3H), 3.80 (s, 6H), 3.78 (s, 3H). ^{13}C NMR (CDCl_3 , 100 MHz): δ (ppm) 193.4, 157.7, 154.4, 152.4, 143.2, 138.8, 132.2, 129.9, 129.8, 125.0, 120.5, 115.5, 111.6, 111.1, 96.9, 56.4, 56.2, 55.9, 55.6.

108 ((*E*)-1-(4-methoxyphenyl)-3-(2,4,5-trimethoxyphenyl)prop-2-en-1-one). ^1H NMR (CDCl_3 , 400 MHz): δ (ppm) 8.03 (d, $J = 15.6$ Hz, 1H), 7.98 (d, $J = 8.8$ Hz, 2H), 7.44 (d, $J = 15.6$ Hz, 1H), 7.09 (s, 1H), 6.92 (d, $J = 8.8$ Hz, 2H), 6.48 (s, 1H), 3.89 (s, 3H), 3.85 (s, 3H), 3.84 (s, 3H), 3.82 (s, 3H). ^{13}C NMR (CDCl_3 , 100 MHz): δ (ppm) 189.3, 163.1, 154.6, 152.4, 143.3, 139.3, 131.7, 130.7, 120.1, 115.8, 113.7, 111.7, 97.1, 56.6, 56.4, 56.1, 55.4.

109 ((*E*)-1-(2-aminophenyl)-3-(2,4,5-trimethoxyphenyl)prop-2-en-1-one). ^1H NMR ($\text{acetone-}d_6$, 400 MHz): δ (ppm) 8.10 (d, $J = 15.6$ Hz, 1H), 7.99 (d, $J = 8.0$ Hz, 1H), 7.78 (d, $J = 15.2$ Hz, 1H), 7.46 (s, 1H), 7.25 (t, $J = 8.4$ Hz, 1H), 7.05 (s, 2H), 6.82 (d, $J = 8.4$ Hz, 1H), 6.78 (s, 1H), 6.60 (t, $J = 8.0$ Hz, 1H), 3.94 (s, 3H), 3.91 (s, 3H), 3.84 (s, 3H). ^{13}C NMR ($\text{acetone-}d_6$, 100 MHz): δ (ppm) 192.2, 155.4, 154.0, 152.9, 144.8, 138.2, 134.6, 131.9, 121.4, 119.9, 118.0, 116.6, 115.8, 112.8, 98.6, 57.1, 56.9, 56.4.

110 ((*E*)-1-(2-(trifluoromethyl)phenyl)-3-(2,4,5-trimethoxyphenyl)prop-2-en-1-one). ^1H NMR (CDCl_3 , 400 MHz): δ (ppm) 7.75 (d, $J = 7.6$ Hz, 1H), 7.62 (t, $J = 7.2$ Hz, 1H), 7.61 (d, $J = 16.4$ Hz, 1H), 7.57 (t, $J = 7.6$ Hz, 1H), 7.47 (d, $J = 7.6$ Hz, 1H), 7.03 (s, 1H), 6.99 (d, $J = 16.0$ Hz, 1H), 6.47 (s, 1H), 3.93 (s, 3H), 3.86 (s, 3H), 3.81 (s, 3H). ^{13}C NMR (CDCl_3 , 100 MHz): δ (ppm) 195.8, 154.9, 153.4, 143.7, 143.0, 131.7, 129.7, 128.4, 128.1 (q, $J = 32.3$ Hz), 126.9, 126.8, 125.3, 124.9, 115.0, 111.2, 97.0, 56.6, 56.5, 56.2.

111 ((*E*)-1-(2-hydroxy-4-methoxyphenyl)-3-(2,4,5-trimethoxyphenyl)prop-2-en-1-one). ^1H NMR (CDCl_3 , 400 MHz): δ (ppm) 13.68 (s, 1H), 8.14 (d, $J = 15.6$ Hz, 1H), 7.80

(d, $J = 8.8$ Hz, 1H), 7.50 (d, $J = 15.2$ Hz, 1H), 7.09 (s, 1H), 6.50 (s, 1H), 6.44 (dd, $J = 10.4$, 2.4 Hz, 1H), 6.43 (s, 1H), 3.92 (s, 3H), 3.90 (s, 3H), 3.89 (s, 3H), 3.82 (s, 3H). ^{13}C NMR (CDCl_3 , 100 MHz): δ (ppm) 192.6, 166.8, 166.0, 155.1, 153.0, 143.5, 140.0, 131.3, 118.2, 115.6, 114.5, 112.0, 107.5, 101.2, 97.0, 56.7, 56.4, 56.1, 55.6.

112 ((*E*)-1-(2-hydroxy-6-methoxyphenyl)-3-(2,4,5-trimethoxyphenyl)prop-2-en-1-one). ^1H NMR (CDCl_3 , 400 MHz): δ (ppm) 13.34 (s, 1H), 8.14 (d, $J = 16.0$ Hz, 1H), 7.81 (d, $J = 15.6$ Hz, 1H), 7.32 (t, $J = 8.4$ Hz, 1H), 7.10 (s, 1H), 6.59 (d, $J = 8.0$ Hz, 1H), 6.51 (s, 1H), 6.41 (d, $J = 8.0$ Hz, 1H), 3.93 (s, 3H), 3.92 (s, 3H), 3.89 (s, 3H), 3.87 (s, 3H). ^{13}C NMR (CDCl_3 , 100 MHz): δ (ppm) 194.6, 164.9, 161.0, 154.9, 152.7, 143.4, 138.7, 135.9, 135.4, 125.5, 116.2, 111.8, 111.1, 101.7, 97.2, 56.7, 56.5, 56.2, 55.9.

113 ((*E*)-1-(4-bromo-2-hydroxyphenyl)-3-(2,4,5-trimethoxyphenyl)prop-2-en-1-one). ^1H NMR (CDCl_3 , 400 MHz): δ (ppm) 13.20 (s, 1H), 8.17 (d, $J = 15.6$ Hz, 1H), 7.72 (d, $J = 8.8$ Hz, 1H), 7.49 (d, $J = 15.6$ Hz, 1H), 7.14 (d, $J = 1.6$ Hz, 1H), 7.07 (s, 1H), 7.00 (dd, $J = 8.8$, 2.0 Hz, 1H), 6.48 (s, 1H), 3.91 (s, 3H), 3.89 (s, 3H), 3.86 (s, 3H). ^{13}C NMR (CDCl_3 , 100 MHz): δ (ppm) 193.5, 164.1, 155.4, 153.4, 143.4, 141.6, 130.6, 130.1, 122.1, 121.6, 119.2, 117.4, 115.1, 112.1, 96.8, 56.7, 56.4, 56.2. HR-MS (ESI) for $\text{C}_{18}\text{H}_{17}\text{BrO}_5\text{Na}$ [$\text{M}+\text{Na}$] $^+$ requires 415.01571 found 415.01520.

114 ((*E*)-1-(5-bromo-2-hydroxyphenyl)-3-(2,4,5-trimethoxyphenyl)prop-2-en-1-one). ^1H NMR (CDCl_3 , 400 MHz): δ (ppm) 13.01 (s, 1H), 8.23 (d, $J = 15.2$ Hz, 1H), 7.99 (d, $J = 2.4$ Hz, 1H), 7.52 (dd, $J = 8.8$, 2 Hz, 1H), 7.48 (d, $J = 15.2$ Hz, 1H), 7.12 (s, 1H), 6.90 (d, $J = 8.8$ Hz, 1H), 6.52 (s, 1H), 3.95 (s, 3H), 3.93 (s, 3H), 3.92 (s, 3H). ^{13}C NMR (CDCl_3 , 100 MHz): δ (ppm) 193.1, 162.6, 155.6, 153.6, 143.6, 142.1, 138.5, 131.9, 121.7, 120.6, 117.2, 115.2, 112.1, 110.3, 96.9, 56.9, 56.5, 56.2. HR-MS (ESI) for $\text{C}_{18}\text{H}_{17}\text{BrO}_5\text{Na}$ [$\text{M}+\text{Na}$] $^+$ requires 415.01571 found 415.01670.

115 ((*E*)-1-(2,4-dimethoxyphenyl)-3-(2,4,5-trimethoxyphenyl)prop-2-en-1-one). ^1H NMR (CDCl_3 , 400 MHz): δ (ppm) 7.87 (d, $J = 15.6$ Hz, 1H), 7.60 (d, $J = 8.4$ Hz, 1H), 7.32 (d, $J = 15.6$ Hz, 1H), 6.99 (s, 1H), 6.42 (dd, $J = 8.4$, 2.0 Hz, 1H), 6.39 (s, 1H), 6.36 (d,

$J = 2.4$ Hz, 1H), 3.79 (s, 3H), 3.76 (s, 3H), 3.75 (s, 3H), 3.74 (s, 3H), 3.71 (s, 3H). ^{13}C NMR (CDCl_3 , 100 MHz): δ (ppm) 190.6, 163.5, 159.9, 154.1, 151.9, 143.0, 137.2, 132.2, 125.0, 122.4, 115.6, 111.0, 105.0, 98.4, 96.8, 56.2, 56.0, 55.8, 55.4, 55.2.

116 ((*E*)-1-(2,5-dimethoxyphenyl)-3-(2,4,5-trimethoxyphenyl)prop-2-en-1-one). ^1H NMR (CDCl_3 , 400 MHz): δ (ppm) 7.87 (d, $J = 16.0$ Hz, 1H), 7.23 (d, $J = 16.0$ Hz, 1H), 7.10 (d, $J = 2.8$ Hz, 1H), 7.04 (s, 1H), 6.93 (dd, $J = 9.2, 3.2$ Hz, 1H), 6.87 (dd, $J = 9.2, 2.4$ Hz, 1H), 6.43 (s, 1H), 3.84 (s, 3H), 3.79 (s, 3H), 3.77 (s, 3H), 3.76 (s, 3H), 3.71 (s, 3H). ^{13}C NMR (CDCl_3 , 100 MHz): δ (ppm) 192.8, 154.4, 153.4, 152.4, 152.1, 143.2, 138.8, 130.2, 124.8, 118.1, 115.4, 114.4, 113.3, 111.1, 96.9, 56.4, 56.3, 56.2, 55.9, 55.6.

117 ((*E*)-1-(2,6-dimethoxyphenyl)-3-(2,4,5-trimethoxyphenyl)prop-2-en-1-one). ^1H NMR (CDCl_3 , 400 MHz): δ (ppm) 7.60 (d, $J = 16.4$ Hz, 1H), 7.27 (t, $J = 8.4$ Hz, 1H), 7.01 (s, 1H), 6.87 (d, $J = 16.4$ Hz, 1H), 6.58 (d, $J = 8.4$ Hz, 2H), 6.44 (s, 1H), 3.88 (s, 3H), 3.82 (s, 3H), 3.76 (s, 3H), 3.74 (s, 3H). ^{13}C NMR (CDCl_3 , 100 MHz): δ (ppm) 195.4, 157.5, 154.2, 152.5, 143.4, 140.4, 130.4, 126.8, 119.1, 115.4, 111.0, 104.2, 97.1, 56.5, 56.1, 56.0.

118 ((*E*)-1-(2-hydroxy-4,6-dimethoxyphenyl)-3-(2,4,5-trimethoxyphenyl)prop-2-en-1-one). ^1H NMR (CDCl_3 , 400 MHz): δ (ppm) 8.08 (d, $J = 15.6$ Hz, 1H), 7.83 (d, $J = 15.6$ Hz, 1H), 7.08 (s, 1H), 6.48 (s, 1H), 6.06 (d, $J = 2.0$ Hz, 1H), 5.92 (d, $J = 2.0$ Hz, 1H), 3.90 (s, 3H), 3.86 (s, 6H), 3.85 (s, 3H), 3.79 (s, 3H). ^{13}C NMR (CDCl_3 , 100 MHz): δ (ppm) 192.8, 168.4, 165.9, 162.5, 154.6, 152.4, 143.3, 138.0, 125.4, 116.3, 111.7, 106.5, 97.1, 93.9, 91.2, 56.6, 56.4, 56.1, 55.8, 55.6.

119 ((*E*)-1-(3,5-dibromo-2-hydroxyphenyl)-3-(2,4,5-trimethoxyphenyl)prop-2-en-1-one). ^1H NMR (acetone- d_6 , 400 MHz): δ (ppm) 13.88 (s, 1H), 8.45 (d, $J = 2.0$ Hz, 1H), 8.26 (d, $J = 15.2$ Hz, 1H), 8.04 (d, $J = 2.0$ Hz, 1H), 7.79 (d, $J = 15.6$ Hz, 1H), 7.58 (s, 1H), 6.71 (s, 1H), 3.88 (s, 3H), 3.86 (s, 3H), 3.80 (s, 3H). ^{13}C NMR (acetone- d_6 , 100 MHz): δ (ppm) 192.1, 158.0, 155.1, 154.2, 143.0, 141.2, 140.0, 131.6, 121.9, 115.9, 113.6, 112.1, 111.2, 109.8, 97.0, 56.4, 56.2, 55.6. HR-MS (ESI) for $\text{C}_{18}\text{H}_{16}\text{Br}_2\text{O}_5\text{Na}$ $[\text{M}+\text{Na}]^+$ requires 492.92622 found 492.93560.

120 ((*E*)-1-(2-hydroxynaphthalen-1-yl)-3-(2,4,5-trimethoxyphenyl)prop-2-en-1-one). ^1H NMR (acetone- d_6 , 400 MHz): δ (ppm) 8.44 (d, J = 7.6 Hz, 1H), 8.41 (d, J = 15.2 Hz, 1H), 8.13 (d, J = 9.2 Hz, 1H), 7.98 (d, J = 15.6 Hz, 1H), 7.88 (d, J = 8.0 Hz, 1H), 7.69 (td, J = 6.8, 0.8 Hz, 1H), 7.58 (t, J = 8.4 Hz, 1H), 7.57 (s, 1H), 7.39 (d, J = 8.8 Hz, 1H), 6.82 (s, 1H), 4.00 (s, 3H), 3.95 (s, 3H), 3.87 (s, 3H). ^{13}C NMR (acetone- d_6 , 100 MHz): δ (ppm) 194.8, 164.9, 156.4, 155.2, 144.9, 141.4, 138.4, 131.0, 128.5, 126.8, 126.4, 125.6, 124.9, 119.0, 118.3, 115.9, 114.6, 113.1, 98.4, 57.2, 57.0, 56.5.

2.8 Preparation of dihydrochalcones.

Two chalcones **48** and **65** were hydrogenated following the methodology of Krohn *et al.* to broaden the scope of chalcone derivatives with various degrees of saturation (**Figure 2.11**).⁵⁷ The appropriate amount of chalcone **48** or **65** and Pd/C powder 5% mol (compared to molarity of chalcones) were charged in a flask with MeOH. The plastic stopper attached by hydrogen gas balloon was used and the reaction was monitored by TLC. When products appear markedly, the palladium was filtered off by celite powder and the solvent was evaporated to dryness to achieve some compounds **121-124**. Three chalcones **121-123** are new substances reported by HR-MS information below.

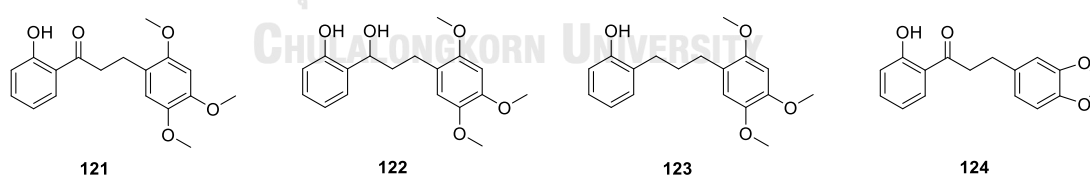


Figure 2.11 Hydrogenated chalcones.

121 (1-(2-hydroxyphenyl)-3-(2,4,5-trimethoxyphenyl)propan-1-one). ^1H NMR (CDCl_3 , 400 MHz): δ (ppm) 12.38 (s, 1H), 7.77 (dd, J = 8.0, 0.8 Hz, 1H), 7.45 (td, J = 8.0, 1.2 Hz, 1H), 6.98 (d, J = 8.0 Hz, 1H), 6.86 (t, J = 7.6 Hz, 1H), 6.75 (s, 1H), 6.52 (s, 1H), 3.88 (s, 3H), 3.82 (s, 3H), 3.80 (s, 3H), 3.24 (t, J = 8.0 Hz, 2H), 2.98 (t, J = 8.0 Hz, 2H). ^{13}C NMR (CDCl_3 , 100 MHz): δ (ppm) 206.6, 162.6, 151.8, 148.4, 143.1, 136.3, 130.2, 120.5, 119.6,

118.9, 118.6, 114.8, 97.2, 56.9, 56.5, 56.2, 39.2, 25.8. HR-MS (ESI) for $C_{18}H_{20}O_5Na$ $[M+Na]^+$ requires 339.12084 found 339.1204.

122 (2-(1-hydroxy-3-(2,4,5-trimethoxyphenyl)propyl)phenol). 1H NMR ($CDCl_3$, 400 MHz): δ (ppm) 8.30 (s, 1H), 7.13 (td, $J = 8.4, 1.6$ Hz, 1H), 6.86 (m, 2H), 6.78 (t, $J = 7.2$ Hz, 1H), 6.70 (s, 1H), 6.55 (s, 1H), 4.67 (dd, $J = 10.0, 4.0$ Hz, 1H), 3.88 (s, 3H), 3.85 (s, 3H), 3.83 (s, 3H), 2.85 (m, 1H), 2.67 (m, 1H), 2.20 (m, 1H), 1.94 (m, 1H). ^{13}C NMR ($CDCl_3$, 100 MHz): δ (ppm) 155.9, 151.3, 148.2, 143.7, 128.7, 127.3, 127.0, 120.8, 119.6, 117.2, 114.4, 98.2, 74.6, 56.8, 56.7, 56.4, 38.3, 25.4. HR-MS (ESI) for $C_{18}H_{22}O_5Na$ $[M+Na]^+$ requires 341.13649 found 341.1359.

123 (2-(3-(2,4,5-trimethoxyphenyl)propyl)phenol). 1H NMR ($DMSO-d_6$, 400 MHz): δ (ppm) 9.24 (s, 1H), 7.03 (dd, $J = 7.6, 0.8$ Hz, 1H), 6.96 (td, $J = 7.6, 1.2$ Hz, 1H), 6.76 (d, $J = 8.0$ Hz, 1H), 6.74 (s, 1H), 6.69 (t, $J = 7.6$ Hz, 1H), 6.62 (s, 1H), 3.75 (s, 3H), 3.73 (s, 3H), 3.67 (s, 3H), 2.51 (m, 4H), 1.74 (p, $J = 8.0$ Hz, 2H). ^{13}C NMR ($DMSO-d_6$, 100 MHz): δ (ppm) 155.1, 151.2, 147.6, 142.5, 129.6, 128.3, 126.6, 121.6, 118.8, 114.8, 114.7, 98.7, 56.4, 56.2, 55.9, 29.9, 29.5, 29.0. HR-MS (ESI) for $C_{18}H_{22}O_4Na$ $[M+Na]^+$ requires 325.14158 found 325.1395.

124 (3-(benzo[d][1,3]dioxol-5-yl)-1-(2-hydroxyphenyl)propan-1-one). 1H NMR ($CDCl_3$, 400 MHz): δ (ppm) 12.31 (s, 1H), 7.72 (d, $J = 8.0$ Hz, 1H), 7.45 (t, $J = 7.6$ Hz, 1H), 6.98 (d, $J = 8.4$ Hz, 1H), 6.88 (t, $J = 7.6$ Hz, 1H), 6.74 (d, $J = 7.2$ Hz, 1H), 6.73 (s, 1H), 6.69 (d, $J = 8.0$ Hz, 1H), 5.91 (s, 2H), 3.26 (t, $J = 7.6$ Hz, 2H), 2.98 (t, $J = 7.6$ Hz, 2H). ^{13}C NMR ($CDCl_3$, 100 MHz): δ (ppm) 205.4, 162.5, 147.8, 146.0, 136.3, 134.5, 129.8, 121.2, 119.3, 118.9, 118.6, 108.9, 108.3, 100.9, 40.2, 29.8.

2.9 AMPK activation activity assessment

The experiments were conducted under the collaboration with Associate Professor Dr. Chatchai Muanprasat, Department of Physiology, Faculty of Science, Mahidol University.

2.9.1 Potency and EC₅₀

In this study, potency is calculated by the fold alteration of AMPK phosphorylation between podocyte cells inoculated with chalcones at 10 μ M and a control sample treated with DMSO medium only. The fold change of AMPK protein expression from Western blot analysis is calculated from the band intensity of pAMPK/total AMPK. A compound can possess high potency if a considerable fold change is measured which means that the increase in AMPK phosphorylation intensity was observed or that compound activates AMPK. The EC₅₀ is the concentration of a drug that gives half-maximal response. The fold modifications of AMPK protein expression of podocyte cells treated at each chalcone concentration (1, 5, 10, 50, 100 μ M) compared to control cells were applied to Hill's equation to obtain the EC₅₀ value.

2.9.2 Assessment procedure

Podocyte cells were cultured following the procedure described by Saleem *et al.*⁵⁸ Firstly, they were cultured at 33°C for 24 h to allow cell proliferation, then the cells were transferred to 37°C culture for 14 days to activate cell differentiation into fully mature podocyte. Thereafter, chalcones were treated at a concentration of 10 μ M for 24h in mature podocyte cells. Subsequently, the cells were monitored under a microscope to check if chalcones were toxic to the cells. If the morphology changed in the abnormal way, it would mean that that chalcone was poisonous to the podocyte cells. Then, cells were extracted for protein collection and AMPK protein expression was measured by Western blot analysis using antibodies. After that, any compounds which could induce at least 5-fold change in AMPK phosphorylation compared to the control samples were chosen. The next step was to evaluate the concentration-response relationship and calculate EC₅₀ of each active compound. The most potent compound was the one with the highest potency and the least toxicity. The general procedure for the evaluation of AMPK activation activity of chalcone compounds is displayed in **Figure 2.12**.

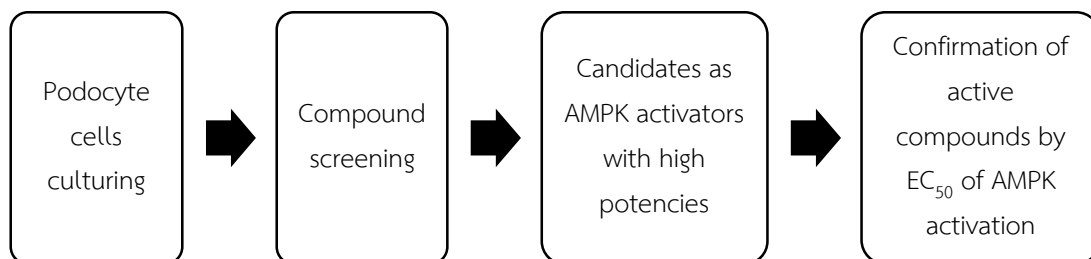


Figure 2.12 General procedure for AMPK phosphorylation activity assessment of chalcone compounds.



CHAPTER III

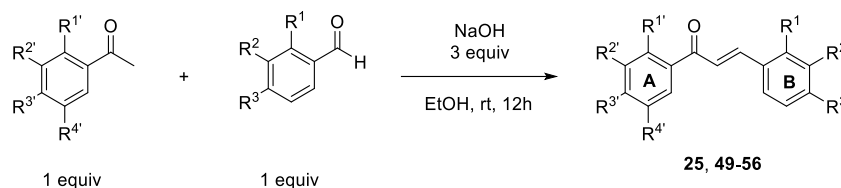
RESULTS AND DISCUSSION

The synthesis of target chalcones could be achieved in moderate to good yields. Structural elucidation of all compounds was carried out by ^1H and ^{13}C -NMR; in addition, HR-MS was collected for new compounds. Furthermore, the structure-activity relationship was investigated according to the potency of chalcones to find some active candidates compared to the reported chalcone **48** as AMPK activator. Thereafter, concentration-response relationship and EC_{50} calculation of each active compound were analyzed to recognize the most promising chalcone for *in vivo* experiment.

3.1 Synthesis and evaluation of chalcones with monosubstitution on B-ring

3.1.1 Synthesis and structural elucidation

Following the procedure of Srinivasan *et al.*, nine chalcones with A-ring fixed as 2'-hydroxy or 3',4',5'-trimethoxyacetophenone (**25** and **49-56**) were prepared (**Figure 3.1**). As mentioned above, 2'-hydroxy substituent had some advantages to boost AMPK activation activity, thus this type of A-ring was fixed. In addition, A-ring as 3',4',5'-trimethoxyacetophenone was reported to be used to prepare chalcones possessing cytotoxicity and anti-inflammatory activity.^{4, 59} B-ring of chalcones possessed only one substituent such as OH or OCH_3 at either of three positions (ortho, meta, and para). All products were obtained as yellow or red crystal with moderate yields (52-69%) as shown in **Table 3.1**. Only three chalcones (**52-54**) were attained by crystallization in MeOH due to their precipitation after acidified by 10% HCl. The other compounds were purified by column chromatography. Chalcones with B-ring bearing OCH_3 group (**52-54**) instead of OH (**25**, **49-51**, **55** and **56**) were achieved in higher yield because the OH group can be deprotonated under basic conditions leading to resonance system formed between negative charge on oxygen atom and carbonyl



49. $R^1 = \text{OH}, R^2 = R^3 = R^4 = \text{H}, R^2 = R^3 = \text{H}, R^1 = \text{OH}$

54. $R^1 = \text{OH}, R^2 = R^3 = R^4 = \text{H}, R^1 = R^2 = \text{H}, R^3 = \text{OCH}_3$

50. $R^1 = \text{OH}, R^2 = R^3 = R^4 = \text{H}, R^1 = R^3 = \text{H}, R^2 = \text{OH}$

55. $R^1 = \text{H}, R^2 = R^3 = R^4 = \text{OCH}_3, R^2 = R^3 = \text{H}, R^1 = \text{OH}$

51. $R^1 = \text{OH}, R^2 = R^3 = R^4 = \text{H}, R^1 = R^2 = \text{H}, R^3 = \text{OH}$

25. $R^1 = \text{H}, R^2 = R^3 = R^4 = \text{OCH}_3, R^1 = R^3 = \text{H}, R^2 = \text{OH}$

52. $R^1 = \text{OH}, R^2 = R^3 = R^4 = \text{H}, R^2 = R^3 = \text{H}, R^1 = \text{OCH}_3$

56. $R^1 = \text{H}, R^2 = R^3 = R^4 = \text{OCH}_3, R^1 = R^2 = \text{H}, R^3 = \text{OH}$

53. $R^1 = \text{OH}, R^2 = R^3 = R^4 = \text{H}, R^1 = R^3 = \text{H}, R^2 = \text{OCH}_3$

Figure 3.1 Synthesis of chalcones with monosubstitution on B-ring.

group of aldehyde molecules. Due to electron donation from minor oxygen atom, the carbon atom of carbonyl component would have less positive property, resulting in being less active. All synthetic chalcones are known compounds.

The structural identification of these compounds was conducted by ^1H and ^{13}C NMR analysis. The important signals of chalcones are two doublets with high value of J coupling constant (15 – 17 Hz) derived from two protons of α,β -unsaturated ketone ($-\text{CH}=\text{CH}-\text{C}=\text{O}$). They are much downfield because of conjugation between alkene and ketone groups pulling most electrons toward ketone functional group (**Figure 3.2**).

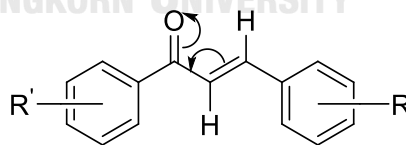


Figure 3.2 Resonance system of α,β -unsaturated ketone.

The ^1H and ^{13}C -NMR spectral assignments of **25** and **49-56** are presented in **Tables 3.2-3.4**. Most of the signals in ^1H and ^{13}C -NMR spectra associating to couples of **49** and **52**, **50** and **53** or **51** and **54** were similar to each other, respectively as they replaced OH to OCH_3 group on B-ring. All of six compounds (**49-54**) have alike chemical shifts of peaks derived from proton and carbon on A-ring and a tertiary carbon of

Table 3.1 Yields and characteristics of chalcones (**25**, **49-56**).

Chalcones	Appearance	Yield (%)	Remarks
49	Yellow crystal	55	known
50	Yellow crystal	53	known
51	Yellow crystal	52	known
52	Yellow crystal	69	known
53	Yellow crystal	68	known
54	Yellow crystal	65	known
55	Red crystal	53	known
25	Yellow crystal	55	known
56	Yellow crystal	60	known

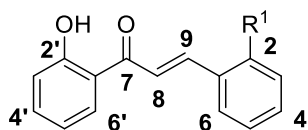
carbonyl group. Sometimes the signals of proton and carbon belonging to α,β -unsaturated ketone were likely fluctuating among them due to the different intensity of the resonance effect of electron-donating group on B-ring. Lastly, the peaks of proton and carbon on B-ring would be varied among three couples such as **49** and **52**, **50** and **53** along with **51** and **54** owing to the particular position of substituents on B-ring such as positions 2, 3 and 4.

The spectra data of three derivatives **25**, **55** and **56** with A-ring as 3',4',5'-trimethoxyacetophenone were distinct from six above derivatives.

3.1.2 Biological activity evaluation

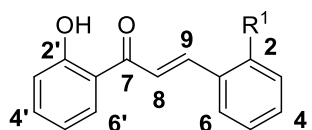
After podocyte cells differentiate into mature cells and are ready for subculturing, they were treated by nine chalcones at 10 μ M for 24 h. The outcomes of biological activity from nine chalcones are shown in **Figure 3.3**. Regarding 2'-hydroxychalcone (**49-54**), it is clear that OCH₃ group at 3 or 4-positions on B-ring would boost the AMPK activation activity better than OH group at the same position. For example, changing from 3-OH (**50**) to 3-OCH₃ (**53**) enhanced the potency from 1.73 to 4.85. Similarly, the potency calculated as 0.65 in **51** bearing 4-OH group altered to

Table 3.2 Tentative NMR chemical shift assignment of chalcones 49-51.

49. R¹ = 2-OH50. R¹ = 3-OH51. R¹ = 4-OH

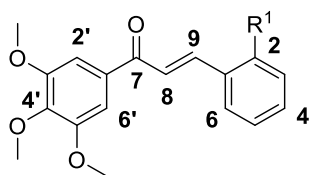
Position	49 (acetone- <i>d</i> ₆)		50 (CDCl ₃)		51 (acetone- <i>d</i> ₆)	
	δH	δC	δH	δC	δH	δC
1'	-	122.5	-	120.2	-	120.8
2'	-	164.2	-	163.7	-	164.3
3'	7.03, d <i>J</i> = 8.0 Hz	118.7	7.04, d <i>J</i> = 8.0 Hz	118.8	6.96, m	118.7
4'	7.55, td <i>J</i> = 8.4, 1.6 Hz	136.9	7.51, t <i>J</i> = 8.0 Hz	136.6	7.54, td <i>J</i> = 8.4, 1.6 Hz	136.8
5'	6.99, t <i>J</i> = 7.2 Hz	120.7	7.31, t <i>J</i> = 7.6 Hz	119.1	6.96, m	119.5
6'	8.19, dd <i>J</i> = 8.0, 1.2 Hz	133.0	7.92, d <i>J</i> = 8.0 Hz	129.8	8.23, dd <i>J</i> = 8.4, 1.6 Hz	130.9
1	-	120.8	-	136.4	-	127.1
2	-	158.2	7.14, s	120.8	7.77, d <i>J</i> = 8.8 Hz	131.9
3	6.92, d <i>J</i> = 7.2 Hz	117.0	-	156.2	6.96, m	116.7
4	7.31, td <i>J</i> = 8.4, 1.6 Hz	130.9	6.92, d <i>J</i> = 7.6 Hz	115.0	-	161.3
5	6.97, t <i>J</i> = 6.4 Hz	119.5	6.95, t <i>J</i> = 7.6 Hz	130.4	6.96, m	116.7
6	7.85, dd <i>J</i> = 7.6, 1.2 Hz	130.1	7.24, d <i>J</i> = 7.6 Hz	121.7	7.77, d <i>J</i> = 8.8 Hz	131.9
7	-	195.1	-	193.9	-	194.7
8	8.07, d <i>J</i> = 15.6 Hz	120.5	7.63, d <i>J</i> = 15.6 Hz	118.2	7.85, d <i>J</i> = 15.2 Hz	117.8
9	8.33, d <i>J</i> = 15.6 Hz	141.8	7.86, d <i>J</i> = 15.6 Hz	145.2	7.91, d <i>J</i> = 15.6 Hz	146.5
2'-OH	13.03, s	-	12.79, s	-	13.08, s	-
OH	9.51, s	-	-	-	9.27, s	-

Table 3.3 Tentative NMR chemical shift assignment of chalcones 52-54.



52. R¹ = 2-OCH₃ 53. R¹ = 3-OCH₃ 54. R¹ = 4-OCH₃

Position	52 (CDCl ₃)		53 (CDCl ₃)		54 (CDCl ₃)	
	δ H	δ C	δ H	δ C	δ H	δ C
1'	-	120.4	-	120.0	-	120.3
2'	-	163.7	-	163.6	-	163.7
3'	7.03, d <i>J</i> = 8.4 Hz	118.7	7.06, d <i>J</i> = 8.4 Hz	118.6	7.02, d <i>J</i> = 8.4 Hz	118.7
4'	7.49, td <i>J</i> = 8.4, 1.2 Hz	136.2	7.53, td <i>J</i> = 8.0, 1.2 Hz	136.4	7.48, td <i>J</i> = 8.4, 1.6 Hz	136.2
5'	7.02, t <i>J</i> = 8.0 Hz	121.0	6.97, t <i>J</i> = 7.6 Hz	121.3	6.94, t <i>J</i> = 7.6 Hz	118.9
6'	7.92, dd <i>J</i> = 8.0, 1.2 Hz	132.3	7.94, d <i>J</i> = 8.4 Hz	130.0	7.91, dd <i>J</i> = 8.0, 1.2 Hz	129.6
1	-	123.8	-	136.0	-	127.5
2	-	159.2	7.19, s	113.8	7.62, d <i>J</i> = 8.0 Hz	130.6
3	6.96, d <i>J</i> = 8.0 Hz	111.5	-	160.0	6.95, d <i>J</i> = 8.8 Hz	114.6
4	7.40, td <i>J</i> = 8.4, 1.2 Hz	129.8	7.01, dd <i>J</i> = 8.4, 2.0 Hz	116.6		162.2
5	6.94, t <i>J</i> = 7.6 Hz	118.9	7.38, t <i>J</i> = 7.6 Hz	129.7	6.95, d <i>J</i> = 8.8 Hz	114.6
6	7.65, dd <i>J</i> = 7.6, 0.8 Hz	129.7	7.29, d <i>J</i> = 7.2 Hz	120.5	7.62, d <i>J</i> = 8.0 Hz	130.6
7	-	194.5	-	193.7	-	193.8
8	7.78, d <i>J</i> = 15.6 Hz	120.9	7.66, d <i>J</i> = 15.6 Hz	118.8	7.53, d <i>J</i> = 15.2 Hz	117.8
9	8.23, d <i>J</i> = 15.6 Hz	141.3	7.91, d <i>J</i> = 16.0 Hz	145.4	7.90, d <i>J</i> = 15.6 Hz	145.5
2'-OH	12.95, s	-		-	12.95, s	-
CH ₃	3.94, s	55.7	3.89, s	55.4	3.86, s	55.6

Table 3.4 Tentative NMR chemical shift assignment of chalcones **25**, **55** and **56**.55. R¹ = 2-OH25. R¹ = 3-OH56. R¹ = 4-OH

Position	55 (CDCl ₃)		25 (DMSO- <i>d</i> ₆)		56 (DMSO- <i>d</i> ₆)	
	δH	δC	δH	δC	δH	δC
1'	-	133.7	-	133.0	-	133.4
2'	7.29, s	106.6	7.42, s	106.2	7.39, s	106.0
3'	-	153.2	-	152.9	-	152.9
4'	-	142.6	-	142.0	-	141.8
5'	-	153.2	-	152.9	-	152.9
6'	7.29, s	106.6	7.42, s	106.2	7.39, s	106.0
1	-	122.3	-	136.0	-	125.9
2	-	156.5	7.26, m	120.0	7.75, d <i>J</i> = 8.4 Hz	131.1
3	6.96, d <i>J</i> = 8.4 Hz	120.7	-	157.7	6.84, d <i>J</i> = 8.4 Hz	115.8
4	7.25, t <i>J</i> = 8.0, 1.6 Hz	129.5	6.88, dd <i>J</i> = 7.6, 1.6 Hz	115.3	-	160.1
5	6.92, t <i>J</i> = 8.0 Hz	122.5	7.26, m	129.8	6.84, d <i>J</i> = 8.4 Hz	115.8
6	7.58, dd <i>J</i> = 8.0, 1.2 Hz	132.0	7.32, d <i>J</i> = 7.6 Hz	121.8	7.75, d <i>J</i> = 8.4 Hz	131.1
7	-	191.3	-	187.9	-	187.8
8	7.64, d <i>J</i> = 16.0 Hz	116.8	7.65, d <i>J</i> = 15.2 Hz	117.7	7.68, d <i>J</i> = 15.2 Hz	118.4
9	8.20, d <i>J</i> = 16.0 Hz	141.6	7.85, d <i>J</i> = 15.6 Hz	144.1	7.73, d <i>J</i> = 14.8 Hz	144.3
OH	7.72, s	-	9.64, s	-	10.10, s	-
CH ₃	3.93, 3.91 s	61.1, 56.5	3.90, 3.76 s	60.1, 56.2	3.89, 3.76 s	60.2, 56.2

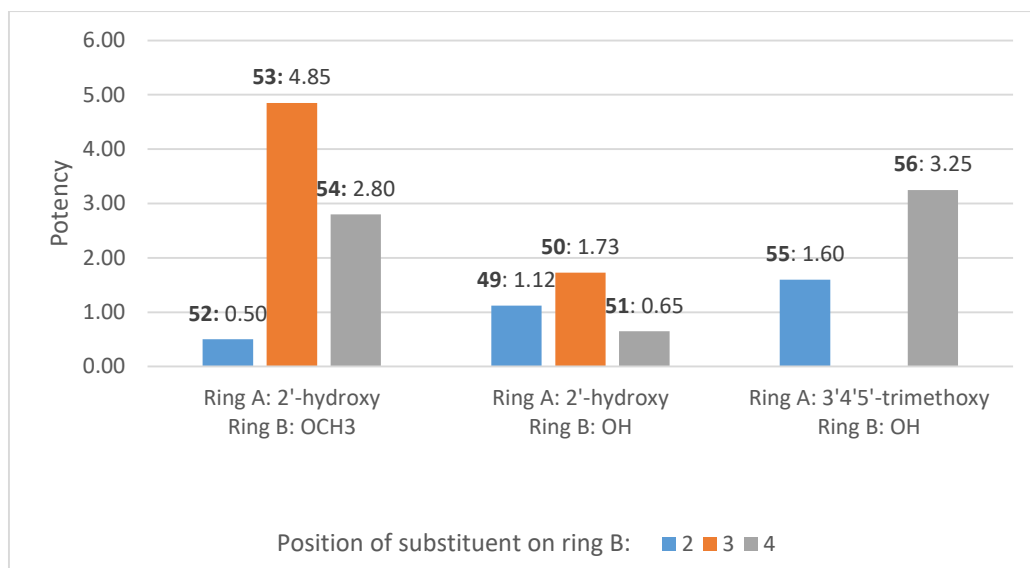
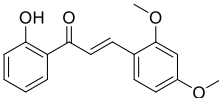
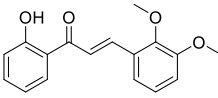
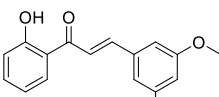
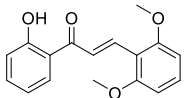
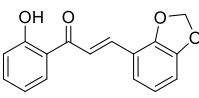
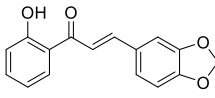
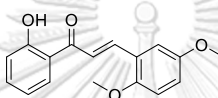
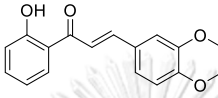


Figure 3.3 Biological evaluation of chalcones with monosubstitution on B-ring.

2.80 in **54** bearing 4-OCH₃. Nonetheless, with respect to 2-position on B-ring, methylation of **49** to **52** seemed to reduce by half of potency, their potencies as 0.50 and 1.12, respectively. In addition, substituents at 3-position on B-ring caused 2'-hydroxychalcone to be more active than at 2- or 4-positions, regardless of types of substituents. In case of 3',4',5'-trimethoxychalcone, the OH at 3-position on B-ring made **25** toxic to the cells, so it did not further monitor. Moreover, with regard to OH at 2- or 4-positions on B-ring, replacing A-ring from 2'-hydroxy- to 3',4',5'-trimethoxyacetophenone led to a 1.5- and 5-fold increase in potency, respectively. The potencies of 3',4',5'-trimethoxyacetophenone with 2- and 4-OH on B-ring (**55** and **56**) were 1.60 and 3.25, respectively. Overall, **53** was the most potent candidate with the potency of 4.85 which was around 1.5 times as much as the second potent **56**. It can be seen that OCH₃ group at 3-position on B-ring might keep an important role in the potency of chalcones. Besides, 3',4',5'-trimethoxychalcones exhibited their competitive activity compared to 2'-hydroxychalcones; therefore, a series of chalcone derivatives with A-ring maintained as 2'-hydroxy- or 3',4',5'-trimethoxyacetophenones and B-ring bearing two OCH₃ groups, methylenedioxy or one OH along with one OCH₃ group were prepared to continue finding for other better candidates.

Table 3.5 Theory about the crucial function of the 3-methoxy group for AMPK activation activity of chalcone derivatives.

Chalcones without 3- or 5-OCH ₃ group	Chalcones with 3- or 5-OCH ₃ group	3,5-Dimethoxychalcone
 60	 57	 66
 62	 59	 65
	 61	
	 63	

From the assumption that the structure containing 3-OCH₃ group on B-ring might be required as AMPK activators, some compounds with dimethoxy groups fixed at 3-position along with any other positions on B-ring were prepared to confirm this hypothesis (**Table 3.5**). Because of the symmetry of the phenyl ring, 3- and 5-positions are the same as long as methoxy substituent was at *meta*-position to the α,β -unsaturated ketone. This can be seen from **Table 3.5** that **66** should be the most potent one among these eight compounds according to the hypothesis “3-methoxy is the best” due to bearing 3,5-dimethoxy group. Subsequently, the next five chalcones (**57**, **59**, **61**, **63** and **65**) revealed moderate potency thanks to one OCH₃ group lying at 3- or 5-position. Eventually, two last chalcones (**60** and **62**) were assumed to bear weak biological activity owing to no OCH₃ group settling at 3- or 5-position.

3.2 Synthesis and evaluation of chalcones with disubstitution (OH, OCH₃ and OCH₂O) on B-ring.

3.2.1 Synthesis and structural elucidation

Twelve chalcones with A-ring fixed as 2'-hydroxy or 3',4',5'-trimethoxyacetophenone (**57-68**) were synthesized by Claisen-Schmidt reaction (**Figure 3.4**). A variety of benzaldehydes with disubstitution such as OH, OCH₃ or methylenedioxy were used to condense with two types of acetophenone to furnish chalcones in moderate yield (52-82%) except for **58** (15%). Almost compounds were purified by crystallization in MeOH to achieve the products as yellow or white crystals except for **58**, **59** and **62** which were purified by column chromatography (**Table 3.6**).

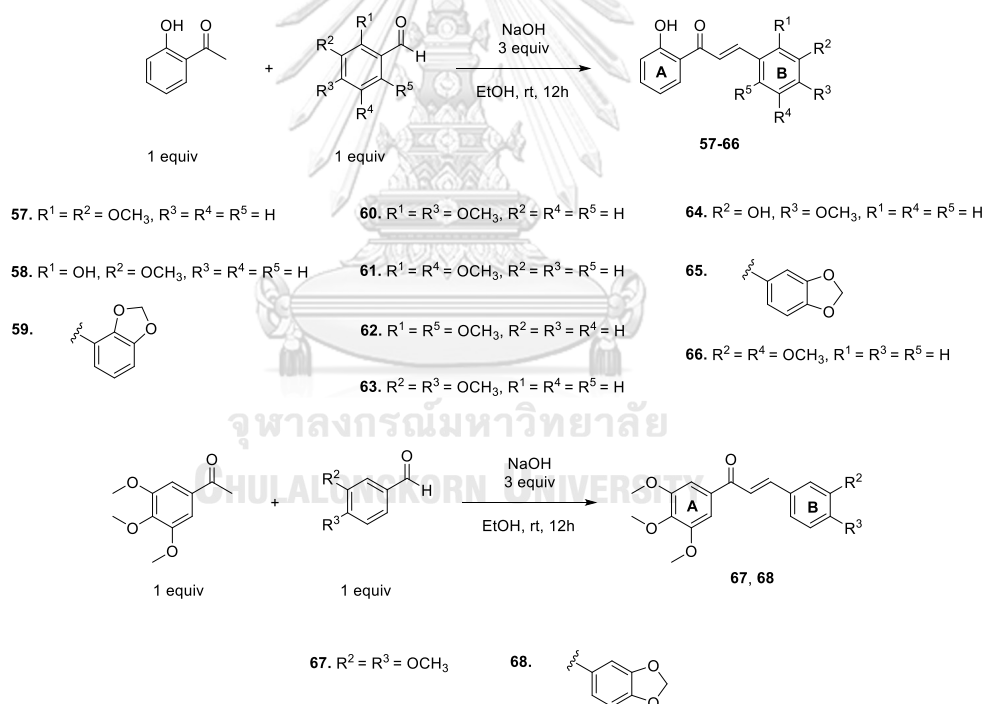


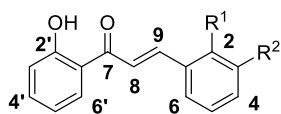
Figure 3.4 Synthesis of chalcones with disubstitution including hydroxy, methoxy and methylenedioxy on B-ring.

Table 3.6 Yields and characteristics of chalcones **57-68**.

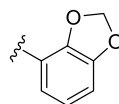
Chalcones	Appearance	Yield (%)	Remarks
57	Yellow crystal	52	known
58	Yellow crystal	15	known
59	Yellow crystal	62	new
60	Yellow crystal	66	known
61	Yellow crystal	68	known
62	Yellow crystal	58	known
63	Yellow crystal	78	known
64	Yellow crystal	62	known
65	Yellow crystal	82	known
66	Yellow crystal	70	known
67	White crystal	69	known
68	White crystal	67	known

The structural identification of these compounds was conducted by ^1H and ^{13}C NMR analysis, as shown in **Tables 3.7-3.10**. Ten chalcones (**57-66**) bear a resemblance in the peaks of ^1H and ^{13}C NMR on A-ring because of derivation from 2'-hydroxyacetophenone together. Three compounds (**57-59**) bearing two substituents at 2,3-position on B-ring have similar ^1H and ^{13}C NMR signals together. The same case was also applied for three chalcones (**63-65**) possessing two substituents at 3,4-position on B-ring. The ^1H and ^{13}C NMR signals on B-ring of **60-62** and **66** were varied according to different positions of dimethoxy groups. Besides, the NMR signals on A-ring of **67** and **68** were distinct to the other ten chalcones due to the generation from 3',4',5'-trimethoxyacetophenone but their NMR signals on B-ring were relatively similar to those of chalcones (**63-65**) owing to carrying two substituents at 3,4-position on B-ring. In addition, **59** is a new compound and its structure was confirmed by HR-MS (ESI) for $\text{C}_{16}\text{H}_{12}\text{O}_4\text{Na}$ $[\text{M}+\text{Na}]^+$ required 291.06333 while the result was found as 291.06270.

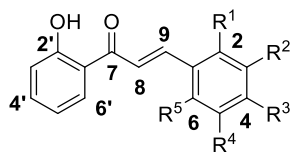
Table 3.7 Tentative NMR chemical shift assignment of chalcones 57-59.

57. $R^1 = R^2 = \text{OCH}_3$ 58. $R^1 = \text{OH}, R^2 = \text{OCH}_3$

59.

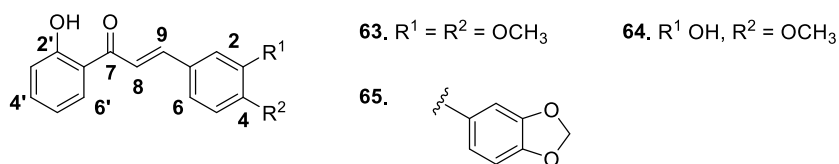


Position	57 (CDCl ₃)		58 (CDCl ₃)		59 (CDCl ₃)	
	δH	δC	δH	δC	δH	δC
1'	-	120.2	-	119.9	-	120.2
2'	-	163.7	-	163.7	-	163.8
3'	7.01, d $J = 8.4$ Hz	118.6	7.20, dd $J = 6.8, 1.6$ Hz	118.7	6.88, d $J = 4.4$ Hz	118.7
4'	7.48, t $J = 8.0$ Hz	136.3	7.49, t $J = 7.6$ Hz	136.3	7.49, td $J = 7.2, 1.2$ Hz	136.5
5'	7.09, t $J = 8.0$ Hz	118.9	6.94, t $J = 7.6$ Hz	118.9	7.01, m	119.0
6'	7.90, d $J = 8.0$ Hz	129.8	7.94, d $J = 7.6$ Hz	130.0	7.90, dd $J = 6.8, 1.6$ Hz	129.9
1	-	128.8	-	129.7	-	117.9
2	-	149.3	-	146.3	-	147.0
3	-	153.3	-	147.1	-	148.2
4	6.97, d $J = 8.0$ Hz	114.8	6.90, d $J = 8.0$ Hz	112.5	6.88, d $J = 4.4$ Hz	110.5
5	6.92, t $J = 8.0$ Hz	124.3	6.91, t $J = 8.0$ Hz	122.4	6.94, t $J = 7.6, 0.8$ Hz	123.8
6	7.27, d $J = 7.6$ Hz	121.7	7.02, d $J = 8.4$ Hz	121.8	7.01, m	123.1
7	-	194.2	-	194.6	-	194.2
8	7.73, d $J = 15.6$ Hz	120.0	7.92, d $J = 15.2$ Hz	120.0	7.81, d $J = 15.2$ Hz	122.2
9	8.20, d $J = 15.6$ Hz	140.5	8.14, d $J = 15.6$ Hz	141.0	7.89, d $J = 16.0$ Hz	140.1,
2'-OH	12.88, s	-	12.94, s	-	12.86, s	-
OH	-	-	6.40, s	-	-	-
CH ₃ /methylene	3.90, 3.88 s	61.4, 56.0	3.94 s	56.4	6.14 s	101.8

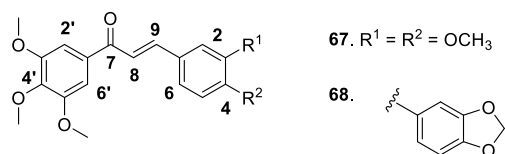
Table 3.8 Tentative NMR chemical shift assignment of chalcones **60-62** and **66**.60. R¹ = R³ = OCH₃, R² = R⁴ = R⁵ = H61. R¹ = R⁴ = OCH₃, R² = R³ = R⁵ = H62. R¹ = R⁵ = OCH₃, R² = R³ = R⁴ = H66. R² = R⁴ = OCH₃, R¹ = R³ = R⁵ = H

Position	60 (CDCl ₃)		61 (CDCl ₃)		62 (CDCl ₃)		66 (CDCl ₃)	
	δH	δC	δH	δC	δH	δC	δH	δC
1'	-	120.4	-	120.3	-	120.7	-	120.0
2'	-	163.7	-	163.7	-	163.7	-	163.6
3'	7.00, d <i>J</i> = 8.4 Hz	118.5	7.02, d <i>J</i> = 8.4 Hz	118.7	7.01, dd <i>J</i> = 8.4, 0.8 Hz	118.6	7.01, d <i>J</i> = 8.4 Hz	118.6
4'	7.46, t <i>J</i> = 8.4 Hz	135.9	7.49, t <i>J</i> = 8.0 Hz	136.3	7.47, td <i>J</i> = 8.4, 1.6 Hz	135.9	7.47, t <i>J</i> = 8.0 Hz	136.4
5'	6.91, t <i>J</i> = 8.0 Hz	118.7	6.90, t <i>J</i> = 8.0 Hz	118.9	6.93, td <i>J</i> = 8.4, 1.2 Hz	118.7	6.92, t <i>J</i> = 7.6 Hz	118.9
6'	7.90, d <i>J</i> = 8.0 Hz	129.7	7.92, d <i>J</i> = 8.0 Hz	129.8	7.91, dd <i>J</i> = 8.0, 1.2 Hz	129.9	7.88, d <i>J</i> = 7.6 Hz	129.7
1	-	117.0	-	124.4	-	112.9	-	136.5
2	-	160.8	-	153.7	-	160.8	6.76, s	106.7
3	6.46, d <i>J</i> = 2.0 Hz	98.6	6.96, m	121.2	6.60, d <i>J</i> = 8.4 Hz	104.0	-	161.2
4	-	163.6	6.96, m	114.4	7.32, t <i>J</i> = 8.4 Hz	132.2	6.52, s	103.1
5	6.53, dd <i>J</i> = 8.4, 2.0 Hz	105.8	-	153.8	6.60, d <i>J</i> = 8.4 Hz	104.0	-	161.2
6	7.56, d <i>J</i> = 8.8 Hz	131.5	7.17, s	112.7	-	160.8	6.76, s	106.7
7	-	194.3	-	194.4	-	195.6	-	193.7
8	7.67, d <i>J</i> = 15.2 Hz	118.2	7.74, d <i>J</i> = 15.6 Hz	117.8	8.15, d <i>J</i> = 15.6 Hz	122.9	7.56, d <i>J</i> = 15.2 Hz	120.6
9	8.16, d <i>J</i> = 15.6 Hz	141.4	8.19, d <i>J</i> = 15.6 Hz	141.0	8.40, d <i>J</i> = 15.6 Hz	136.6	7.79, d <i>J</i> = 15.6 Hz	145.5
2'-OH	13.11, s	-	12.92, s	-	13.12, s	-	12.81, s	-
CH ₃	3.90, 3.84 s	55.7, 55.6	3.89, 3.83 s	56.3, 56.0	3.94 s	56.1	3.82 s	55.5

Table 3.9 Tentative NMR chemical shift assignment of chalcones 63-65.



Position	63 (CDCl ₃)		64 (CDCl ₃)		65 (CDCl ₃)	
	δH	δC	δH	δC	δH	δC
1'	-	120.2	-	120.3	-	120.1
2'	-	163.7	-	163.7	-	163.6
3'	6.94, dd $J = 7.2, 0.8 \text{ Hz}$	118.7	7.02, d $J = 8.4 \text{ Hz}$	118.7	7.04, d $J = 8.0 \text{ Hz}$	118.6
4'	7.48, td $J = 7.2, 1.6 \text{ Hz}$	136.3	7.48, td $J = 7.8, 1.6 \text{ Hz}$	136.3	7.51, td $J = 8.0, 1.6 \text{ Hz}$	136.2
5'	6.91, t $J = 8.4 \text{ Hz}$	118.8	6.93, t $J = 7.2 \text{ Hz}$	118.9	6.95, t $J = 8.0 \text{ Hz}$	118.8
6'	7.92, dd $J = 8.0, 0.8 \text{ Hz}$	129.6	7.92, d $J = 8.0 \text{ Hz}$	129.7	7.91, dd $J = 8.0, 0.8 \text{ Hz}$	129.5
1	-	127.8	-	127.4	-	129.1
2	7.16, d $J = 1.6 \text{ Hz}$	110.6	7.14, s	115.2	7.19, d $J = 1.2 \text{ Hz}$	106.8
3	-	152.0	-	147.0	-	150.3
4	-	149.5	-	148.9	-	148.5
5	7.01, d $J = 8.4 \text{ Hz}$	111.4	7.25, dd $J = 8.0, 1.2 \text{ Hz}$	110.5	6.87, d $J = 8.0 \text{ Hz}$	108.8
6	7.26, dd $J = 8.4, 1.6 \text{ Hz}$	123.7	6.97, d $J = 8.4 \text{ Hz}$	123.8	7.16, d $J = 8.0 \text{ Hz}$	125.7
7	-	193.7	-	193.8	-	193.6
8	7.51, d $J = 15.2 \text{ Hz}$	118.0	7.50, d $J = 15.2 \text{ Hz}$	117.7	7.50, d $J = 15.2 \text{ Hz}$	118.0
9	7.87, d $J = 15.6 \text{ Hz}$	145.8	7.87, d $J = 15.2 \text{ Hz}$	146.0	7.86, d $J = 15.2 \text{ Hz}$	145.3
2'-OH	12.92, s	-	12.93, s	-	12.92, s	-
OH	-	-	6.04, s	-	-	-
CH ₃ / methylene	3.96, 3.93 s	56.2	3.97, s	56.2	6.05, s	101.8

Table 3.10 Tentative NMR chemical shift assignment of chalcones **67** and **68**.

Position	67 (CDCl ₃)		68 (CDCl ₃)	
	δ H	δ C	δ H	δ C
1'	-	133.9	-	133.8
2'	7.25, s	106.3	7.26, s	106.2
3'	-	153.2	-	153.3
4'	-	142.6	-	142.6
5'	-	153.2	-	153.3
6'	7.25, s	106.3	7.26, s	106.2
1	-	128.0	-	129.5
2	7.13, d $J = 1.6$ Hz	110.7	7.17, d $J = 0.8$ Hz	106.8
3	-	151.6	-	150.0
4	-	149.4	-	148.6
5	6.89, d $J = 8.0$ Hz	111.3	6.85, d $J = 8.0$ Hz	108.8
6	7.24, dd $J = 7.2, 1.6$ Hz	123.0	7.13, dd $J = 8.0, 1.2$ Hz	125.3
7	-	189.5	-	189.2
8	7.31, d $J = 15.6$ Hz	120.0	7.32, d $J = 15.6$ Hz	119.9
9	7.74, d $J = 15.6$ Hz	145.0	7.74, d $J = 15.6$ Hz	144.7
CH ₃ / methylene	3.93, 3.92, s	61.0, 56.6, 56.2, 56.1	6.03, 3.95, 3.93, s	101.8, 61.1, 56.5

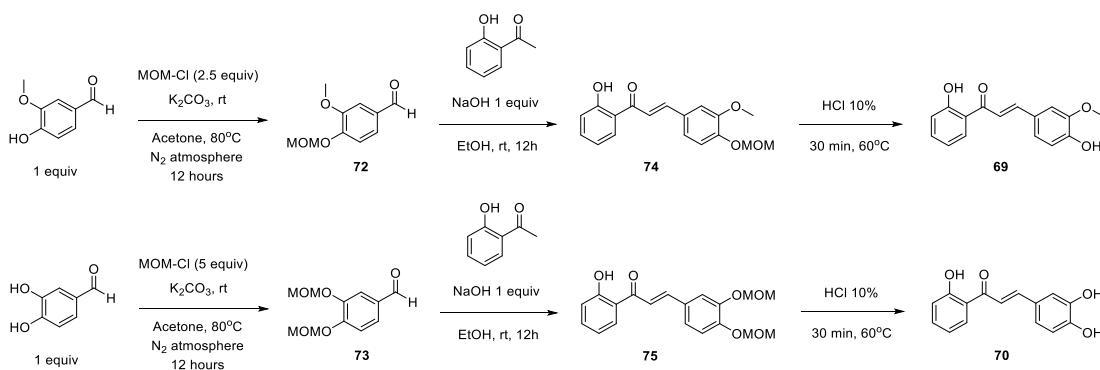


Figure 3.5 Synthesis of disubstituted chalcones with 4-OH on B-ring.

Table 3.11 The yields and characteristics of products **69**, **70**, **72-74**.

Products	Appearance	Yield (%)	Remarks
72	Yellow liquid	92	-
73	Yellow liquid	95	-
74	Yellow crystal	70	new
69	Yellow crystal	96	known
70	Orange crystal	66	known

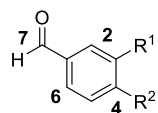
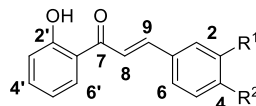
Because of the disadvantage of the direct preparation of 4-OH substituent, **69** and **70** were prepared *via* three steps covering the participation of protecting group (Chloromethyl methyl ether) (**Figure 3.5**). After preparing the protecting agent – MOMCl in high yield (74%), it was used to convert sensitive OH groups in benzaldehydes into less sensitive ether functional group in quantitative yield using the ratio between MOMCl and one OH group approximately 3 – 1 or more. These benzaldehydes were proceeded to react with 2'-hydroxyacetophenone to furnish chalcones **74** and **75**. **74** was obtained by column chromatography with 70% yield while **75** was not stable after acidified with 10% HCl leading to **70**. Chalcone **70** was purified by column chromatography with the yield of 66%. If **74** was used, the decomposition would accomplish **69**, the deprotection of MOM group by stirred **74** in 10% HCl at 60 °C for 15 min was carried out. Then, **69** was achieved in higher yield nearly 96% by

crystallization in MeOH. The yield and characterization of products in each step are illustrated in **Table 3.11**.

The structural identification of **69**, **70** and **72-74** was conducted by ^1H and ^{13}C NMR analysis, as shown in **Table 3.12**. Benzaldehyde bearing MOM **72** and chalcone **74** derived from **72** had a resemblance in the NMR signals on benzaldehyde ring part. Furthermore, the most similarity in ^1H and ^{13}C NMR between chalcones **69** and **74** was observed owing to their structural differentiation only from MOM. Unfortunately, **75** was not isolated to achieve NMR data; therefore, it is quite hard to compare ^1H and ^{13}C NMR between benzaldehyde **73** bearing MOM group and MOM-protected chalcone **70**, yet they still resemble together in the NMR signals on B-ring except MOM peaks not seen in chalcone **70**. The structural confirmation of the new compound **74** was indicated in HR-MS results. The exact mass of $\text{C}_{18}\text{H}_{18}\text{O}_5\text{Na}$ $[\text{M}+\text{Na}]^+$ requires 337.10519 and the outcome was shown as 337.10480.

3.2.2 Biological activity evaluation

Ten compounds (**57**, **60**, **61**, **63-68**, **70**) among fourteen have already been assessed for AMPK activation activity (**Figure 3.6**). Because this part includes analyses for disubstituted chalcones containing only OH, OCH_3 and methylenedioxy groups, **74** bearing MOM would be analyzed in the next part. From the graph, three compounds (**63**, **65** and **70**) with the potencies of 9.16, 8.90 and 5.10, respectively were the most active compounds even more potent than **53** with potency as 4.58. Regarding chalcones bearing dimethoxy substituents on B-ring, five compounds have already been screened for biological activity except **62**. **57** was found to be toxic to the cell so AMPK activation activity was not tested further. Three chalcones **60**, **61** and **66** carrying 2,4-dimethoxy, 2,5-dimethoxy and 3,5-dimethoxy substituents on B-ring exhibited low abilities to activate AMPK compared to **53** with potencies as 2.15, 1.81 and 2.69, respectively. Interestingly, 3,4-dimethoxy substituents on B-ring mediated **63** a dramatic potential with a value as 9.16 which was approximately twice as much as that of **53**. From this outcome, it can be seen that the hypothesis relating to chalcone

Table 3.12 Tentative NMR chemical shift assignment of chalcones **69**, **70**, **72-74**.72. R¹ = OCH₃, R² = OMOM73. R¹ = OMOM, R² = OMOM69. R¹ = OCH₃, R² = OH70. R¹ = R² = OH74. R¹ = OCH₃, R² = OMOM

Position	72 (CDCl ₃)		74 (CDCl ₃)		69 (CDCl ₃)		73 (CDCl ₃)		70 (acetone-d ₆)	
	δH	δC	δH	δC	δH	δC	δH	δC	δH	δC
1'	-	-	-	120.3	-	120.3	-	-	-	121.0
2'	-	-	-	163.7	-	163.7	-	-	-	164.4
3'	-	-	6.94, d <i>J</i> = 8.4 Hz	118.7	6.97, d <i>J</i> = 8.4 Hz	118.7	-	-	6.96, dd <i>J</i> = 8.4, 1.2 Hz	118.9
4'	-	-	7.49, td <i>J</i> = 7.8, 1.6 Hz	136.3	7.48, t <i>J</i> = 8.0 Hz	136.3	-	-	7.53, td <i>J</i> = 8.4, 1.6 Hz	137.0
5'	-	-	6.95, td <i>J</i> = 8.0, 0.8 Hz	118.9	6.94, t <i>J</i> = 7.6 Hz	118.9	-	-	6.97, td <i>J</i> = 8.4, 1.2 Hz	119.7
6'	-	-	7.93, dd <i>J</i> = 8.0, 1.2 Hz	129.8	7.92, d <i>J</i> = 7.6 Hz	129.6	-	-	8.22, dd <i>J</i> = 8.4, 1.6 Hz	131.1
1	-	130.6	-	128.0	-	127.4	-	131.2	-	128.1
2	7.12, s	114.4	7.50, s	115.8	7.14, s	110.5	7.62, s	115.5	7.40, d <i>J</i> = 2.0 Hz	116.2
3	-	149.6	-	147.1	-	148.9	-	147.5	-	146.4
4	-	151.4	-	152.6	-	147.0	-	152.7	-	149.6
5	6.93, d <i>J</i> = 8.8 Hz	109.3	7.02, dd <i>J</i> = 8.0, 0.4 Hz	111.9	7.02, d <i>J</i> = 8.4 Hz	115.1	7.23, d <i>J</i> = 8.4 Hz	116.0	7.27, dd <i>J</i> = 8.0, 2.0 Hz	116.5
6	7.11, d <i>J</i> = 8.8 Hz	125.3	7.32, dd <i>J</i> = 8.4, 2.0 Hz	125.0	7.25, d <i>J</i> = 8.0 Hz	123.8	7.45, d <i>J</i> = 8.0 Hz	126.3	6.93, d <i>J</i> = 8.0 Hz	123.9
7	9.54, s	190.2	-	193.8	-	193.8	9.80, s	190.8	-	194.8
8	-	-	7.51, d <i>J</i> = 15.2 Hz	118.3	7.50, d <i>J</i> = 14.4 Hz	117.7	-	-	7.79, d <i>J</i> = 15.2 Hz	118.1
9	-	-	7.87, d <i>J</i> = 15.6 Hz	145.6	7.87, d <i>J</i> = 15.2 Hz	146.0	-	-	7.85, d <i>J</i> = 15.2 Hz	147.0
2'-OH	-	-	12.91, s	-	12.94, s	-	-	-	13.08, s	-
OH	-	-	-	-	6.06, s	-	-	-	8.43, s	-
CH ₂	5.01 s	94.4	5.30 s	95.8	-	-	5.27, 5.24 s	95.4, 95.0	-	-
CH ₃	3.61, 3.21 s	55.7, 55.2	3.94, 3.56 s	56.5, 56.2	3.97, s	56.2	3.47 s	56.4, 56.3	-	-

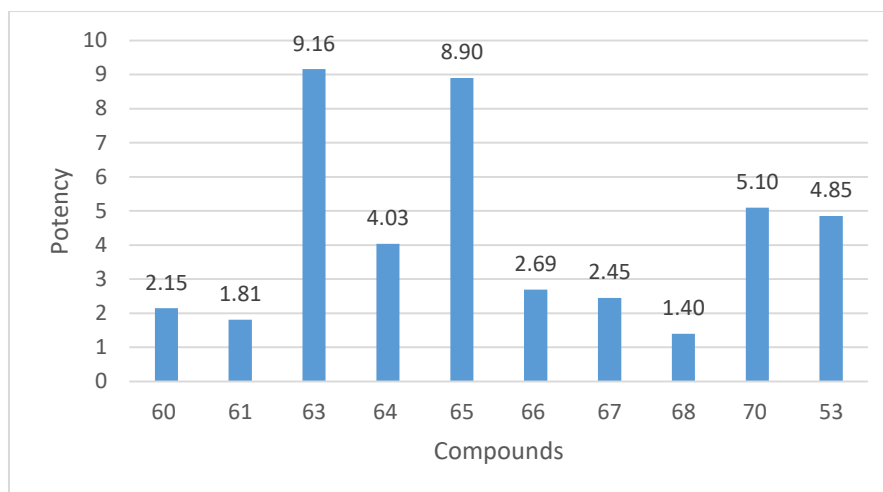


Figure 3.6 Biological evaluation of disubstituted chalcones with OH, OCH₃ and methylenedioxy on B-ring.

with 3-methoxy group being the potent one seemed to be not totally suitable; for example, **66** bearing 3,5-dimethoxy displayed the potency higher than **60** and **61** with no 3- or 5-OCH₃ and 5-OCH₃ substituents, respectively which correlated with the hypothesis, but **66** was less active than **63** carrying 3-OCH₃ around 3.4 times. Therefore, it was considered that 3-OCH₃ on B-ring should be the vital factor for improving the AMPK activation activity. The sufficient issue that made **63** distinct from the other three chalcones was 3,4-dimethoxy group on B-ring of **63** more compact than 2,4-, 2,5- and 3,5-dimethoxy. Thanks to compact B-ring, **63** may easily rotate B-ring around its symmetric axis, which was likely convenient for the interaction with AMPK kinase of **63** compared to the other three compounds with steric structure on B-ring. Ultimately, 3,4-disubstitution on B-ring seemed to play a radical role to boost the AMPK activation activity of chalcone derivatives compared to disubstitution at the other position. Thus, three compounds possessing 3,4-disubstitution covering OCH₃, OH and methylenedioxy such as **64**, **65** and **70** were evaluated thereafter. The results showed that two compounds **64** and **70** had potencies approximate with **53**, (4.03 and 5.10, respectively). However, **65** demonstrated a dominated AMPK activation with potency as 8.90, which was comparable to chalcone **63**. Moreover, 3',4',5'-trimethoxychalcones

with 3,4-disubstitution on B-ring such as **67** and **68** were also utilized to evaluate their activity. They bear the same B-ring with **63** and **65** but low activities with potencies as 2.45 and 1.40 respectively were observed, which underlined that A-ring as 3',4',5'-trimethoxyacetophenone might not be a suitable component to improve AMPK activation activity of chalcone derivatives. Finally, **63** and **65** were chosen as promising compounds for activating AMPK and it was found that 3,4-position on B-ring of 2'-hydroxychalcones could be potent places to settle substituents in order to develop activities of chalcones compared to the other position couples. Therefore, a series of chalcone derivatives were prepared with A-ring as 2'-hydroxyacetophenone while B-ring bore a diverse variety of substituents at 3,4-position to compare with **63** and **65** possessing dimethoxy and methylenedioxy substituents.

3.3 Synthesis of chalcones with 3,4-disubstitution on B-ring

3.3.1 Synthesis and structural elucidation

Firstly, vanillin, isovanillin and 3,4-dihydroxybenzaldehyde were alkylated following the method addressed by Matsuda *et al.* to furnish twelve benzaldehyde derivatives (**76–87**) with various groups at 3,4-position on phenyl ring.⁵⁶ Twelve chalcones with 3,4-disubstitution on B-ring (**88–99**) were synthesized from these benzaldehyde derivatives (**76–87**) by aldol condensation with 2'-hydroxyacetophenone (**Figure 3.7**). The yield and appearance of these chalcones were described in **Table 3.13**. Most benzaldehyde products were obtained in moderate to good yields.

The structural determination of twenty-four benzaldehyde derivatives and chalcones were elucidated by ¹H and ¹³C NMR analysis as shown in **Tables 3.14–3.19**. Each table shows the ¹H and ¹³C NMR signals of benzaldehyde derivatives and their corresponding chalcones. The signals of benzaldehyde products resemble the ones on B-ring of their corresponding chalcones. All chalcones had the same signals of those in A-ring of 2'-hydroxyacetophenone. The differences of signals on B-ring only came

from various substituents connected at 3,4-position but the ones on B-ring bear a resemblance to one another because of substituents being fixed at 3,4-position. There are seven new compounds (**89**, **92-95**, **98**, **99**) and their molecular weights were confirmed by HR-MS. The results of MS are presented in **Table 3.13**.

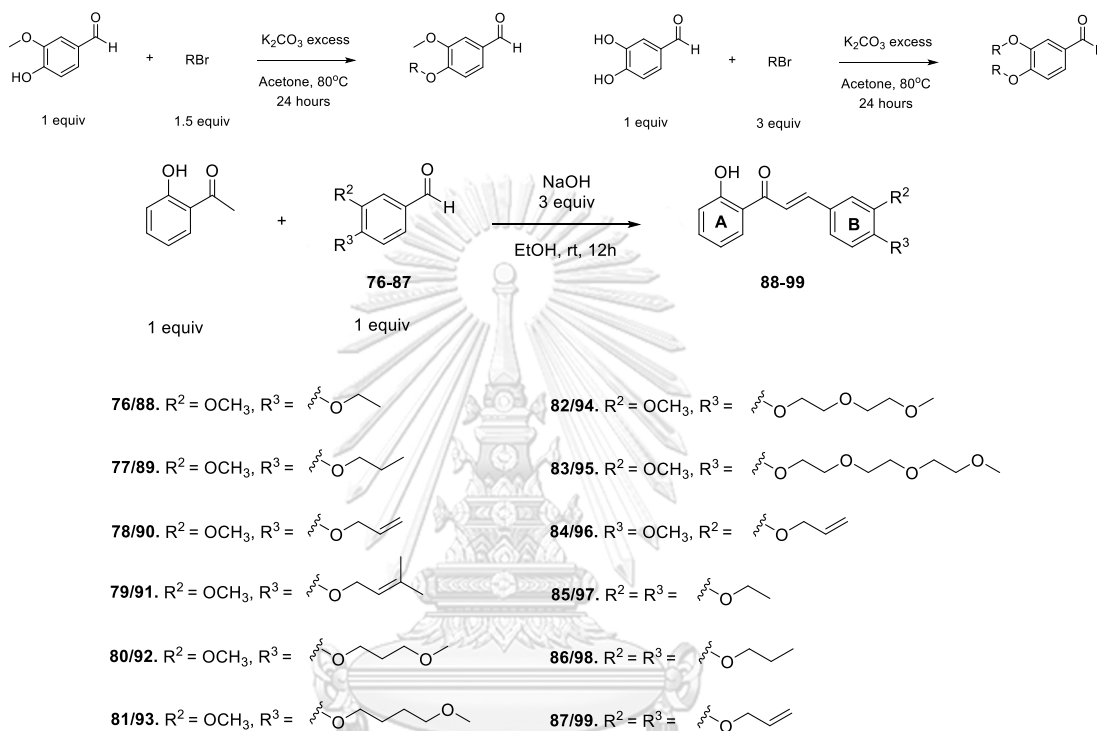


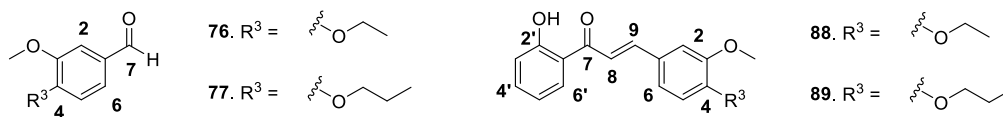
Figure 3.7 Synthesis of di-substituted benzaldehydes and chalcones with 3,4-disubstitution on B-ring.

3.3.2 Biological activity evaluation

There are eleven chalcones with AMPK activation potency results except **97** (**Figure 3.8**). The results were illustrated by the bar chart including the potency of **74** bearing MOM and **63** for comparison. A variety of alkyl substituents were connected to OH groups of vanillin, isovanillin and 3,4-dihydroxybenzaldehyde to modify the

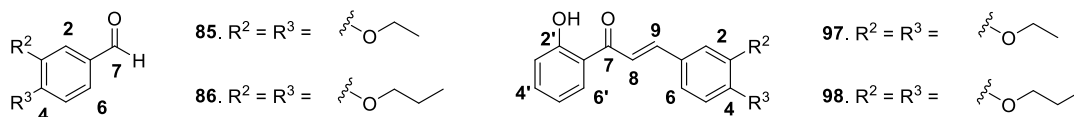
Table 3.13 Yields, characteristics and HR-MS (ESI) outcomes of products 82-105.

Benzaldehydes/ Chalcones	Appearance	Yield (%)	Remarks	Exact Mass	HR-MS (ESI)
76	White liquid	80	-	-	-
77	White liquid	85	-	-	-
78	Brown liquid	86	-	-	-
79	Brown liquid	88	-	-	-
80	Brown liquid	78	-	-	-
81	Brown liquid	85	-	-	-
82	Brown liquid	82	-	-	-
83	Brown liquid	76	-	-	-
84	Brown liquid	78	-	-	-
85	Brown liquid	89	-	-	-
86	Brown liquid	91	-	-	-
87	Brown liquid	87	-	-	-
88	Yellow crystal	64	known	-	-
89	Yellow crystal	75	new	335.12593	335.12410
90	Yellow crystal	78	known	-	-
91	Yellow crystal	61	known	-	-
92	Yellow crystal	74	new	365.13649	365.13620
93	Yellow crystal	65	new	379.15214	379.15150
94	Yellow liquid	79	new	395.14706	395.14650
95	Yellow liquid	54	new	439.17327	439.17360
96	Yellow crystal	67	known	-	-
97	Yellow crystal	51	known	-	-
98	Yellow crystal	80	new	363.15723	363.15710
99	Yellow crystal	69	new	359.12593	359.12590

Table 3.14 NMR chemical shift assignment of benzaldehydes and chalcones **76**, **77**,**88** and **89**.

Position	76 (CDCl ₃)		88 (CDCl ₃)		77 (CDCl ₃)		89 (CDCl ₃)	
	δ H	δ C	δ H	δ C	δ H	δ C	δ H	δ C
1'	-	-	-	120.3	-	-	-	120.1
2'	-	-	-	163.7	-	-	-	163.6
3'	-	-	6.91, d <i>J</i> = 8.4 Hz	118.8	-	-	7.00, dd <i>J</i> = 8.4, 0.8 Hz	118.6
4'	-	-	7.49, td <i>J</i> = 8.8, 1.6 Hz	136.3	-	-	7.45, td <i>J</i> = 8.4, 1.6 Hz	136.
5'	-	-	6.94, td <i>J</i> = 8.0, 0.8 Hz	118.9	-	-	6.90, td <i>J</i> = 8.0, 0.8 Hz	118.7
6'	-	-	7.93, dd <i>J</i> = 8.0, 1.6 Hz	129.7	-	-	7.91, dd <i>J</i> = 8.4, 1.6 Hz	129.6
1	-	129.9	-	127.6	-	130.1	-	127.4
2	7.32, s	109.2	7.18, d <i>J</i> = 1.6 Hz	111.0	7.40, d <i>J</i> = 1.6 Hz	109.6	7.15, d <i>J</i> = 2.0 Hz	111.0
3	-	149.7	-	151.5	-	150.1	-	151.6
4	-	153.9	-	149.7	-	154.4	-	149.7
5	6.88, d <i>J</i> = 8.0 Hz	111.3	7.25, dd <i>J</i> = 8.4, 2.0 Hz	112.5	6.96, d <i>J</i> = 8.4 Hz	111.6	7.21, dd <i>J</i> = 8.4, 2.0 Hz	112.5
6	7.34, d <i>J</i> = 8.4 Hz	126.6	7.03, d <i>J</i> = 8.0 Hz	123.7	7.43, dd <i>J</i> = 8.0, 2.0 Hz	126.9	6.87, d <i>J</i> = 8.4 Hz	123.6
7	9.75, s	190.7	-	193.8	9.84, s	191.0	-	193.6
8	-	-	7.52, d <i>J</i> = 15.6 Hz	117.9	-	-	7.49, d <i>J</i> = 15.2 Hz	117.6
9	-	-	7.89, d <i>J</i> = 15.2 Hz	145.9	-	-	7.85, d <i>J</i> = 15.2 Hz	145.8
2'-OH	-	-	12.92, s	-	-	-	12.96, s	-
CH ₂	4.10, q <i>J</i> = 6.4 Hz	64.5	4.17, q <i>J</i> = 7.2 Hz	64.6	4.06, t <i>J</i> = 6.8 Hz 1.90, sext <i>J</i> = 7.2 Hz	70.8, 22.4	4.00, t <i>J</i> = 6.8 Hz 1.88, sext <i>J</i> = 7.6 Hz	70.5, 22.4
CH ₃	3.84, s 1.42, t <i>J</i> = 7.2 Hz	55.9, 14.5	3.96, s 1.50, t <i>J</i> = 7.2 Hz	56.3, 14.8	3.92, s 1.06, t <i>J</i> = 7.6 Hz	56.2, 10.5	3.92, s 1.04, t <i>J</i> = 7.6 Hz	56.2, 10.4

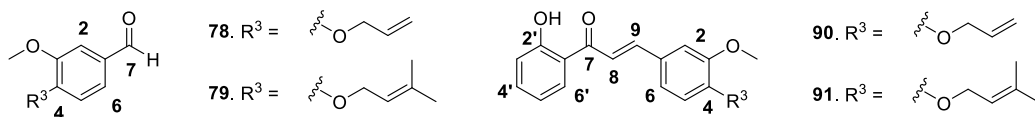
Table 3.15 NMR chemical shift assignment of benzaldehydes and chalcones **85**, **86**, **97** and **98**.



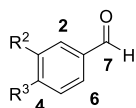
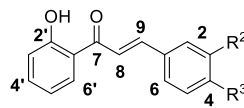
Position	85 (CDCl ₃)		97 (CDCl ₃)		86 (CDCl ₃)		98 (CDCl ₃)	
	δ H	δ C	δ H	δ C	δ H	δ C	δ H	δ C
1'	-	-		120.4	-	-	-	120.2
2'	-	-		163.7	-	-	-	163.6
3'	-	-	7.25, m	118.8	-	-	7.01, d $J = 8.4$ Hz	118.6
4'	-	-	7.49, t $J = 8.0$ Hz	136.3	-	-	7.47, t $J = 8.4$ Hz	136.1
5'	-	-	6.94, t $J = 7.6$ Hz	118.9	-	-	6.93, t $J = 7.6$ Hz	118.8
6'	-	-	7.93, d $J = 8.0$ Hz	129.7	-	-	7.92, dd $J = 8.0, 1.2$ Hz	129.6
1	-	130.0		127.7	-	130.0	-	127.6
2	7.38, s	111.0	7.20, s	113.0	7.39, s	111.4	7.19, s	113.2
3	-	149.2		152.0	-	149.6	-	149.4
4	-	154.4		154.4	-	154.8	-	152.3
5	6.93, d $J = 8.4$ Hz	111.8	6.89, d $J = 8.4$ Hz	113.1	6.94, d $J = 8.0$ Hz	112.0	7.22, dd $J = 8.0, 1.2$ Hz	113.4
6	7.39, d $J = 8.0$ Hz	126.6	7.03, d $J = 8.4$ Hz	123.8	7.40, dd $J = 8.8, 1.6$ Hz	126.6	6.89, d $J = 8.0$ Hz	123.8
7	9.80, s	191.0		193.8	9.81, s	191.1	-	193.7
8	-	-	7.50, d $J = 15.2$ Hz	117.8	-	-	7.49, d $J = 15.2$ Hz	117.7
9	-	-	7.88, d $J = 15.2$ Hz	146.0	-	-	7.86, d $J = 15.2$ Hz	145.9
2'-OH	-	-	12.93, s		-	-	12.97, s	-
CH ₂	4.16, q $J = 6.8$ Hz	64.7, 64.6	4.17, q $J = 6.8$ Hz	65.1, 64.7	4.03, t, $J = 6.8$ Hz	70.7, 22.6	4.03, t, $J = 6.8$ Hz	71.1, 70.6, 22.8, 22.6
	4.13, q $J = 6.8$ Hz		4.16, q $J = 6.8$ Hz		4.01, t, $J = 6.8$ Hz		4.01, t, $J = 6.8$ Hz	
					1.87, sext, $J = 7.2$ Hz		1.88, sext, $J = 7.0$ Hz	
CH ₃	1.47, t $J = 7.2$ Hz	14.7, 14.6	1.50, t $J = 6.8$ Hz	15.0, 14.8	1.05, t $J = 7.2$ Hz	10.5	1.08, t $J = 7.6$ Hz	10.6, 10.5
	1.45, t $J = 7.2$ Hz		1.49, t $J = 7.2$ Hz		1.04, t $J = 7.2$ Hz		1.06, t $J = 7.6$ Hz	

Table 3.16 NMR chemical shift assignment of benzaldehydes and chalcones **78**, **79**,

90 and 91.



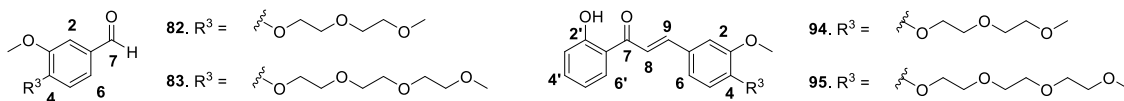
Position	78 (CDCl ₃)		90 (CDCl ₃)		79 (CDCl ₃)		91 (CDCl ₃)	
	δH	δC	δH	δC	δH	δC	δH	δC
1'	-	-	-	120.2	-	-	-	120.3
2'	-	-	-	163.6	-	-	-	163.7
3'	-	-	6.93, d, <i>J</i> = 8.0 Hz	118.6	-	-	6.92, d, <i>J</i> = 8.4 Hz	118.7
4'	-	-	7.47, t, <i>J</i> = 8.0 Hz	136.2	-	-	7.48, t, <i>J</i> = 7.2 Hz	136.2
5'	-	-	6.90, t, <i>J</i> = 8.0 Hz	118.8	-	-	6.94, t, <i>J</i> = 8.0 Hz	118.8
6'	-	-	7.91, d, <i>J</i> = 8.0 Hz	129.6	-	-	7.93, d, <i>J</i> = 8.0 Hz	129.7
1	-	124.4	-	127.9	-	130.0	-	127.6
2	7.42, s	109.6	7.16, s	111.0	7.36, d <i>J</i> = 1.6 Hz	109.3	7.17, s	110.8
3	-	130.4	-	151.0	-	138.7	-	151.4
4	-	153.7	-	149.8	-	154.0	-	149.9
5	6.98, d <i>J</i> = 8.8 Hz	112.2	7.00, d <i>J</i> = 8.4 Hz	113.1	6.93, d <i>J</i> = 8.4 Hz	111.8	7.24, dd <i>J</i> = 8.4, 1.6 Hz	112.9
6	7.43, d <i>J</i> = 6.4 Hz	126.7	7.21, d <i>J</i> = 8.4 Hz	123.4	7.39, dd <i>J</i> = 8.4, 2.0 Hz	126.7	7.02, d <i>J</i> = 8.4 Hz	123.6
7	9.85, s	191.0	-	193.6	9.80, s	190.9	-	193.8
8	-	-	7.50, d <i>J</i> = 15.2 Hz	118.0	-	-	7.51, d <i>J</i> = 15.6 Hz	117.8
9	-	-	7.85, d <i>J</i> = 15.6 Hz	145.7	-	-	7.88, d <i>J</i> = 15.2 Hz	145.9
2'-OH	-	-	12.93, s	-	-	-	12.93, s	-
C tert	-	-	-	-	-	150.0	-	138.4
CH	6.08, ddt <i>J</i> = 16.4, 10.8, 5.2 Hz	132.4	6.08, ddt <i>J</i> = 16, 10.8, 5.6 Hz	132.8	5.47, tt <i>J</i> = 6.8, 1.2 Hz	119.0	5.52, t <i>J</i> = 6 Hz	119.5
CH ₂	5.44, d, <i>J</i> = 17.2 Hz 5.34, d, <i>J</i> = 10.4 Hz 4.71, d, <i>J</i> = 5.6 Hz	118.9, 70.0	5.42, d, <i>J</i> = 16.8 Hz 5.32, d, <i>J</i> = 10.4 Hz 4.65, d, <i>J</i> = 5.6 Hz	118.5, 69.8	4.63, d <i>J</i> = 6.8 Hz	66.0	4.65, d <i>J</i> = 6.4 Hz	66.0
CH ₃	3.94, s	56.2	3.94, s	56.2	3.88, 1.75, 1.72, s	56.0, 25.8, 18.3	3.95, 1.79, 1.76, s	56.2, 25.9, 18.4

Table 3.17 NMR chemical shift assignment of benzaldehydes and chalcones **84**, **87**,**96** and **99**.**84.** R³ = OCH₃, R² = **87.** R² = R³ = **96.** R³ = OCH₃, R² = **99.** R² = R³ =

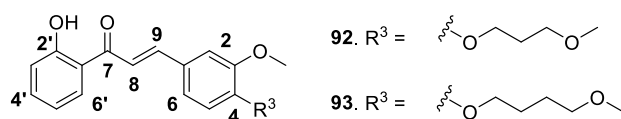
Position	84 (CDCl ₃)		96 (CDCl ₃)		87 (CDCl ₃)		99 (CDCl ₃)	
	δ H	δ C	δ H	δ C	δ H	δ C	δ H	δ C
1'	-	-	-	120.2	-	-	-	120.3
2'	-	-	-	163.7	-	-	-	163.7
3'	-	-	6.91, d <i>J</i> = 8.0 Hz	118.7	-	-	7.25, dd <i>J</i> = 9.2, 2.4 Hz	118.8
4'	-	-	7.48, t, <i>J</i> = 8.8 Hz	136.2	-	-	7.48, t, <i>J</i> = 8.8 Hz	136.3
5'	-	-	6.93, t, <i>J</i> = 7.6 Hz	118.8	-	-	6.94, t, <i>J</i> = 8.4 Hz	118.9
6'	-	-	7.91, dd <i>J</i> = 8.0, 1.6 Hz	129.6	-	-	7.91, d <i>J</i> = 8.0 Hz	129.6
1	-	129.6	-	127.7	-	129.7	-	128.0
2	7.20, s	110.4	7.19, s	111.7	7.18, s	111.2	7.21, s	113.7
3	-	154.5	-	152.5	-	148.3	-	151.6
4	-	148.1	-	148.4	-	153.4	-	148.8
5	6.78, d <i>J</i> = 8.4 Hz	110.7	7.27, dd <i>J</i> = 8.0, 1.6 Hz	113.1	6.74, d <i>J</i> = 8.0 Hz	112.0	6.92, d <i>J</i> = 8.4 Hz	113.8
6	7.25, dd <i>J</i> = 8.4, 1.6 Hz	126.2	7.02, d <i>J</i> = 8.4 Hz	123.8	7.19, d <i>J</i> = 8.0 Hz	125.8	7.02, d <i>J</i> = 8.4 Hz	123.8
7	9.63, s	190.3	-	193.7	9.60, s	190.1	-	193.7
8	-	-	7.49, d <i>J</i> = 15.2 Hz	118.0	-	-	7.49, d <i>J</i> = 15.6 Hz	118.2
9	-	-	7.86, d <i>J</i> = 15.2 Hz	145.7	-	-	7.86, d <i>J</i> = 15.2 Hz	145.7
2'-OH	-	-	12.92, s	-	-	-	12.91, s	-
CH	5.90, ddt <i>J</i> = 16.0, 10.4, 5.2 Hz	132.3	6.10, m	133.1	5.85, ddt <i>J</i> = 16.0, 10.4, 5.2 Hz	132.4, 132.1	6.10, m	133.3, 132.9
CH ₂	5.26, d, <i>J</i> = 17.2 Hz 5.12, d, <i>J</i> = 10.4 Hz 4.44, d, <i>J</i> = 4.8 Hz	117.8, 69.2	5.46, d, <i>J</i> = 17.2 Hz 5.34, d, <i>J</i> = 10.4 Hz 4.68, d, <i>J</i> = 5.6 Hz	118.4, 70.2	5.25, d, <i>J</i> = 17.2 Hz 5.09, d, <i>J</i> = 9.6 Hz 4.41, d, <i>J</i> = 4.8 Hz	117.4, 117.2, 69.1, 69.0	5.47, d, <i>J</i> = 17.2 Hz 5.45, d, <i>J</i> = 17.2 Hz 5.33, d, <i>J</i> = 10.8 Hz 5.32, d, <i>J</i> = 10.4 Hz 4.68, d, <i>J</i> = 4.4 Hz 4.67, d, <i>J</i> = 5.2 Hz	118.1, 118.0, 70.4, 69.9
CH ₃	3.73, s	55.6	3.92, s	56.2	-	-	-	-

Table 3.18 NMR chemical shift assignment of benzaldehydes and chalcones **82**, **83**,

94 and 95.



Position	82 (acetone- <i>d</i> ₆)		94 (CDCl ₃)		83 (acetone- <i>d</i> ₆)		95 (CDCl ₃)	
	δH	δC	δH	δC	δH	δC	δH	δC
1'	-	-	-	120.3	-	-	-	120.2
2'	-	-	-	163.7	-	-	-	163.6
3'	-	-	6.95, d, <i>J</i> = 8.0 Hz	118.7	-	-	6.92, d, <i>J</i> = 8.0 Hz	118.6
4'	-	-	7.49, t, <i>J</i> = 8.8 Hz	136.3	-	-	7.46, t, <i>J</i> = 7.6 Hz	136.2
5'	-	-	6.94, t, <i>J</i> = 7.2 Hz	118.8	-	-	6.91, t, <i>J</i> = 7.6 Hz	118.8
6'	-	-	7.93, d, <i>J</i> = 8.0 Hz	129.7	-	-	7.91, d, <i>J</i> = 8.0 Hz	129.6
1	-	129.5	-	128.1	-	130.6	-	128.0
2	7.38, s	109.0	7.16, s	111.4	7.39, d, <i>J</i> = 1.6 Hz	110.1	7.14, s	111.2
3	-	149.0	-	151.4	-	150.1	-	151.3
4	-	153.2	-	149.9	-	154.2	-	149.8
5	7.08, d <i>J</i> = 8.0 Hz	111.3	7.02, d <i>J</i> = 8.4 Hz	113.4	7.10, d <i>J</i> = 8.0 Hz	112.4	6.99, d <i>J</i> = 8.0 Hz	113.2
6	7.47, d <i>J</i> = 7.6 Hz	125.2	7.24, d <i>J</i> = 8.4 Hz	123.5	7.48, dd <i>J</i> = 8.0, 1.2 Hz	126.1	7.21, d <i>J</i> = 8.4 Hz	123.4
7	9.81, s	190.2	-	193.7	9.83, s	190.9	-	193.6
8	-	-	7.51, d <i>J</i> = 15.6 Hz	118.1	-	-	7.49, d <i>J</i> = 14.8 Hz	118.0
9	-	-	7.87, d <i>J</i> = 15.6 Hz	145.7	-	-	7.84, d <i>J</i> = 15.2 Hz	145.7
2'-OH	-	-	12.91, s	-	-	-	12.91, s	-
CH ₂	4.21, t, <i>J</i> = 4.6 Hz 3.84, t, <i>J</i> = 5.2 Hz 3.64, t, <i>J</i> = 4.4 Hz 3.48, t, <i>J</i> = 4.8 Hz	70.9, 69.5, 68.3, 67.7	4.25, t, <i>J</i> = 4.8 Hz 3.92, t, <i>J</i> = 4.4 Hz 3.73, t, <i>J</i> = 4.4 Hz 3.57, t, <i>J</i> = 4.8 Hz	72.1, 71.0, 69.7, 68.6,	4.22, t, <i>J</i> = 4.4 Hz 3.85, t, <i>J</i> = 4.8 Hz 3.66, t, <i>J</i> = 4.8 Hz 3.58, t, <i>J</i> = 4.8 Hz 3.56, t, <i>J</i> = 5.0 Hz 3.45, t, <i>J</i> = 4.6 Hz	72.0, 70.8, 70.5, 70.4, 69.4, 68.7	4.22, t, <i>J</i> = 4.6 Hz 3.89, t, <i>J</i> = 4.8 Hz 3.72, t, <i>J</i> = 4.4 Hz 3.66, t, <i>J</i> = 4.8 Hz 3.63, t, <i>J</i> = 4.8 Hz 3.52, t, <i>J</i> = 4.8 Hz	72.0, 70.9, 70.7, 70.6, 69.5, 68.5,
CH ₃	3.86, 3.28, s	57.2, 54.6	3.93, 3.39, s	59.2, 56.3	3.87, 3.26, s	58.2, 55.4	3.91, 3.35, s	59.0, 56.1

Table 3.19 NMR chemical shift assignment of chalcones **92** and **93**.

Position	92 (CDCl ₃)		93 (CDCl ₃)	
	δ H	δ C	δ H	δ C
1'	-	120.2	-	120.2
2'	-	163.6	-	163.6
3'	6.90, d, $J = 8.0$ Hz	118.6	7.23, dd, $J = 8.0, 1.6$ Hz	118.7
4'	7.44, t, $J = 7.2$ Hz	136.1	7.47, t, $J = 7.6$ Hz	136.2
5'	6.89, t, $J = 6.8$ Hz	118.7	6.92, t, $J = 7.2$ Hz	118.8
6'	7.90, d, $J = 7.6$ Hz	129.6	7.92, d, $J = 7.6$ Hz	129.6
1	-	127.6	-	127.6
2	7.14, s	111.1	7.16, s	111.2
3	-	151.5	-	151.6
4	-	149.7	-	149.8
5	6.98, d, $J = 8.4$ Hz	112.7	6.89, d, $J = 8.4$ Hz	112.7
6	7.21, d, $J = 8.0$ Hz	123.6	7.01, d, $J = 8.4$ Hz	123.7
7	-	193.6	-	193.7
8	7.48, d, $J = 15.2$ Hz	117.7	7.50, d, $J = 15.6$ Hz	117.8
9	7.84, d, $J = 15.2$ Hz	145.7	7.86, d, $J = 15.2$ Hz	145.8
2'-OH	12.95, s		12.93, s	
CH ₂	4.14, t, $J = 6.4$ Hz, 3.55, t, $J = 6.0$ Hz 2.10, p, $J = 6.0$ Hz	69.1, 66.1, 29.5	4.09, t, $J = 6.4$ Hz 3.45, t, $J = 6.0$ Hz 1.93, p, $J = 6.8$ Hz 1.76, p, $J = 6.4$ Hz	72.4, 68.9, 26.2, 26.0
CH ₃	3.91, 3.34, s	58.7, 56.1	3.92, 3.34, s	58.6, 56.2

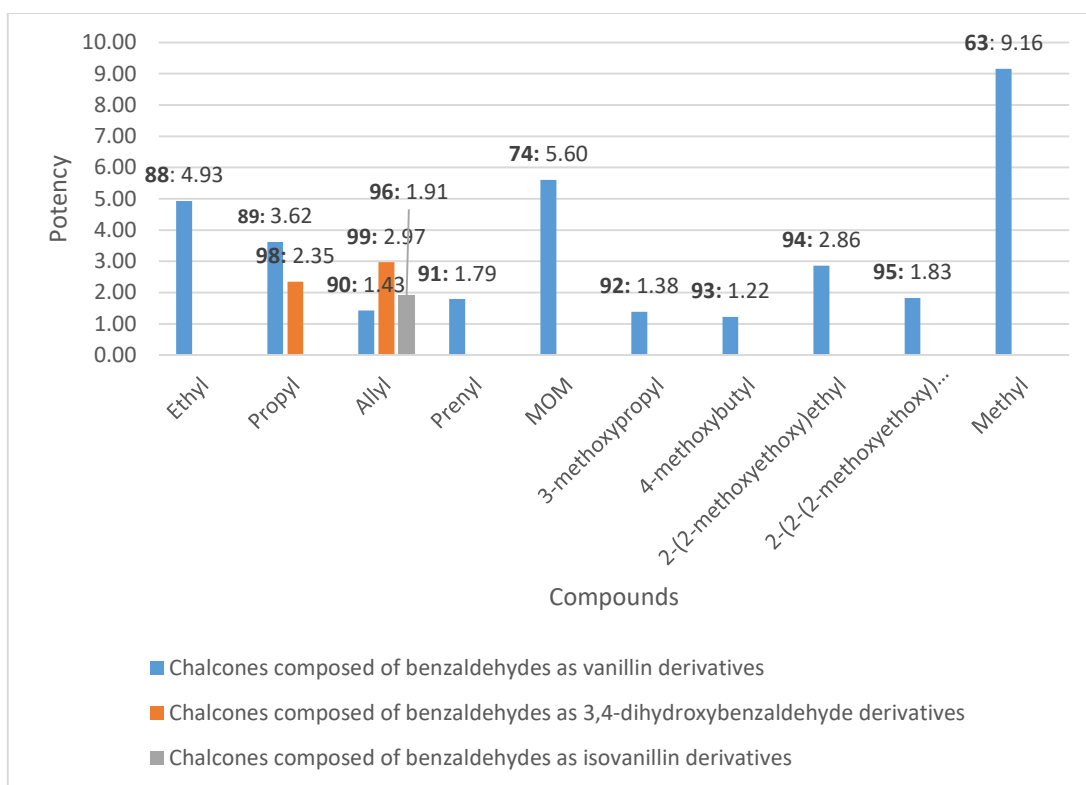


Figure 3.8 Biological evaluation of chalcones with 3,4-disubstitution on B-ring.

structures of chalcones. The effect of the substituents was exclusively evaluated at 3,4-position on B-ring in order to find other compounds more potent than **63** and **65**. If chalcones were derived from vanillin derivatives (**74**, **88-95**), the OCH₃ group at 3-position will remain and different substituents will extend the OH group at 4-position. In the case that the chalcone was derived from isovanillin derivatives (**96**), 4-position will be maintained with OCH₃ group while allyl substituent linked to the OH group at 3-position will be evaluated. Regarding chalcones prepared from 3,4-dihydroxybenzaldehyde derivatives (**98**, **99**), both substituents at 3,4-position will be varied. Firstly, from biological outcomes of chalcones derived from vanillin derivatives (**74**, **88-95**), MOM and ethyl groups seemed to be the most potent substituents to produce **74** and **88** with the potencies of 5.60 and 4.93, respectively. These two compounds were the best candidates in eleven compounds as well; nevertheless, their potencies were only around two-third to that of **63**. In addition, **89** along with **94** bearing propyl and 2-(2-methoxyethoxy)ethyl substituents exhibited lower potencies

of 3.62 and 2.86, respectively. Moreover, the other molecules synthesized from vanillin derivatives (**90-93, 95**) were recognized to have potencies lower than 2. As a result, it could be realized that shorter saturated carbon chains should be powerful connectors for improving AMPK activation activity of chalcones more than longer saturated carbon chains; for instance, the potency of **63** was higher than that of **88** and the potency of **88** was better than that of **89** while **63, 88** and **89** possessed methyl, ethyl and propyl groups, respectively. However, unsaturated carbon chains such as allyl and prenyl seemed to lessen biological activity of chalcones (**90, 91**). Besides, saturated carbon chains containing oxygen atoms were also a good choice; for example, **74** and **94** bearing MOM and 2-(2-methoxyethoxy)ethyl respectively displayed quite noticeable potencies. There were some fluctuations in potencies among chalcones carrying substituents including oxygen atoms and they were rationalized by the assumption in **Table 3.20**. It can be noticed that the higher the ratios of a number of carbon and oxygen atoms of substituents, the less potency of chalcones. Because the ratio of a number of carbon and oxygen atoms in a molecule has a close linkage to the water-solubility and hydrogen bonding formation of that molecule; therefore, these factors may take responsibility for the differences among chalcones having substituents comprising oxygen atoms (**74, 92-95**). On the other hand, with respect to chalcones derived from 3,4-dihydroxybenzaldehyde and isovanillin derivatives, three chalcones with allyl substituents (**90, 96** and **99**) could be used to compare one another. It was found that **99** prepared from 3,4-dihydroxybenzaldehyde derivatives was more potent than **96** synthesized from isovanillin derivatives whilst **96** was better than **90** derived from vanillin derivatives with potencies such as 2.97, 1.91 and 1.43, respectively. Nonetheless, in the case of propyl substituent, **89** prepared from vanillin derivatives was more powerful than **98** synthesized from 3,4-dihydroxybenzaldehyde derivatives. Thus, more tested compounds obtained from isovanillin and 3,4-dihydroxybenzaldehyde derivatives were required to confirm the trend in the biological activity of chalcones with 3,4-disubstitution on B-ring.

Table 3.20 Relationship between the ratio of a number of carbon and oxygen atoms of substituents and compound potency.

Compound	Substituent	The ratio of a number of carbon and oxygen atoms of substituents	Potency
74		1	5.6
92		2	1.38
93		2.5	1.22
94		1.67	2.86
95		1.75	1.83

3.4 Synthesis of chalcones with 2,4,5-trisubstitution on B-ring

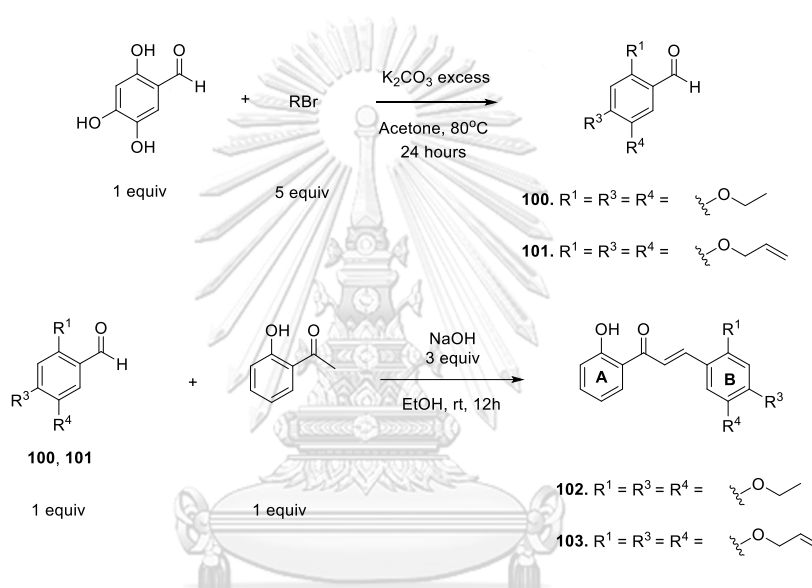
3.4.1 Synthesis and structural elucidation

As mentioned above, **48** was recognized to be the most promising candidate for inhibiting CFTR via AMPK activation.⁵³ Therefore, **48** was a skeletal model of chalcones with 2,4,5-trisubstitution on B-ring activating AMPK. Therefore, **48** was chosen as the potent former structure and then some structural modifications were performed to ameliorate its AMPK activation activity. Two separate routes were applied to form two different series.

In the first route, 2,4,5-trihydroxybenzaldehyde was used to carry out S_N2 reaction with two alkyl halides to achieve two benzaldehyde derivatives (**100**, **101**) in high yield (more than 85%). Some by-products were also observed when substitution reaction only occurred on one or two OH groups; therefore, the ratio of the amount between alkyl halide and 2,4,5-trihydroxybenzaldehyde should be 4 or 5 instead of 3 in order to obtain trisubstituted products in high yield (85 and 87%). **100** and **101** then followed by aldol condensation with 2'-hydroxyacetophenone to furnish **102** and **103**

Table 3.21 Yields and characteristics of products **106-109**.

Products	Appearance	Yield (%)	Remarks
100	White crystal	85	-
101	White crystal	87	-
102	Yellow crystal	76	new
103	Yellow crystal	85	new

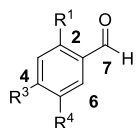
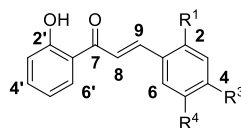
**Figure 3.9** Synthesis of tri-substituted benzaldehydes and 2'-hydroxychalcones with 2,4,5-trisubstitution on B-ring.

(**Figure 3.9**). Both chalcones were obtained in good yield (76 and 85%). **100**, **101** and **102** were isolated by column chromatography while **103** was precipitated after acidified by 10% HCl, then purified by crystallization in MeOH. The yield and appearance of these benzaldehydes and chalcones are illustrated in **Table 3.21**.

The structural identification of four benzaldehyde derivatives and chalcones were operated by ¹H and ¹³C NMR analysis, as presented in **Table 3.22**. The ¹H and ¹³C NMR signals of two benzaldehydes were similar to those on the B-ring of two corresponding chalcones. Both chalcones are new compounds. The exact masses of

Table 3.22 NMR chemical shift assignment of benzaldehydes and chalcones 100-

103.

100. R¹ = R³ = R⁴ = 101. R¹ = R³ = R⁴ = 102. R¹ = R³ = R⁴ = 103. R¹ = R³ = R⁴ =

Position	100 (CDCl ₃)		102 (CDCl ₃)		101 (CDCl ₃)		103 (DMSO-d ₆)	
	δH	δC	δH	δC	δH	δC	δH	δC
1'	-	-	-	120.2	-	-	-	120.5
2'	-	-	-	163.7	-	-	-	162.2
3'	-	-	7.02, d, J = 8.4 Hz	118.7	-	-	6.98, d, J = 8.4 Hz	118.1
4'	-	-	7.47, td J = 7.6, 1.2 Hz	135.9	-	-	7.55, t, J = 8.0 Hz	136.0
5'	-	-	6.93, t, J = 7.6 Hz	118.8	-	-	7.00, t, J = 7.6 Hz	118.9
6'	-	-	7.91, d, J = 8.0 Hz	129.6	-	-	8.24, d, J = 8.0 Hz	130.5
1	-	110.0	-	109.4	-	118.2	-	114.9
2	-	158.0	-	155.0	-	157.6	-	153.6
3	6.47, s	98.5	6.51, s	99.4	6.48, s	99.5	6.78, s	100.2
4	-	153.2	-	151.4	-	155.3	-	152.6
5	-	138.9	-	138.6	-	143.0	-	142.2
6	7.32, s	111.3	7.16, s	116.0	7.30, s	112.0	7.61, s	113.7
7	10.32, s	188.4	-	194.4	10.30, s	187.9	-	193.6
8	-	-	7.70, d, J = 15.6 Hz	118.3	-	-	7.87, d, J = 15.2 Hz	118.0
9	-	-	8.16, d, J = 15.6 Hz	141.5	-	-	8.20, d, J = 15.6 Hz	139.5
2'-OH	-	-	13.10, s	-	-	-	12.87, s	-
CH	-	-	-	-	6.02 (m)	133.1, 132.6, 132.4	6.09, m	134.0, 133.4, 133.2
CH ₂	4.15, q, J = 7.2 Hz 4.11, q, J = 6.8 Hz 4.08, q, J = 6.8 Hz	65.2, 65.1, 64.9	4.13, m	66.1, 65.1, 64.9	5.41, dd, J = 17.2, 1.2 Hz 5.39, dd, J = 17.2, 1.2 Hz 5.38, dd, J = 17.2, 1.2 Hz 5.30, dd, J = 10.4, 1.2 Hz 5.29, dd, J = 10.4, 1.2 Hz 5.24, dd, J = 10.4, 1.2 Hz 4.63, d, J = 5.2 Hz 4.56, d, J = 5.2 Hz 4.53, d, J = 5.2 Hz	118.3, 118.1, 117.9, 70.3, 70.2, 69.9	5.44, d, J = 17.2 Hz 5.32, d, J = 10.4 Hz 5.30, d, J = 11.2 Hz 5.27, d, J = 10.8 Hz 4.68 (d, J = 4.8 Hz 4.62 (d, J = 5.2 Hz	117.8, 117.7, 117.4, 70.0, 69.6, 69.1
CH ₃	1.50, t, J = 7.2 Hz 1.45, t, J = 6.8 Hz 1.42, t, J = 7.2 Hz	14.9, 14.7	1.53, t, J = 7.2 Hz 1.49, t, J = 7.2 Hz 1.45, t, J = 7.2 Hz	15.2, 15.1, 14.9	-	-	-	-

102 and **103** required 379.15214 and 415.15214 while their HR-MS (ESI) results were calculated as 379.15290 and 415.152140, respectively.

The second route is that B-ring remained as 2,4,5-trimethoxybenzaldehyde and substituents on A-ring were altered. There are eighteen chalcones obtained by Claisen-Schmidt reaction (**Figure 3.10**). The yield and appearance of these benzaldehydes and chalcones are illustrated in **Table 3.23**. The yields of these reactions were varied from 34 to 98%. Almost compounds were obtained by crystallization in MeOH.

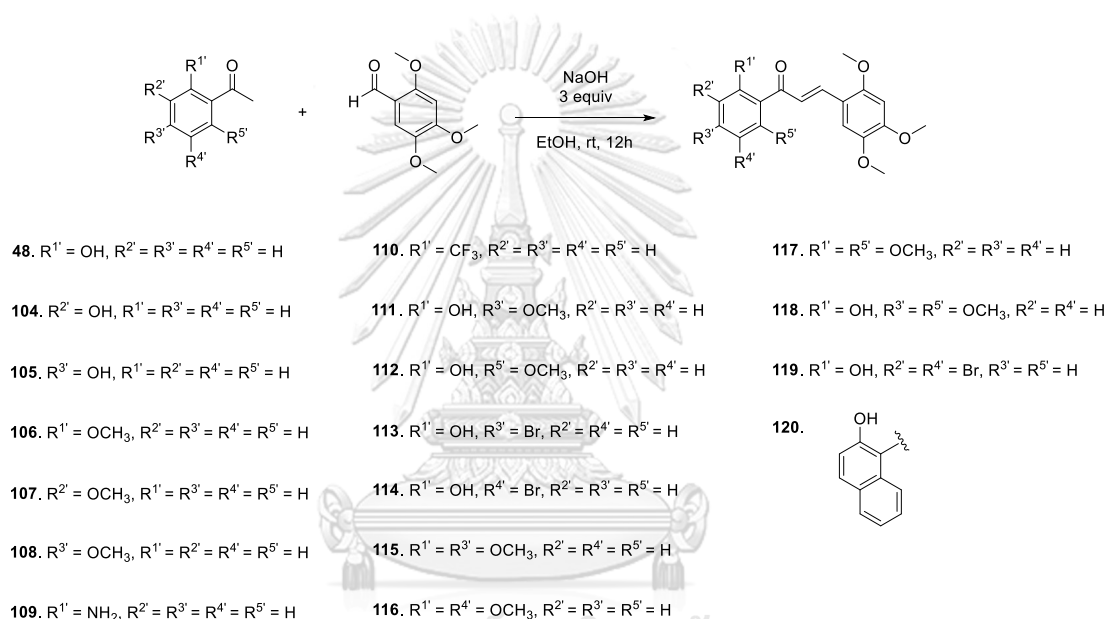


Figure 3.10 Synthesis of chalcones with 2,4,5-trimethoxy on B-ring.

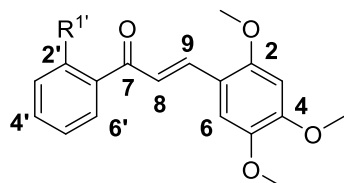
The structural identification of eighteen chalcones was operated by ¹H and ¹³C NMR analysis, as described in **Tables 3.24-3.29**; nonetheless, the NMR data of **107** has not been collected. All products bear a resemblance in the signals of B-ring as 2,4,5-trimethoxybenzaldehyde. They were only differentiated by the peaks in distinct A-rings. Three chalcones **113**, **114** and **119** are new compounds. The exact masses of **113**, **114** and **119** required 415.01571, 415.01571 and 492.92622 while their HR-MS (ESI) results were calculated as 415.01520, 415.01670 and 492.93560, respectively.

Table 3.23 Yields and characteristics of products 48, 104-120.

Products	Appearance	Yield (%)	Remarks
48	Orange crystal	79	known
104	Yellow crystal	45	known
105	Yellow crystal	68	known
106	Yellow crystal	80	known
107	Yellow crystal	42	known
108	Yellow crystal	76	known
109	Yellow crystal	41	known
110	Yellow crystal	86	known
111	Red crystal	61	known
112	Orange crystal	56	known
113	Yellow crystal	98	new
114	Orange crystal	45	New
115	Yellow crystal	81	known
116	Yellow crystal	75	known
117	Yellow crystal	77	known
118	Yellow crystal	61	known
119	Red crystal	80	new
120	Red crystal	34	known

3.4.2 Biological activity evaluation

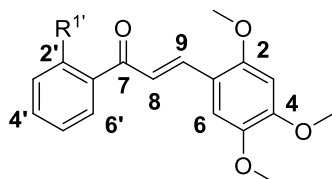
There are eleven chalcones (48, 103-105, 108-110, 113, 114, 118 and 120) with 2,4,5-trisubstitution on B-ring reported about AMPK activation activity as presented in Figure 3.11 among twenty synthesized compounds. 109 and 110 changed the morphologies of podocyte cells so they were assessed to be toxic to the cells. Besides, the other candidates mostly expressed quite similar potencies to one another including 48 (potency of 4.97) but the most potent one (103) still had its potency two-

Table 3.24 NMR chemical shift assignment of chalcones **48**, **104** and **105**.

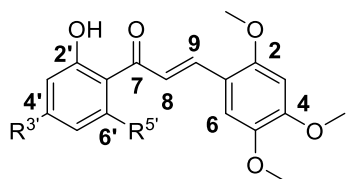
48. R^{1'} = 2'-OH **104.** R^{1'} = 3'-OH **105.** R^{1'} = 4'-OH

Position	48 (CDCl ₃)		104 (acetone-d ₆)		105 (acetone-d ₆)	
	δH	δC	δH	δC	δH	δC
1'	-	120.4	-	141.4	-	142.7
2'	-	163.6	7.52, t <i>J</i> = 2.0 Hz	120.4	8.03, d <i>J</i> = 8.8 Hz	131.5
3'	7.00, dd <i>J</i> = 8.0, 0.8 Hz	118.6	-	158.7	6.94, d <i>J</i> = 8.8 Hz	116.0
4'	7.46, td <i>J</i> = 8.4, 1.2 Hz	136.0	7.08, dd <i>J</i> = 8.0, 2.4 Hz	120.3	-	162.4
5'	6.92, t <i>J</i> = 8.0, 0.8 Hz	118.7	7.36, t <i>J</i> = 7.6 Hz	130.6	6.94, d <i>J</i> = 8.8 Hz	116.0
6'	7.92, dd <i>J</i> = 8.0, 1.2 Hz	129.7	7.58, d <i>J</i> = 7.6 Hz	120.6	8.03, d <i>J</i> = 8.8 Hz	131.5
1	-	115.4	-	116.2	-	116.2
2	-	143.5	-	144.8	-	144.6
3	6.52, s	97.0	6.78, s	98.5	6.78, s	98.4
4	-	155.3	-	155.8	-	155.4
5	-	153.2	-	154.4	-	154.0
6	7.12, s	112.1	7.46, s	112.8	7.45, s	112.6
7	-	194.2	-	190.1	-	188.3
8	7.61, d <i>J</i> = 15.2 Hz	118.0	7.66, d <i>J</i> = 15.6 Hz	115.7	7.72, d <i>J</i> = 15.6 Hz	120.0
9	8.20, d <i>J</i> = 15.6 Hz	141.0	8.14, d <i>J</i> = 15.6 Hz	139.8	8.11, d <i>J</i> = 15.6 Hz	138.6
OH	13.07, s	-	8.66, s	-	9.37, s	-
CH ₃	3.95, 3.92, 3.91, s	56.8, 56.5, 56.2	3.94, 3.92, 3.85, s	57.1, 56.9, 56.4	3.94, 3.91, 3.84, s	57.0, 56.7, 56.2

Table 3.25 NMR chemical shift assignment of chalcones 106, 108-110.

106. R^{1'} = 2'-OCH₃108. R^{1'} = 4'-OCH₃109. R^{1'} = 2'-NH₂110. R^{1'} = 2'-CF₃

Position	106 (CDCl ₃)		108 (CDCl ₃)		109 (acetone-d ₆)		110 (CDCl ₃)	
	δH	δC	δH	δC	δH	δC	δH	δC
1'	-	129.8	-	131.7	-	119.9	-	125.3
2'	-	157.7	7.98, d <i>J</i> = 8.8 Hz	130.7	-	155.4	-	126.8
3'	6.92, d <i>J</i> = 8.8 Hz	111.1	6.92, d <i>J</i> = 8.8 Hz	113.7	6.82, d <i>J</i> = 8.4 Hz	115.8	7.47, d <i>J</i> = 7.6 Hz	126.9
4'	7.37, t <i>J</i> = 7.6 Hz	132.2	-	163.1	7.25, t <i>J</i> = 8.4 Hz	134.6	7.62, t <i>J</i> = 7.2 Hz	131.7
5'	6.96, t <i>J</i> = 7.2 Hz	125.0	6.92, d <i>J</i> = 8.8 Hz	113.7	6.60, t <i>J</i> = 8.0 Hz	118.0	7.57, t <i>J</i> = 7.6 Hz	129.7
6'	7.51, d <i>J</i> = 7.6 Hz	129.9	7.98, d <i>J</i> = 8.8 Hz	130.7	7.99, d <i>J</i> = 8.0 Hz	131.9	7.75, d <i>J</i> = 7.6 Hz	128.4
1	-	115.5	-	115.8	-	116.6	-	115.0
2	-	143.2	-	143.3	-	144.8	-	143.7
3	6.44, s	96.9	6.48, s	97.1	6.78, s	98.6	6.47, s	97.0
4	-	154.4	-	154.6	-	154.0	-	154.9
5	-	152.4	-	152.4	-	152.9	-	153.4
6	7.03, s	111.6	7.09, s	111.7	7.46, s	112.8	7.03, s	111.2
7	-	193.4	-	189.3	-	192.2	-	195.8
8	7.20, d <i>J</i> = 16.0 Hz	120.5	7.44, d <i>J</i> = 15.6 Hz	120.1	7.78, d <i>J</i> = 15.2 Hz	121.4	6.99, d <i>J</i> = 16.0 Hz	124.9
9	7.86, d <i>J</i> = 16.0 Hz	138.8	8.03, d <i>J</i> = 15.6 Hz	139.3	8.10, d <i>J</i> = 15.6 Hz	138.2	7.61, d <i>J</i> = 16.4 Hz	143.0
NH ₂					7.05, s	-	-	-
CF ₃					-	-	-	128.1, q <i>J</i> = 32.3 Hz
CH ₃	3.85, 3.80, 3.78, s	56.4, 56.2, 55.9, 55.6	3.89, 3.85, 3.84, 3.82, s	56.6, 56.4, 56.1, 55.4	3.94, 3.91, 3.84, s	57.1, 56.9, 56.4	3.93, 3.86, 3.81, s	56.6, 56.5, 56.2

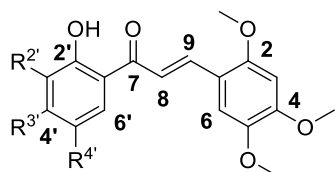
Table 3.26 NMR chemical shift assignment of chalcones **111**, **112** and **118**.

111. R^{3'} = OCH₃, R^{5'} = H

112. R^{3'} = H, R^{5'} = OCH₃

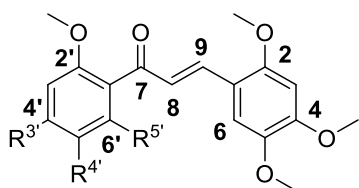
118. R^{3'} = R^{5'} = OCH₃

Position	111 (CDCl ₃)		112 (CDCl ₃)		118 (CDCl ₃)	
	δ H	δ C	δ H	δ C	δ H	δ C
1'	-	115.6	-	135.9	-	106.5
2'	-	166.0	-	161.0	-	162.5
3'	6.50, s	101.2	6.59, d <i>J</i> = 8.0 Hz	111.1	5.92, d <i>J</i> = 2.0 Hz	93.9
4'	-	166.8	7.32, t <i>J</i> = 8.4 Hz	135.4	-	168.4
5'	6.44, dd <i>J</i> = 10.4, 2.4 Hz	107.5	6.41, d <i>J</i> = 8.0 Hz	101.7	6.06, d <i>J</i> = 2.0 Hz	91.2
6'	7.80, d <i>J</i> = 8.8 Hz	131.3	-	164.9	-	165.9
1	-	114.5	-	116.2	-	116.3
2	-	143.5	-	143.4	-	143.3
3	6.43, s	97.0	6.51, s	97.2	6.48, s	97.1
4	-	155.1	-	154.9	-	154.6
5	-	153.0	-	152.7	-	152.4
6	7.09, s	112.0	7.10, s	111.8	7.08, s	111.7
7	-	192.6	-	194.6	-	192.8
8	7.50, d <i>J</i> = 15.2 Hz	118.2	7.81, d <i>J</i> = 15.6 Hz	125.5	7.83, d <i>J</i> = 15.6 Hz	125.4
9	8.14, d <i>J</i> = 15.6 Hz	140.0	8.14, d <i>J</i> = 16.0 Hz	138.7	8.08, d <i>J</i> = 15.6 Hz	138.0
2'-OH	13.68, s	-	13.34, s	-	-	-
CH ₃	3.92, 3.90, 3.89, 3.82, s	56.7, 56.4, 56.1, 55.6	3.93, 3.92, 3.89, 3.87, s	56.7, 56.5, 56.2, 55.9	3.90, 3.86, 3.85, 3.79, s	56.6, 56.4, 56.1, 55.8, 55.6

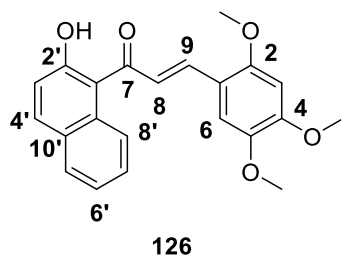
Table 3.27 NMR chemical shift assignment of chalcones **113**, **114** and **119**.113. R^{2'} = H, R^{3'} = Br, R^{4'} = H114. R^{2'} = H, R^{3'} = H, R^{4'} = Br119. R^{2'} = R^{4'} = Br, R^{3'} = H

Position	113 (CDCl ₃)		114 (CDCl ₃)		119 (acetone-d ₆)	
	δ _H	δ _C	δ _H	δ _C	δ _H	δ _C
1'	-	130.1	-	121.7	-	121.9
2'	-	164.1	-	162.6	-	158.0
3'	7.14, d <i>J</i> = 1.6 Hz	121.6	6.90, d <i>J</i> = 8.8 Hz	120.6	-	109.8
4'	-	119.2	7.52, dd <i>J</i> = 8.8, 2 Hz	138.5	8.45, d <i>J</i> = 2.0 Hz	140.0,
5'	7.00, dd <i>J</i> = 8.8, 2.0 Hz	122.1	-	110.3	-	112.1
6'	7.72, d <i>J</i> = 8.8 Hz	130.6	7.99, d <i>J</i> = 2.4 Hz	131.9	8.04, d <i>J</i> = 2.0 Hz	131.6
1	-	115.1	-	115.2	-	113.6
2	-	143.4	-	143.6	-	143.0
3	6.48, s	96.8	6.52, s	96.9	6.71, s	97.0
4	-	155.4	-	155.6	-	155.1
5	-	153.4	-	153.6	-	154.2
6	7.07, s	112.1	7.12, s	112.1	7.58, s	111.2
7	-	193.5	-	193.1	-	192.1
8	7.49, d <i>J</i> = 15.6 Hz	117.4	7.48, d <i>J</i> = 15.2 Hz	117.2	7.79, d <i>J</i> = 15.6 Hz	115.9
9	8.17, d <i>J</i> = 15.6 Hz	141.6	8.23, d <i>J</i> = 15.2 Hz	142.1	8.26, d <i>J</i> = 15.2 Hz	141.2
2'-OH	13.20, s	-	13.01, s	-	13.88, s	-
CH ₃	3.91, 3.89, 3.86, s	56.7, 56.4, 56.2	3.95, 3.93, 3.92, s	56.9, 56.5, 56.2	3.88, 3.86, 3.80, s	56.4, 56.2, 55.6

Table 3.29 NMR chemical shift assignment of chalcones 115-117.

115. R^{3'} = OCH₃, R^{4'} = H, R^{5'} = H116. R^{3'} = H, R^{4'} = OCH₃, R^{5'} = H117. R^{3'} = H, R^{4'} = H, R^{5'} = OCH₃

Position	115 (CDCl ₃)		116 (CDCl ₃)		117 (CDCl ₃)	
	δH	δC	δH	δC	δH	δC
1'	-	122.4	-	130.2	-	119.1
2'	-	159.9	-	152.1	-	157.5
3'	6.36, d <i>J</i> = 2.4 Hz	98.4	6.87, dd <i>J</i> = 9.2, 2.4 Hz	111.1	6.58, d <i>J</i> = 8.4 Hz	104.2
4'	-	163.5	6.93, dd <i>J</i> = 9.2, 3.2 Hz	124.8	7.27, t <i>J</i> = 8.4 Hz	130.4
5'	6.42, dd <i>J</i> = 8.4, 2.0 Hz	105.0	-	152.4	6.58, d <i>J</i> = 8.4 Hz	104.2
6'	7.60, d <i>J</i> = 8.4 Hz	132.2	7.10, d <i>J</i> = 2.8 Hz	114.4	-	157.5
1	-	115.6	-	115.4	-	115.4
2	-	143.0	-	143.2	-	143.4
3	6.39, s	96.8	6.43, s	96.9	6.44, s	97.1
4	-	154.1	-	154.4	-	154.2
5	-	151.9	-	153.4	-	152.5
6	6.99, s	111.0	7.04, s	113.3	7.01, s	111.0
7	-	190.6	-	192.8	-	195.4
8	7.32, d <i>J</i> = 15.6 Hz	125.0	7.23, d <i>J</i> = 16.0 Hz	118.1	6.87, d <i>J</i> = 16.4 Hz	126.8
9	7.87, d <i>J</i> = 15.6 Hz	137.2	7.87, d <i>J</i> = 16.0 Hz	138.8	7.60, d <i>J</i> = 16.4 Hz	140.4
CH ₃	3.79, 3.76, 3.75, 3.74, 3.71, s	56.2, 56.0, 55.8, 55.4, 55.2	3.84, 3.79, 3.77, 3.76, 3.71, s	56.4, 56.3, 56.2, 55.9, 55.6	3.88, 3.82, 3.76, 3.74, s	56.5, 56.1, 56.0

Table 3.30 NMR chemical shift assignment of chalcone **120**.

Position	120 (acetone- d_6)	
	δ H	δ C
1'	-	115.9
2'	-	164.9
3'	7.39, d, $J = 8.8$ Hz	118.3
4'	7.88, d, $J = 8.0$ Hz	131.0
5'	8.13, d, $J = 9.2$ Hz	125.6
6'	7.58, t, $J = 8.4$ Hz	119.0
7'	7.69, td, $J = 6.8, 0.8$ Hz	128.5
8'	8.44, d, $J = 7.6$ Hz	124.9
9'	-	138.4
10'	-	126.4
1	-	114.6
2	-	144.9
3	6.82, s	98.4
4	-	156.4
5	-	155.2
6	7.57, s	113.1
7	-	194.8
8	7.98, d, $J = 15.6$ Hz	126.8
9	8.41, d, $J = 15.2$ Hz	141.4
CH ₃	4.00, 3.95, 3.87, s	57.2, 57.0, 56.5

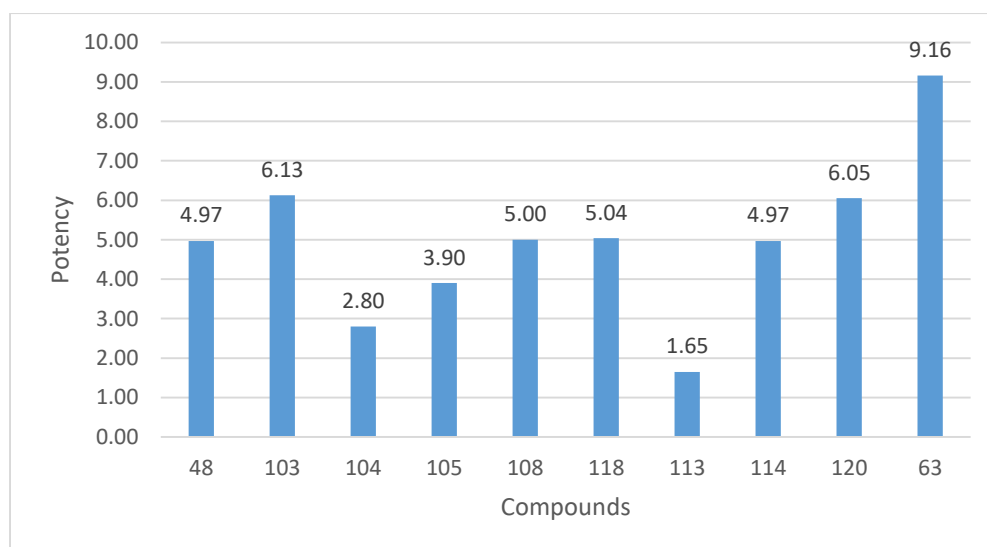


Figure 3.11 Biological evaluation of chalcones with 2,4,5-trisubstitution on B-ring.

third as much as chalcone **63**. In the first route, only **103** with allyloxy group at 2,4,5-position exhibited potency result so far and it showed the highest quality compared to the other candidates in the second route with potency of 6.13 and definitely it would dominate the reported chalcone **48** for AMPK activity which paved the way for further synthesized compounds with various substituents at 2,4,5-position. On the other hand, in the second route, it could be seen among three compounds **48**, **104** and **105** with potency of 4.97, 2.80 and 3.90, respectively that monohydroxy group on A-ring should settle at 2'-position to achieve the highest potency for activating AMPK compared to 3'-or 4'-position. Differentiation the potency between **105** (5.00) and **108** (3.90) suggested that OCH₃ group seem to be more active than OH at 4'-position which may imply that **106** bearing OCH₃ group at 2'-position was likely to exceed **48** in potency. From this idea, the other chalcones **115-117** carrying dimethoxy substituents at 2',4'-, 2',5'- and 2',6', respectively were synthesized to confirm the effect of OCH₃ group on A-ring compared to OH group. **118** was prepared to compare with **48** since it contained two more OCH₃ groups at 4',6'-position along with OH group at 2'-position the same as **48**. The potency of **118** (5.04) was quite similar to that of **48**. Two OCH₃ groups at 4',6'-position had no advantage on biological activity of **118**; thus, two compounds **111** and **112** with 4'- and 6'-OCH₃, respectively along with 2'-OH on A-ring

were prepared to collect more data about structure-activity relationship. In addition, two chalcones **113** and **114** bearing 2'-OH group along with 4'-Br and 5'-Br, respectively were synthesized to differentiate with **48**. **114** with 5'-Br had comparable potency with **48**, which was 4.97, this result reflected that 5'-Br substituent could not enhance chalcone having impressive biological outcome. Surprisingly, 4'-Br substituent lessened the potency of **113** to just one third as much as that of **48** (1.65). Therefore, **119** with 2'-OH and 3',5'-dibromo on A-ring evading 4'-Br substitution was prepared to evaluate biological activity in case of dihalogene chalcone. Interestingly, **120** with A-ring as naphthalene derivatives was observed with comparable potency (6.05) to the highest one (**103**) which proposed an appealing direction for chalcones possessing polycyclicaromatic component. Finally, from these results, the synthesis of more chalcones was necessary to search for good candidates that exceed **48** in potency similar to chalcones **63** and **65**.

3.5 Synthesis of dihydrochalcones

3.5.1 Synthesis and structural elucidation

Hydrogenation reaction was carried out for two potent chalcones **48** and **65** to furnish dihydrochalcones as the target products (**Figure 3.12**). The reactions are monitored by TLC to determine the process of product formation. In case of **48**, after 3 h, there are two products obtained in the mixture containing **121** and **122**. If the mixture was handled to work-up, these two products would be achieved by column chromatography in moderate yield as presented in **Table 3.30**. If the reaction was prolonged for 2 days, TLC plate appeared only one spot of **123** with the yield nearly 100% and purification was not necessary. On the other hand, **65** was applied under the same conditions to prepare **124** in excellent yield (98%) although the reaction was extended in one and a half day. Only one spot of **124** was observed; therefore, purification was not required.

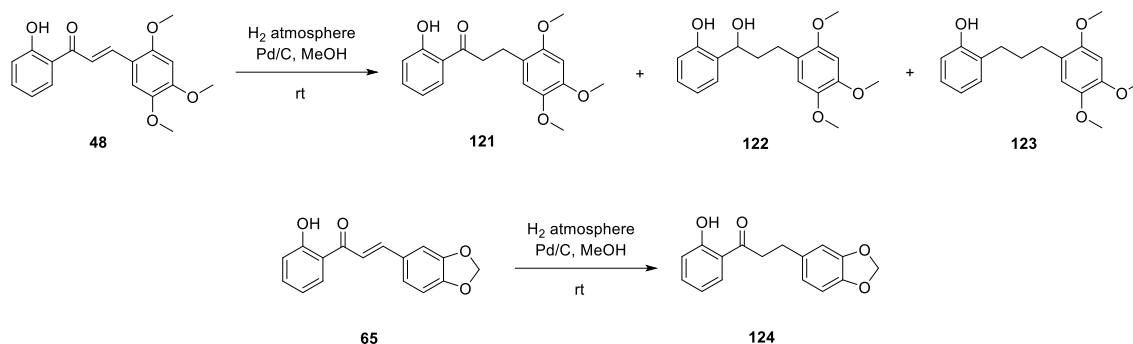


Figure 3.12 Synthesis of dihydrochalcones.

Table 3.31 Yields, characteristics and HR-MS (ESI) results of products **48**, **121-124**.

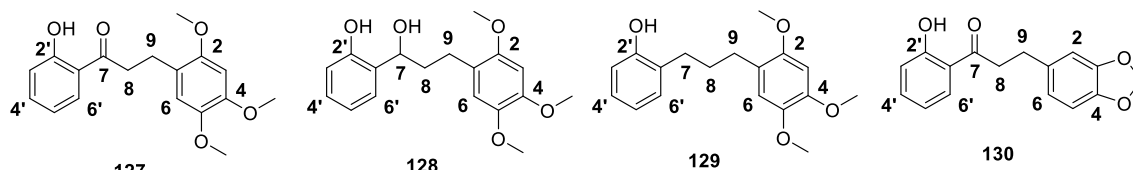
Products	Appearance	Yield (%)	Remarks	Exact mass	HR-MS (ESI)
121	White crystal	53	new	339.12084	339.1204
122	Oil	40	new	341.13649	341.1359
123	White crystal	98	new	325.14158	325.1395
124	White crystal	98	known	-	-

The structural identification of four compounds was operated by ¹H and ¹³C NMR analysis, as shown in **Table 3.31**. The ¹H and ¹³C NMR signals of **121-123** resemble to those of **48** except for the signals designated for the peaks of α,β -unsaturated ketone linker. **124** was also similar to **65** in the ¹H and ¹³C NMR signals excluding the disappearance of the signals of alkene functional group in **124**. **121-123** are new compounds and the exact masses along with HR-MS (ESI) results are presented in **Table 3.30**.

3.5.2 Biological activity evaluation

The AMPK activation activity results of dihydrochalcones are shown in **Figure 3.13**. Firstly, four-column of **48** derivatives with different saturation degree demonstrated that the single carbonyl group made **121** dominated in AMPK activation activity than conjugation enone system with the potency of **121** as 9.07 comparable

Table 3.32 NMR chemical shift assignment of chalcones 127-130.



Position	127 (CDCl ₃)		128 (CDCl ₃)		129 (DMSO- <i>d</i> ₆)		130 (CDCl ₃)	
	δ H	δ C	δ H	δ C	δ H	δ C	δ H	δ C
1'	-	120.5	-	127.3	-	128.3	-	134.5
2'	-	162.6	-	155.9	-	155.1	-	162.5
3'	6.98, d <i>J</i> = 8.0 Hz	118.6	6.86, m	117.2	6.76, d <i>J</i> = 8.0 Hz	114.8	6.74, d <i>J</i> = 7.2 Hz	118.6
4'	7.45, td <i>J</i> = 8.0, 1.2 Hz	136.3	7.13, td <i>J</i> = 8.4, 1.6 Hz	128.7	6.96, td <i>J</i> = 7.6, 1.2 Hz	126.6	7.45, t <i>J</i> = 7.6 Hz	136.3
5'	6.86, t <i>J</i> = 7.6 Hz	118.9	6.78, t <i>J</i> = 7.2 Hz	119.6	6.69, t <i>J</i> = 7.6 Hz	118.8	6.88, t <i>J</i> = 7.6 Hz	118.9
6'	7.77, dd <i>J</i> = 8.0, 0.8 Hz	130.2	6.86, m	127.0	7.03, dd <i>J</i> = 7.6, 0.8 Hz	129.6	7.72, d <i>J</i> = 8.0 Hz	129.8
1	-	119.6	-	120.8	-	121.6	-	119.3
2	-	143.1	-	143.7	-	142.5	6.73, s	108.3
3	6.52, s	97.2	6.55, s	98.2	6.62, s	98.7	-	147.8
4	-	151.8	-	151.3	-	151.2	-	146.0
5	-	148.4	-	148.2	-	147.6	6.69, d <i>J</i> = 8.0 Hz	108.9
6	6.75, s	114.8	6.70, s	114.4	6.74, s	114.7	6.98, d <i>J</i> = 8.4 Hz	121.2
7	-	206.6	4.67, dd <i>J</i> = 10.0, 4.0 Hz	74.6	2.51, m	29.9	-	205.4
8	3.24, t <i>J</i> = 8.0 Hz	39.2	2.85, 2.67, m	38.3	1.74, pentet <i>J</i> = 8.0 Hz	29.0	3.26, t <i>J</i> = 7.6 Hz	40.2
9	2.98, t <i>J</i> = 8.0 Hz	25.8	2.20, 1.94, m	25.4	2.51, m	29.5	2.98, t <i>J</i> = 7.6 Hz	29.8
2'-OH	12.38, s	-	8.30, s	-	9.24, s	-	12.31, s	-
CH ₃ /methylene	3.88, 3.82, 3.80, s	56.9, 56.5, 56.2	3.88, 3.85, 3.83, s	56.8, 56.7, 56.4	3.75, 3.73, 3.67, s	56.4, 56.2, 55.9	5.91, s	100.9

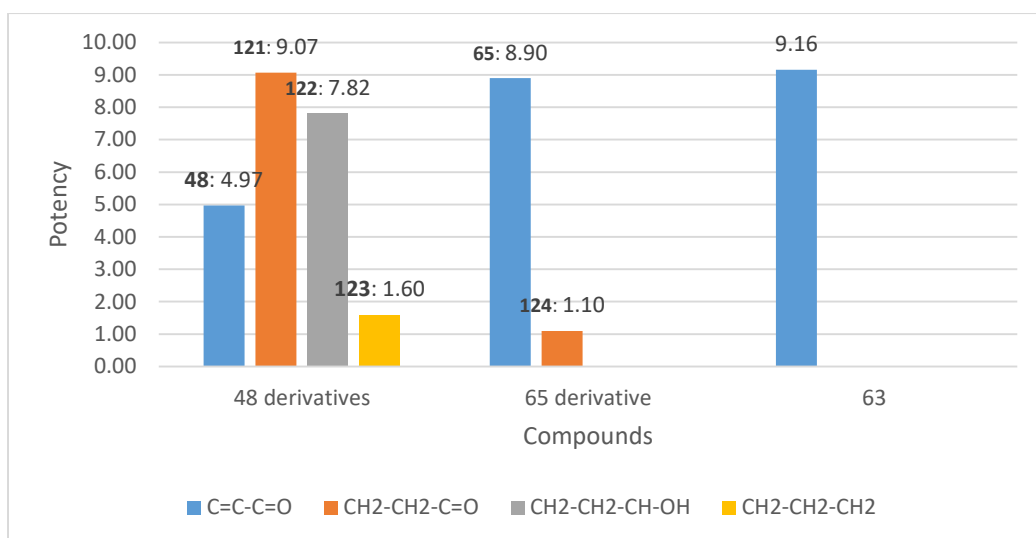


Figure 3.13 Biological evaluation of hydrogenated chalcones.

to that of the most potent **63** so far. Moreover, reducing of carbonyl group of **121** to OH group still encouraged **122** to overwhelm **48** with the potency of 7.82. Nevertheless, the highest degree of saturation of **48** decreased significantly potency of **123** (1.6). As a result, if the alkene group was reduced and carbonyl group was hydrogenated to OH group, they still boost the biological activity of products compared to parent chalcone but the compound bearing saturated carbon chain seemed to be inactive in AMPK activity. From this consideration, the potent chalcone **65** was used to confirm the results by hydrogenation reaction. But surprisingly, dihydrochalcone **124** was found to be incapable to activate AMPK with the potency as 1.1. Therefore, this kind of compounds required to assess more candidates to confirm the trend of AMPK activation activity.

3.6 Concentration-response relationship and EC₅₀ calculation

According to the AMPK activation activity results from forty-six compounds, there were eleven candidates possessing potency higher than **48**, as listed in **Figures 3.14** and **3.15**. Seven compounds (**70**, **74**, **103**, **108**, **114**, **118** and **120**) possessed

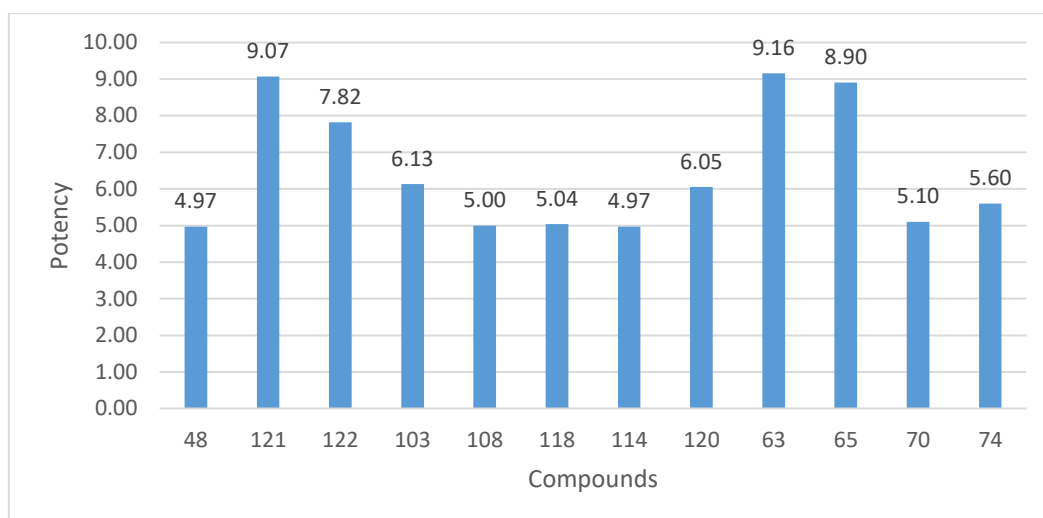


Figure 3.14 Biological activity results of active compounds.

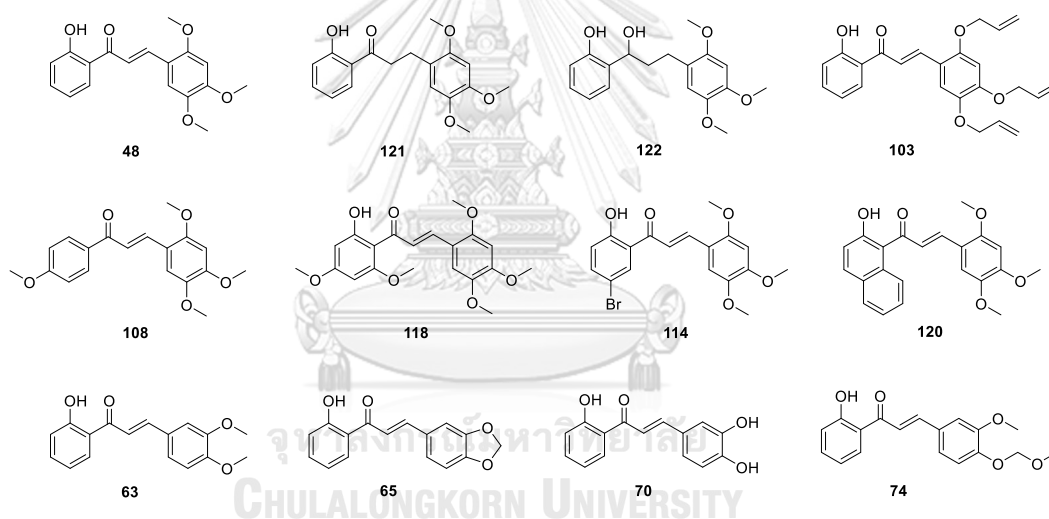


Figure 3.15 Structure of active compounds.

potency around 1.00 to 1.23 times as much as that of **48**. Four compounds (**63**, **65**, **121** and **122**) exclusively exhibited more powerful potency than **48** with the fold change such as 1.84, 1.79, 1.82 and 1.57, respectively. However, **122** was found to be toxic to the podocyte cells when it was treated in a prolonged time as 14 days under diabetic condition. Therefore, only three chalcones along with **48** were processed to calculate the concentration-response relationship and achieved EC_{50} values in **Figure 3.16**. The fold changes of phosphorylation of AMPK between the podocyte samples

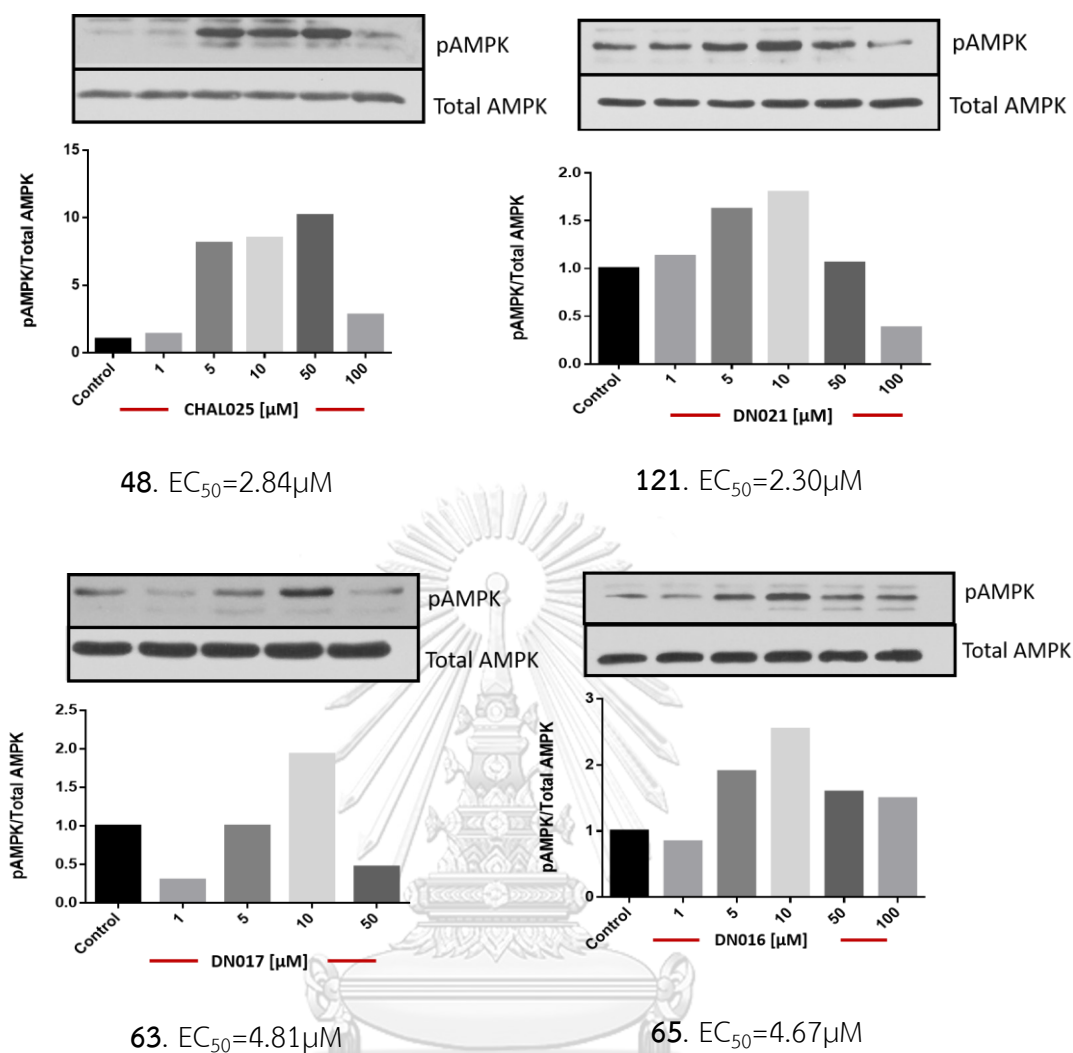


Figure 3.16 Concentration – response relationship and EC₅₀ calculation.

CHULALONGKORN UNIVERSITY

Inoculated at each concentration 0,1, 5, 10, 50, 100 μM of chalcones and the control podocyte sample treated with DMSO were fitted into Hill's equation. Then, resulted Hill's curve could estimate the EC₅₀ relying on the data at all concentrations. From the EC₅₀ results, it could be seen that the increasing trend of EC₅₀ values was following the order of compounds that **121**, **48**, **65** and **63** with values such as 2.30, 2.84, 4.67 and 4.81 respectively. Therefore, **121** was the most active one with the lowest EC₅₀ value which meant that it exhibited half of maximal response at the lowest concentration compared to the other chalcones. These concentration-response relationship results were obtained from two separate experiments and they were averaged to achieve the final outcome. Therefore, it was required to perform more repeated experiments to

confirm the EC_{50} results. After that the cytotoxic effect evaluation of these four active compounds will be performed using MTT assay in podocyte cells. Ultimately, the compounds with the lowest EC_{50} and cytotoxicity will be used for further research.



CHAPTER 4

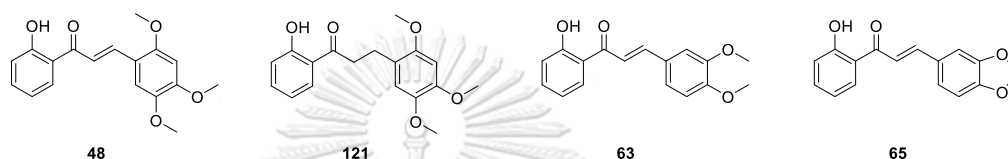
CONCLUSIONS

Sixty chalcones were synthesized by Claisen-Schmidt reaction from various types of acetophenone and benzaldehyde derivatives in moderate to high yield. The substituents on B-ring were evaluated as mono-, di- and trisubstitution while those on A-ring as 2'-hydroxy, 3',4',5'-trimethoxy and different types of groups were assessed. Furthermore, chalcones with different degrees of saturation in α,β -unsaturated ketone connectors were prepared. All of prepared chalcones were tested and compared their AMPK phosphorylation potency with that of **48** – a reported AMPK activator.

Among synthesized chalcones, forty-six candidates were exclusively achieved AMPK activation activity. Regarding monosubstitution on B-ring, 2'-hydroxychalcone with 3-OCH₃ was found as the most potent one. Therefore, in case of disubstitution, a broad variety of chalcone bearing dimethoxy at various positions couples on B-ring was tested, but only dimethoxy or methylenedioxy at 3,4-position were found as the privilege structure to develop the activity of chalcones such as **63** and **65**. Moreover, a series of chalcone derivatives with various substituents at 3,4-position was assessed but they could not exceed the potency of **63** and **65**. Trisubstitution was investigated only for 2,4,5-position based on the structure of reported AMPK activator **48** and there were two routes to apply. The first route was recognized that **103** with 2,4,5-trialkoxy group was more potent than **48** with 2,4,5-trimethoxy group. In the second route, a number of chalcones with B-ring fixed as 2,4,5-trimethoxy group and varied substituents on A-ring were evaluated. There were also some candidates slightly more potent than **48**. But overall, all chalcones in two routes did not possess an impressive potency compared to **63** and **65**. Lastly, four dihydrochalcones were synthesized and their biological outcomes presented that the potency soars by nearly two folds when **48** was reduced to **121** after that rising degree of saturation ensured the decrease of potency which plummeted in chalcone bearing entirely saturated carbon chain linker. However, **121** and **122** were found to possess the potency comparable to **63** and **65**.

Interestingly, **124** having the same saturation degree with **121** showed the low potency for AMPK phosphorylation.

The EC_{50} calculation of four active compounds (**48**, **63**, **65** and **121**) ensued to obtain the concentration-response relationship. Dihydrochalcone **121** was the most active candidate with the lowest EC_{50} value as 2.30 μ M which was more potent than reported AMPK activator **48** (EC_{50} 2.84 μ M). These concentration-response relationship experiments were required to repeat to achieve trusty EC_{50} values.



Suggestion for future work

MTT assay should be carried out subsequently to test the toxicity of chalcones in order to select the most potent one with the lowest EC_{50} value and cytotoxic effect. Then the AMPK activation mechanism should be investigated using the potent chalcones. After that, potent candidate should be applied to assess the impact on insulin resistance disorder and lipotoxicity-induced podocyte dysfunction in *in-vitro* model. Finally, the function of the active compounds should be tested on *db/db* diabetic mouse in *in vivo* model.



APPENDIX

จุฬาลงกรณ์มหาวิทยาลัย
CHULALONGKORN UNIVERSITY

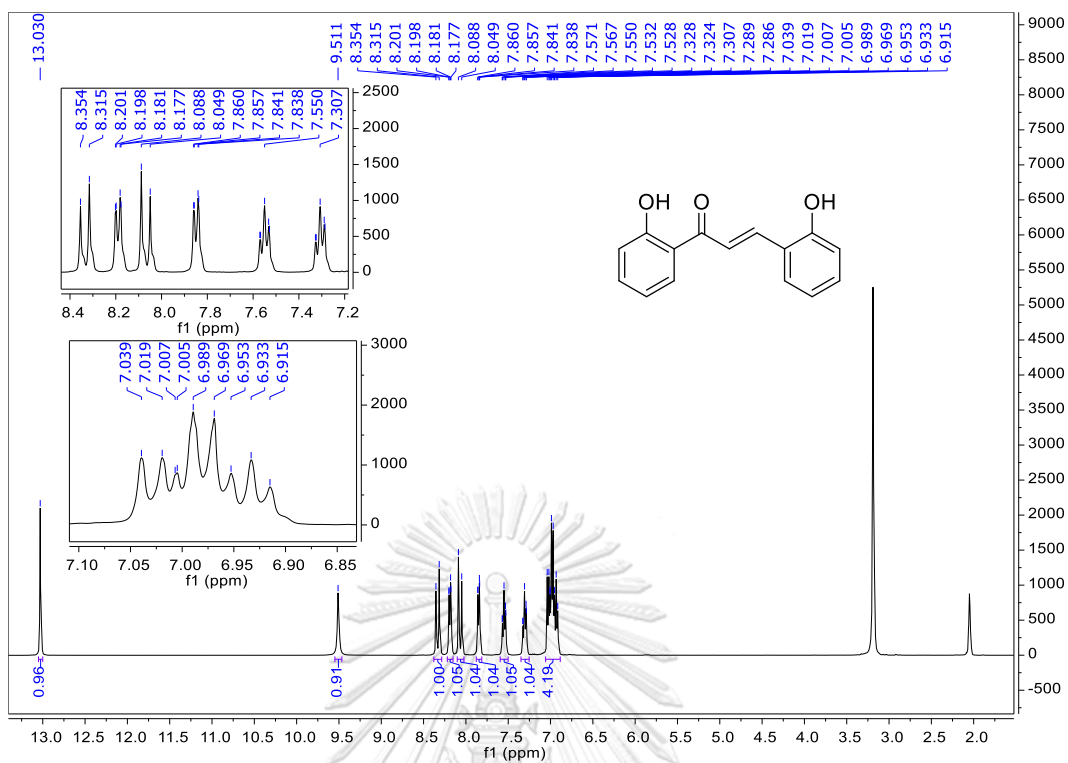


Figure A.1 The ^1H NMR spectrum (acetone- d_6 , 400 MHz) of **49**.

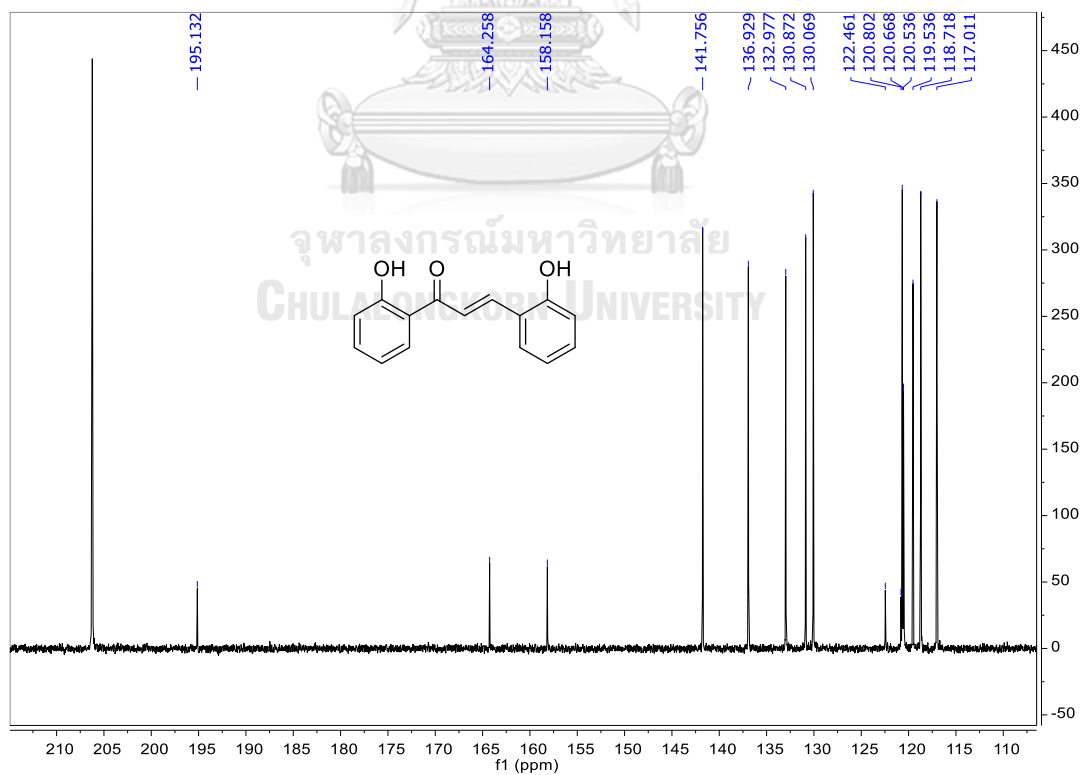


Figure A.2 The ^{13}C NMR spectrum (acetone- d_6 , 100 MHz) of **49**.

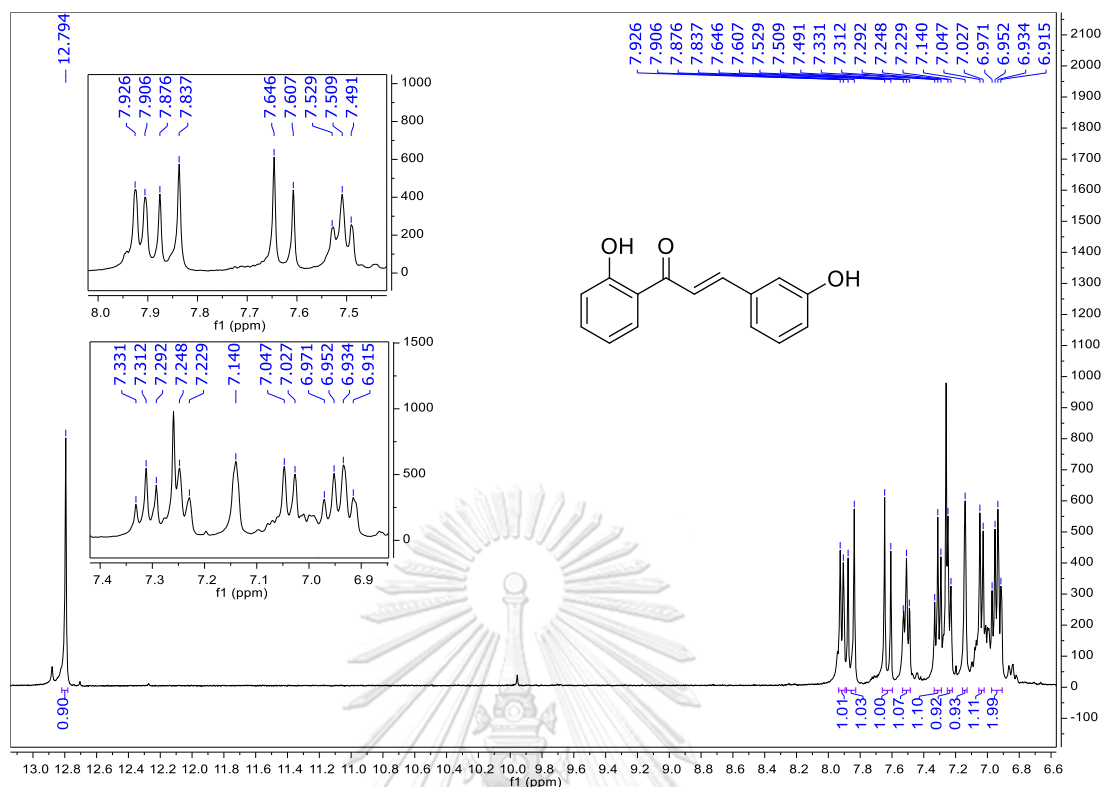


Figure A.3 The ^1H NMR spectrum (CDCl₃, 400 MHz) of 50.

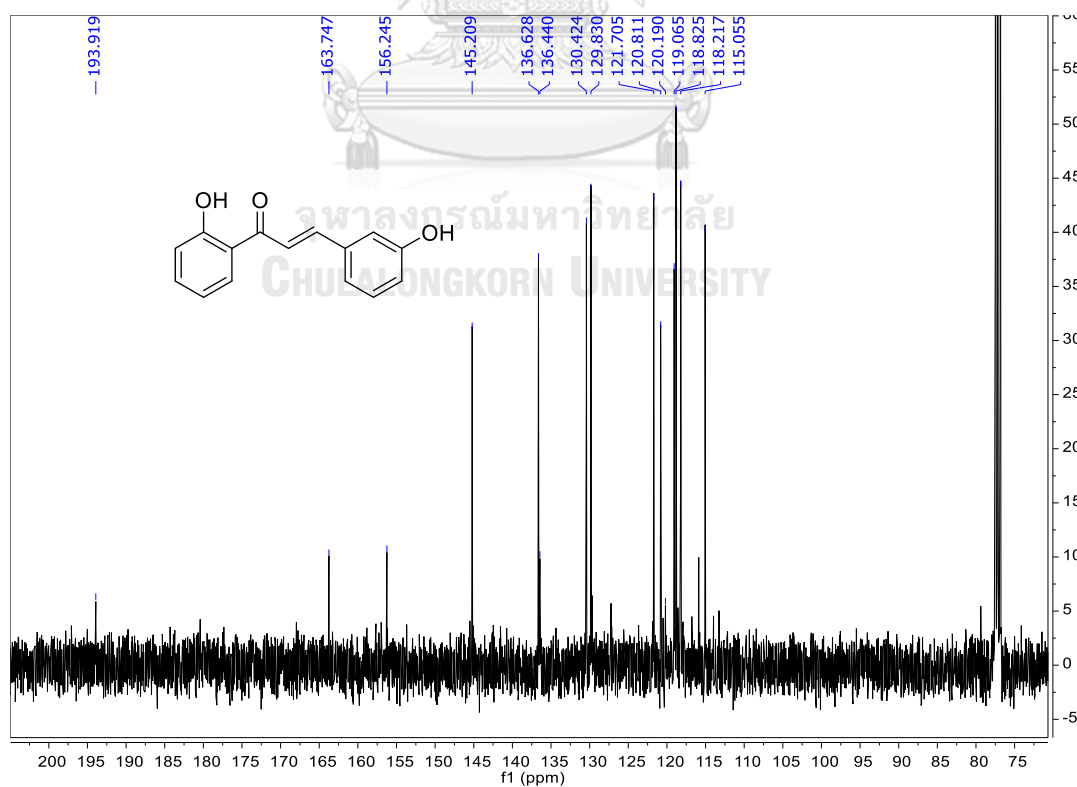


Figure A.4 The ^{13}C NMR spectrum (CDCl₃, 100 MHz) of 50.

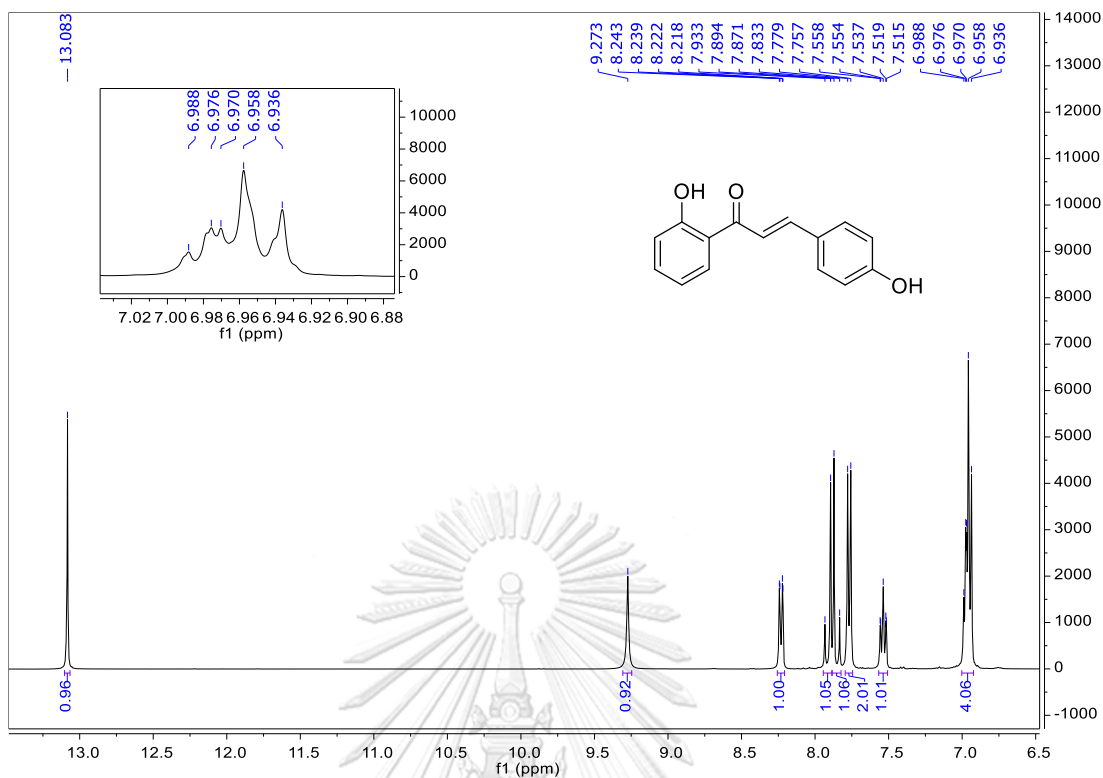


Figure A.5 The ¹H NMR spectrum (acetone-d₆, 400 MHz) of **51**.

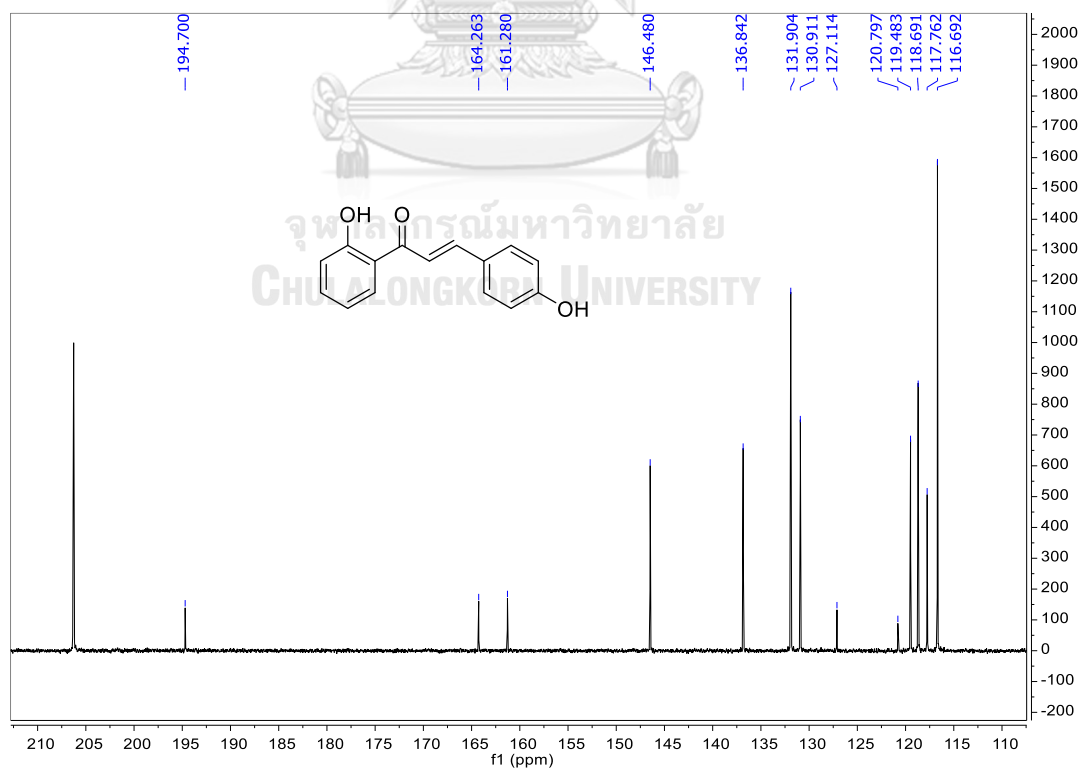


Figure A.6 The ¹³C NMR spectrum (acetone-d₆, 100 MHz) of **51**.

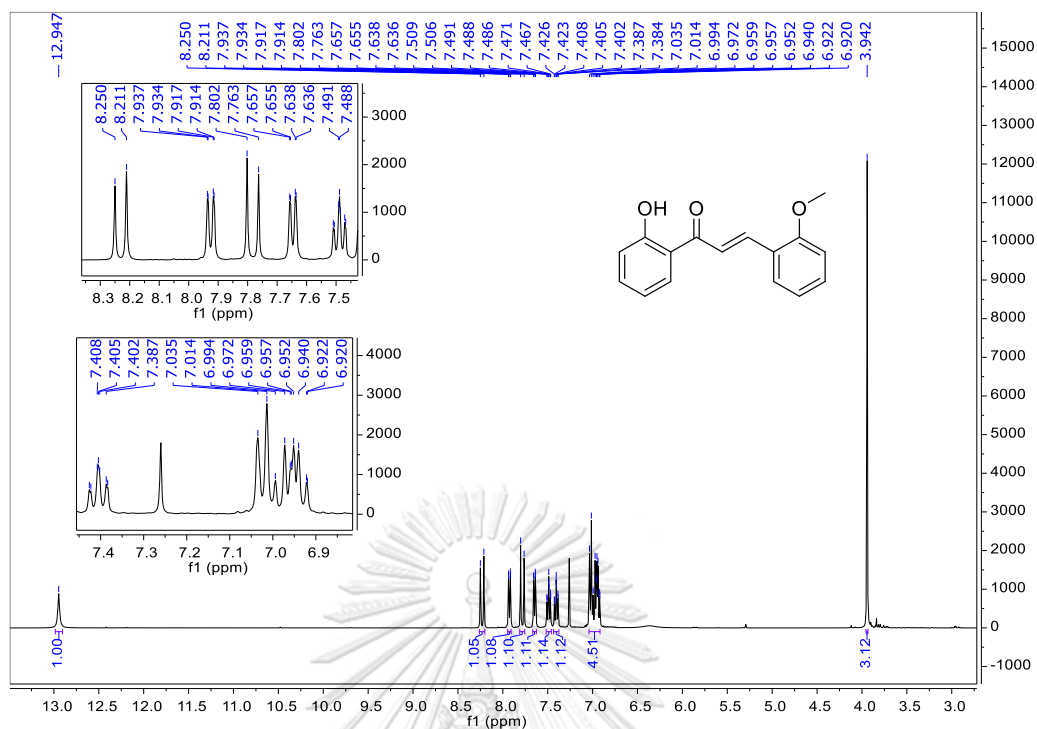


Figure A.7 The ¹H NMR spectrum (CDCl₃, 400 MHz) of 52.

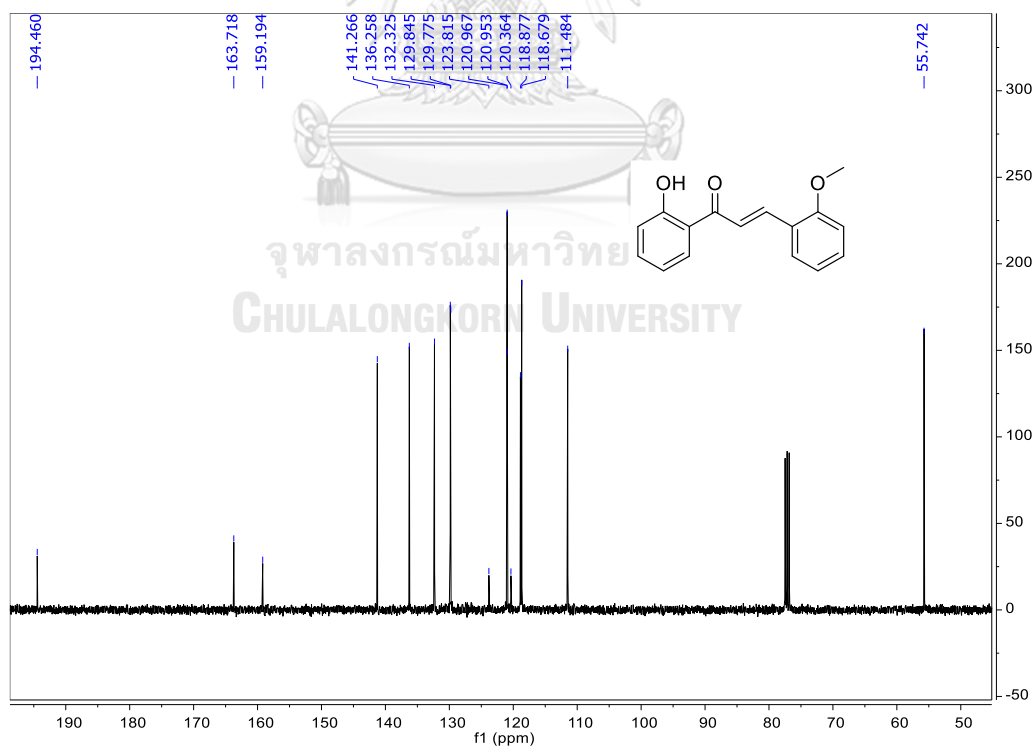


Figure A.8 The ¹³C NMR spectrum (CDCl₃, 100 MHz) of 52.

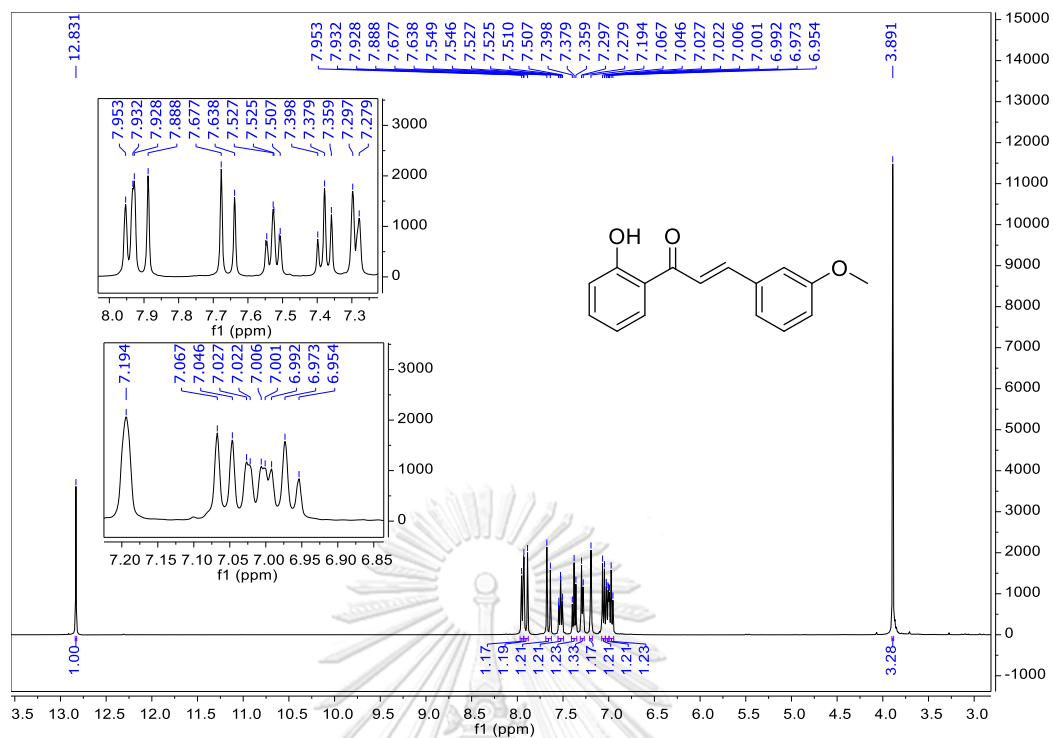


Figure A.9 The ^1H NMR spectrum (CDCl_3 , 400 MHz) of **53**.

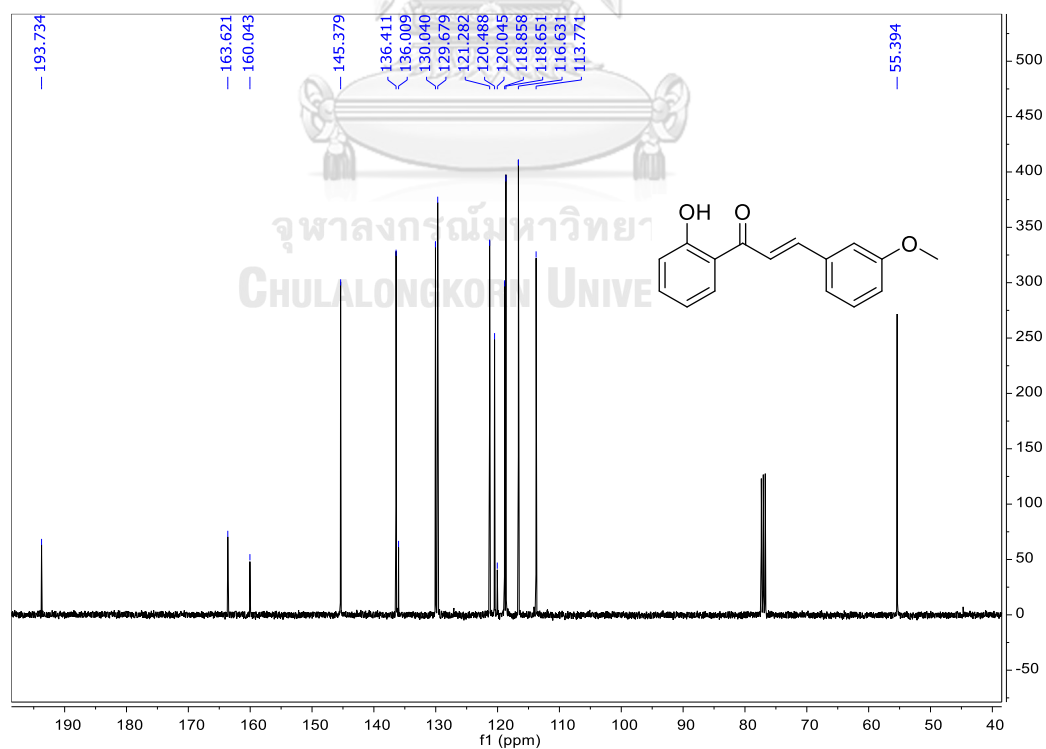


Figure A.10 The ^{13}C NMR spectrum (CDCl_3 , 100 MHz) of **53**.

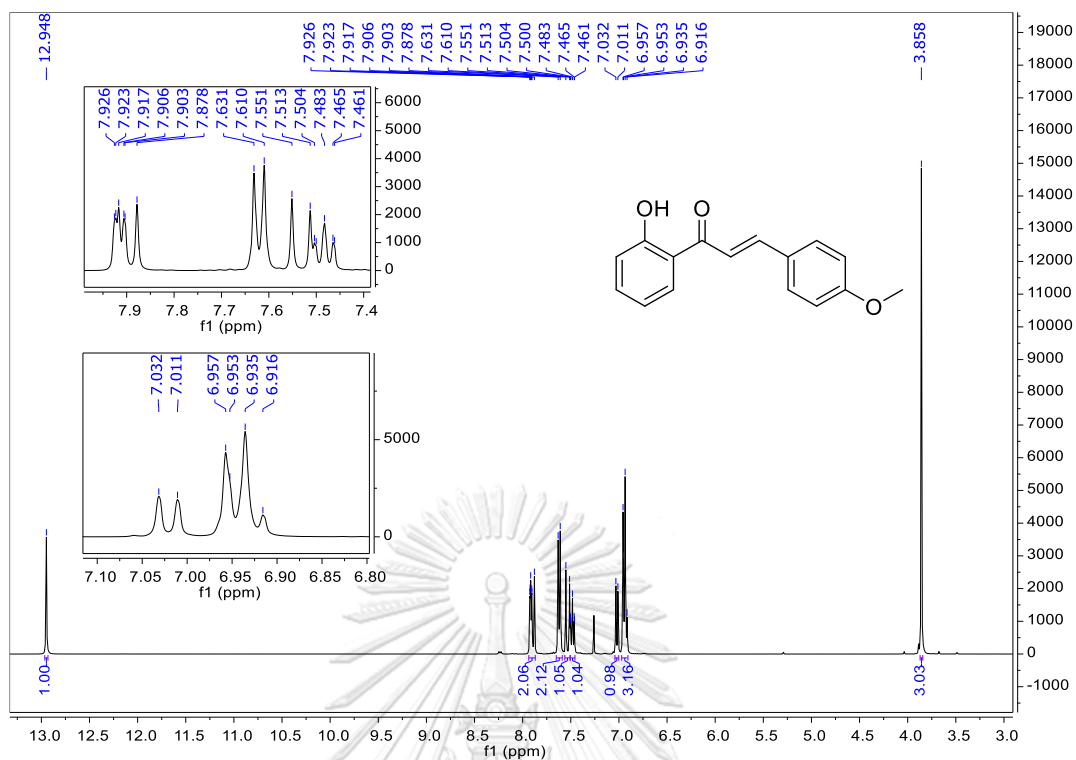


Figure A.11 The ^1H NMR spectrum (CDCl_3 , 400 MHz) of 54.

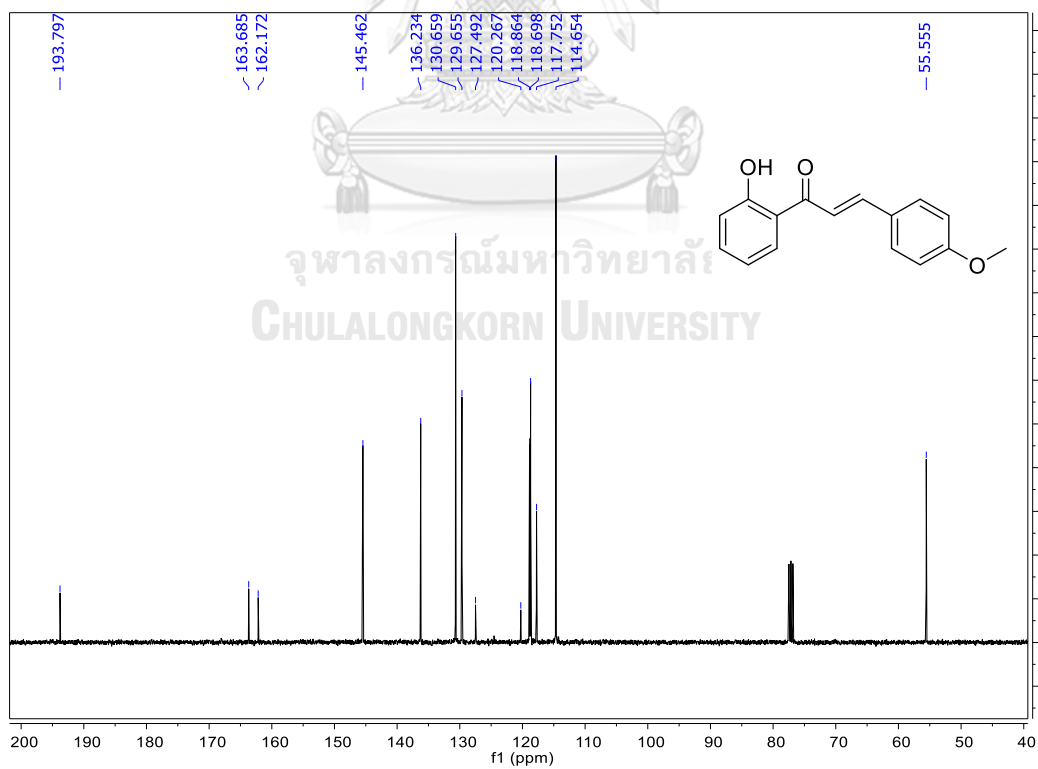


Figure A.12 The ^{13}C NMR spectrum (CDCl_3 , 100 MHz) of 54.

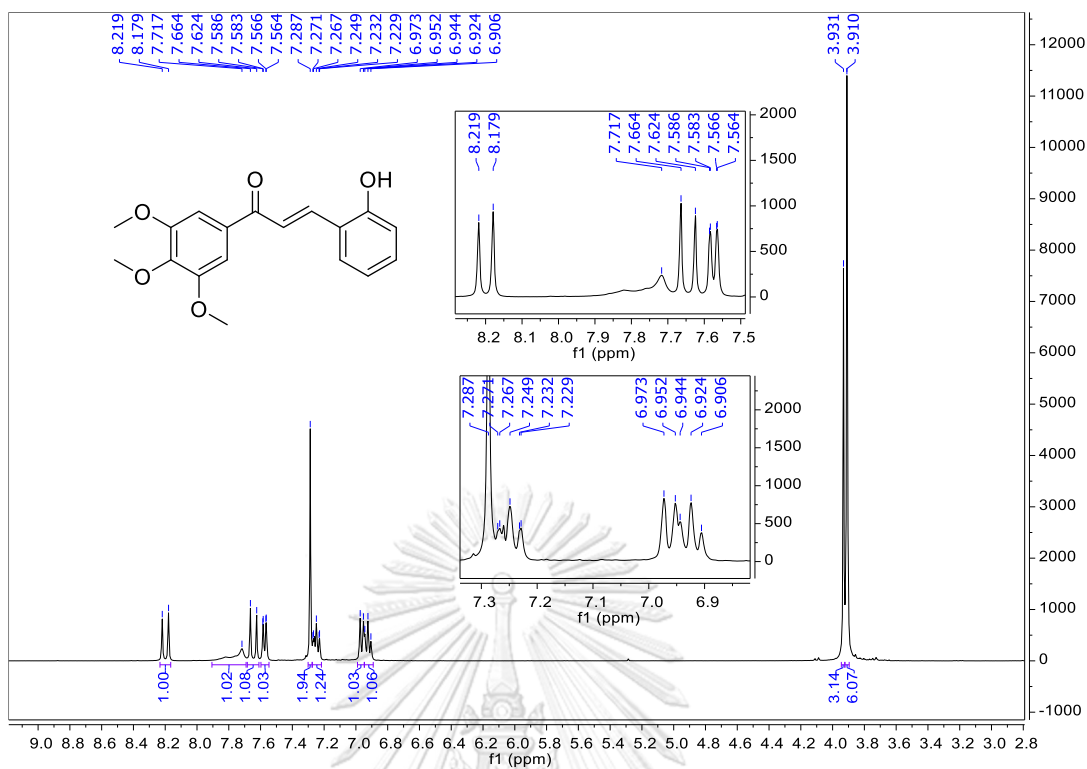


Figure A.13 The ^1H NMR spectrum (CDCl₃, 400 MHz) of 55.

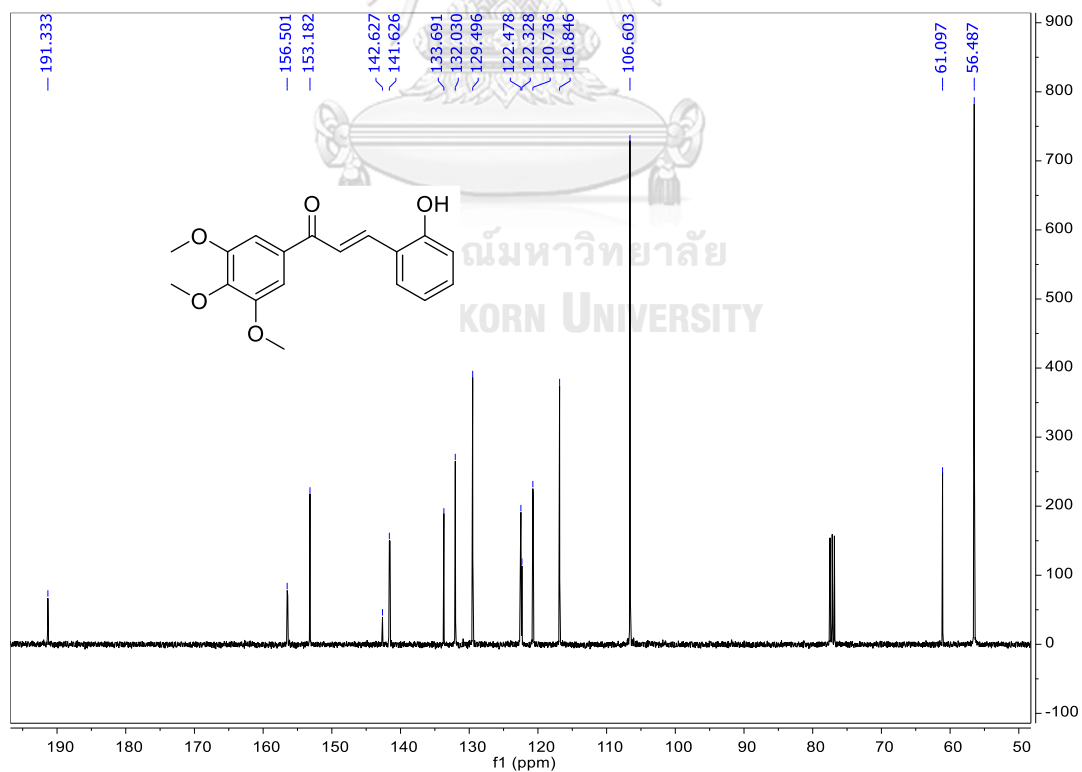


Figure A.14 The ^{13}C NMR spectrum (CDCl₃, 100 MHz) of 55.

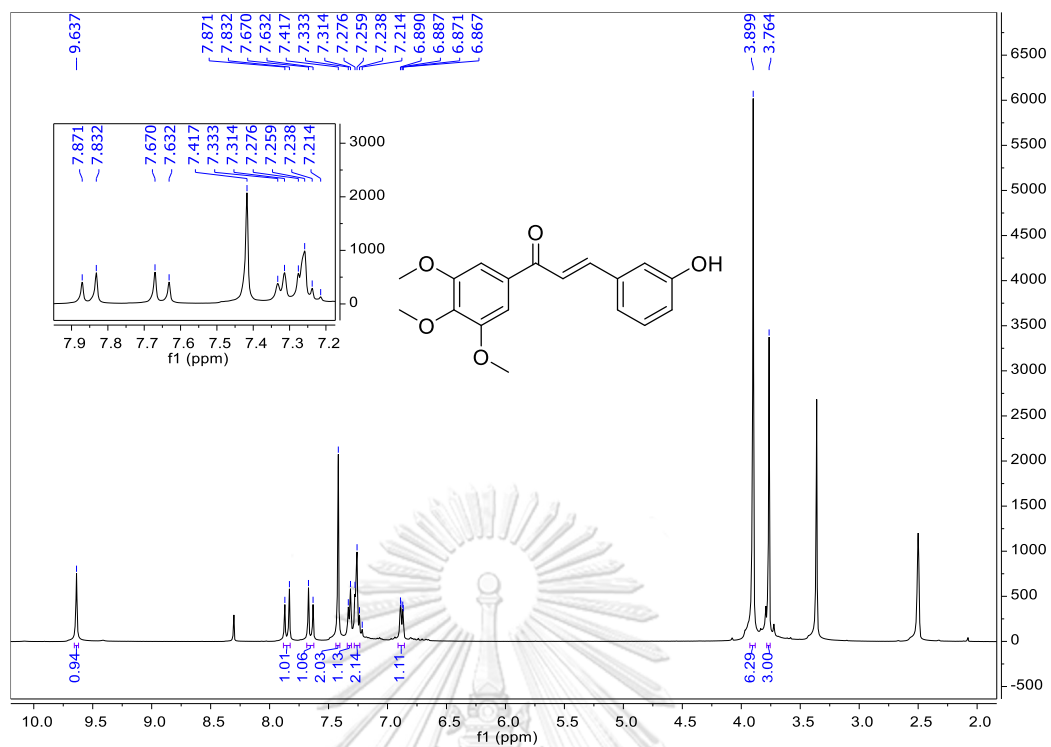


Figure A.15 The ¹H NMR spectrum (DMSO-d₆, 400 MHz) of 25.

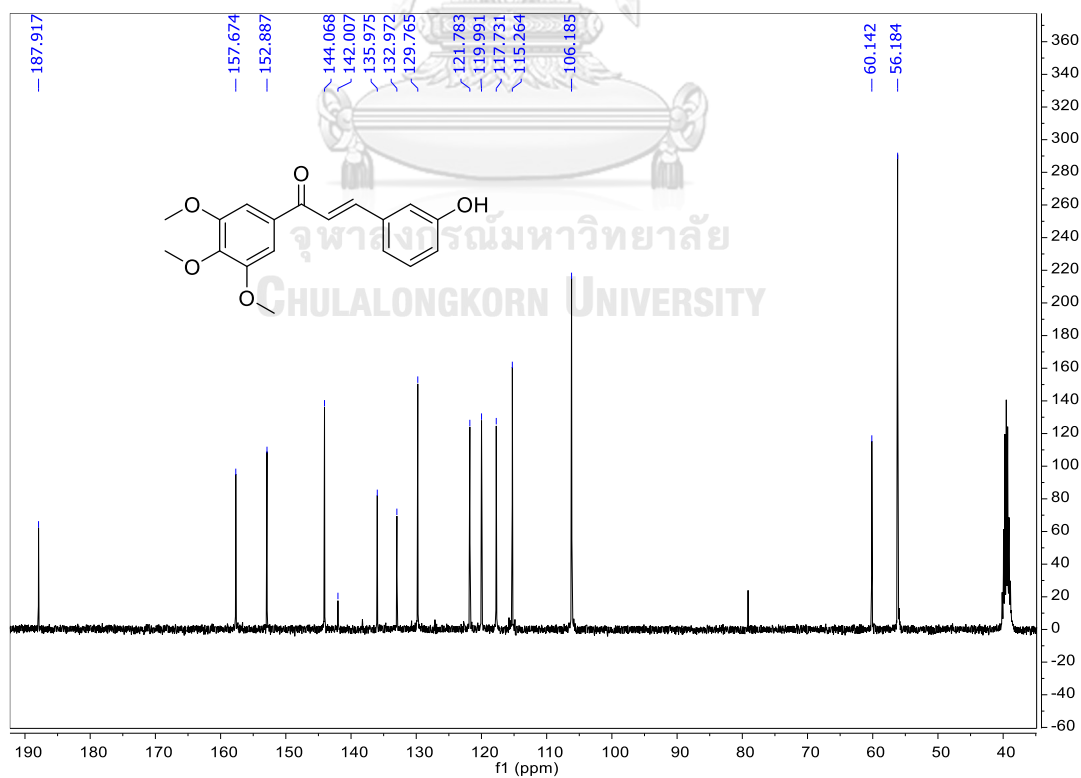


Figure A.16 The ¹³C NMR spectrum (DMSO-d₆, 100 MHz) of 25.

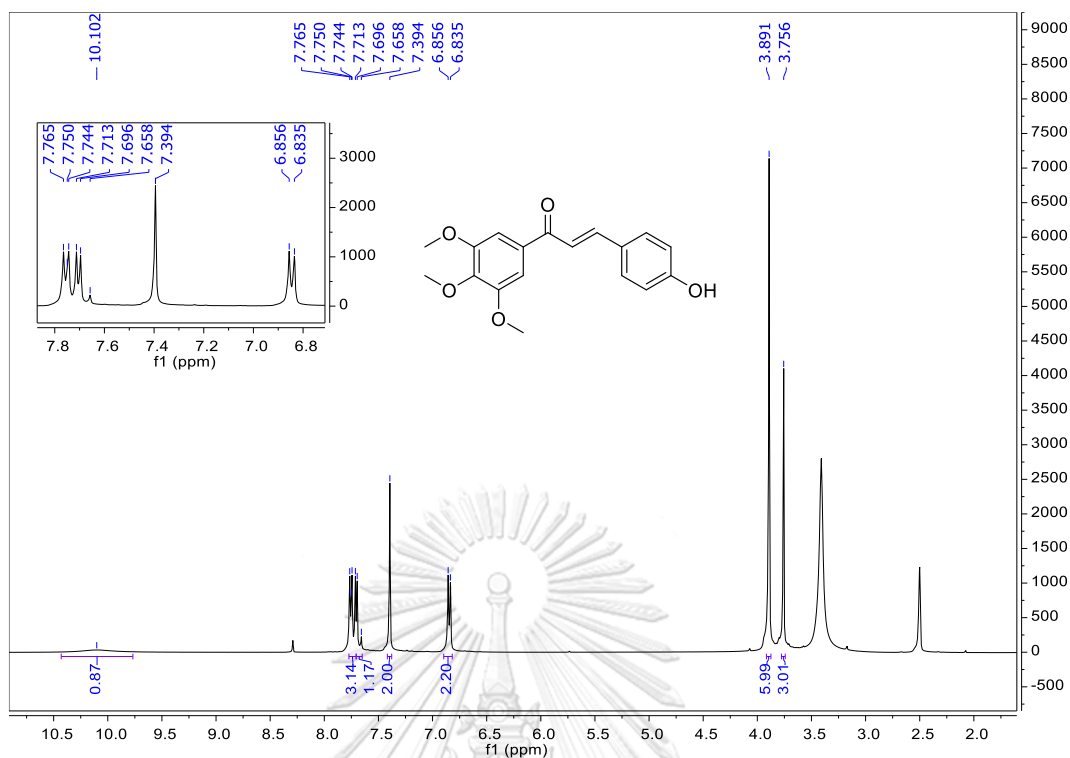


Figure A.17 The ^1H NMR spectrum (DMSO- d_6 , 400 MHz) of **56**.

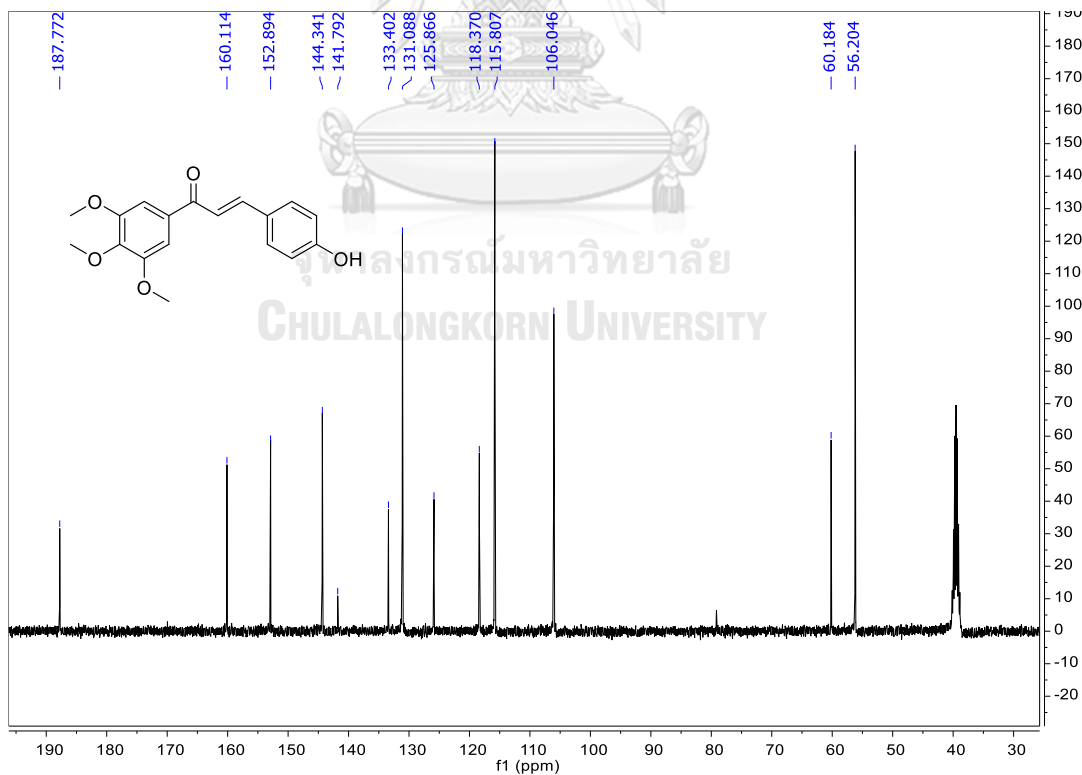


Figure A.18 The ^{13}C NMR spectrum (DMSO- d_6 , 100 MHz) of **56**.

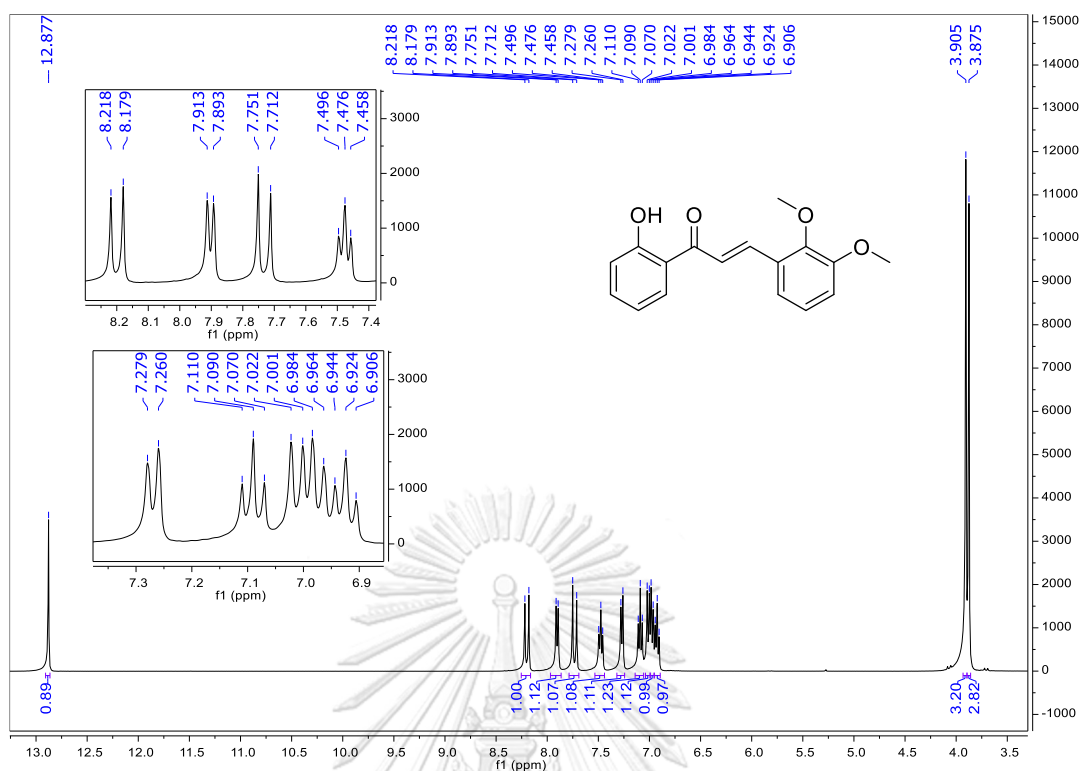


Figure A.19 The ¹H NMR spectrum (CDCl₃, 400 MHz) of **57**.

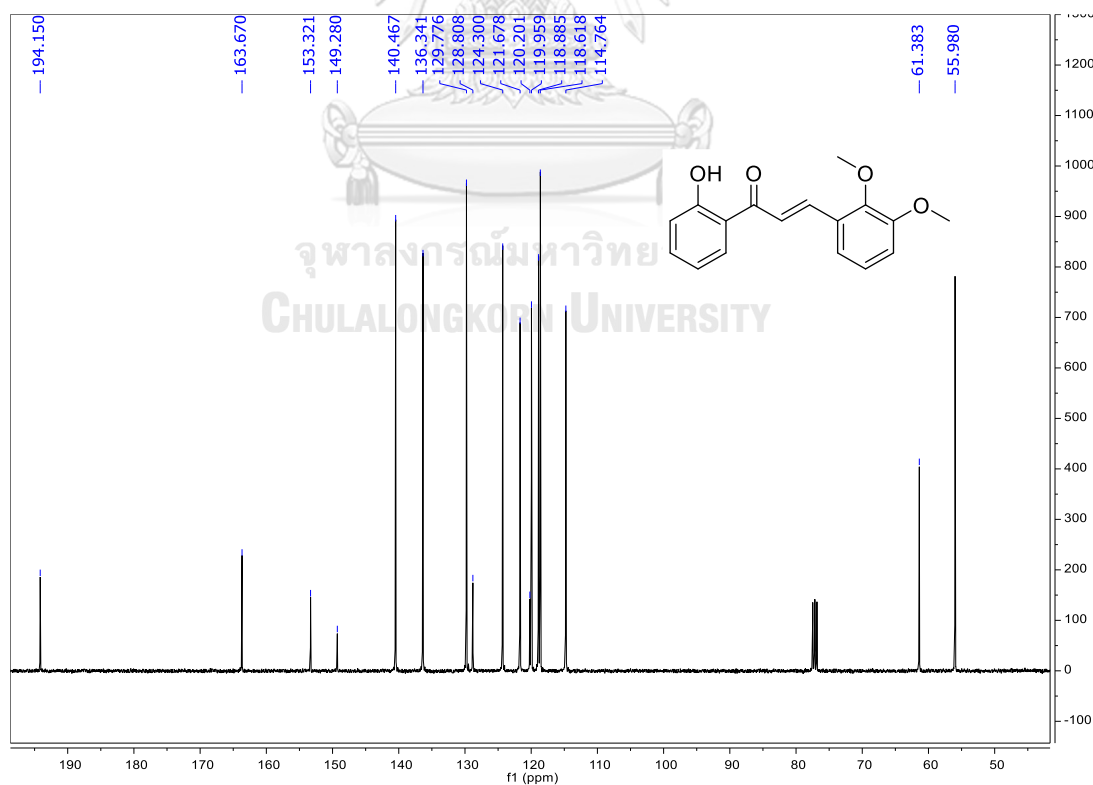


Figure A.20 The ¹³C NMR spectrum (CDCl₃, 100 MHz) of **57**.

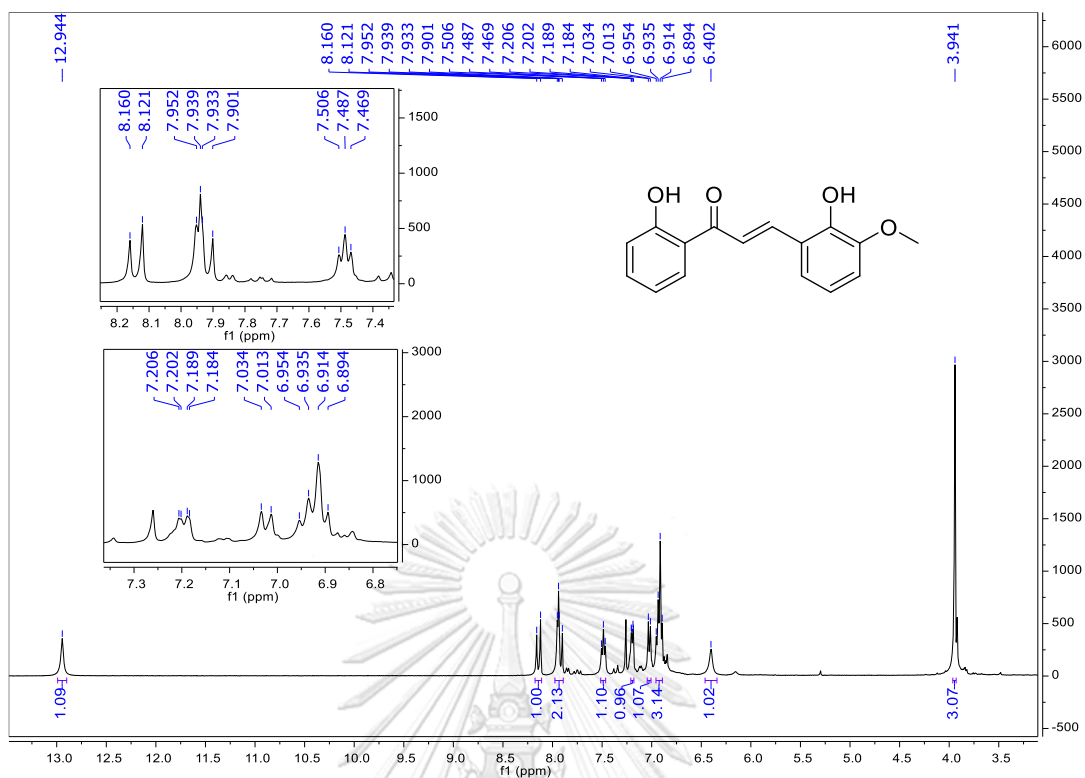


Figure A.21 The ¹H NMR spectrum (CDCl₃, 400 MHz) of 58.

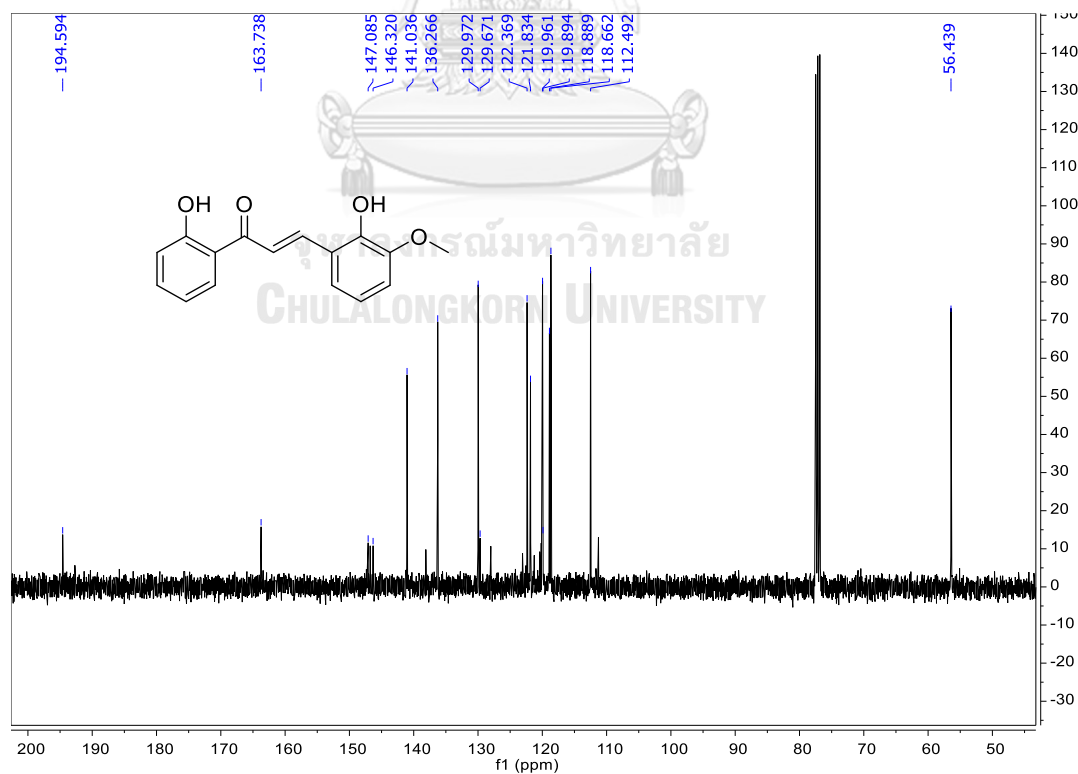


Figure A.22 The ¹³C NMR spectrum (CDCl₃, 100 MHz) of 58.

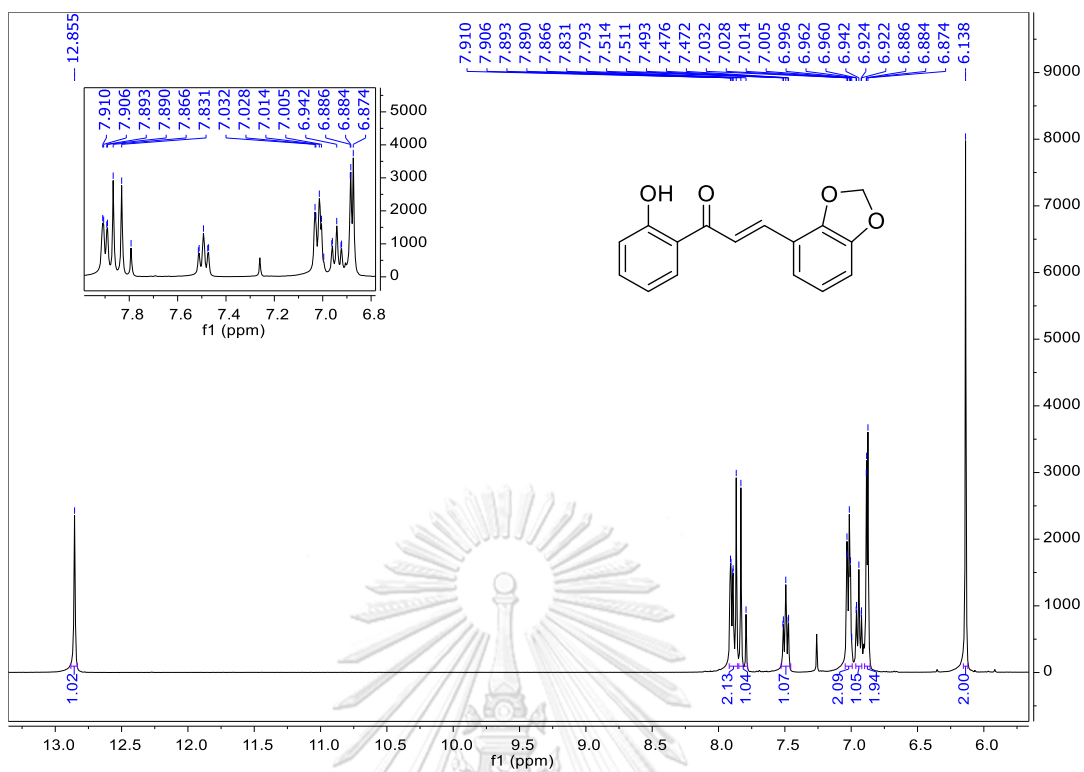


Figure A.23 The ^1H NMR spectrum (CDCl_3 , 400 MHz) of **59**.

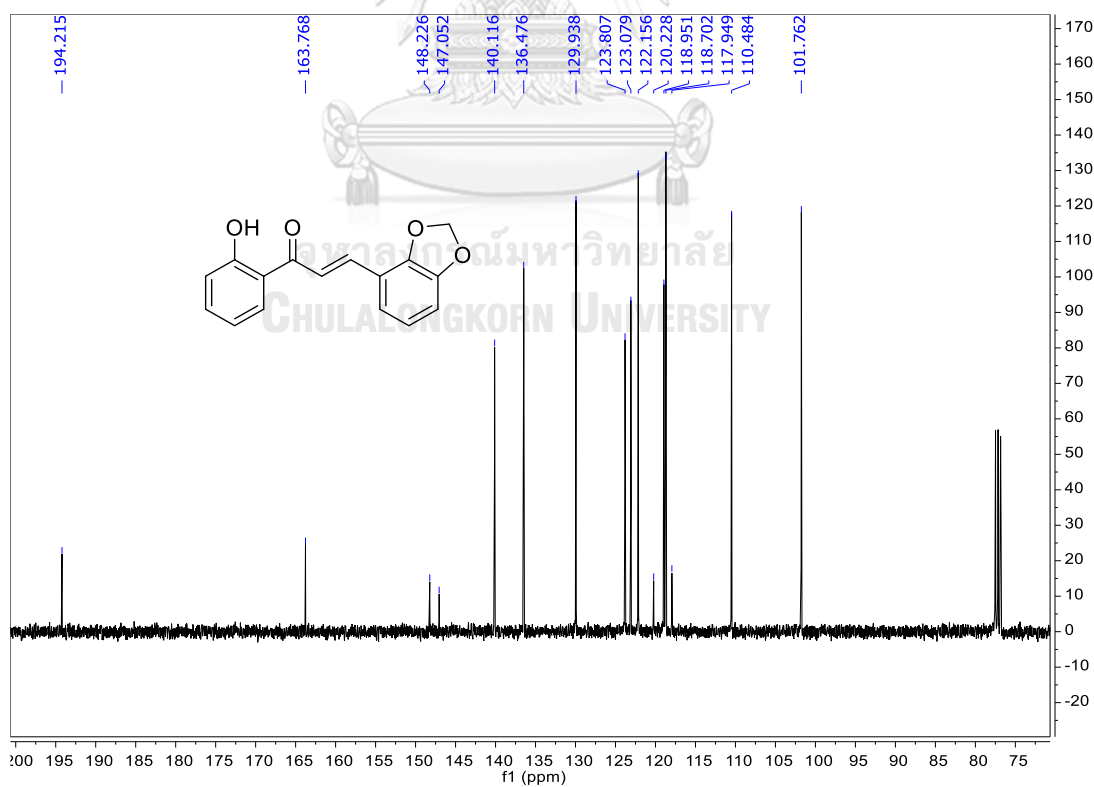


Figure A.24 The ^{13}C NMR spectrum (CDCl_3 , 100 MHz) of **59**.

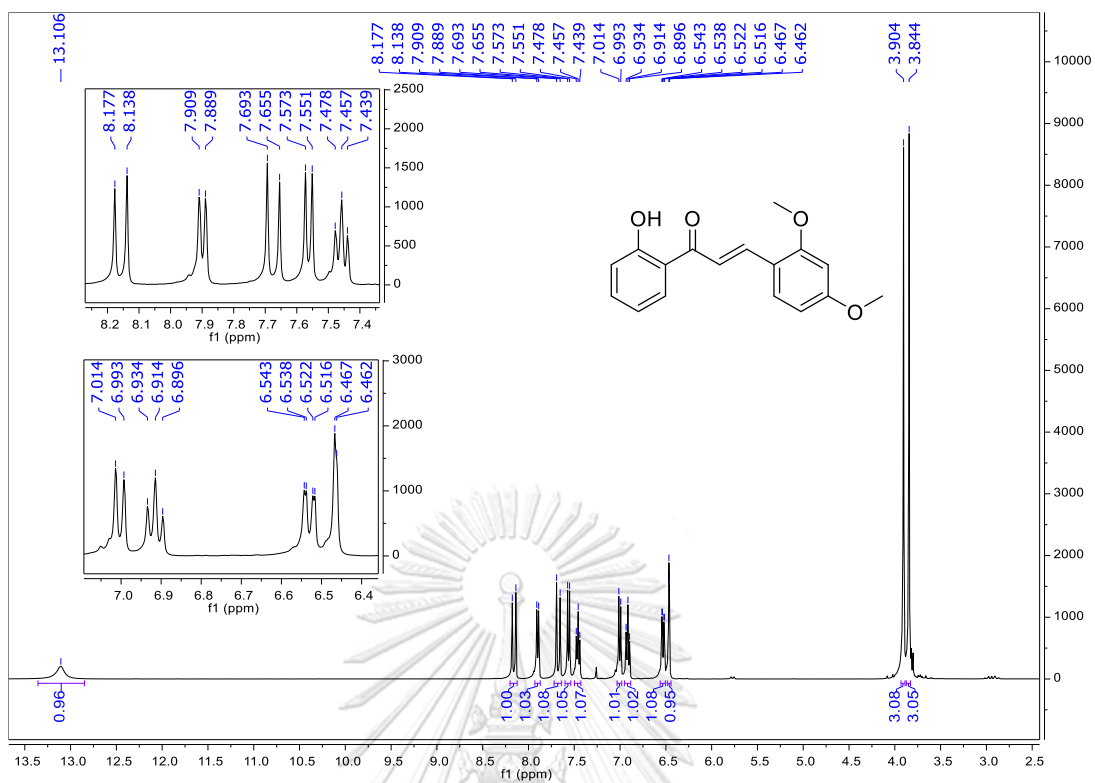


Figure A.25 The ^1H NMR spectrum (CDCl_3 , 400 MHz) of **60**.

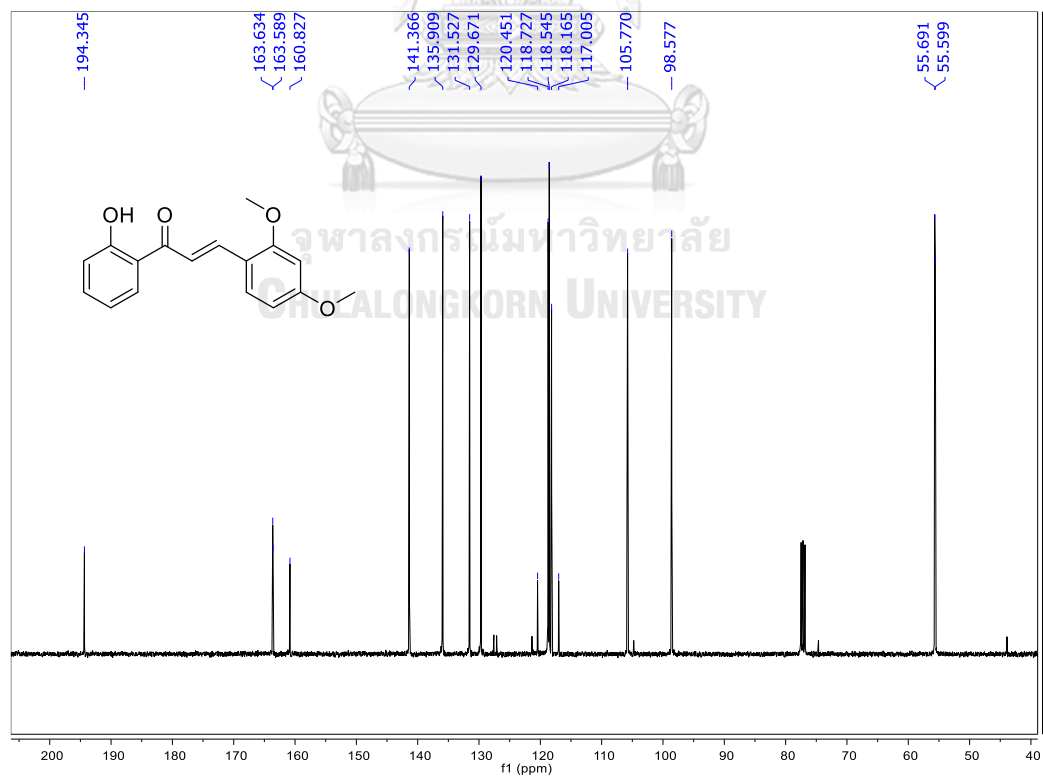


Figure A.26 The ^{13}C NMR spectrum (CDCl_3 , 100 MHz) of **60**.

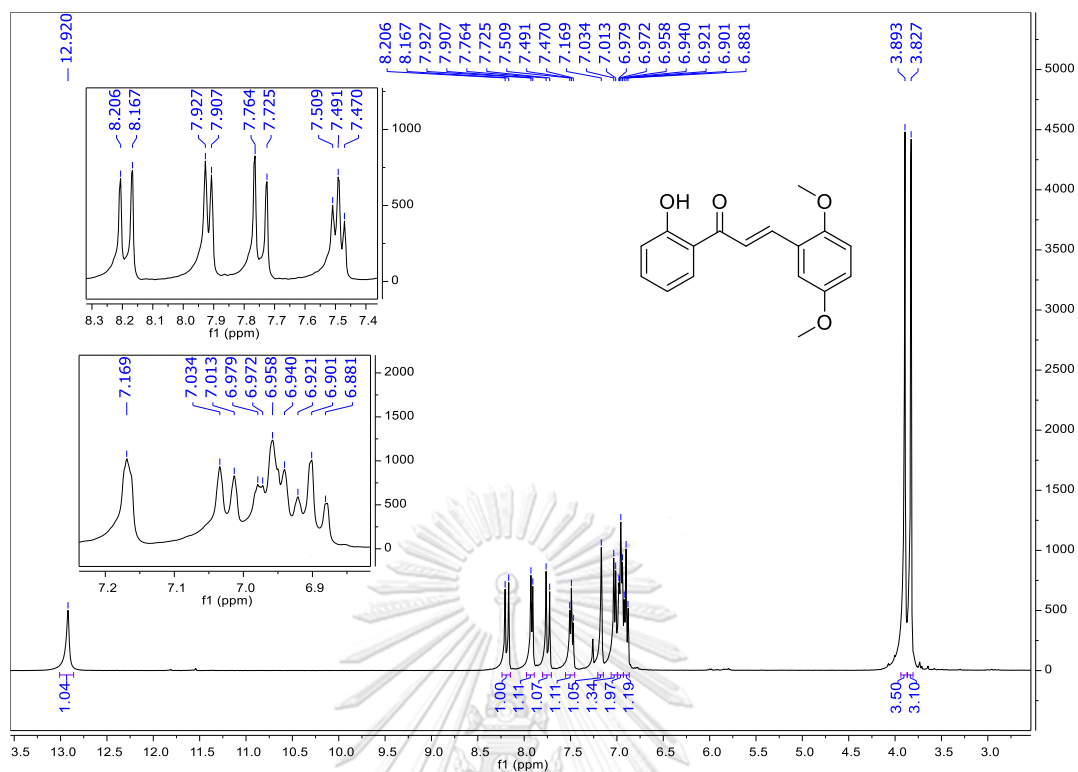


Figure A.27 The ¹H NMR spectrum (CDCl₃, 400 MHz) of **61**.

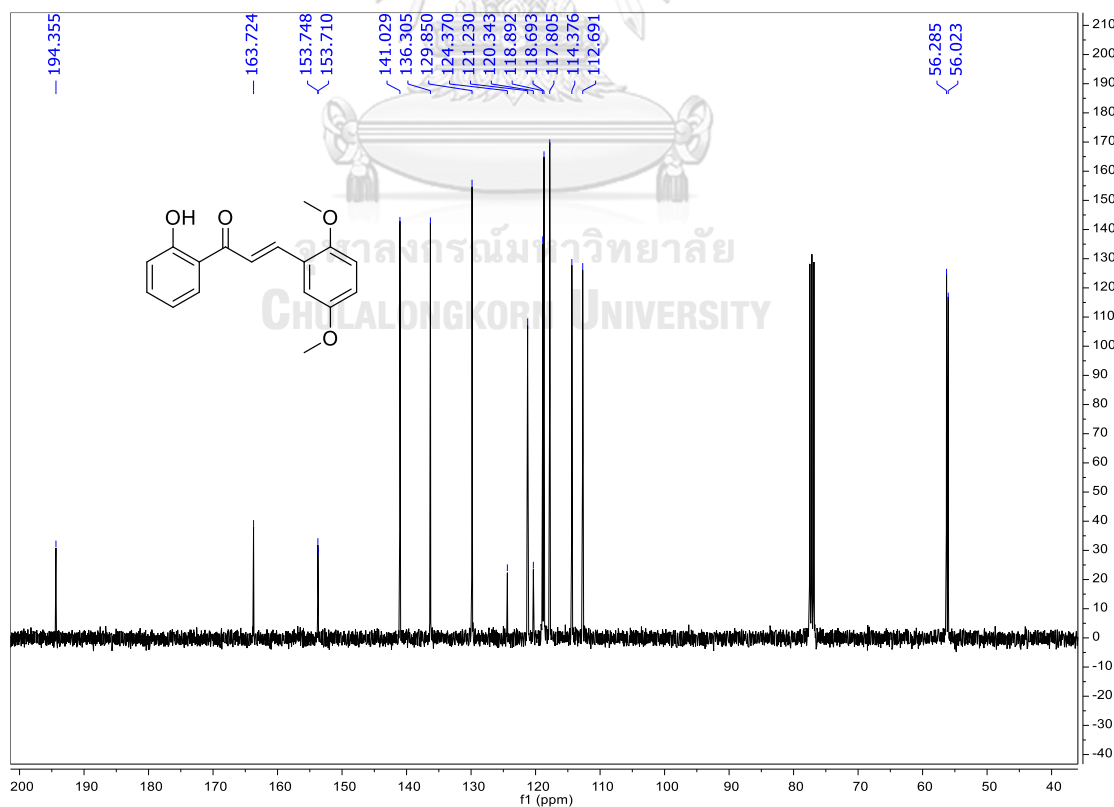


Figure A.28 The ¹³C NMR spectrum (CDCl₃, 100 MHz) of **61**.

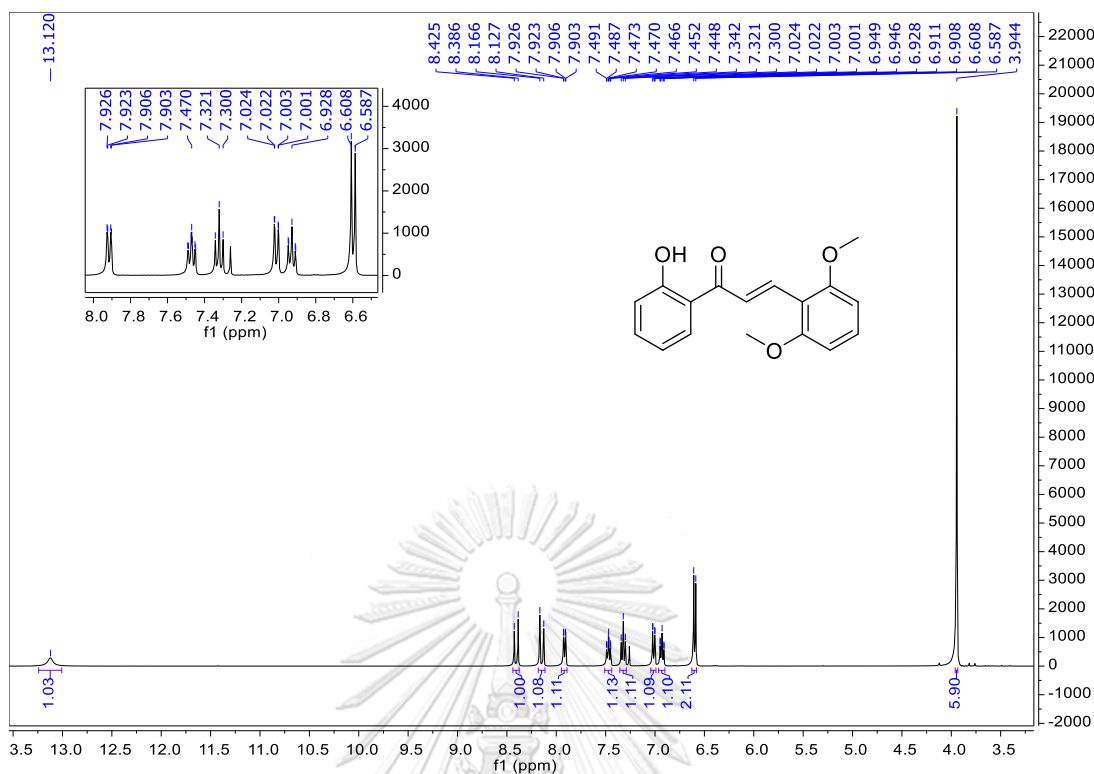


Figure A.29 The ^1H NMR spectrum (CDCl_3 , 400 MHz) of **62**.

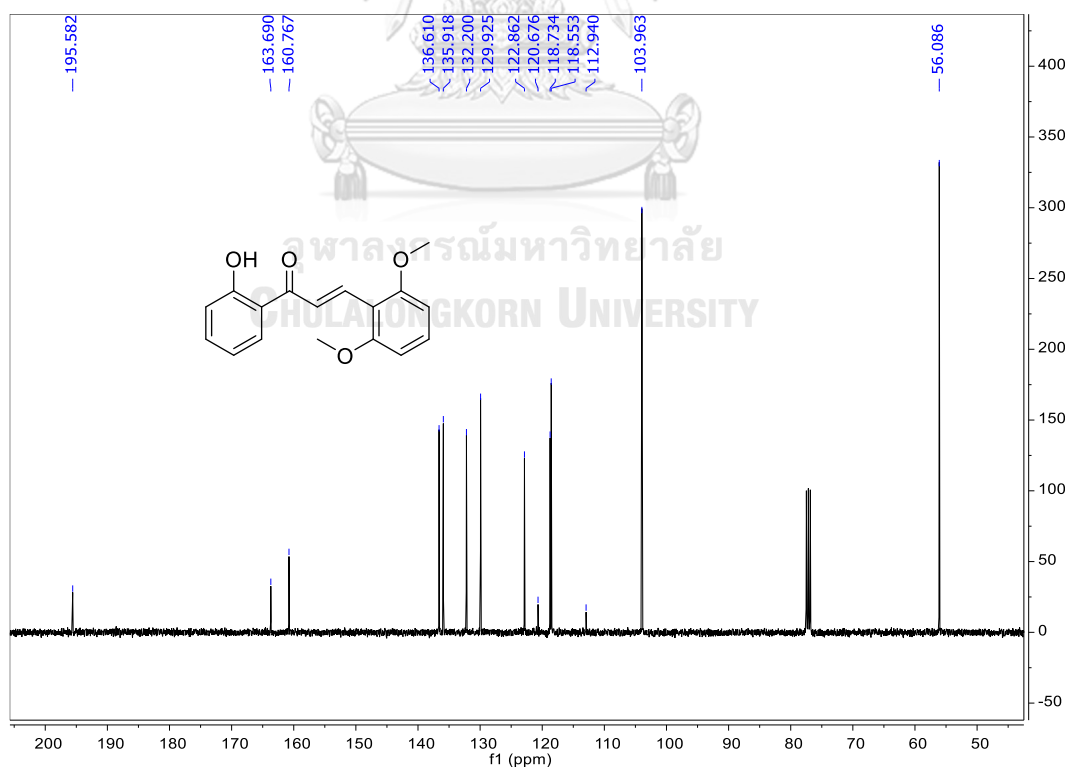


Figure A.30 The ^{13}C NMR spectrum (CDCl_3 , 100 MHz) of **62**.

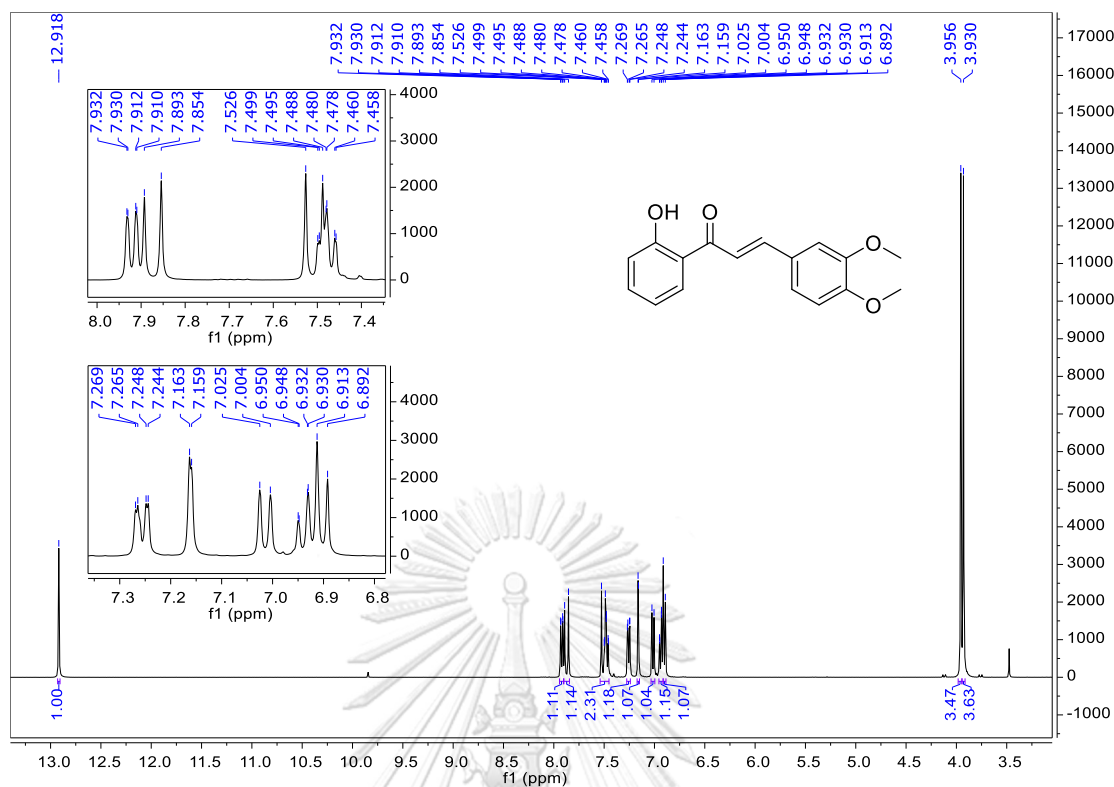


Figure A.31 The ¹H NMR spectrum (CDCl₃, 400 MHz) of **63**.

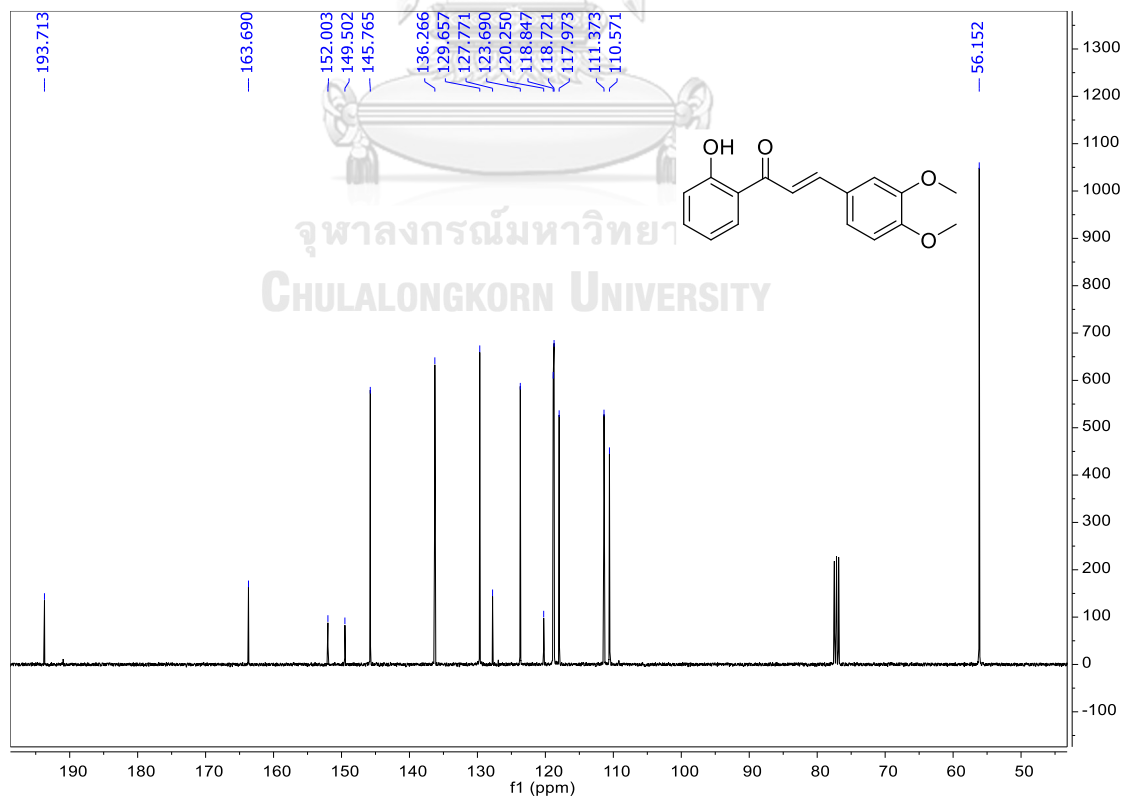


Figure A.32 The ¹³C NMR spectrum (CDCl₃, 100 MHz) of **63**.

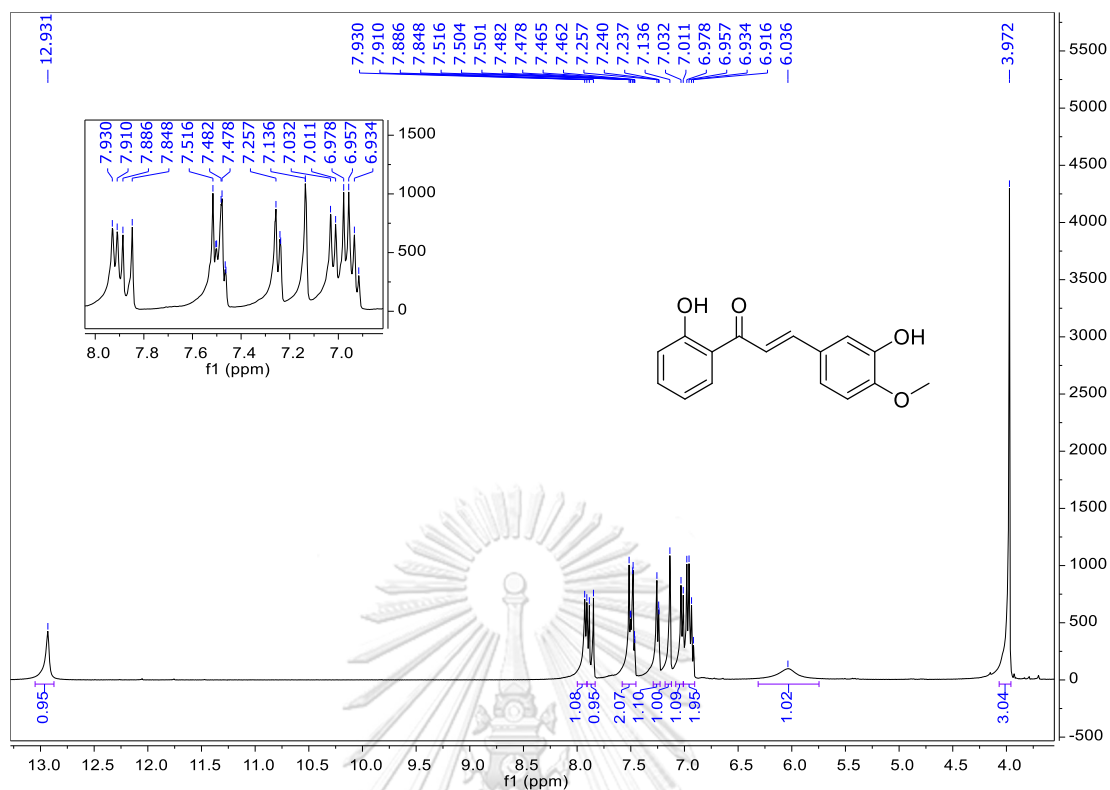


Figure A.33 The ^1H NMR spectrum (CDCl_3 , 400 MHz) of **64**.

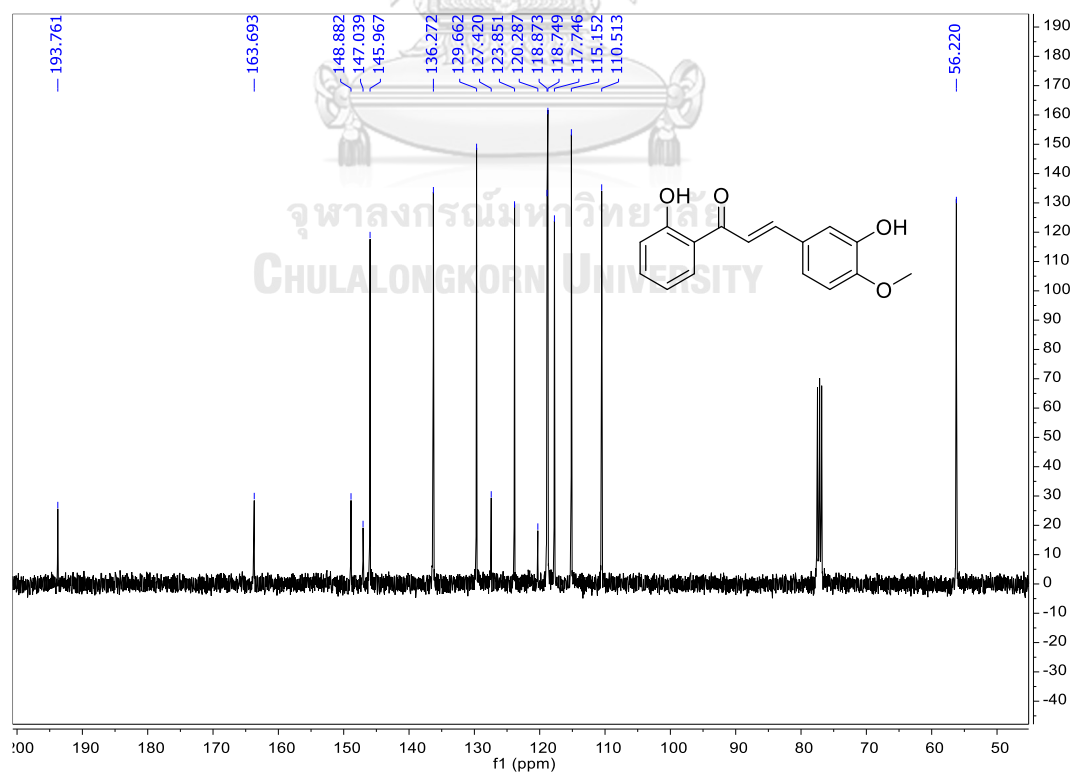


Figure A.34 The ^{13}C NMR spectrum (CDCl_3 , 100 MHz) of **64**.

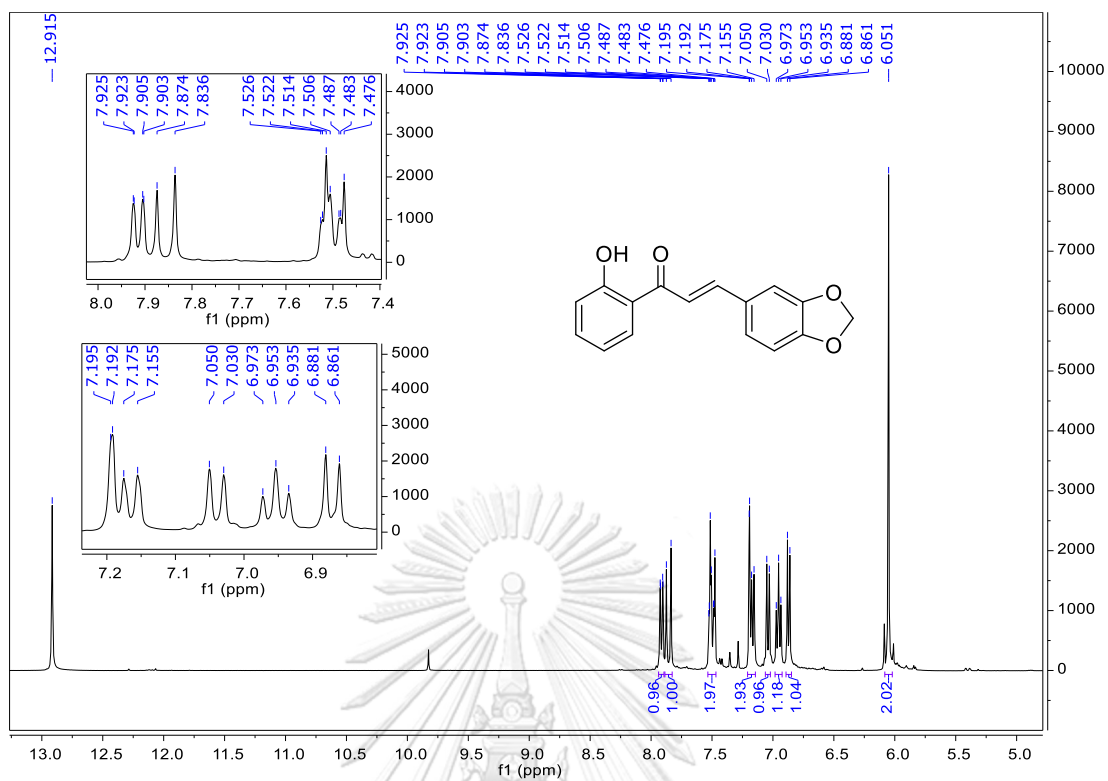


Figure A.35 The ^1H NMR spectrum (CDCl₃, 400 MHz) of 65.

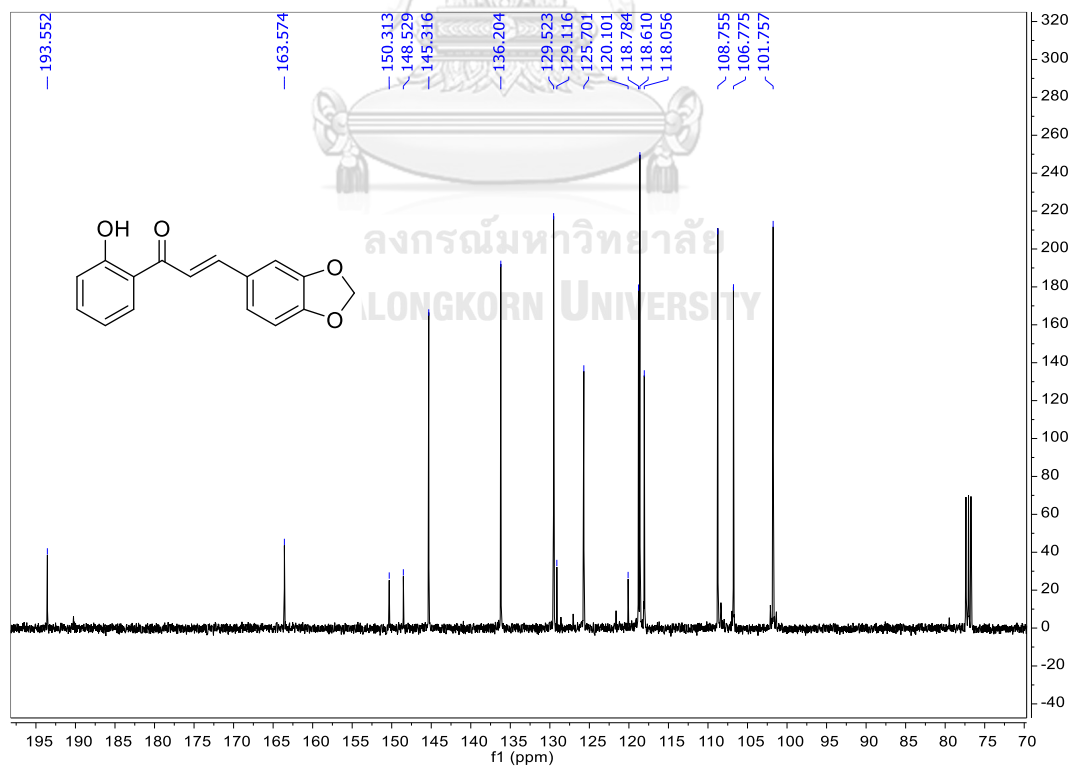


Figure A.36 The ^{13}C NMR spectrum (CDCl₃, 100 MHz) of 65.

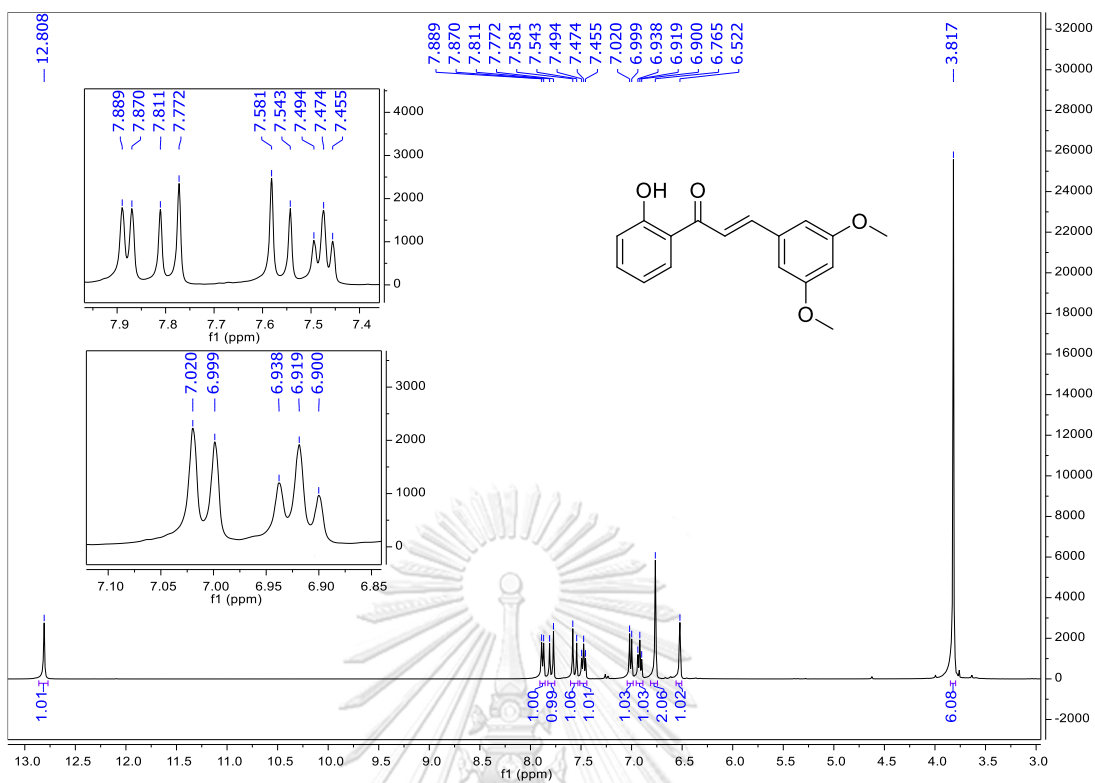


Figure A.37 The ¹H NMR spectrum (CDCl₃, 400 MHz) of **66**.

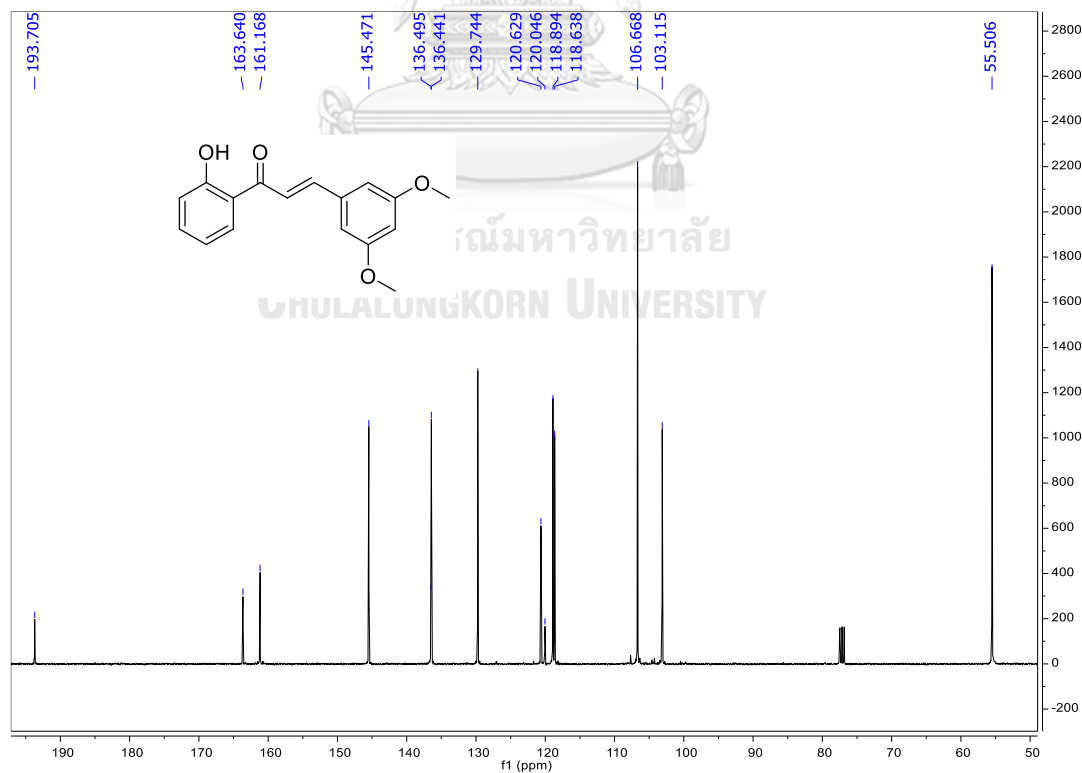


Figure A.38 The ¹³C NMR spectrum (CDCl₃, 100 MHz) of **66**.

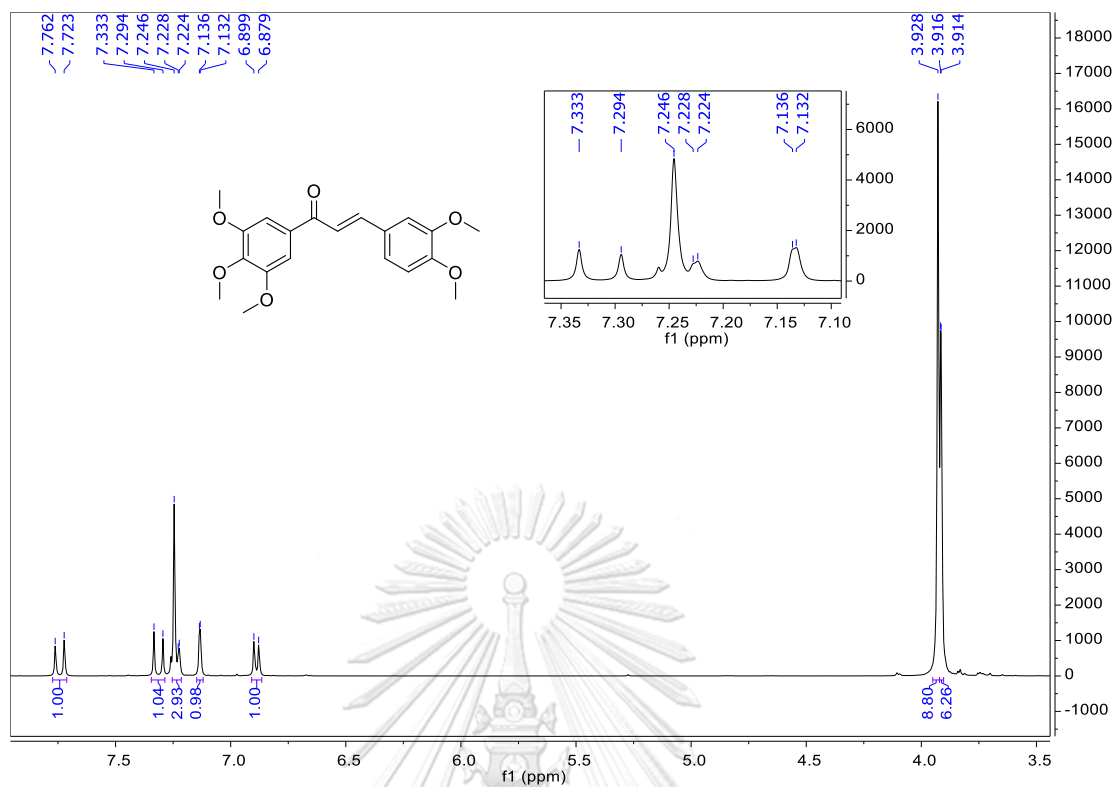


Figure A.39 The ¹H NMR spectrum (CDCl₃, 400 MHz) of 67.

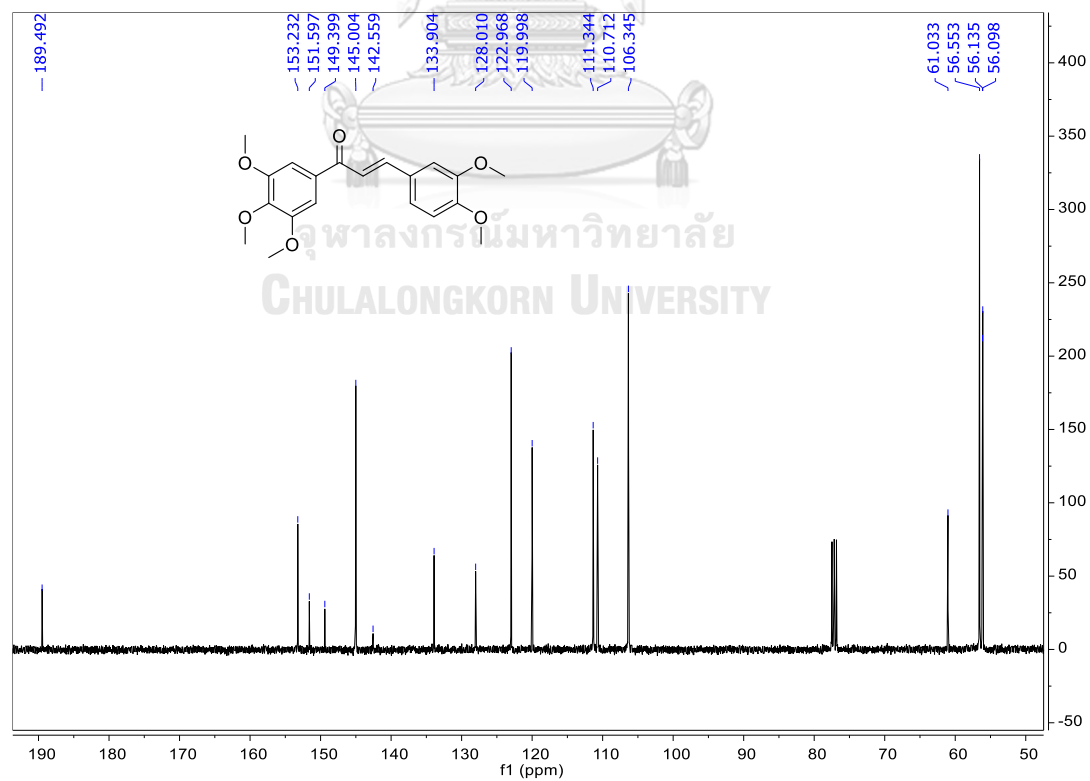


Figure A.40 The ¹³C NMR spectrum (CDCl₃, 100 MHz) of 67.

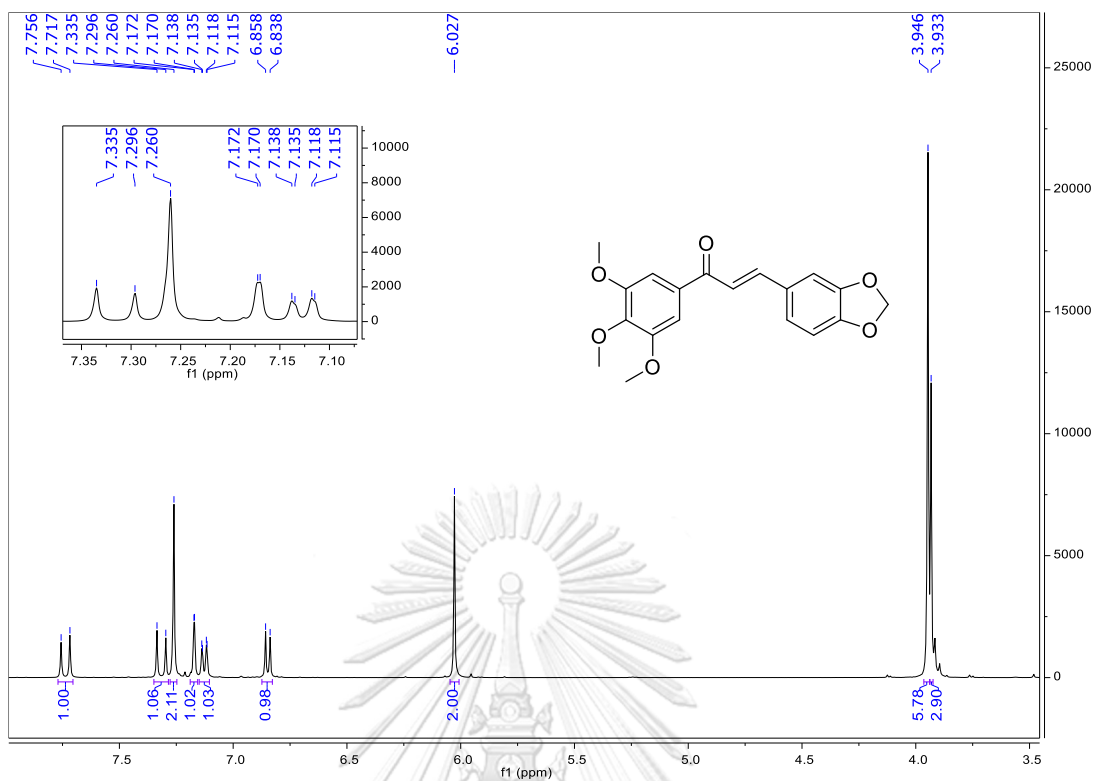


Figure A.41 The ^1H NMR spectrum (CDCl_3 , 400 MHz) of **68**.

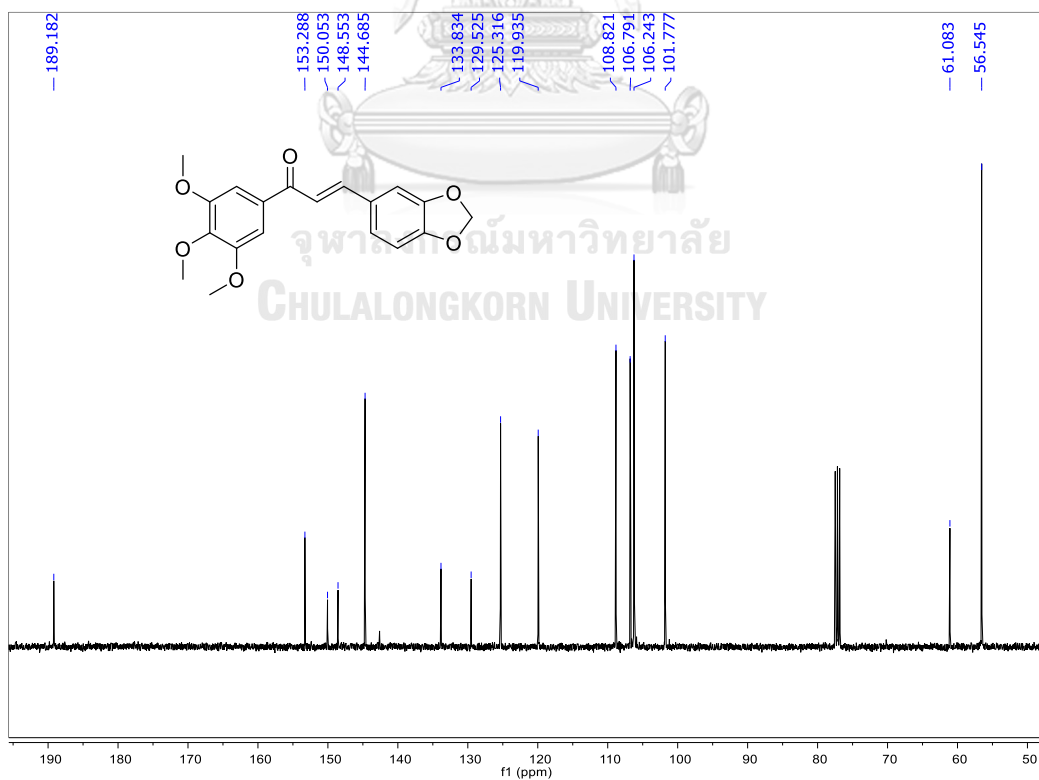


Figure A.42 The ^{13}C NMR spectrum (CDCl_3 , 100 MHz) of **68**.

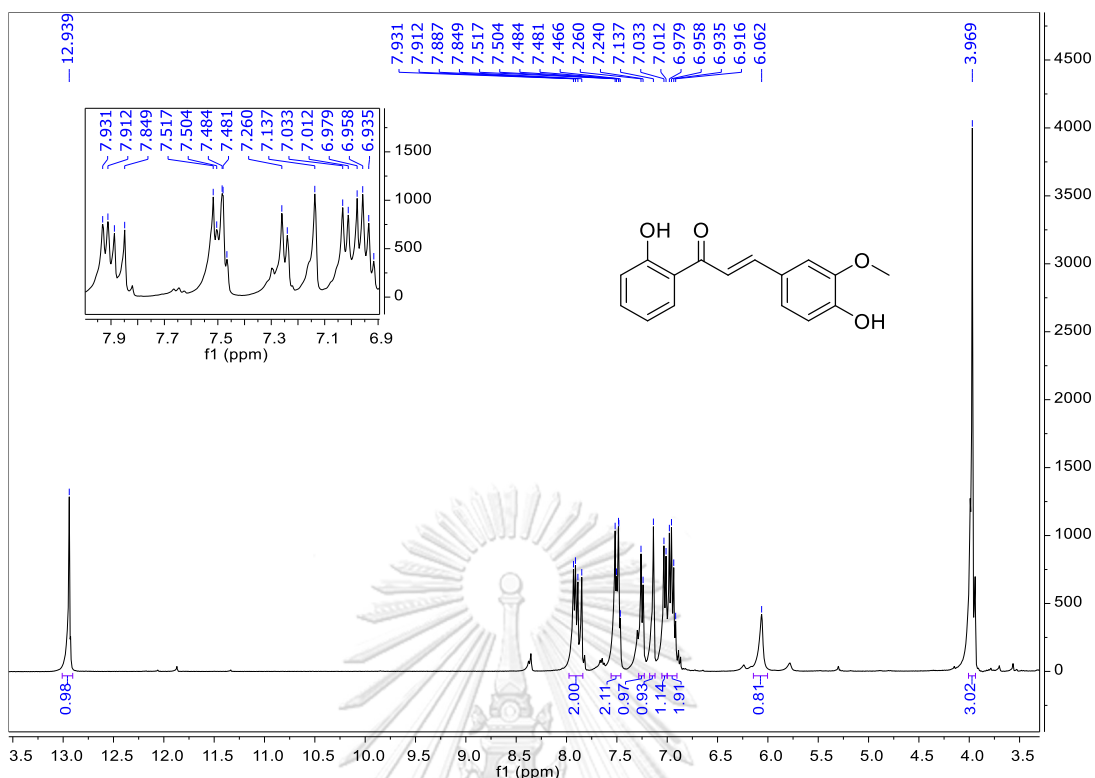


Figure A.43 The ^1H NMR spectrum (CDCl_3 , 400 MHz) of **69**.

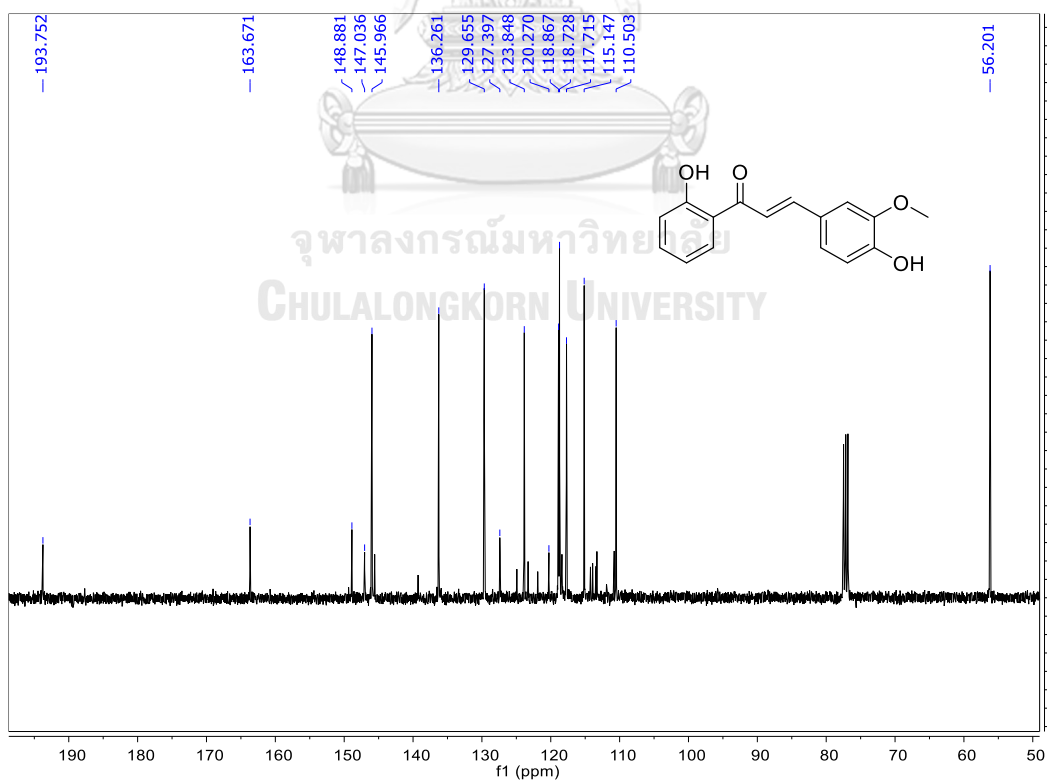


Figure A.44 The ^{13}C NMR spectrum (CDCl_3 , 100 MHz) of **69**.

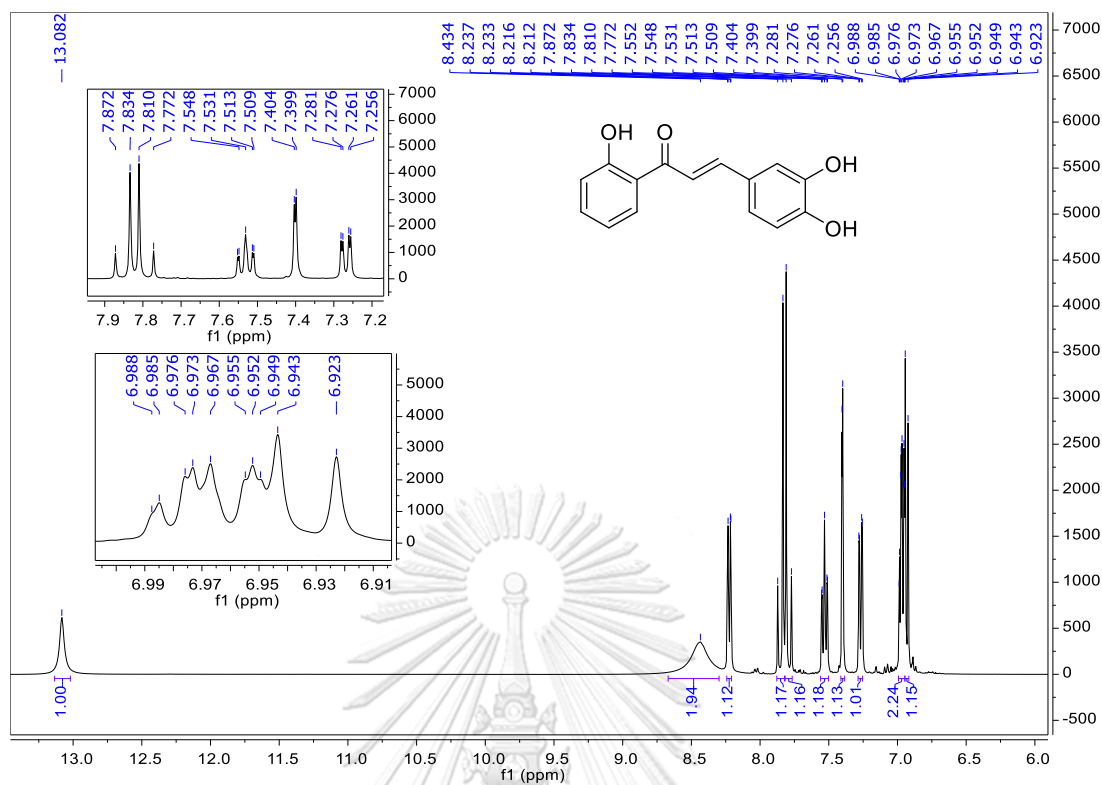


Figure A.45 The ^1H NMR spectrum (acetone- d_6 , 400 MHz) of 70.

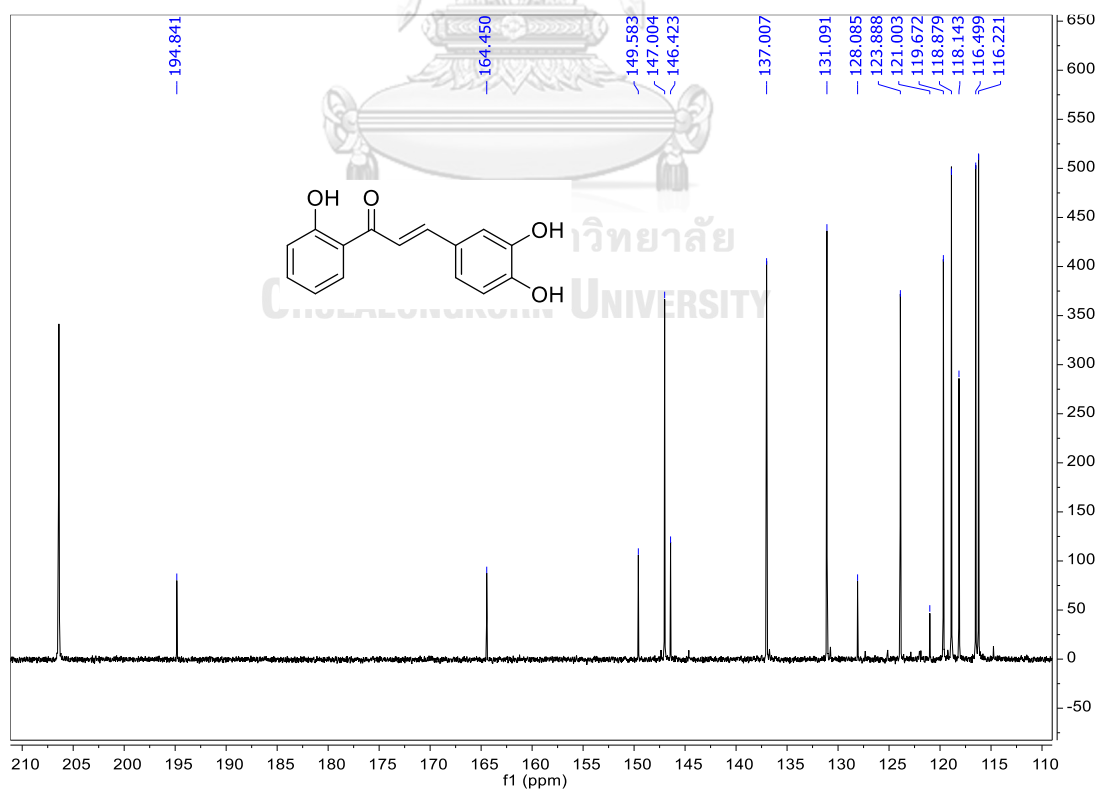
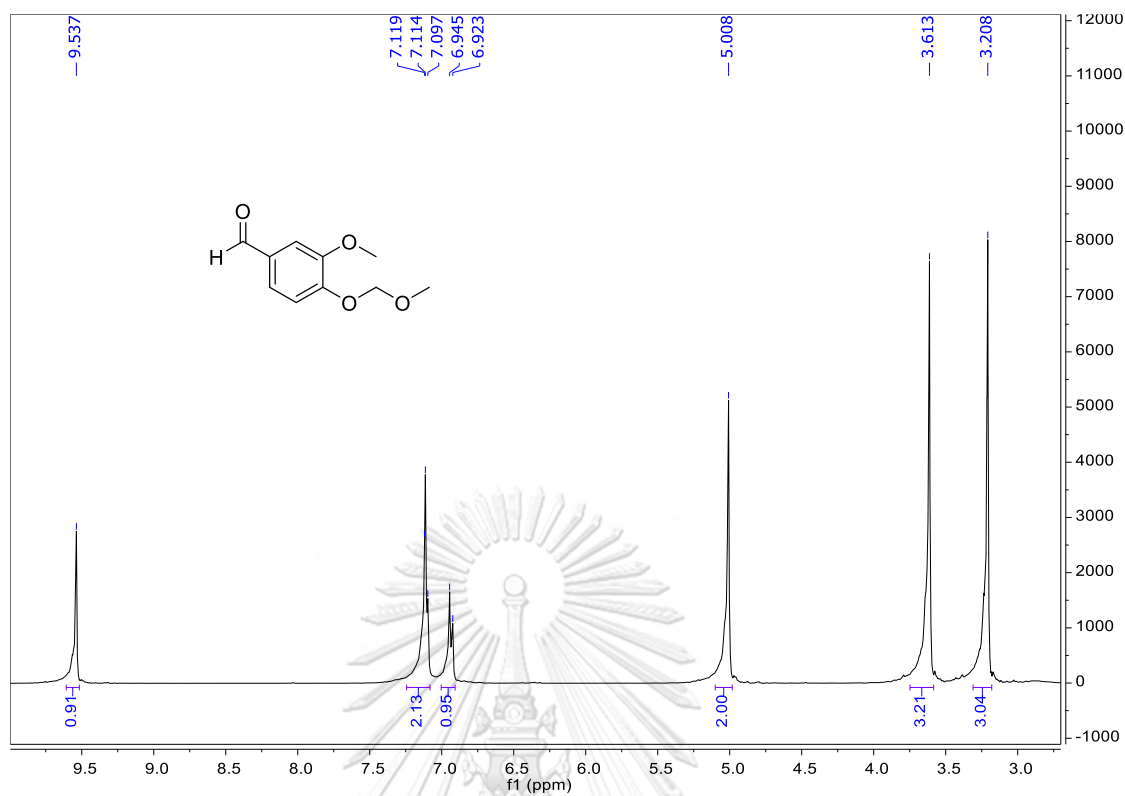
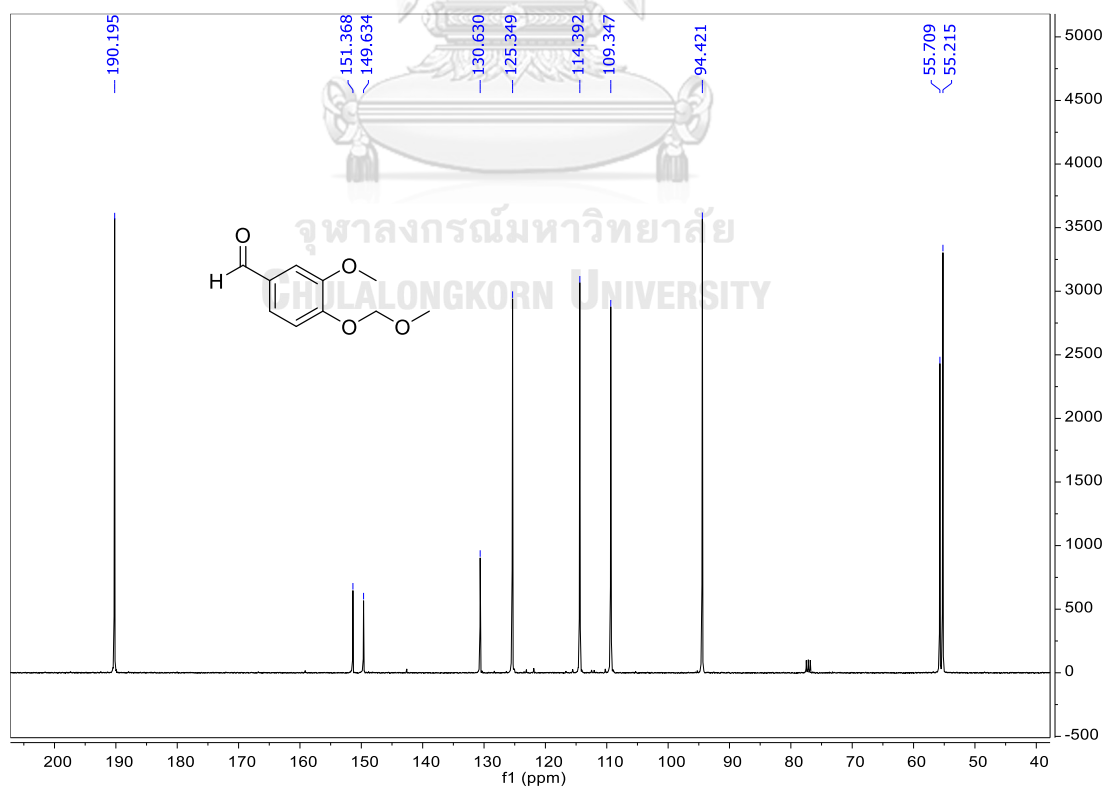


Figure A.46 The ^{13}C NMR spectrum (acetone- d_6 , 100 MHz) of 70.

Figure A.47 The ^1H NMR spectrum (CDCl_3 , 400 MHz) of **72**.Figure A.48 The ^{13}C NMR spectrum (CDCl_3 , 100 MHz) of **72**.

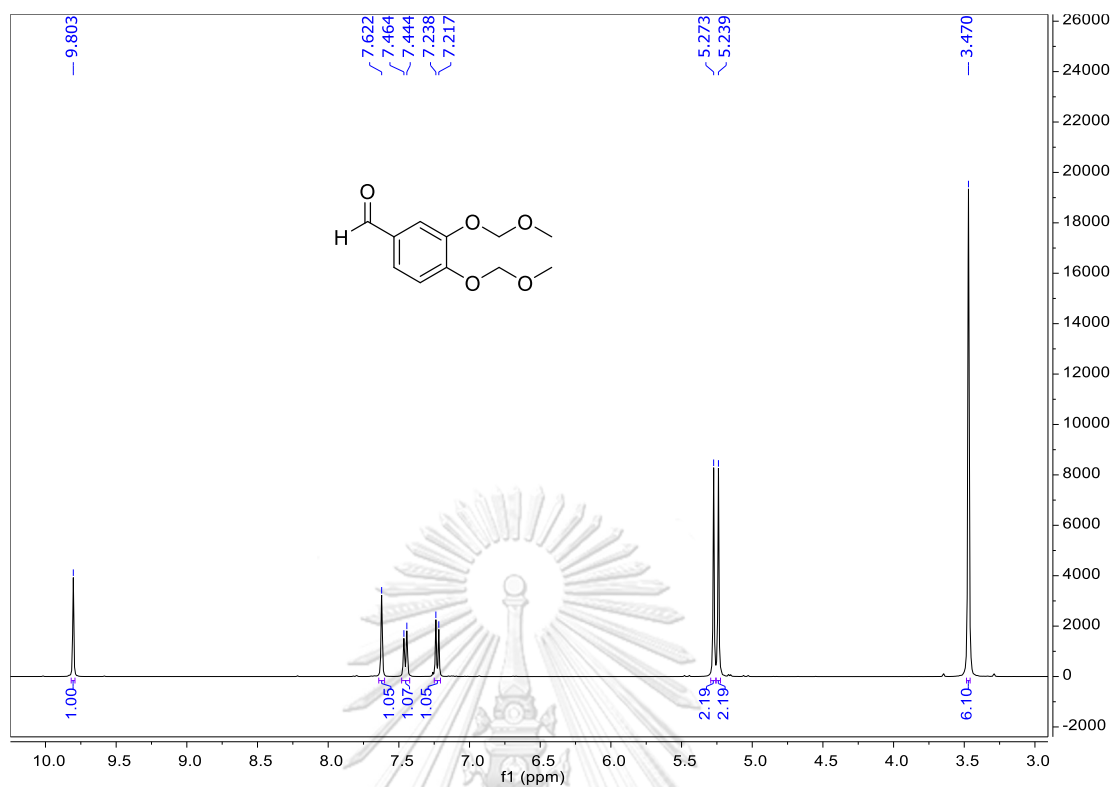


Figure A.49 The ^1H NMR spectrum (CDCl_3 , 400 MHz) of **73**.

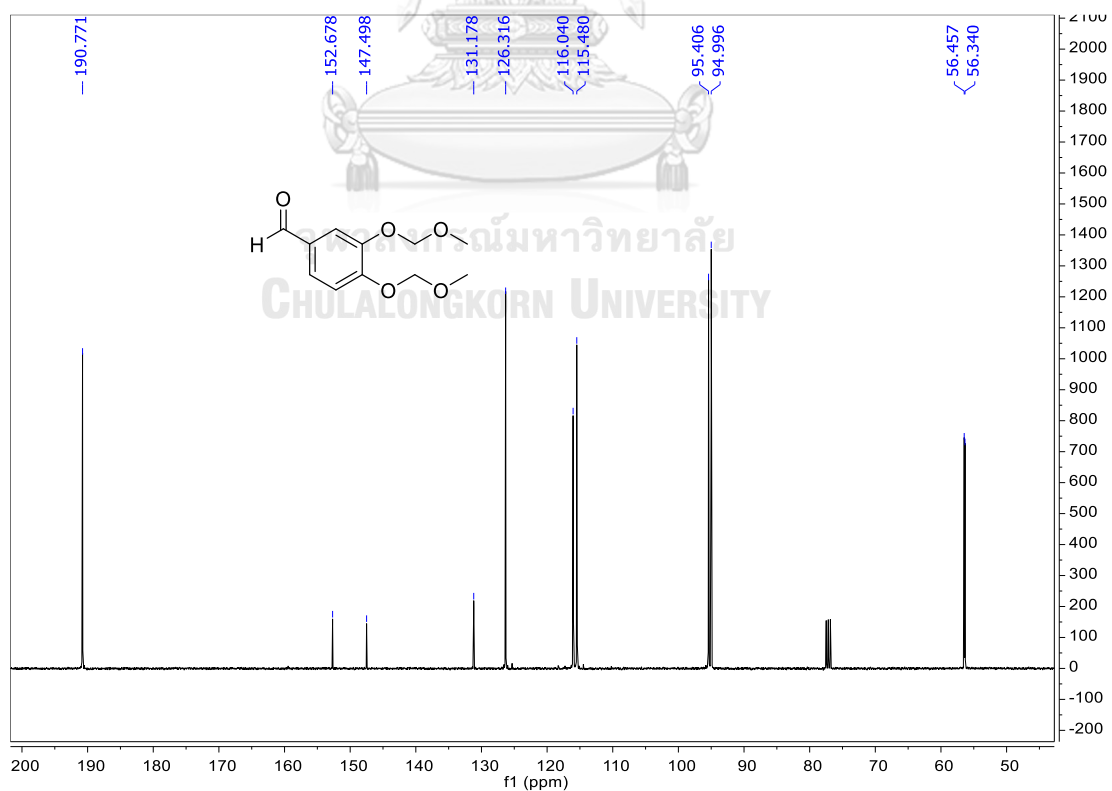


Figure A.50 The ^{13}C NMR spectrum (CDCl_3 , 100 MHz) of **73**.

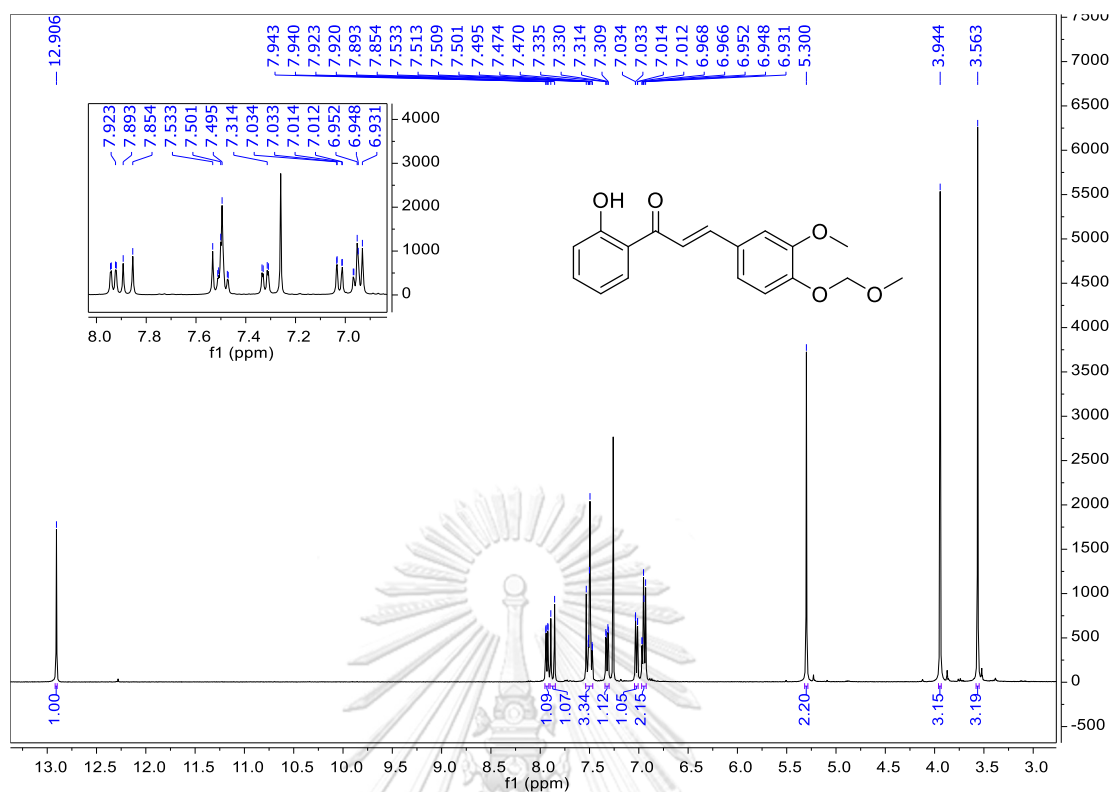


Figure A.51 The ^1H NMR spectrum (CDCl₃, 400 MHz) of 74.

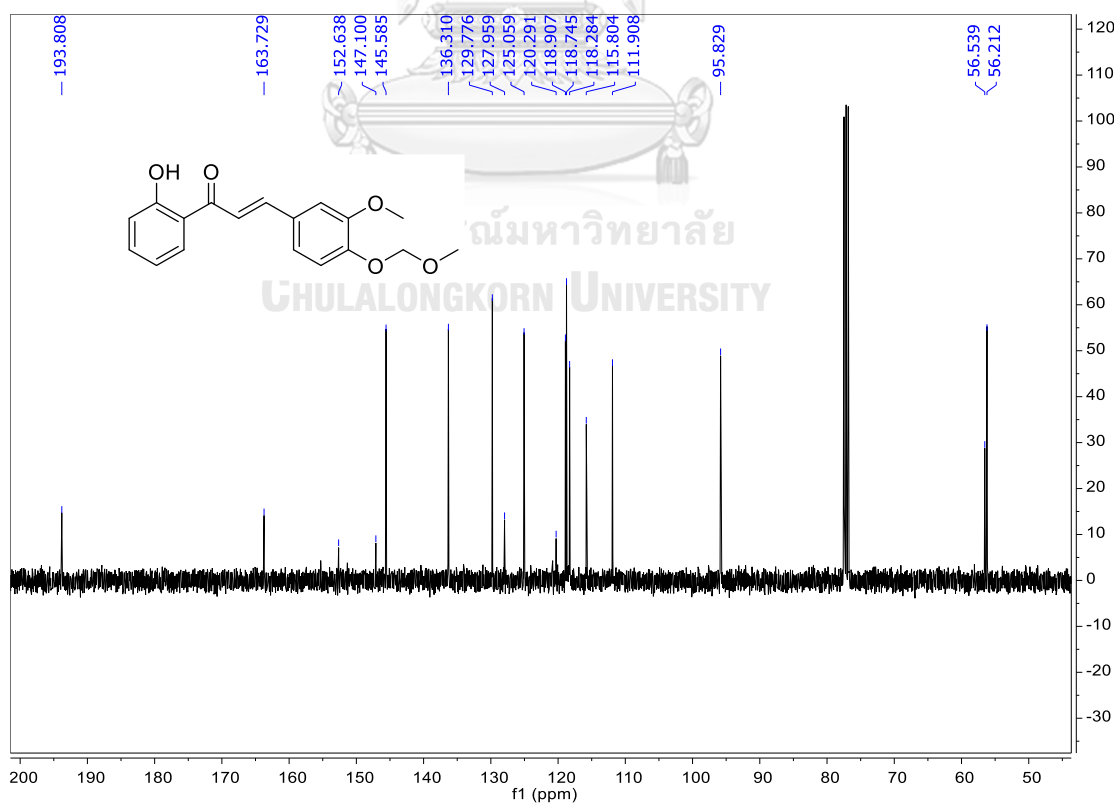


Figure A.52 The ^{13}C NMR spectrum (CDCl₃, 100 MHz) of 74.

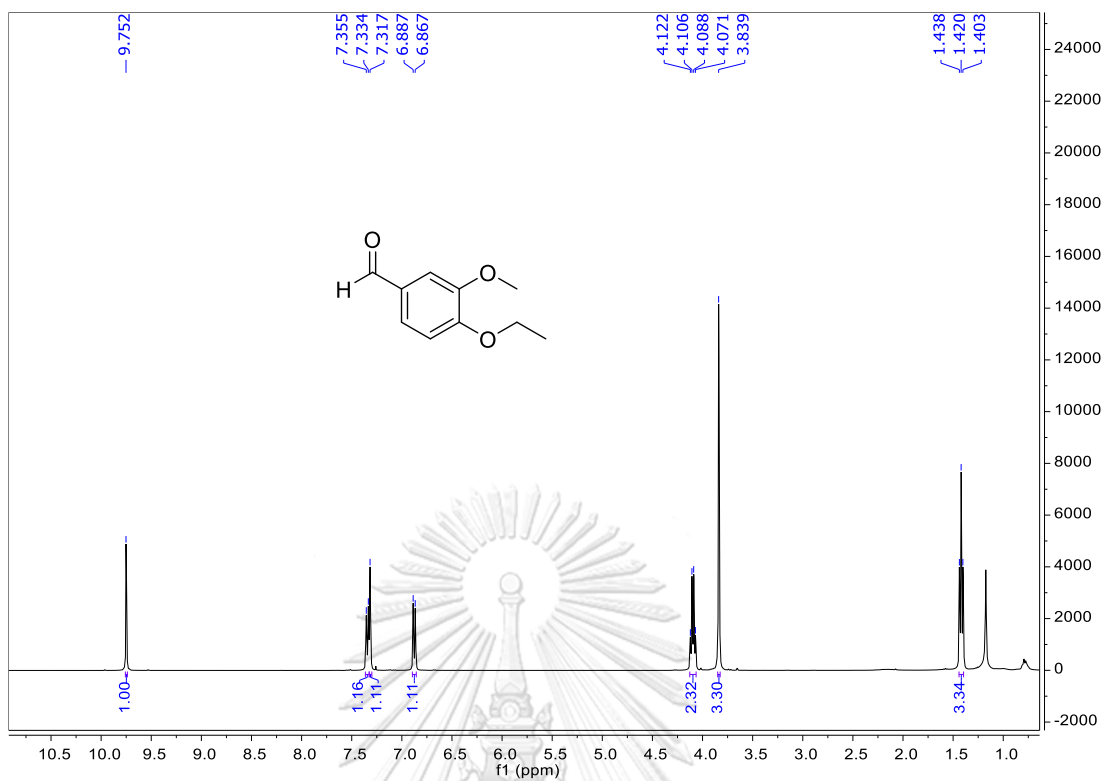


Figure A.53 The ^1H NMR spectrum (CDCl_3 , 400 MHz) of **76**.

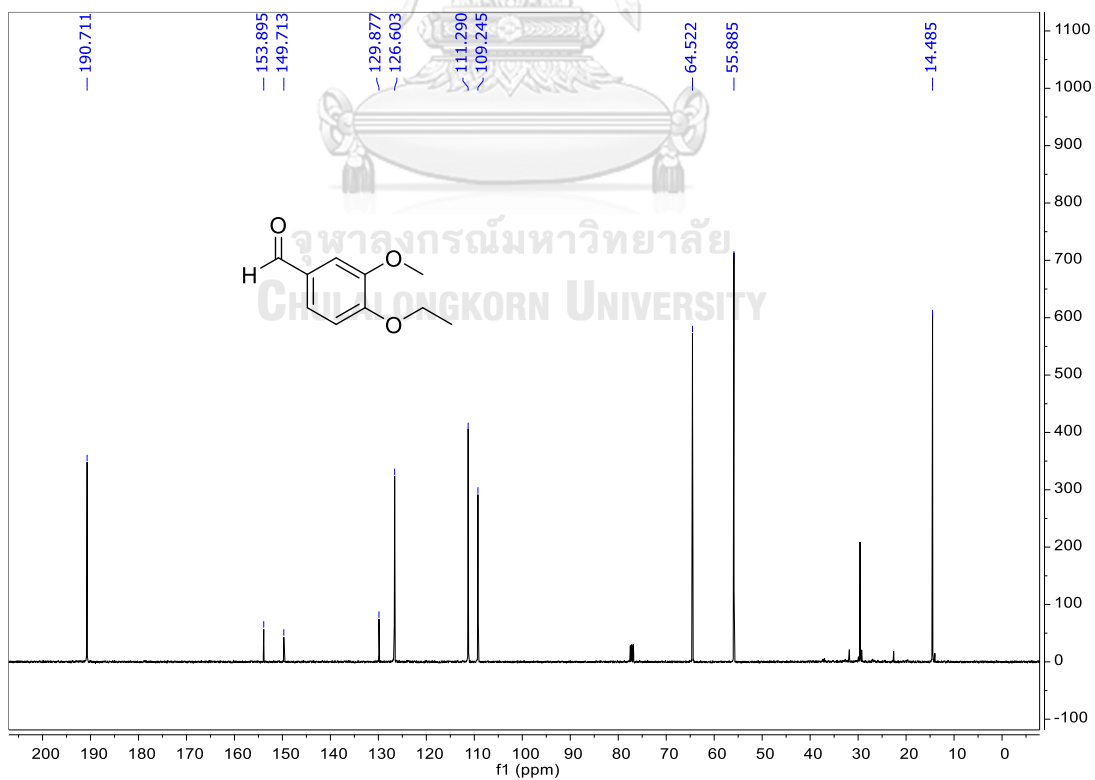


Figure A.54 The ^{13}C NMR spectrum (CDCl_3 , 100 MHz) of **76**.

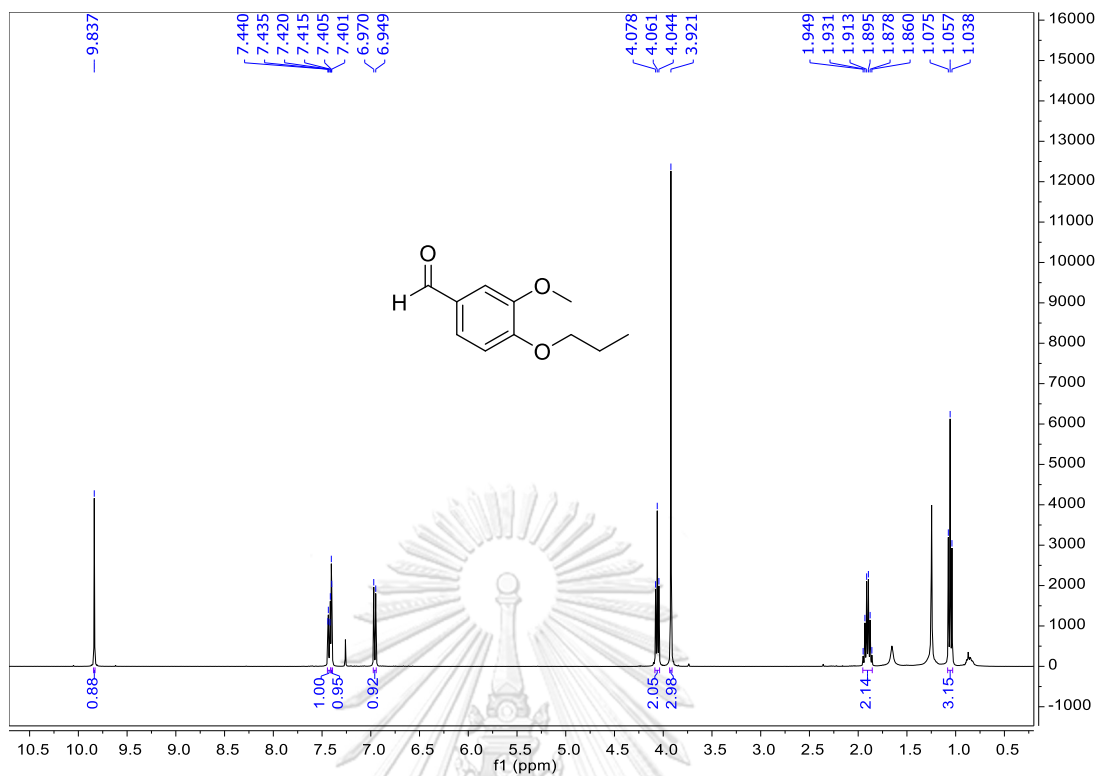


Figure A.55 The ^1H NMR spectrum (CDCl_3 , 400 MHz) of 77.

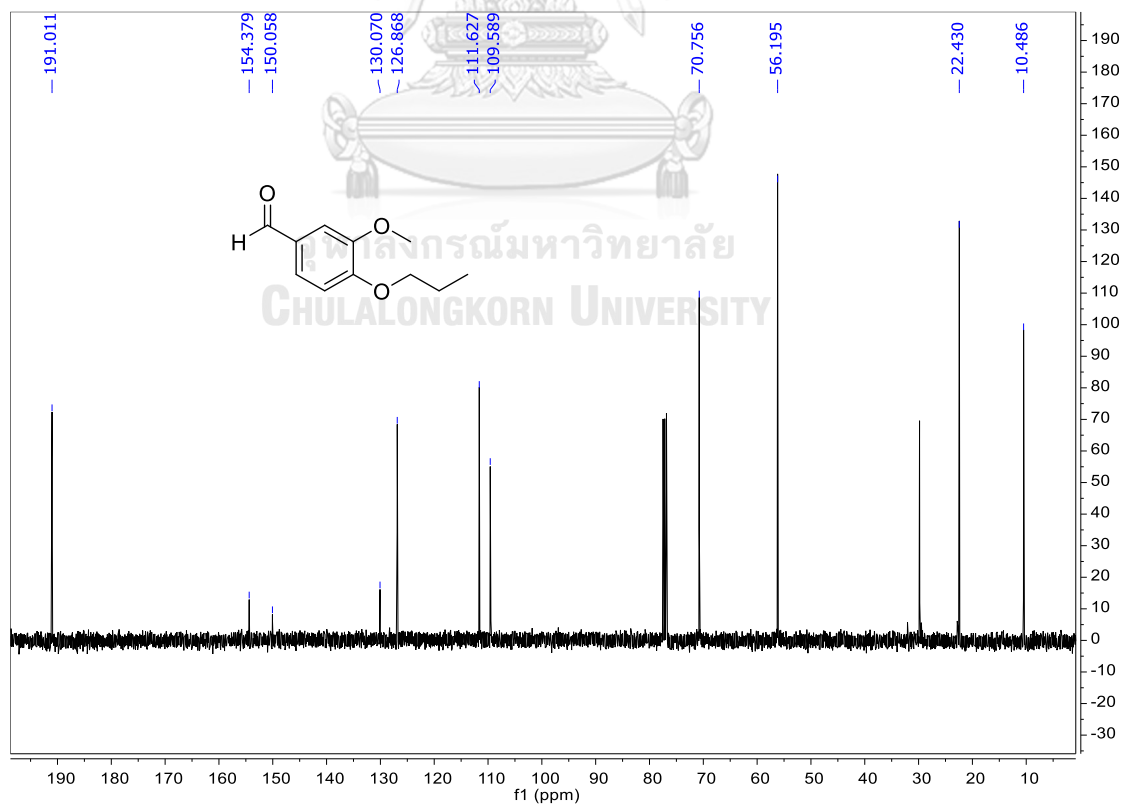


Figure A.56 The ^{13}C NMR spectrum (CDCl_3 , 100 MHz) of 77.

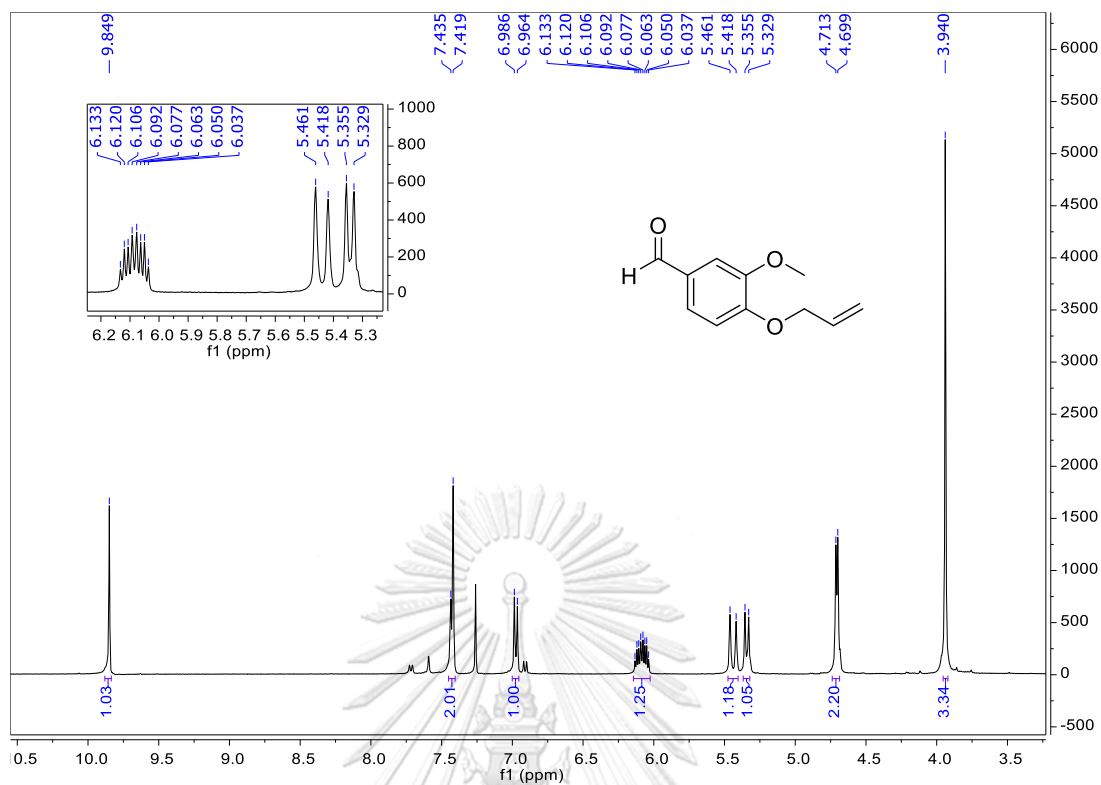


Figure A.57 The ^1H NMR spectrum (CDCl_3 , 400 MHz) of 78.

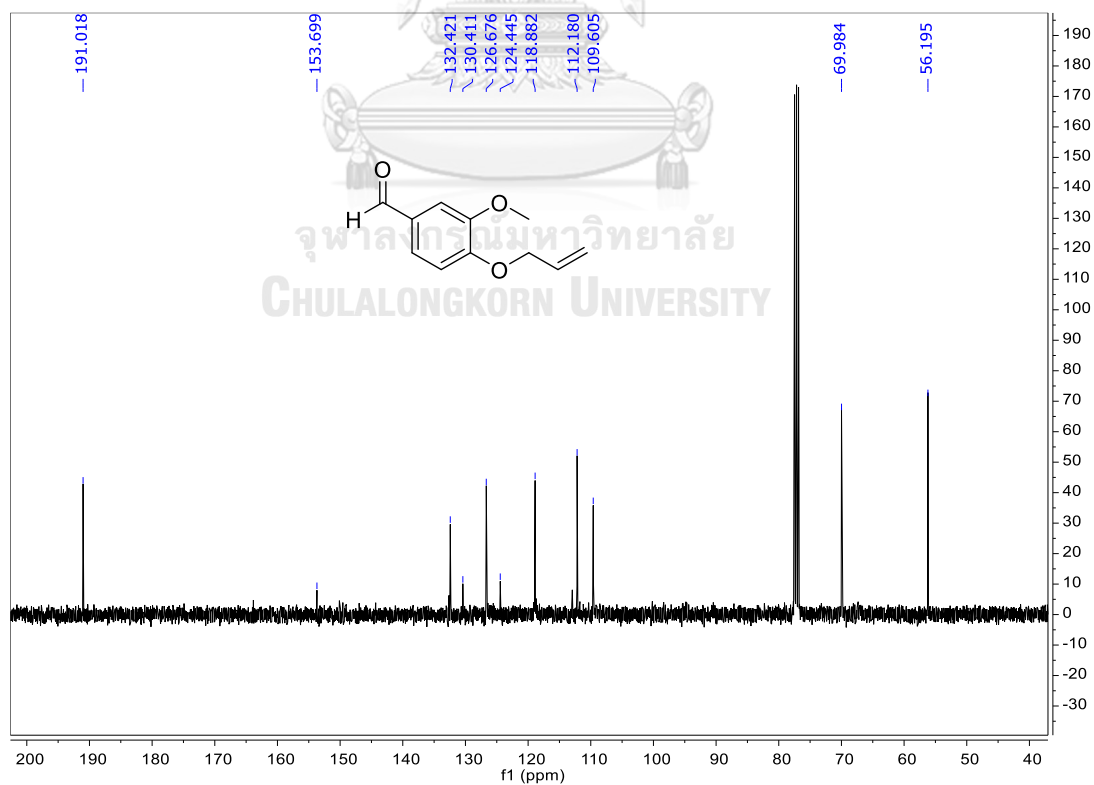


Figure A.58 The ^{13}C NMR spectrum (CDCl_3 , 100 MHz) of 78.

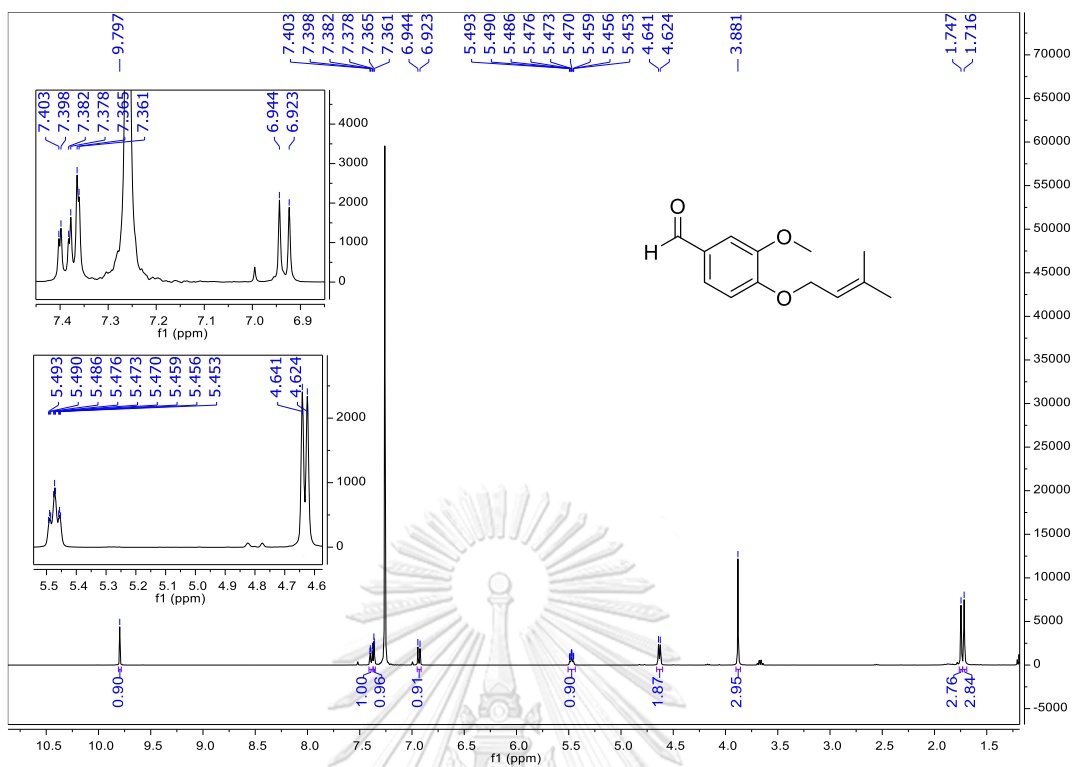


Figure A.59 The ^1H NMR spectrum (CDCl₃, 400 MHz) of 79.

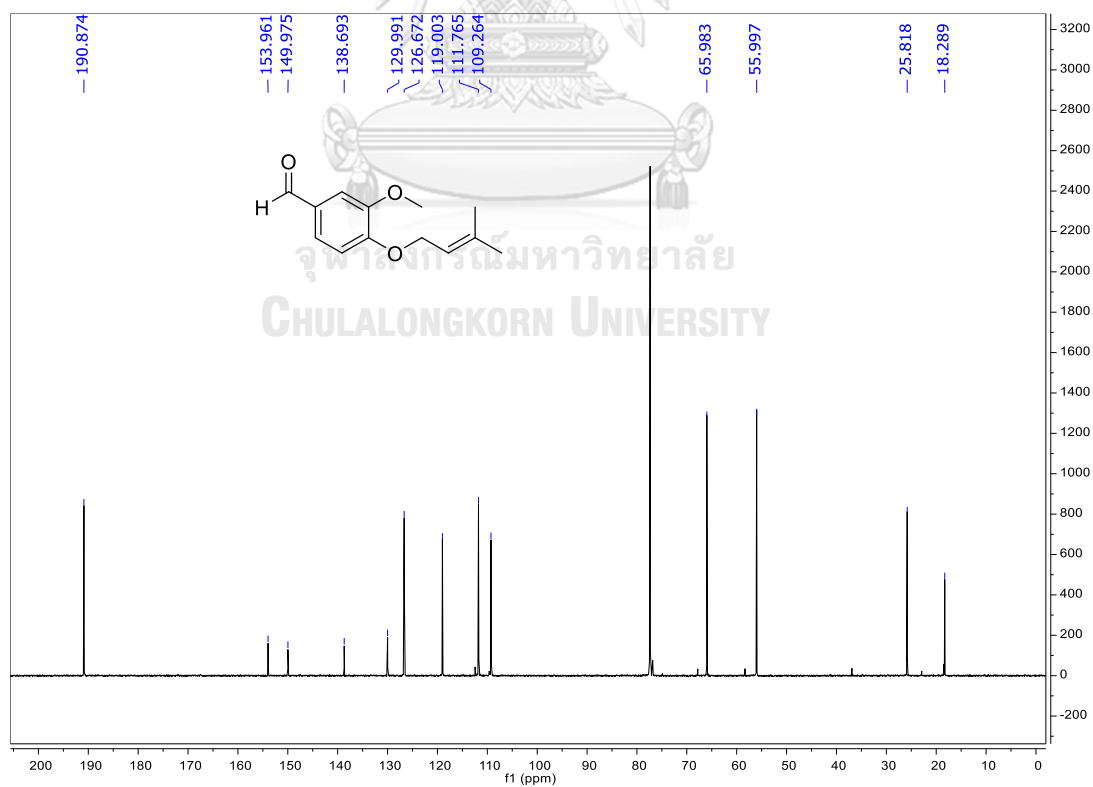
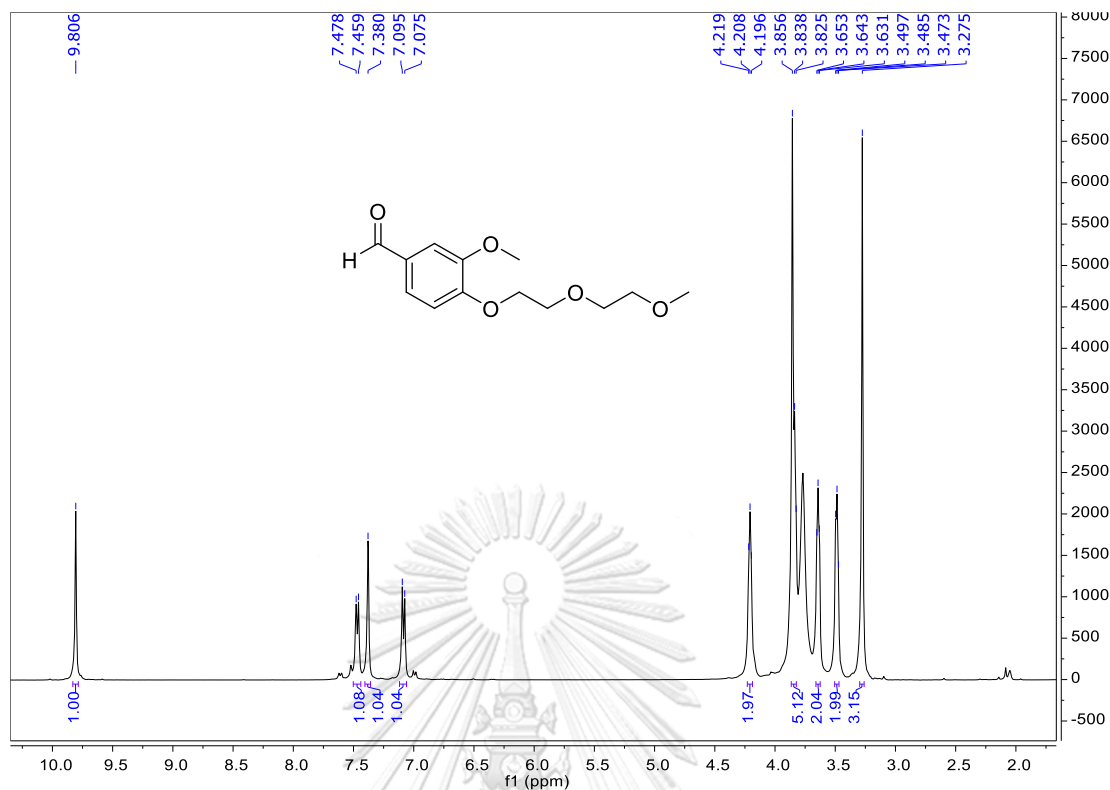
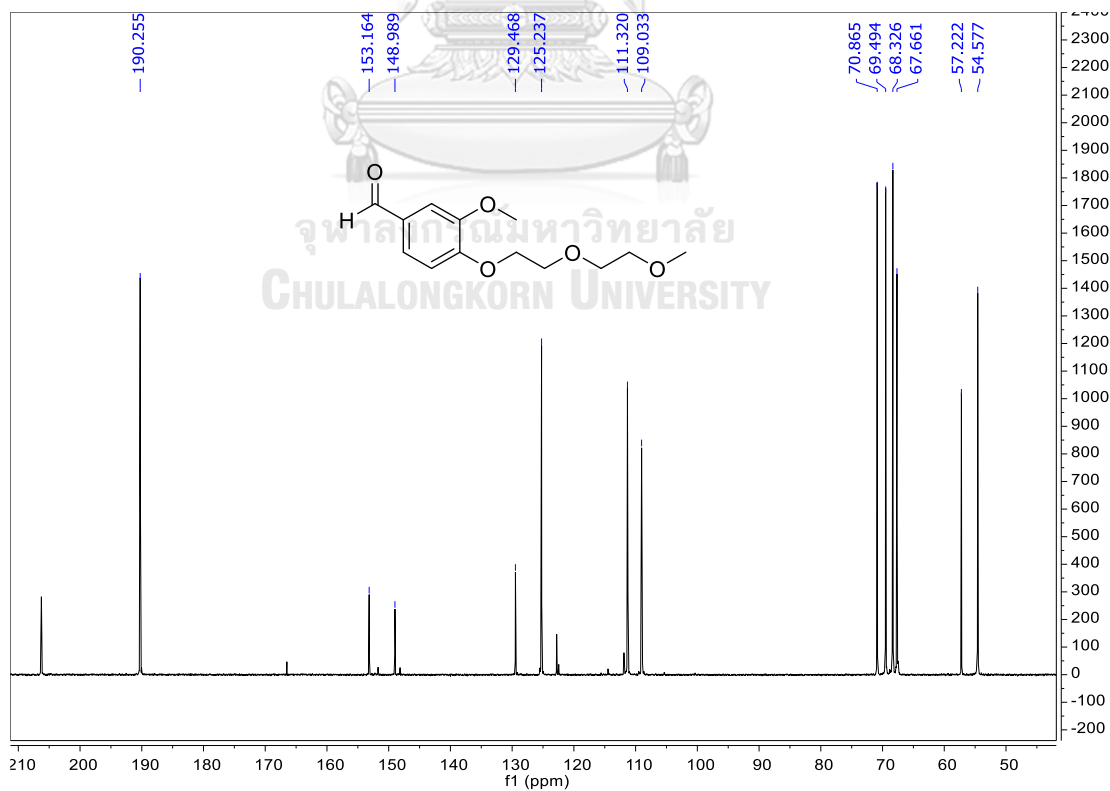


Figure A.60 The ^{13}C NMR spectrum (CDCl₃, 100 MHz) of 79.

Figure A.61 The ^1H NMR spectrum (acetone- d_6 , 400 MHz) of **82**.Figure A.62 The ^{13}C NMR spectrum (acetone- d_6 , 100 MHz) of **82**.

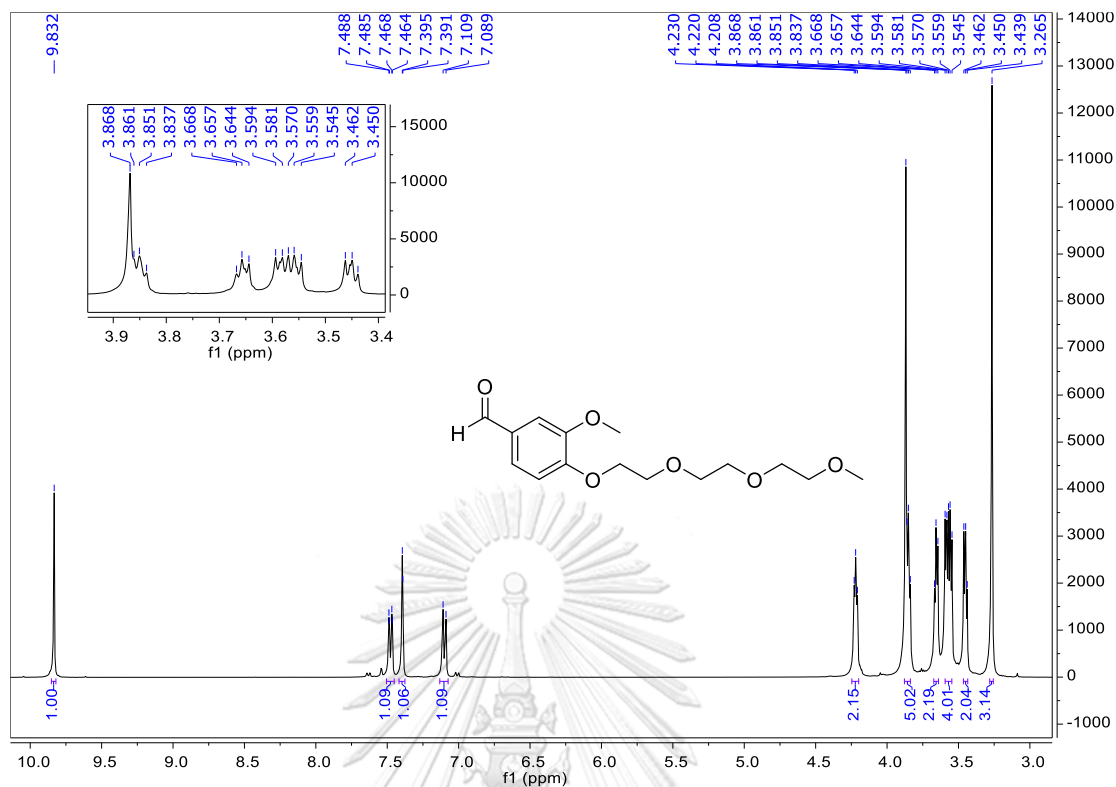


Figure A.63 The ^1H NMR spectrum (acetone- d_6 , 400 MHz) of 83.

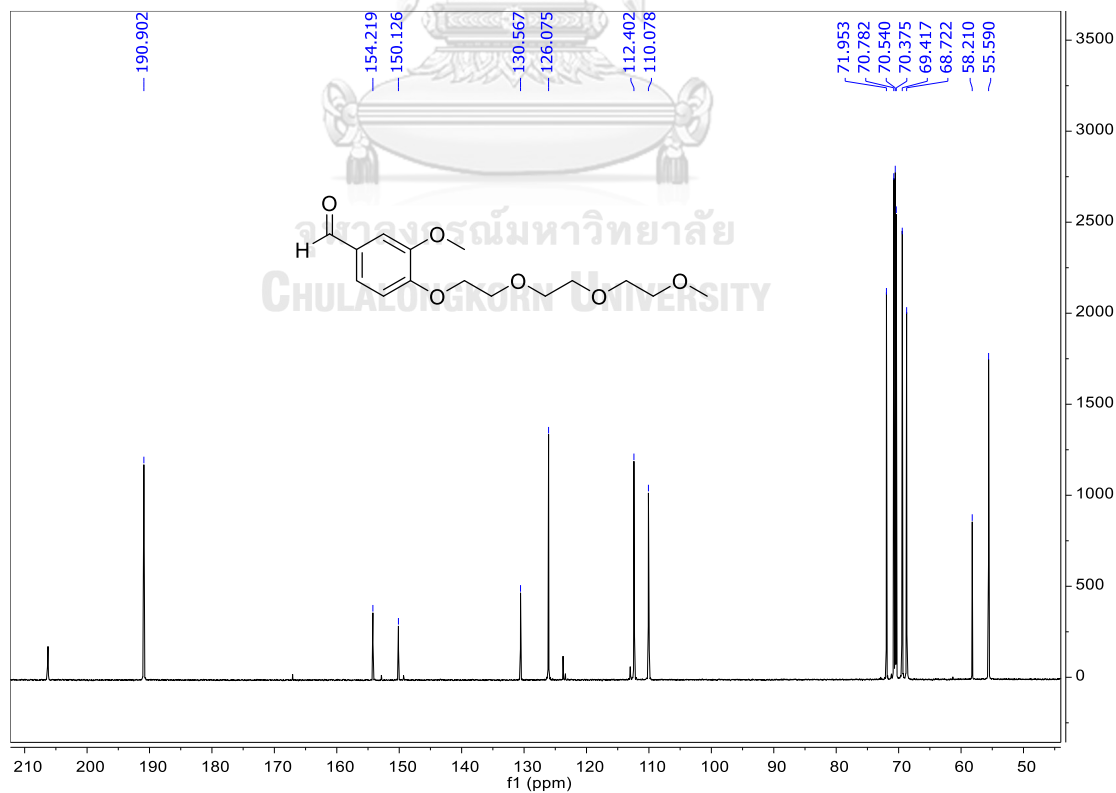


Figure A.64 The ^{13}C NMR spectrum (acetone- d_6 , 100 MHz) of 83.

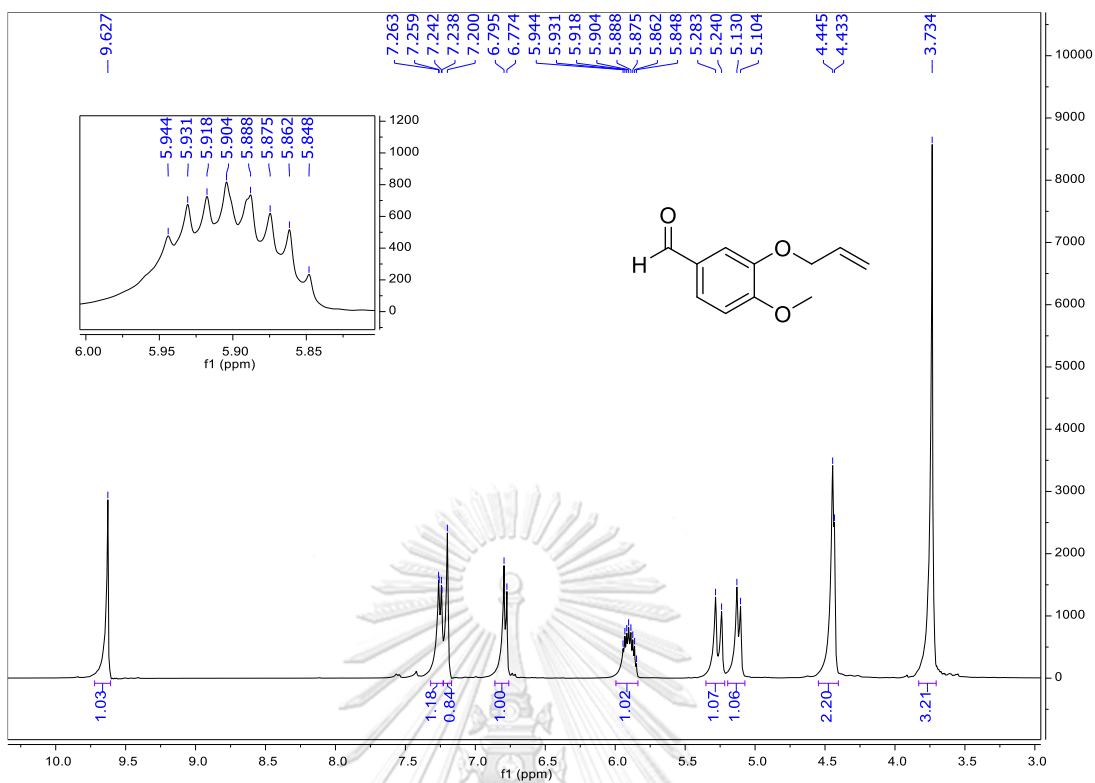


Figure A.65 The ^1H NMR spectrum (CDCl_3 , 400 MHz) of **84**.

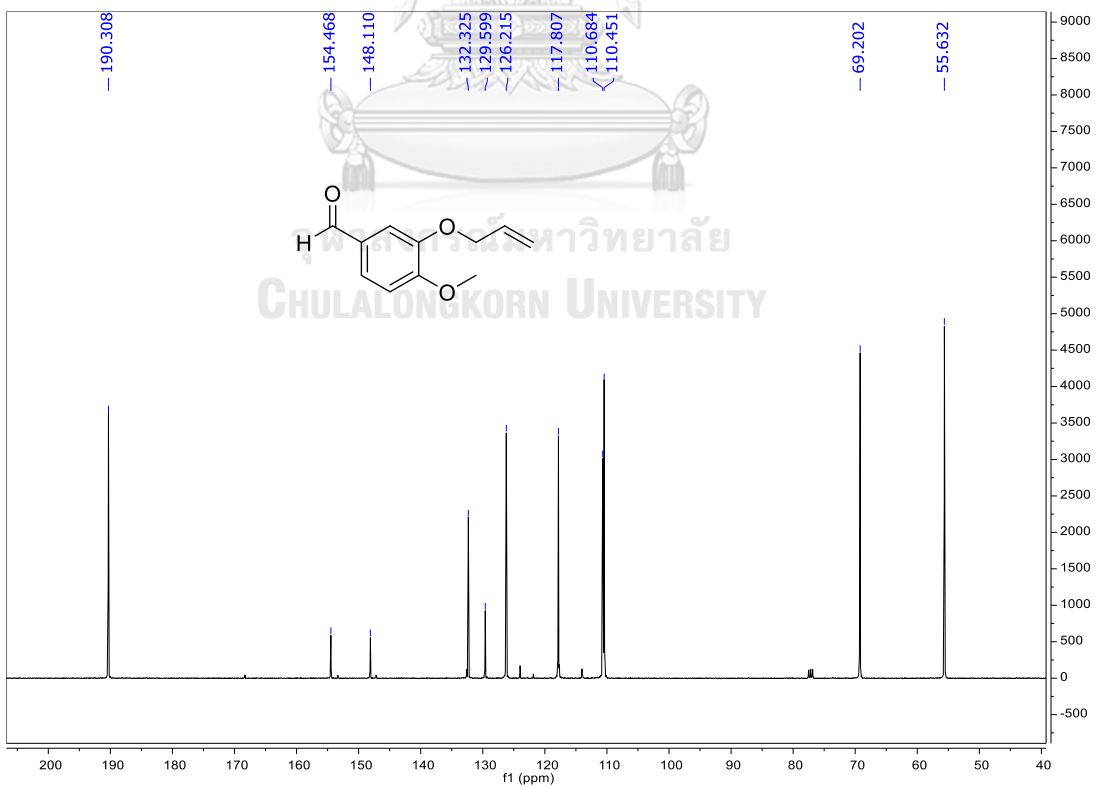


Figure A.66 The ^{13}C NMR spectrum (CDCl_3 , 100 MHz) of **84**.

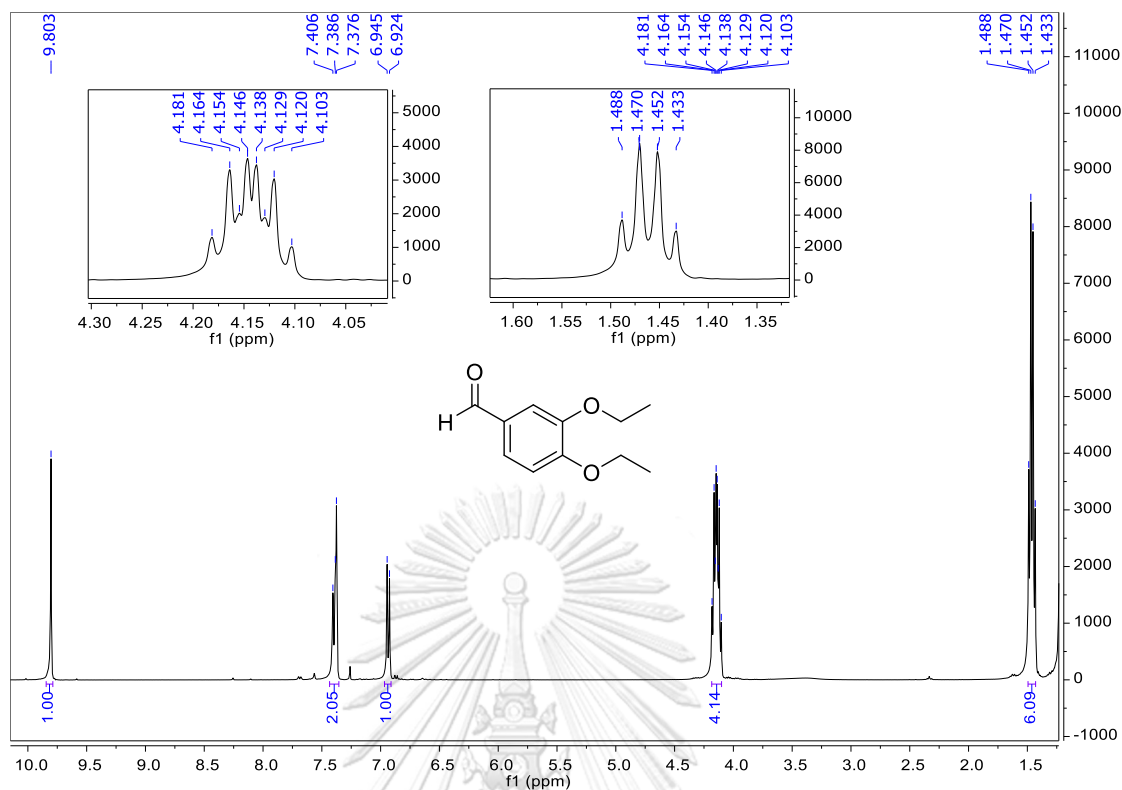


Figure A.67 The ^1H NMR spectrum (CDCl_3 , 400 MHz) of **85**.

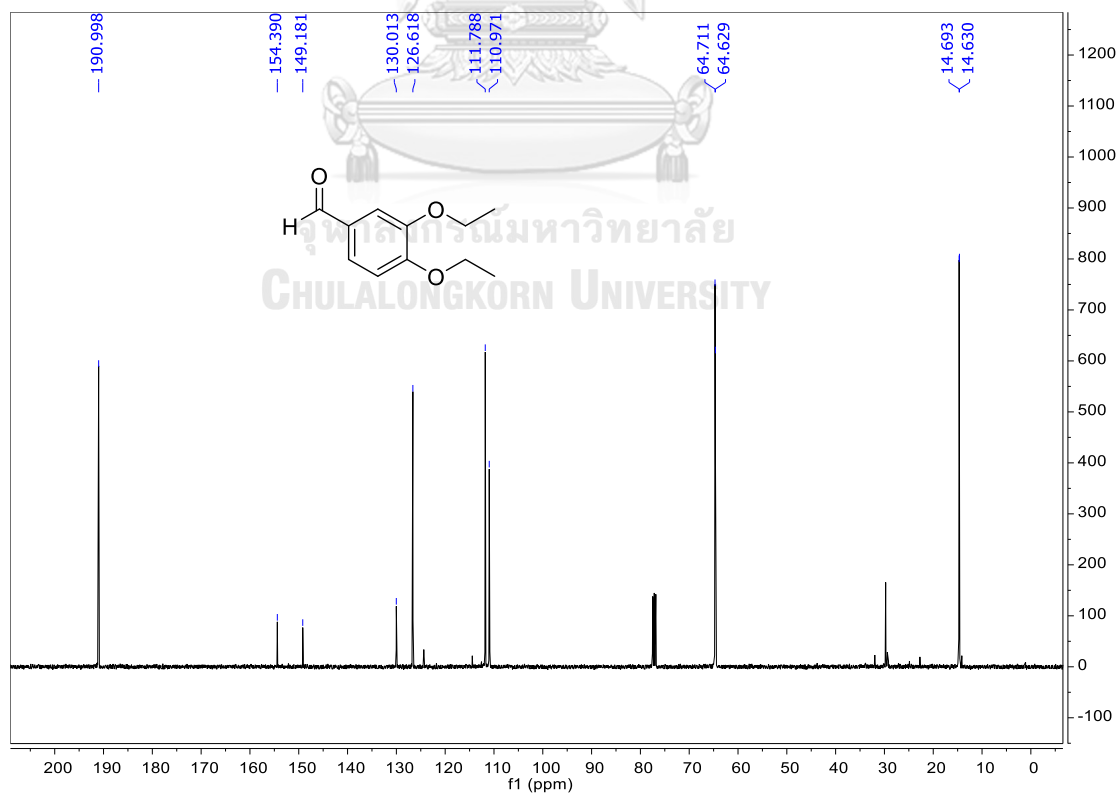


Figure A.68 The ^{13}C NMR spectrum (CDCl_3 , 100 MHz) of **85**.

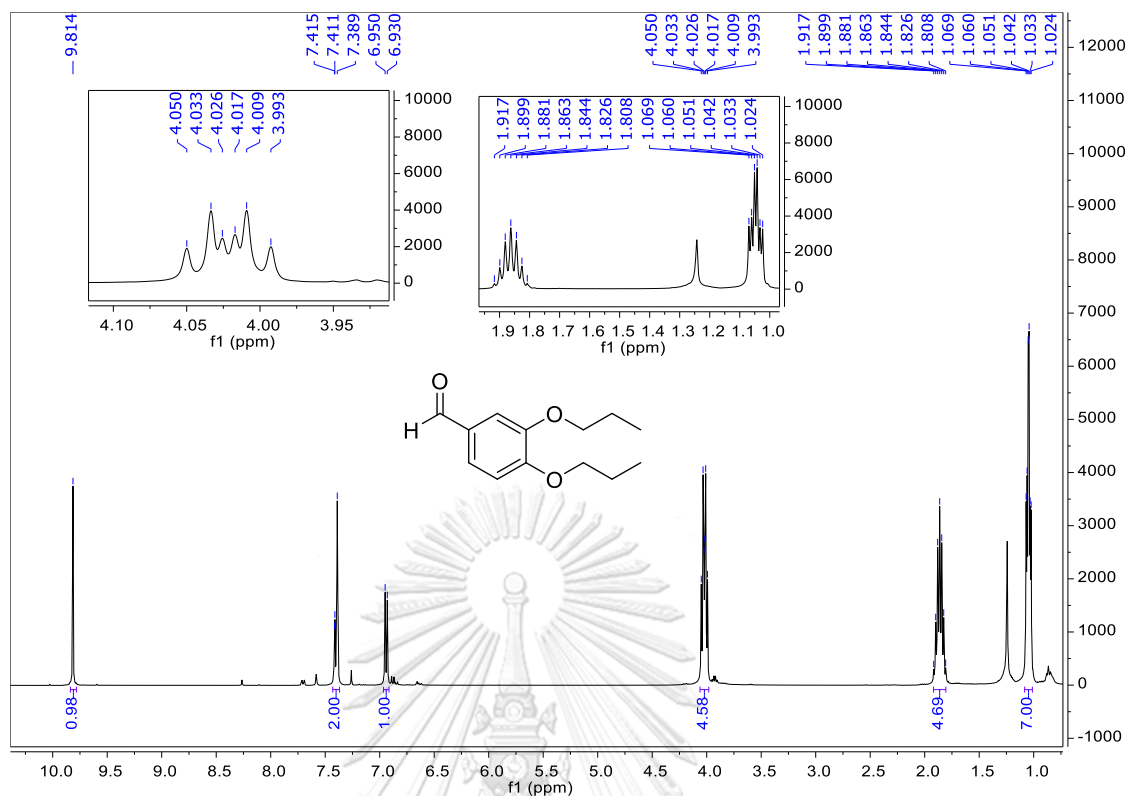


Figure A.69 The ^1H NMR spectrum (CDCl_3 , 400 MHz) of **86**.

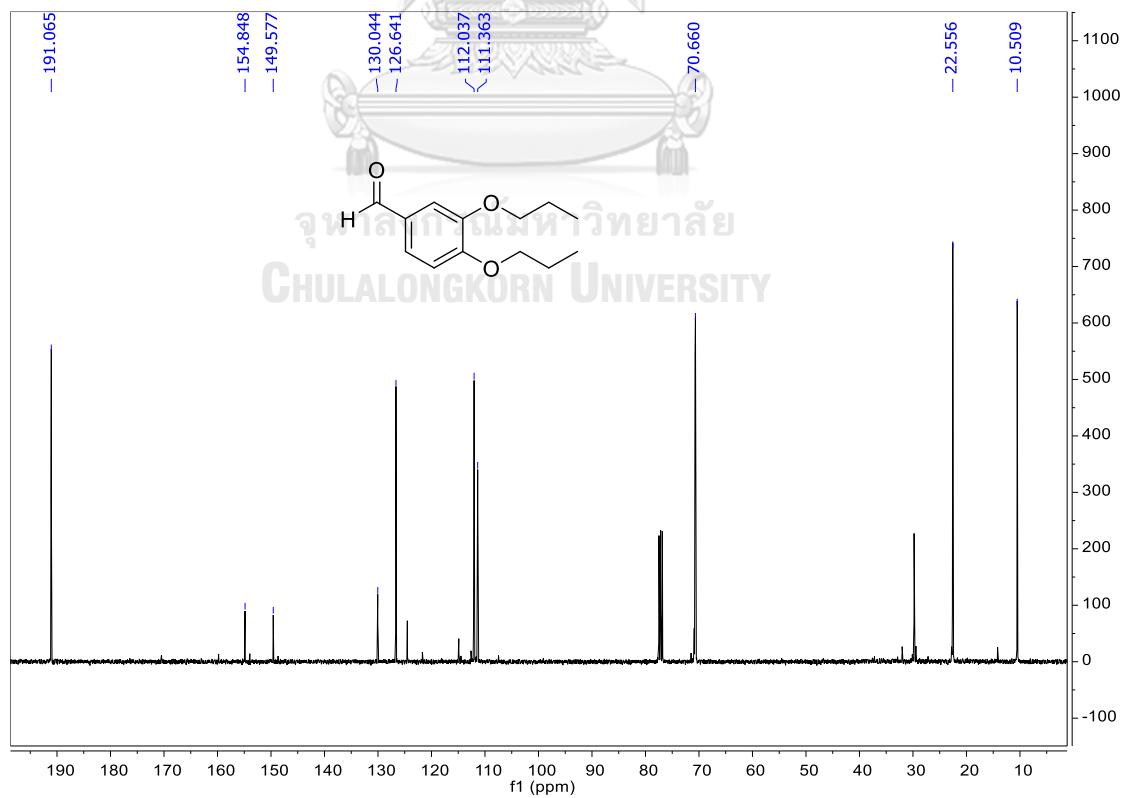


Figure A.70 The ^{13}C NMR spectrum (CDCl_3 , 100 MHz) of **86**.

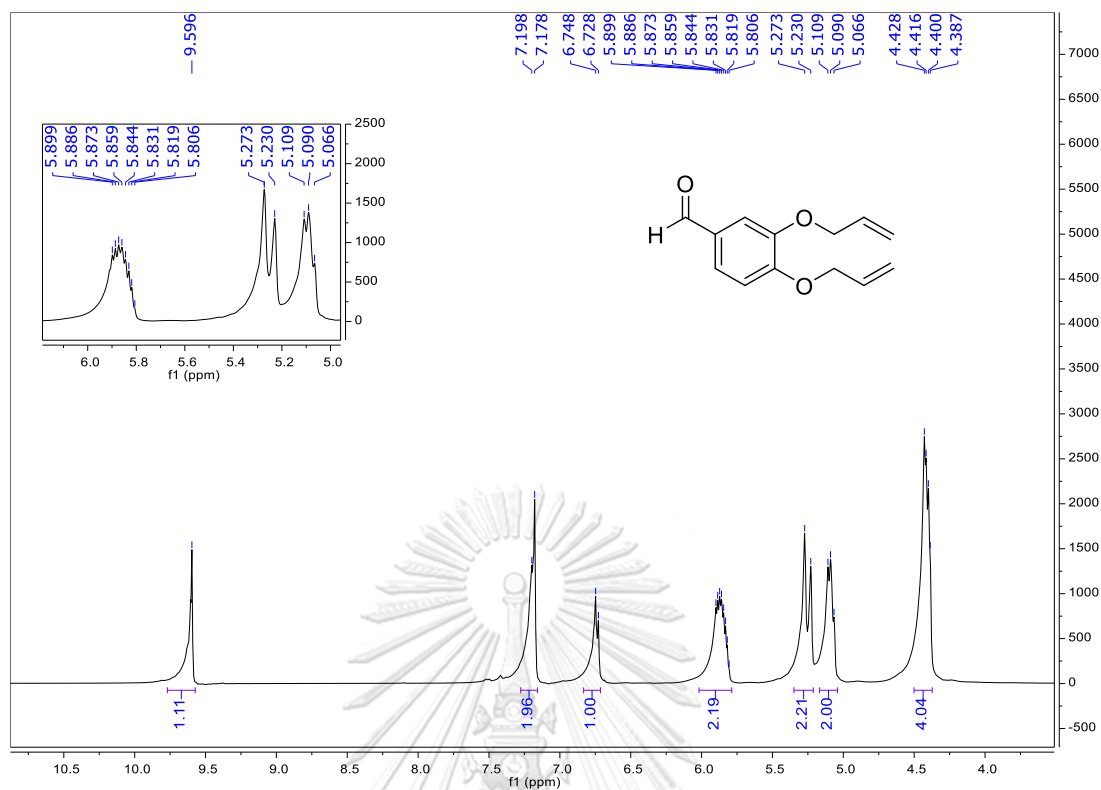


Figure A.71 The ^1H NMR spectrum (CDCl_3 , 400 MHz) of **87**.

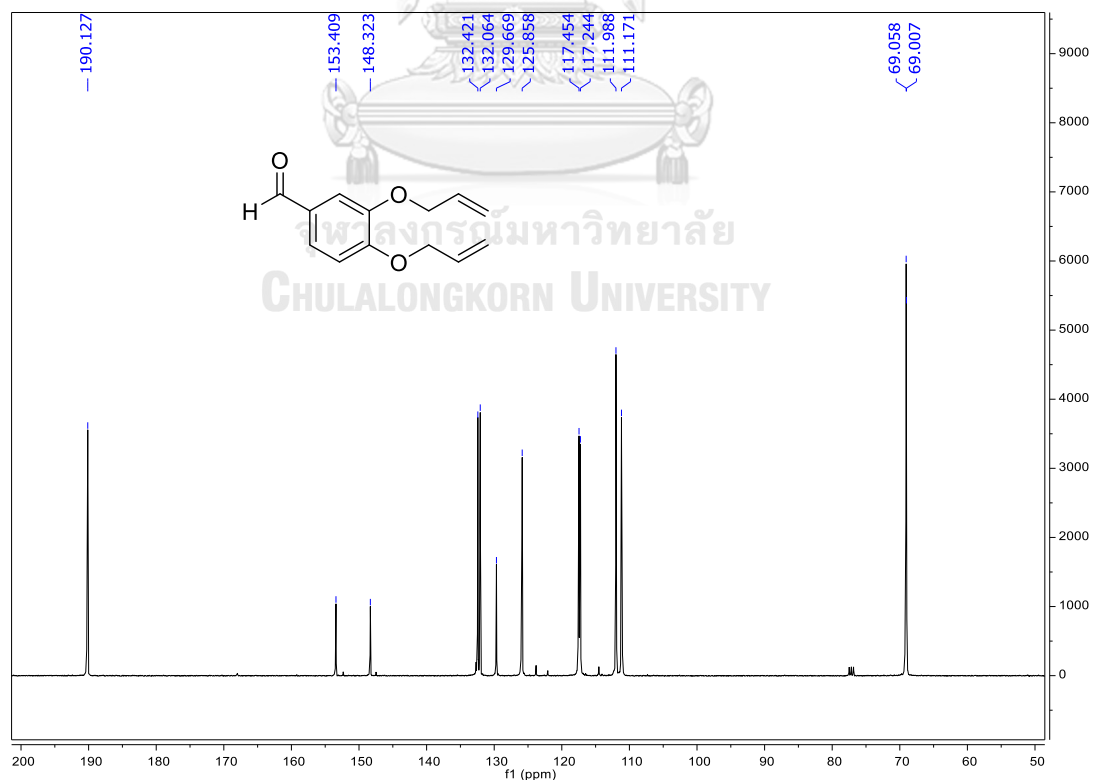


Figure A.72 The ^{13}C NMR spectrum (CDCl_3 , 100 MHz) of **87**.

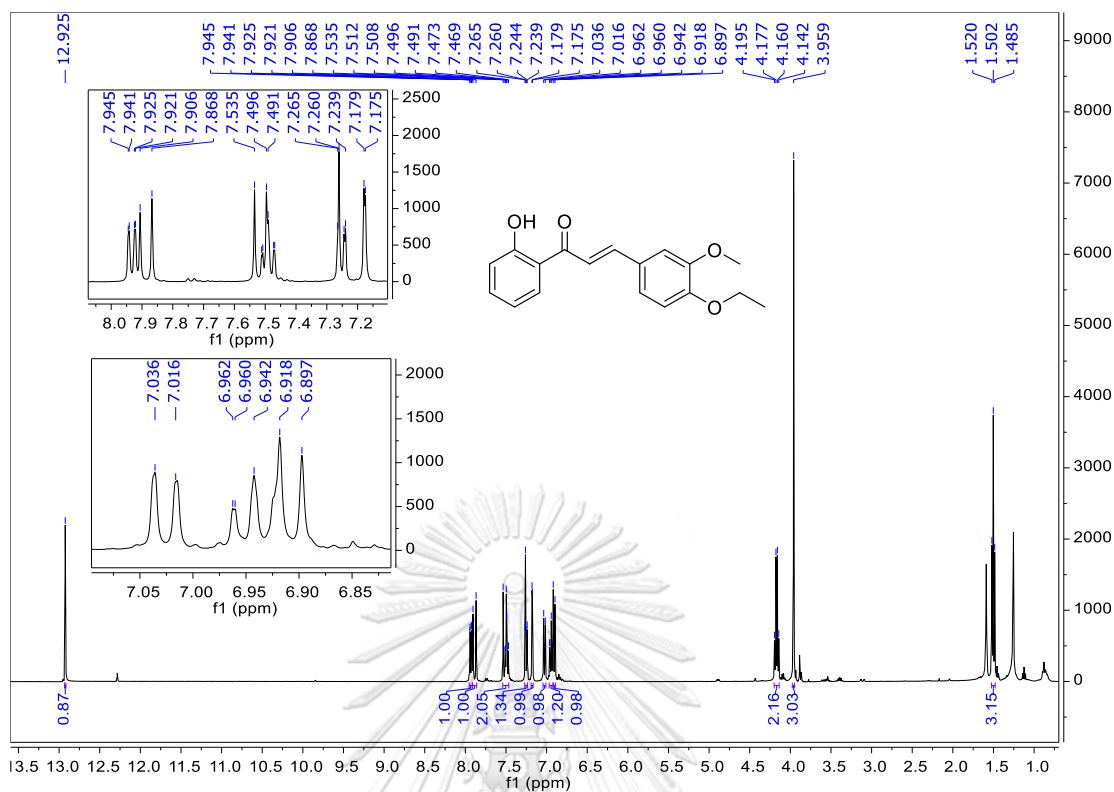


Figure A.73 The ^1H NMR spectrum (CDCl_3 , 400 MHz) of **88**.

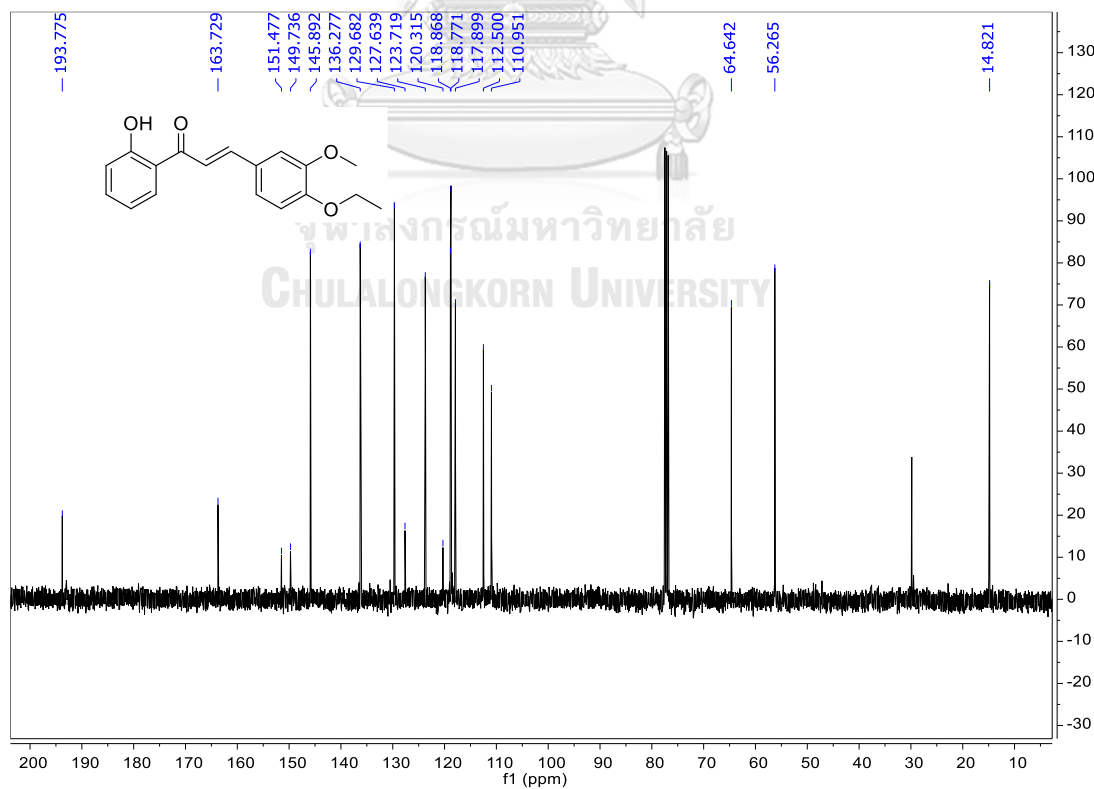


Figure A.74 The ^{13}C NMR spectrum (CDCl_3 , 100 MHz) of **88**.

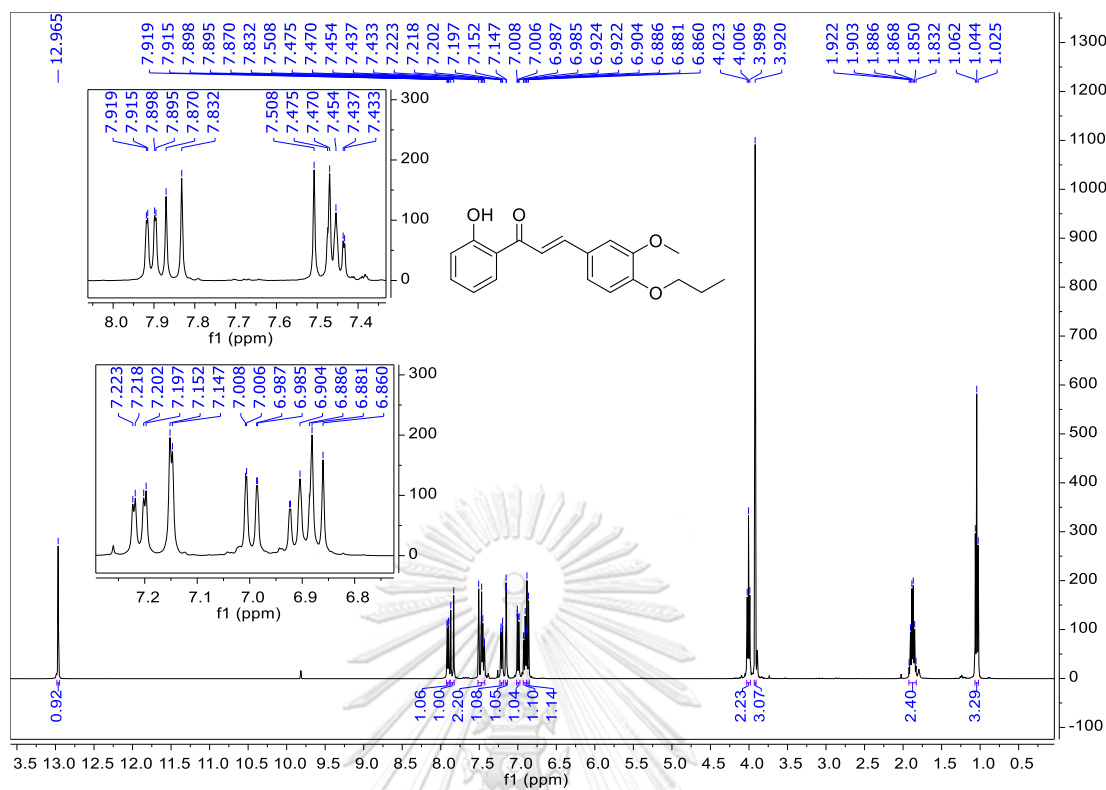


Figure A.75 The ^1H NMR spectrum (CDCl₃, 400 MHz) of 89.

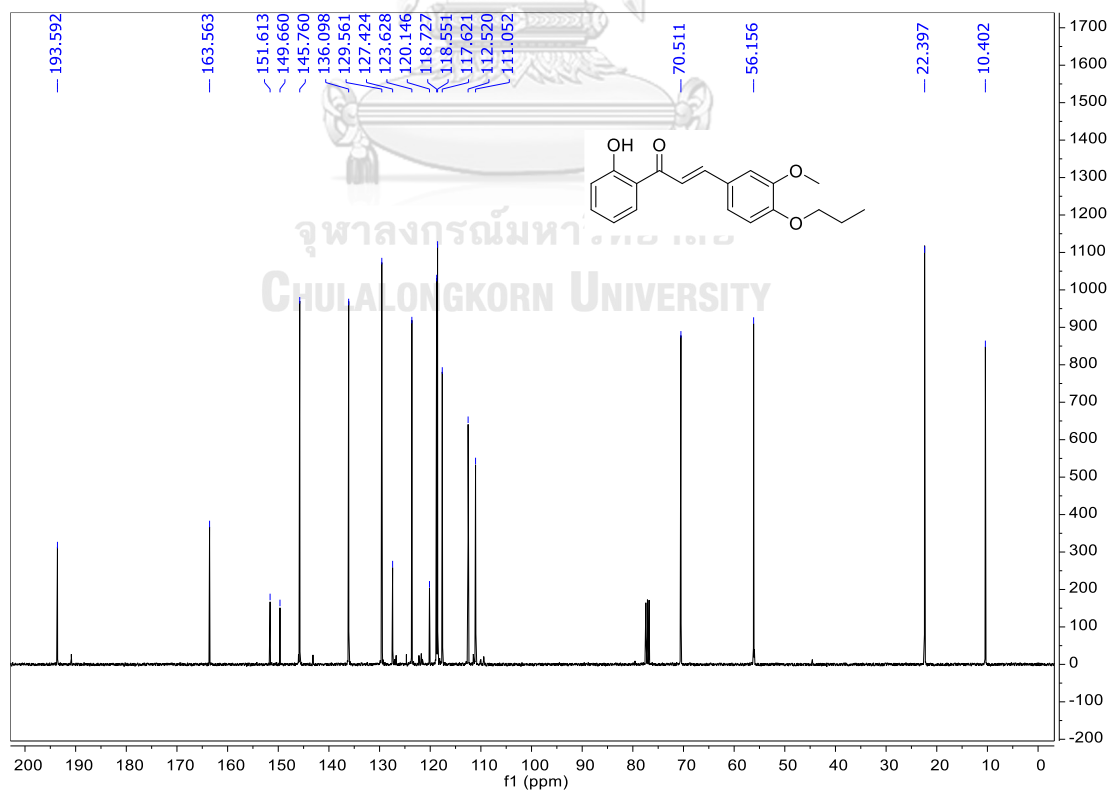


Figure A.76 The ^{13}C NMR spectrum (CDCl₃, 100 MHz) of 89.

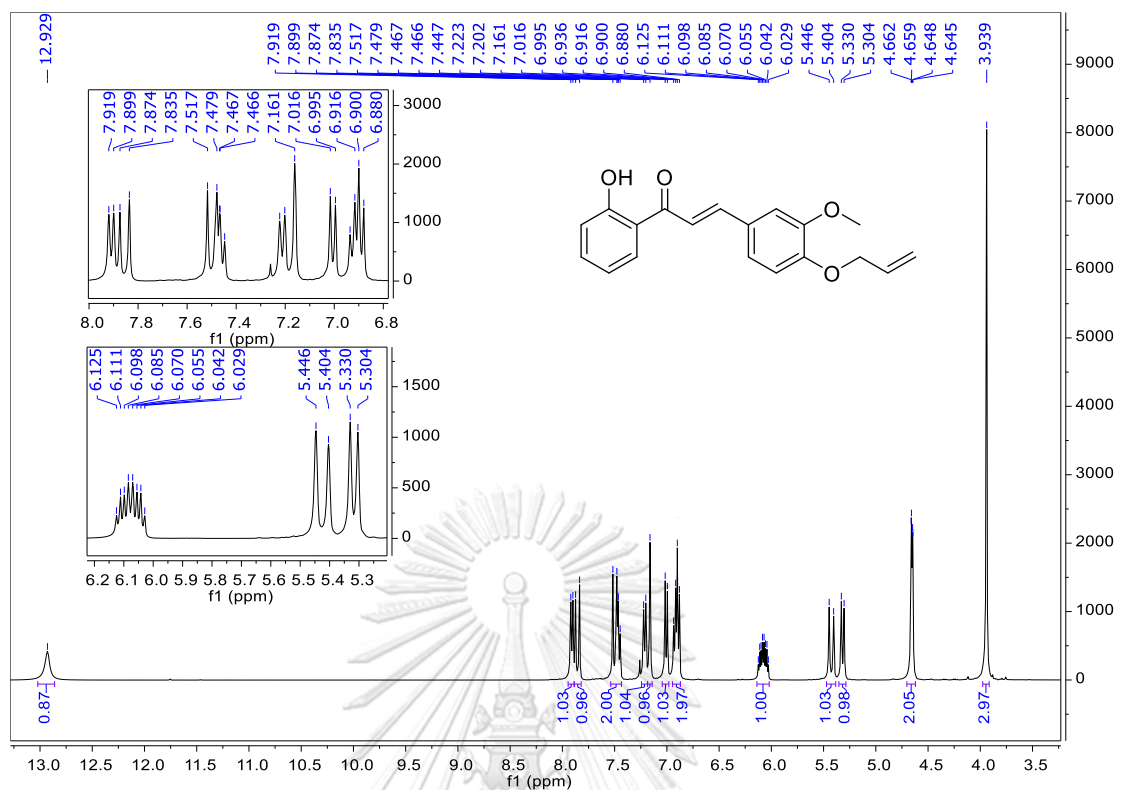


Figure A.77 The ^1H NMR spectrum (CDCl_3 , 400 MHz) of **90**.

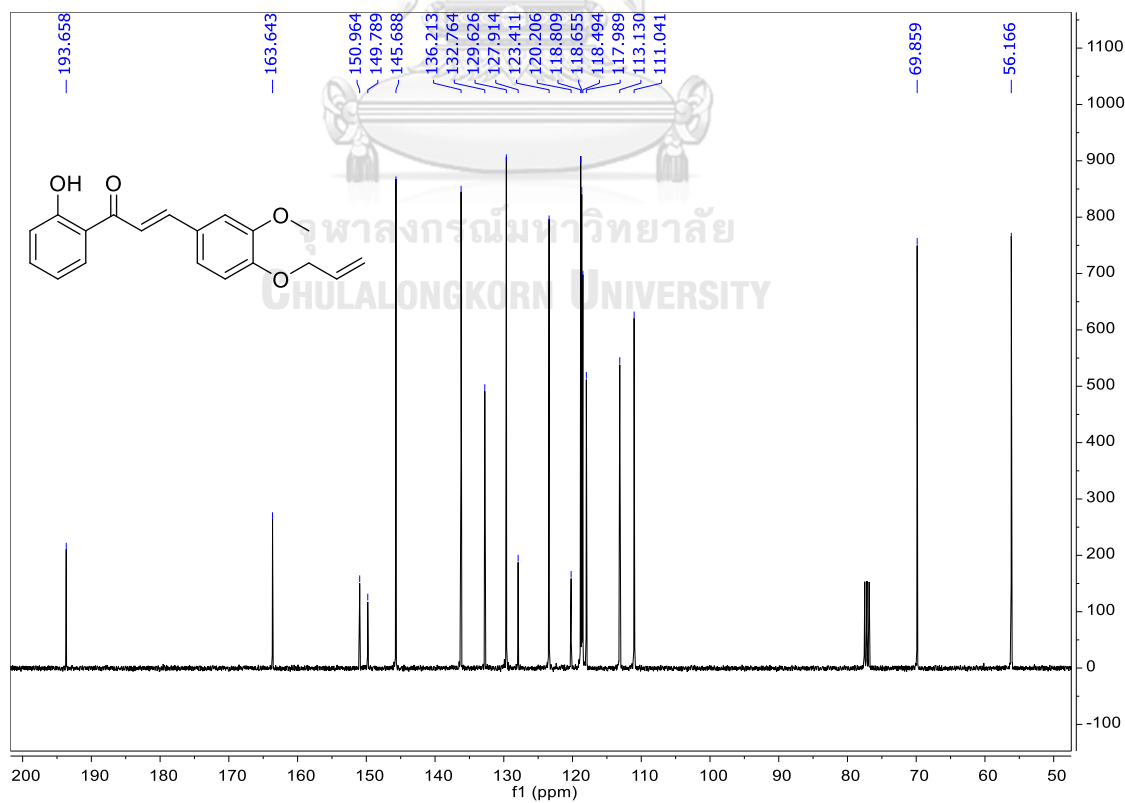


Figure A.78 The ^{13}C NMR spectrum (CDCl_3 , 100 MHz) of **90**.

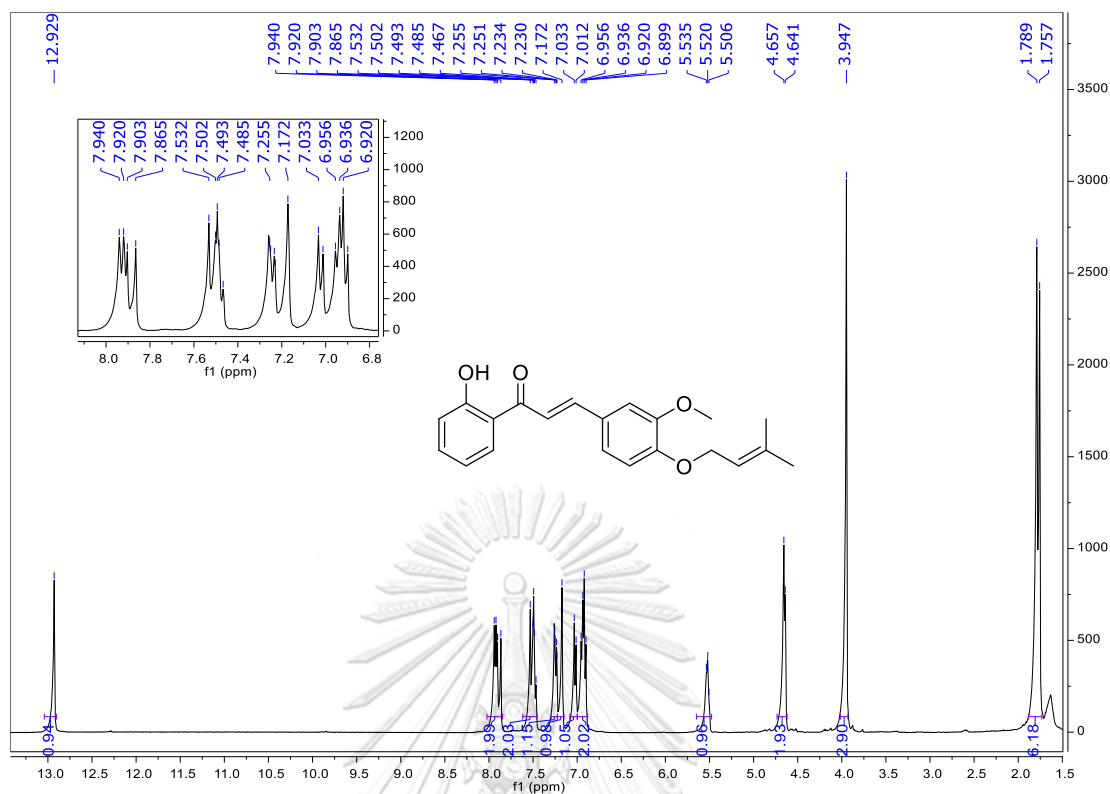


Figure A.79 The ^1H NMR spectrum (CDCl_3 , 400 MHz) of **91**.

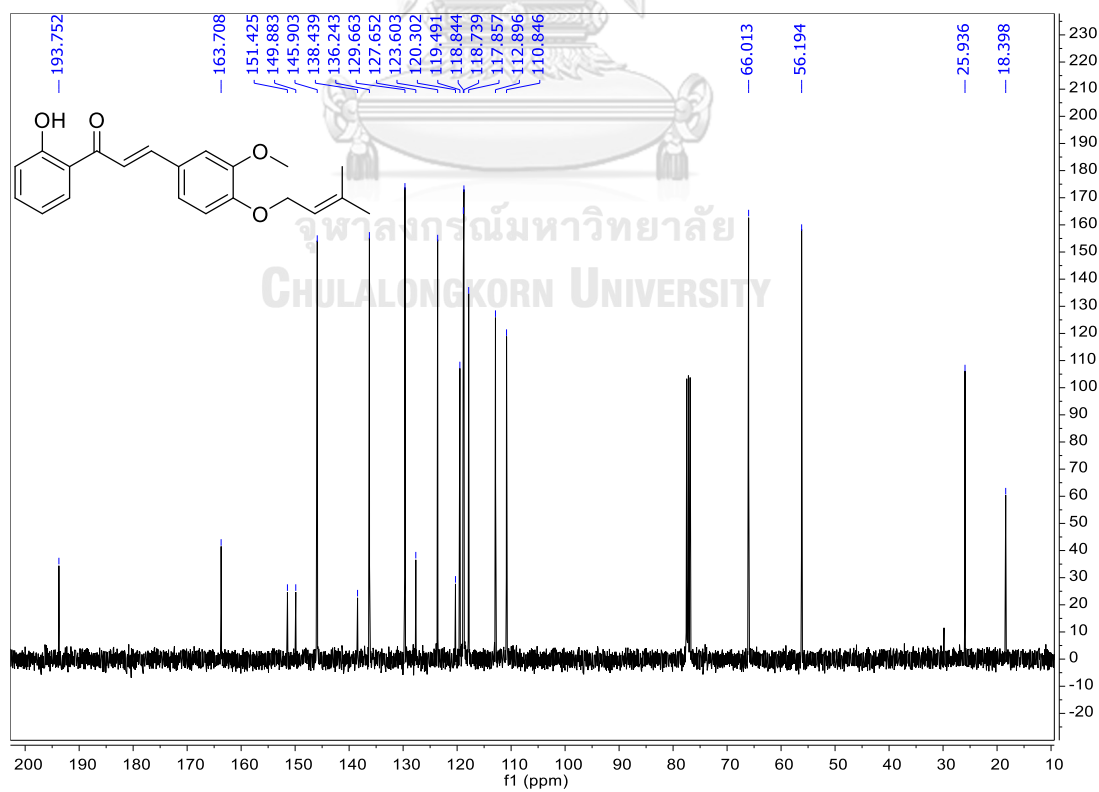


Figure A.80 The ^{13}C NMR spectrum (CDCl_3 , 100 MHz) of **91**.

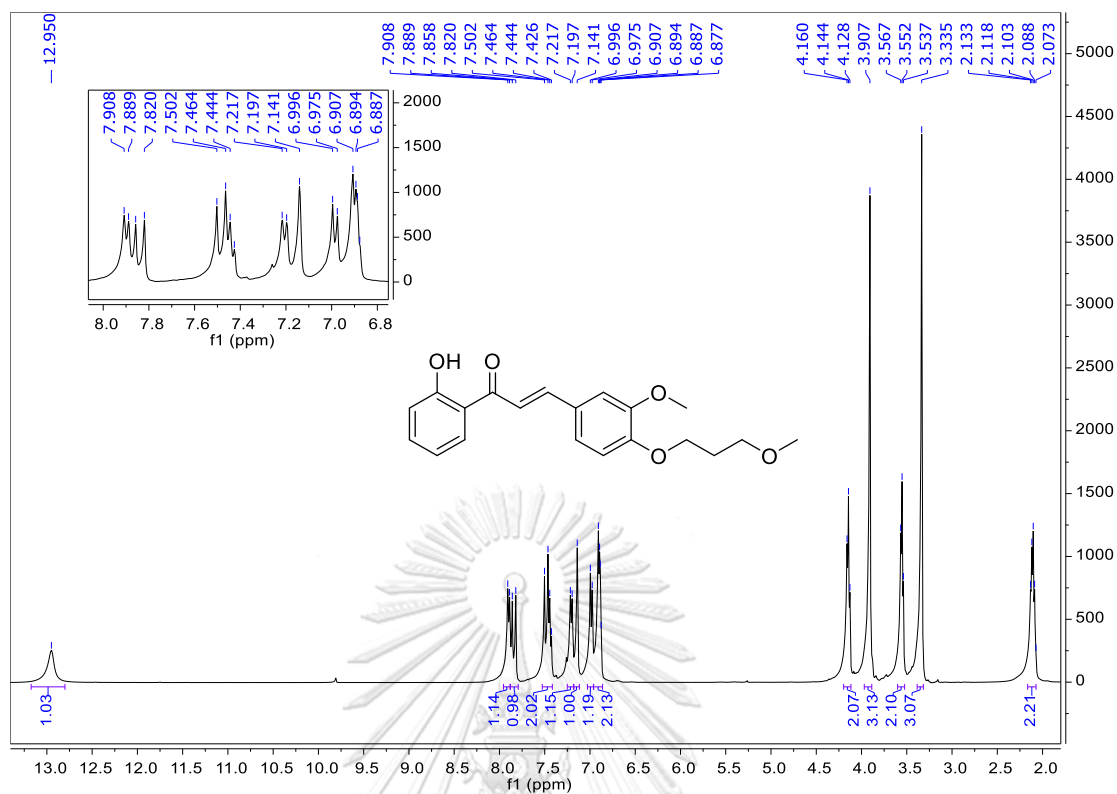


Figure A.81 The ^1H NMR spectrum (CDCl_3 , 400 MHz) of **92**.

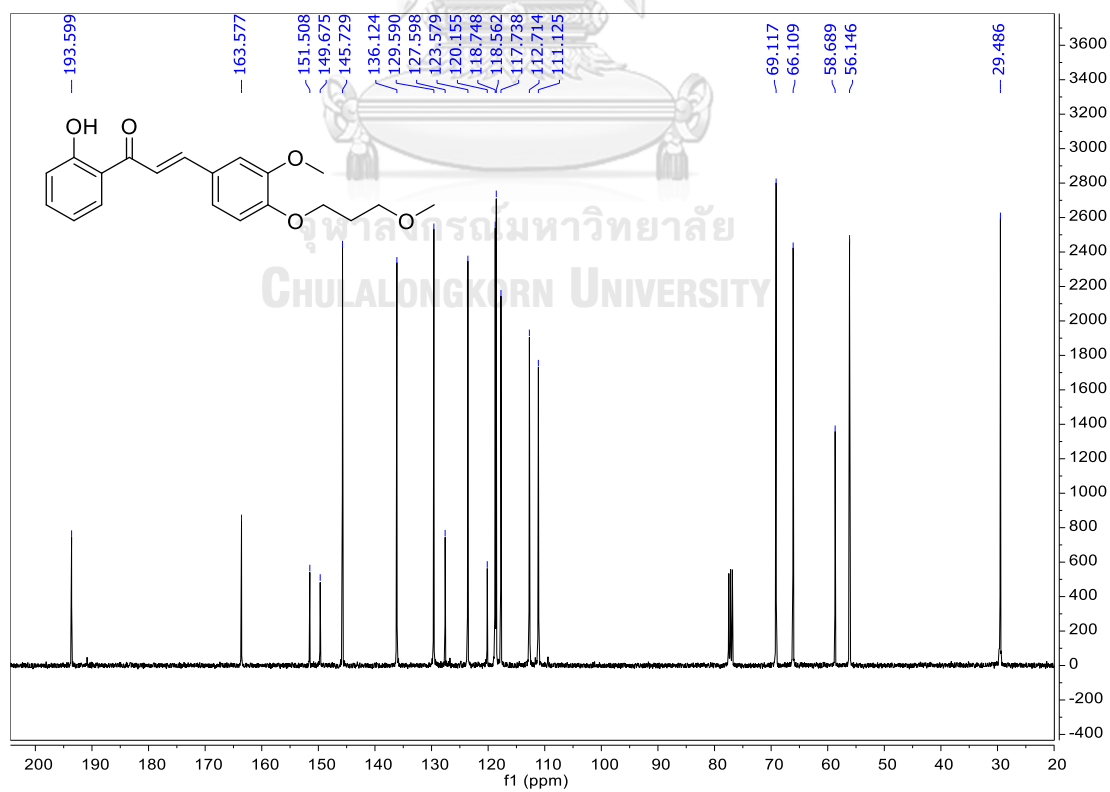


Figure A.82 The ^{13}C NMR spectrum (CDCl_3 , 100 MHz) of **92**.

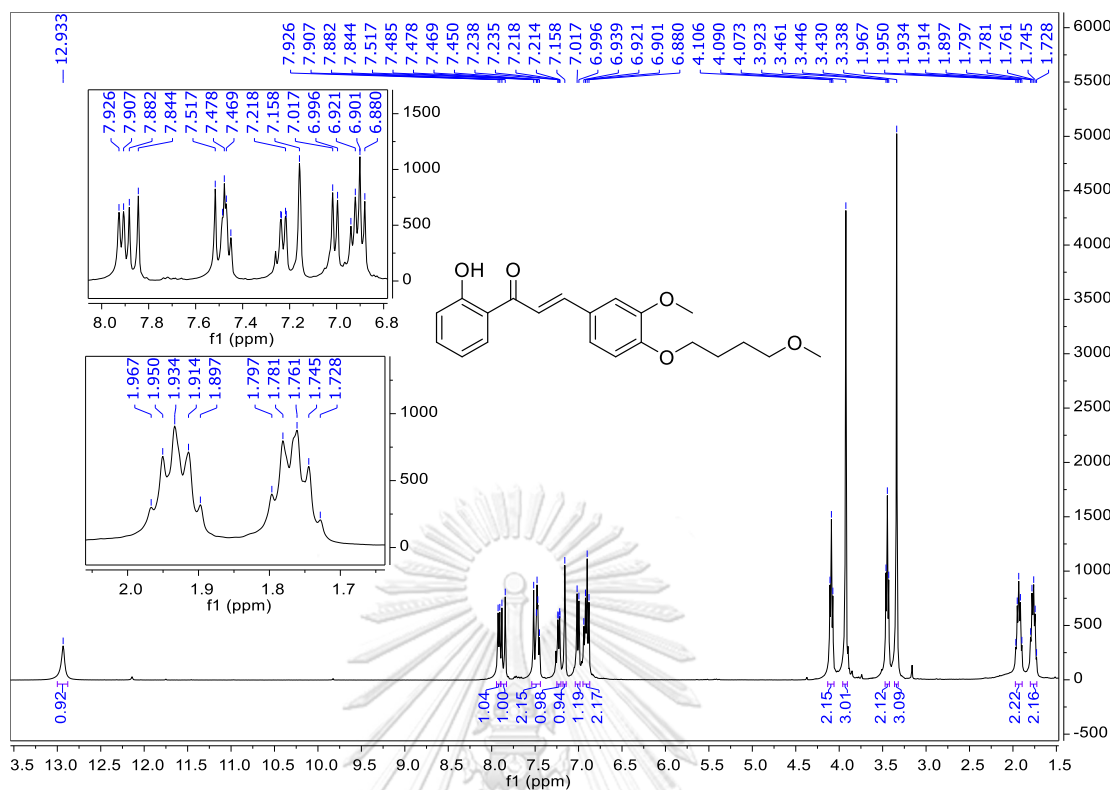


Figure A.83 The ¹H NMR spectrum (CDCl₃, 400 MHz) of **93**.

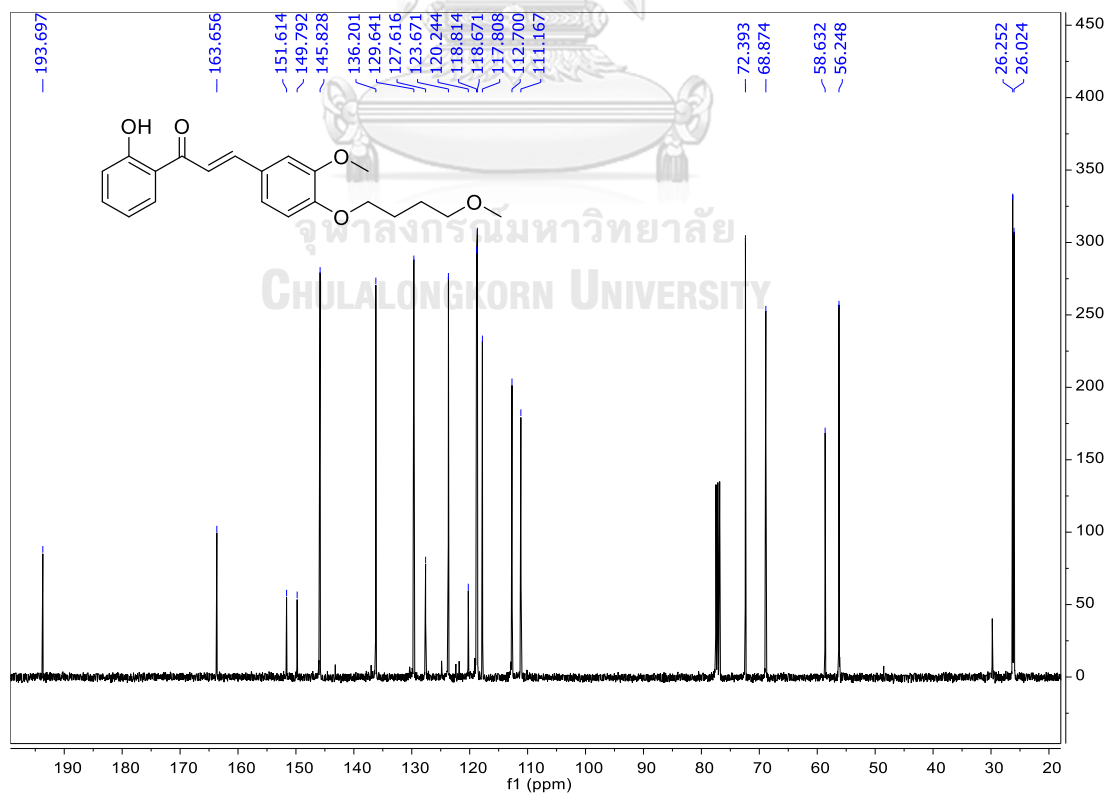


Figure A.84 The ¹³C NMR spectrum (CDCl₃, 100 MHz) of **93**.

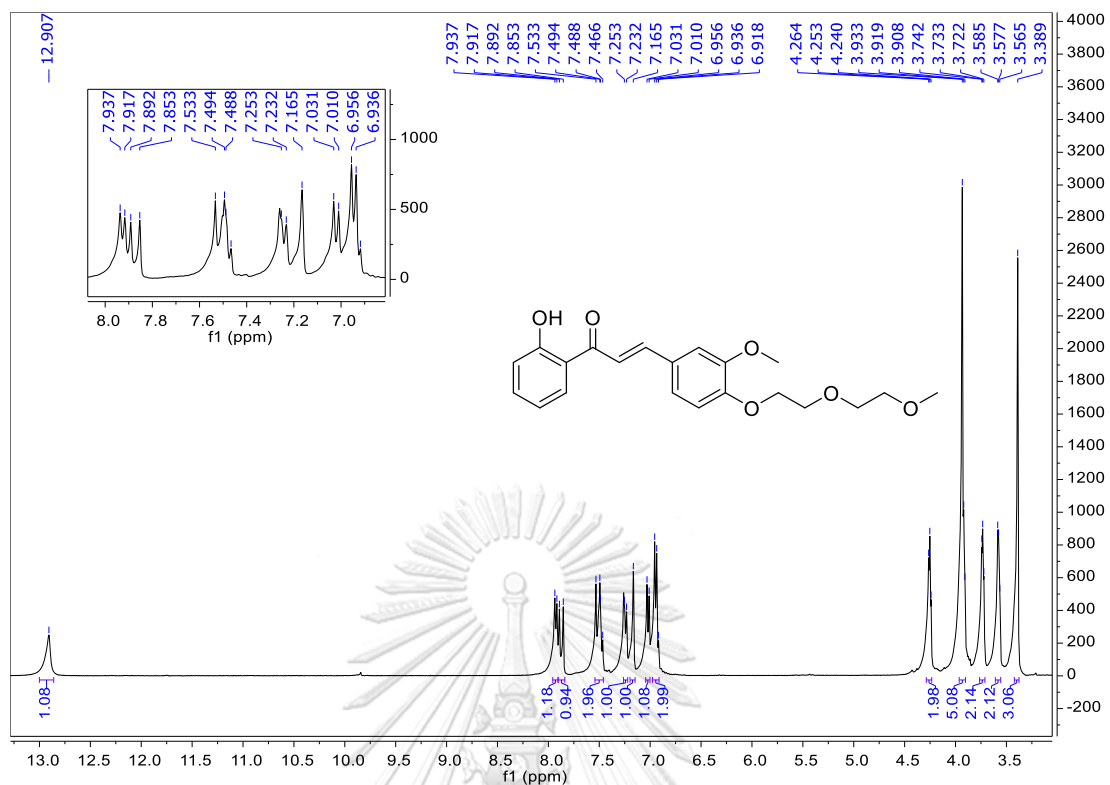


Figure A.85 The ^1H NMR spectrum (CDCl_3 , 400 MHz) of **94**.

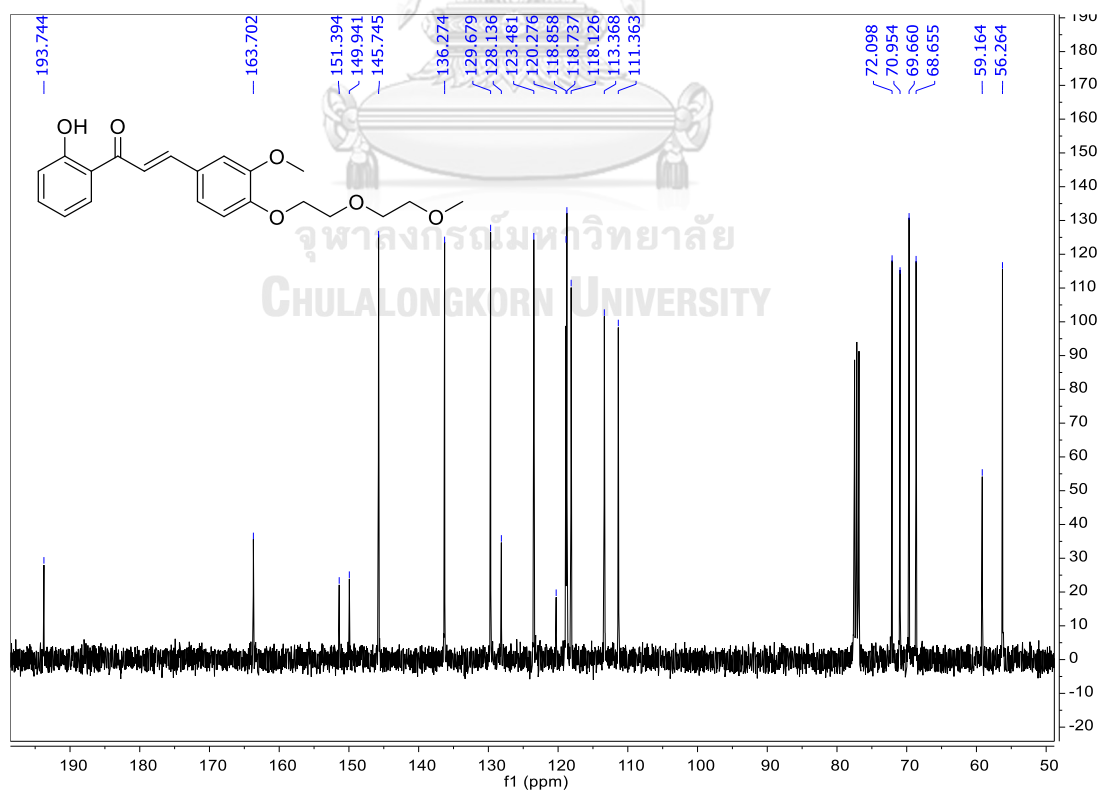


Figure A.86 The ^{13}C NMR spectrum (CDCl_3 , 100 MHz) of **94**.

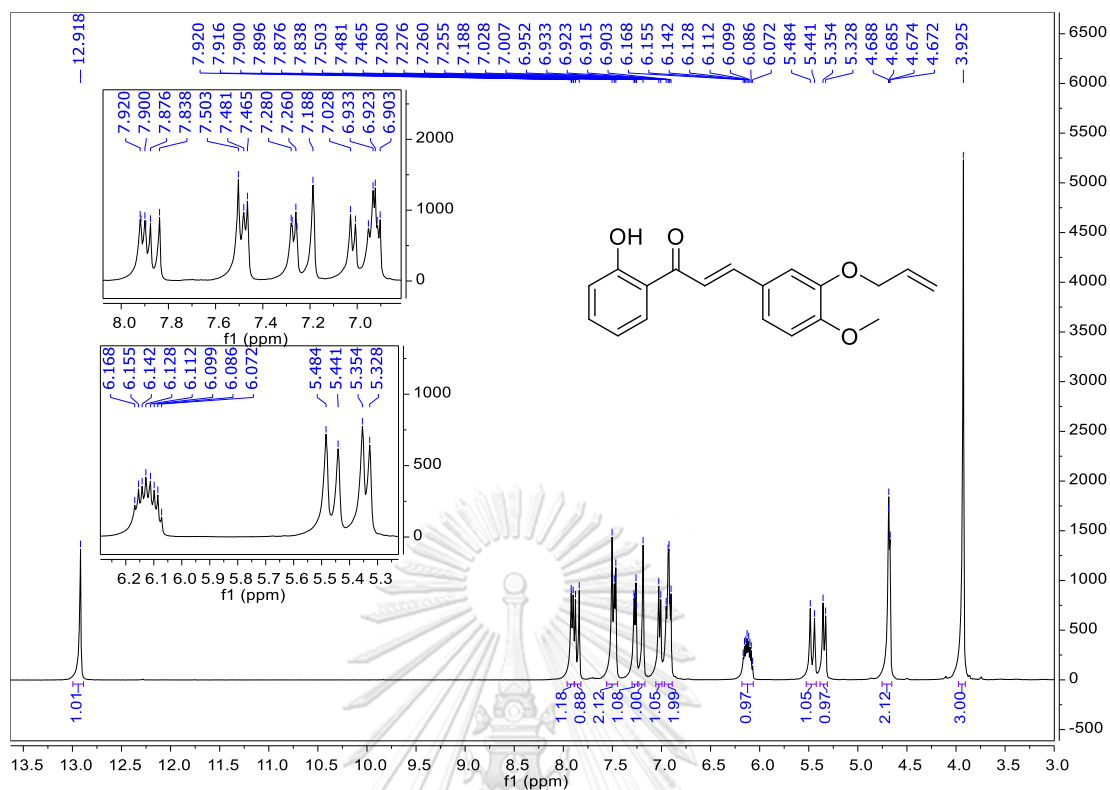


Figure A.89 The ¹H NMR spectrum (CDCl₃, 400 MHz) of **96**.

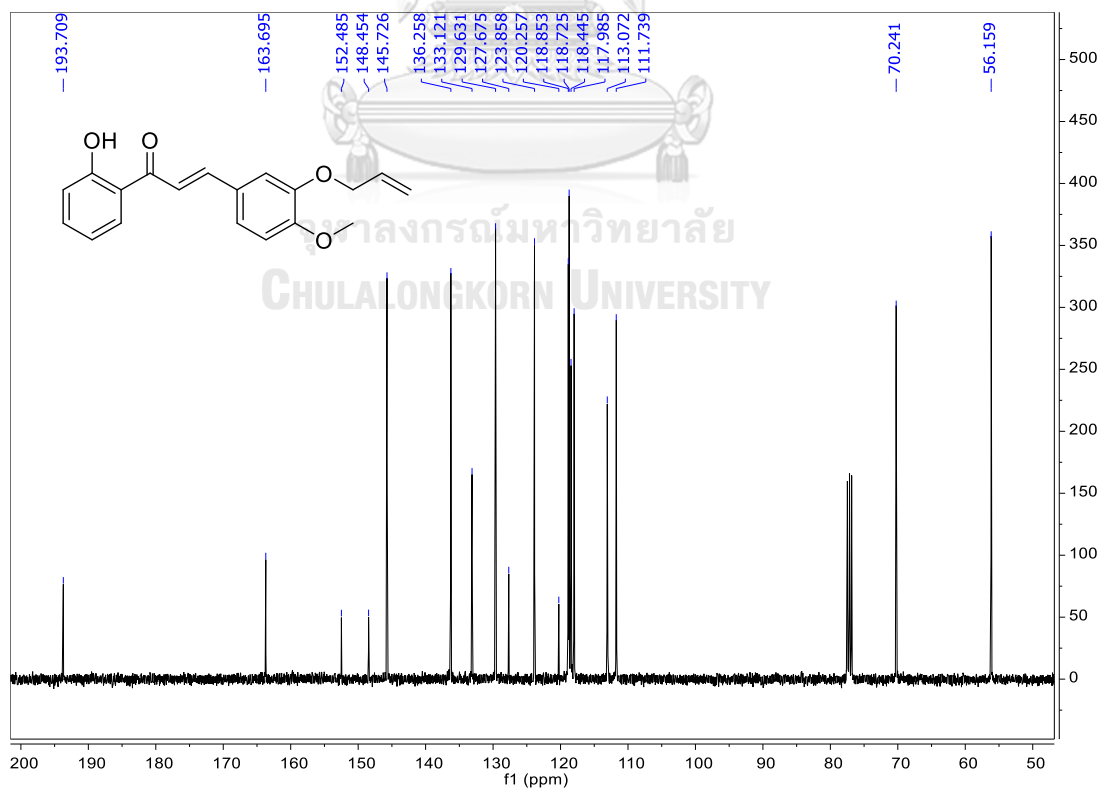


Figure A.90 The ¹³C NMR spectrum (CDCl₃, 100 MHz) of **96**.

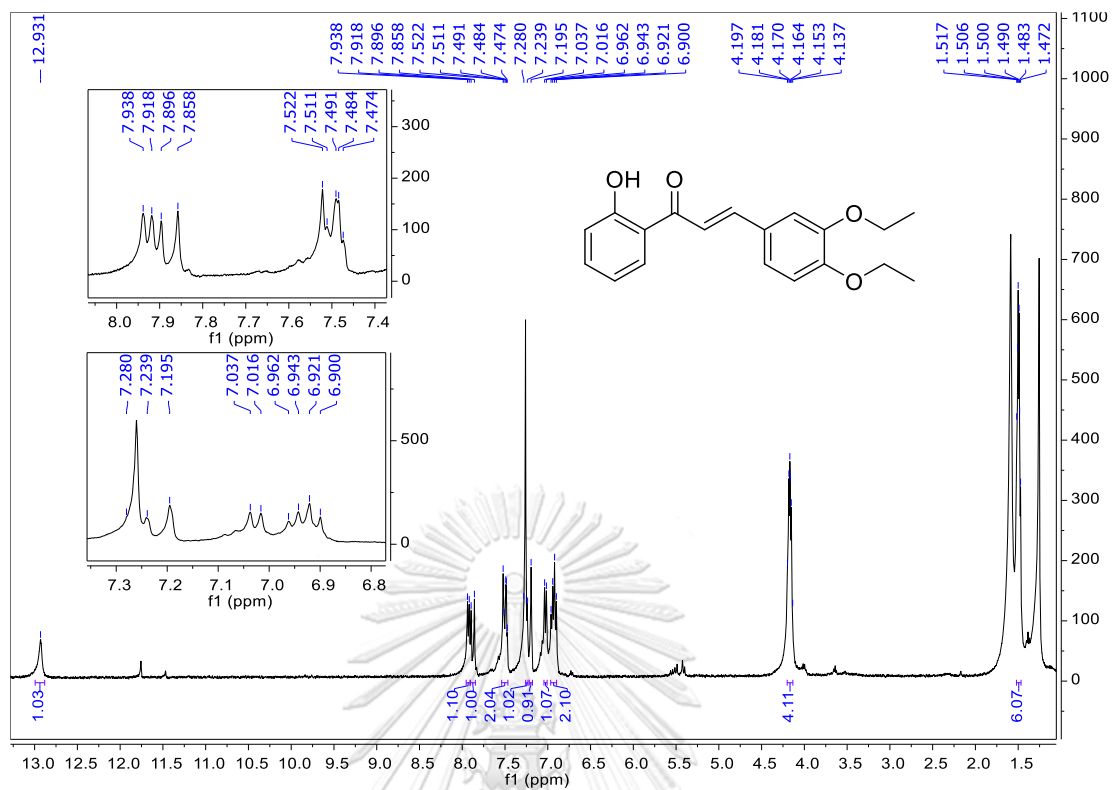


Figure A.91 The ¹H NMR spectrum (CDCl₃, 400 MHz) of 97.

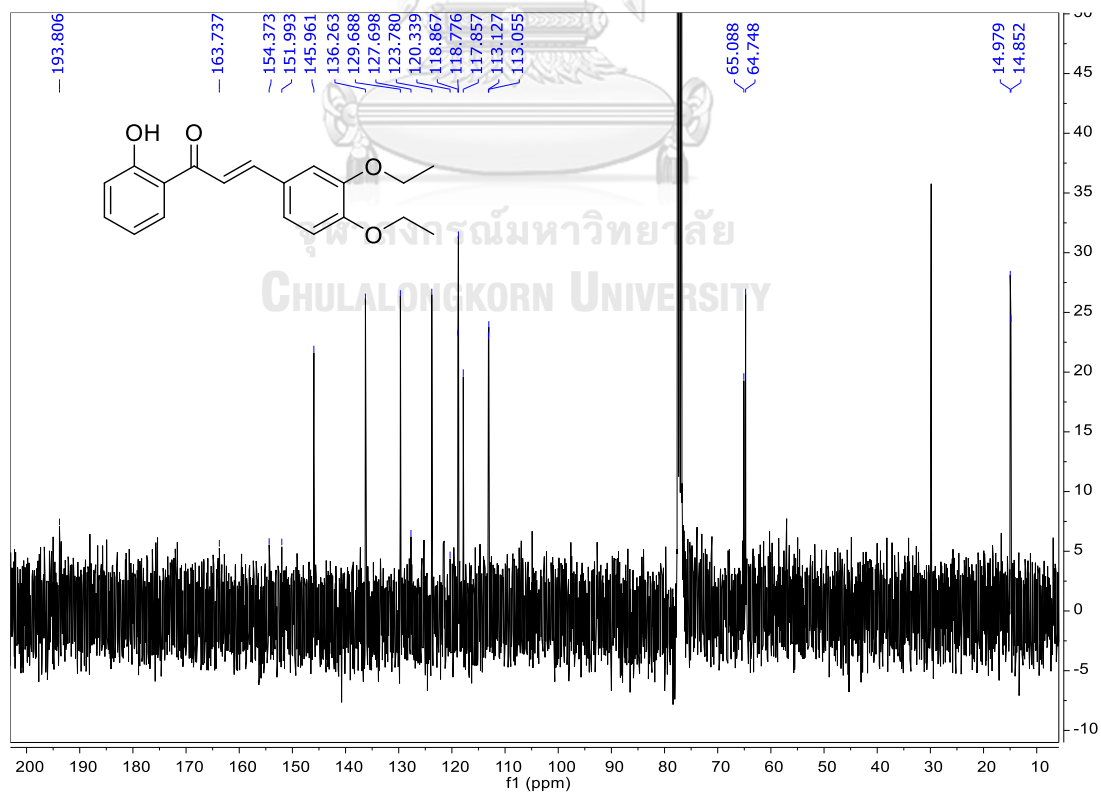


Figure A.92 The ¹³C NMR spectrum (CDCl₃, 100 MHz) of 97.

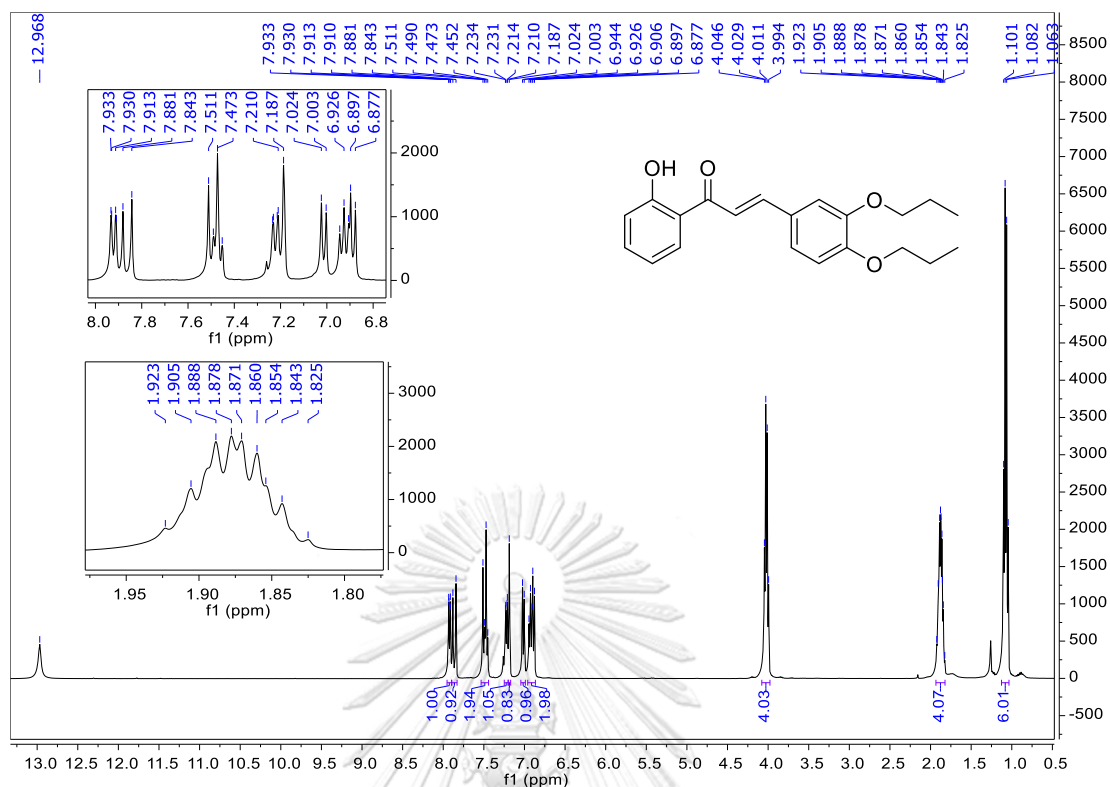


Figure A.93 The ¹H NMR spectrum (CDCl₃, 400 MHz) of **98**.

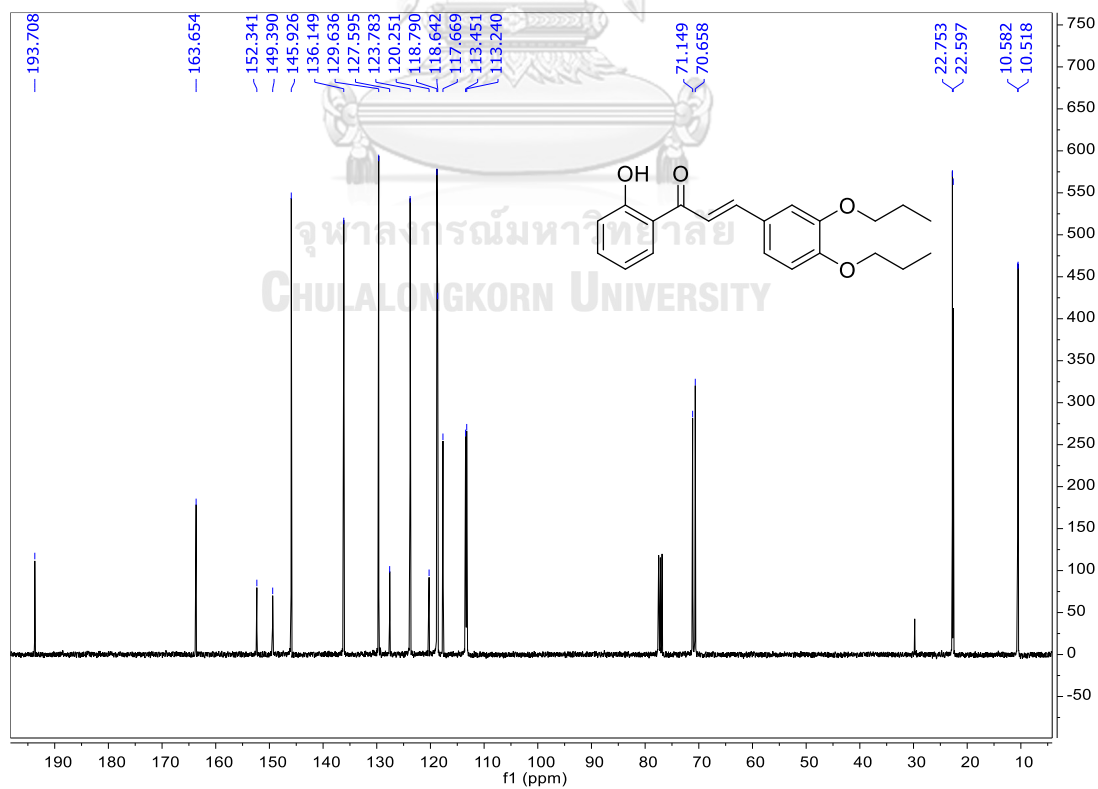


Figure A.94 The ¹³C NMR spectrum (CDCl₃, 100 MHz) of **98**.

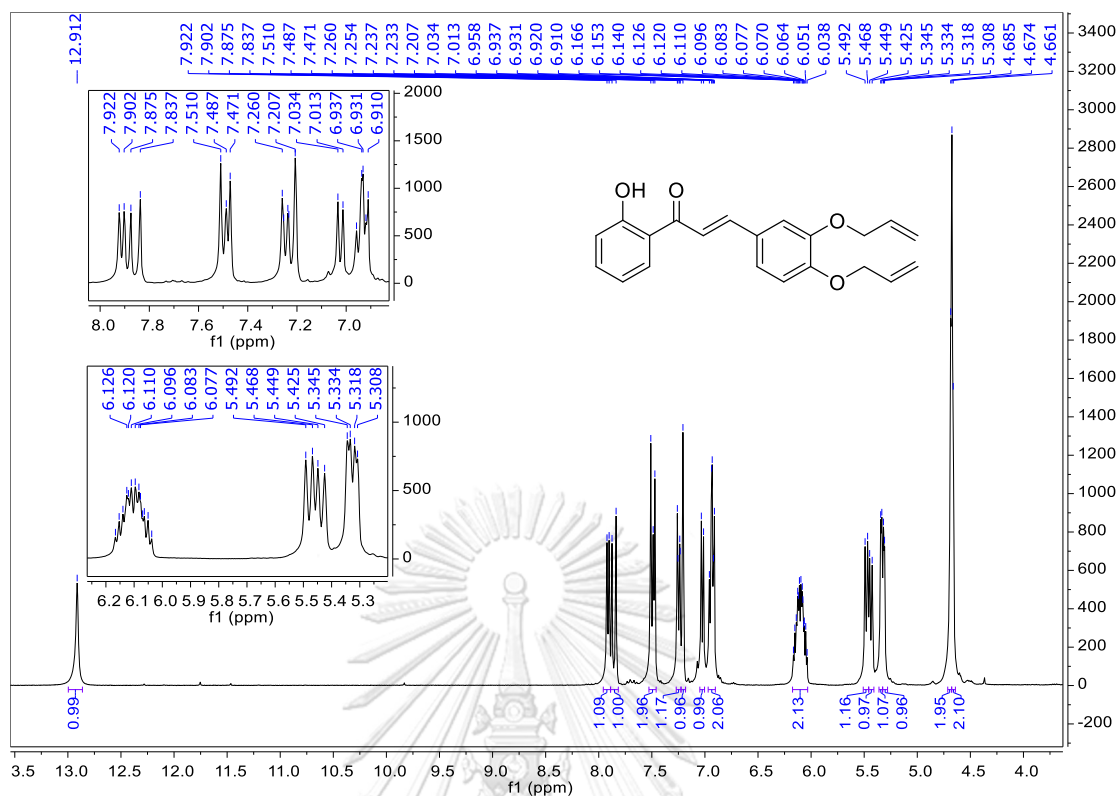


Figure A.95 The ^1H NMR spectrum (CDCl_3 , 400 MHz) of **99**.

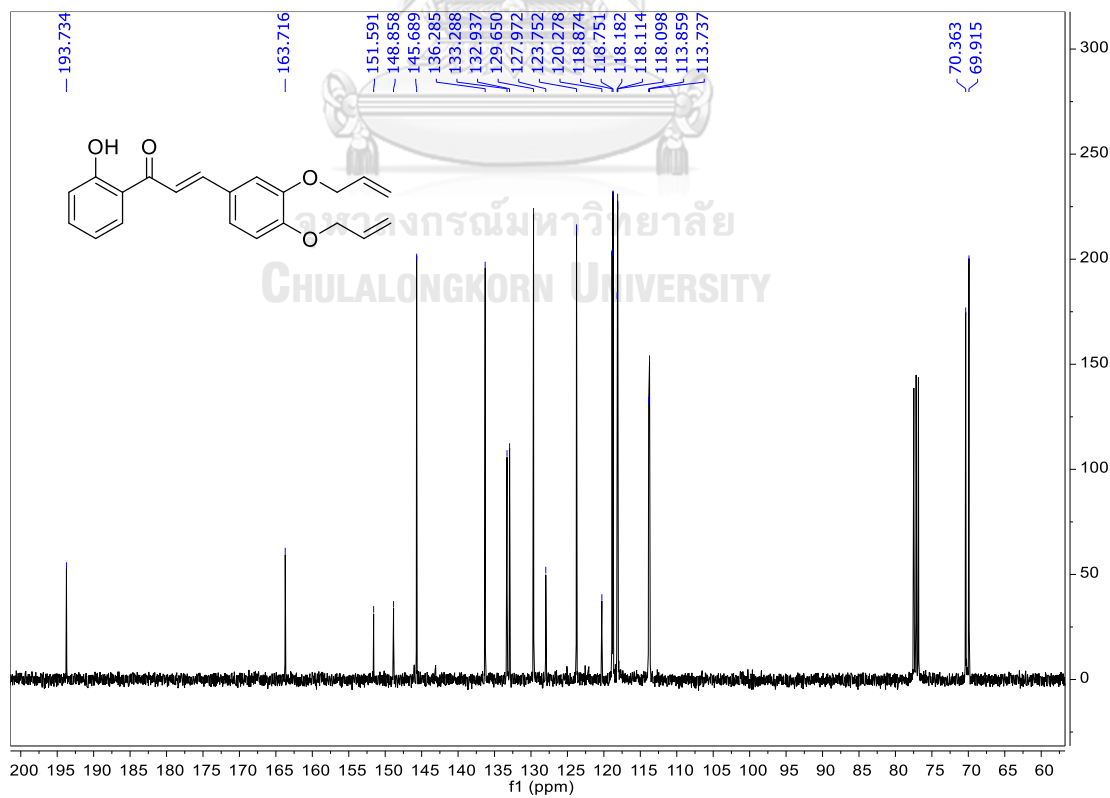


Figure A.96 The ^{13}C NMR spectrum (CDCl_3 , 100 MHz) of **99**.

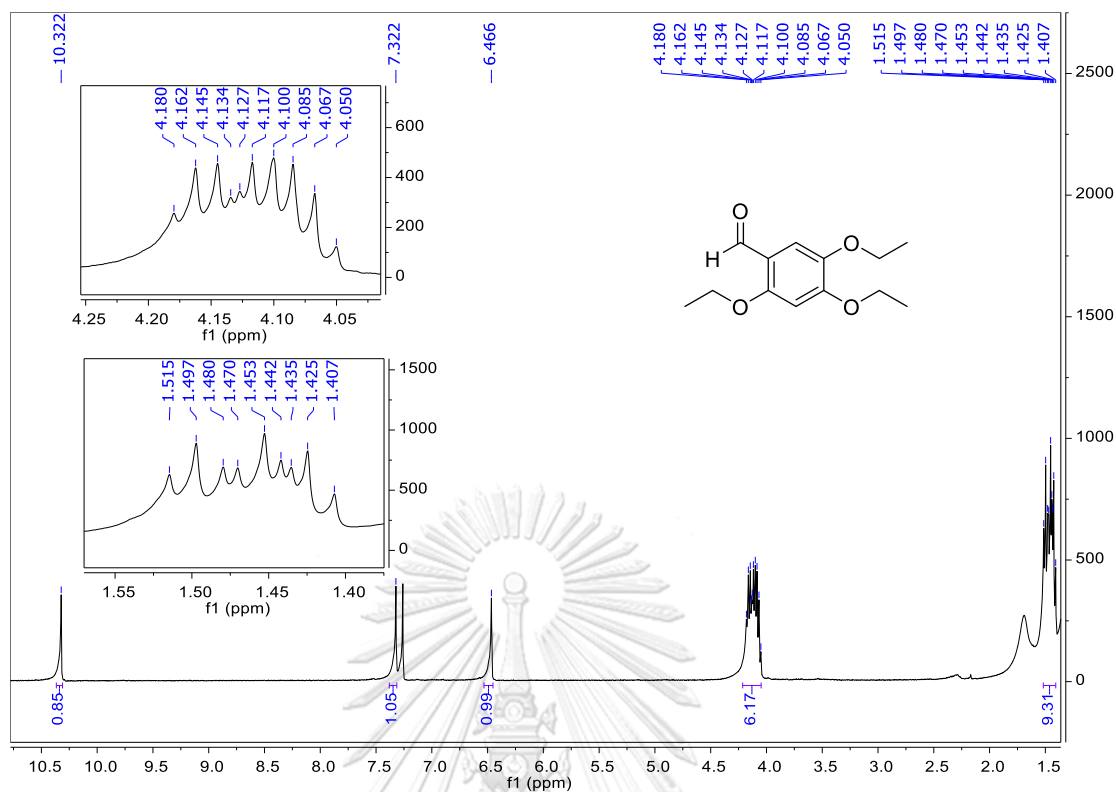


Figure A.97 The ^1H NMR spectrum (CDCl₃, 400 MHz) of **100**.

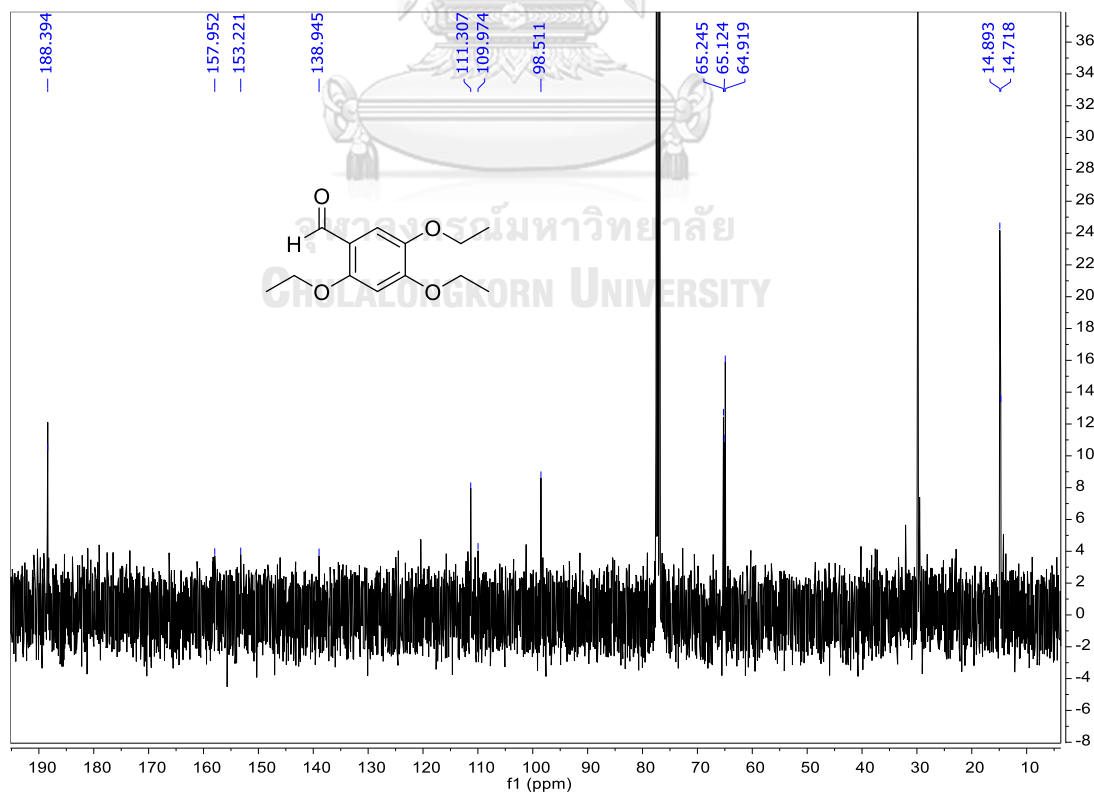


Figure A.98 The ^{13}C NMR spectrum (CDCl₃, 100 MHz) of **100**.

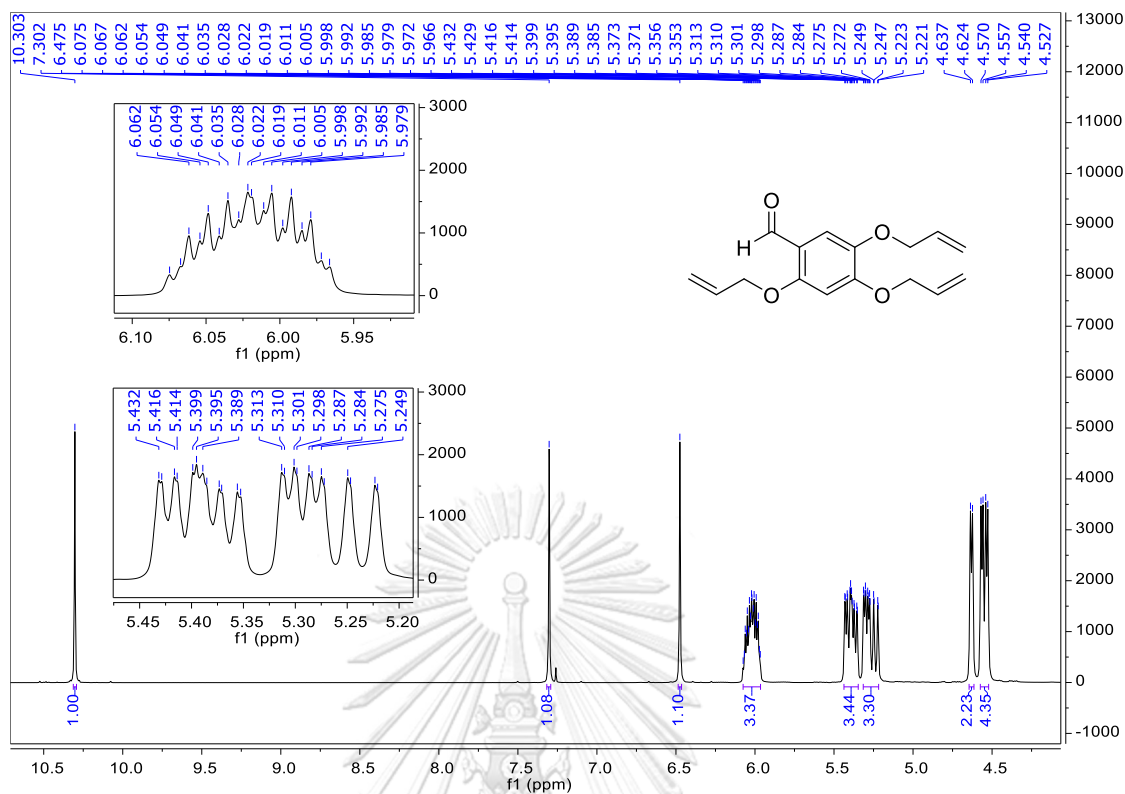


Figure A.99 The $^1\text{H NMR}$ spectrum (CDCl₃, 400 MHz) of 101.

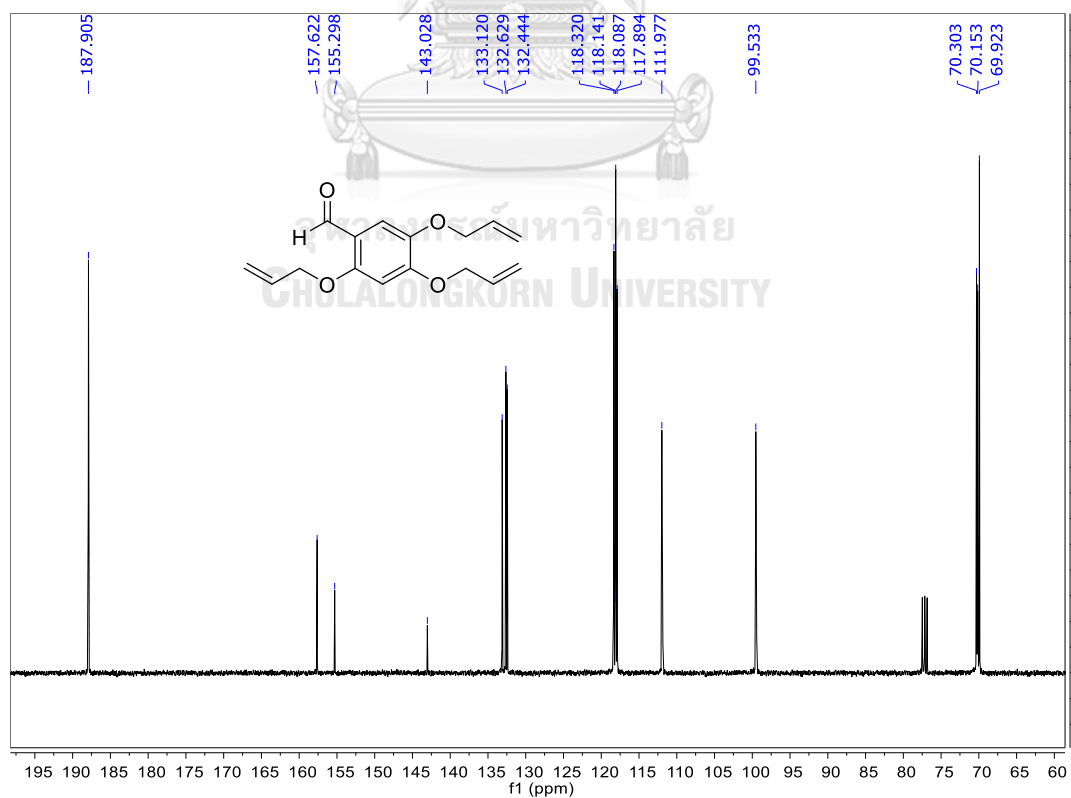


Figure A.100 The $^{13}\text{C NMR}$ spectrum (CDCl₃, 100 MHz) of 101.

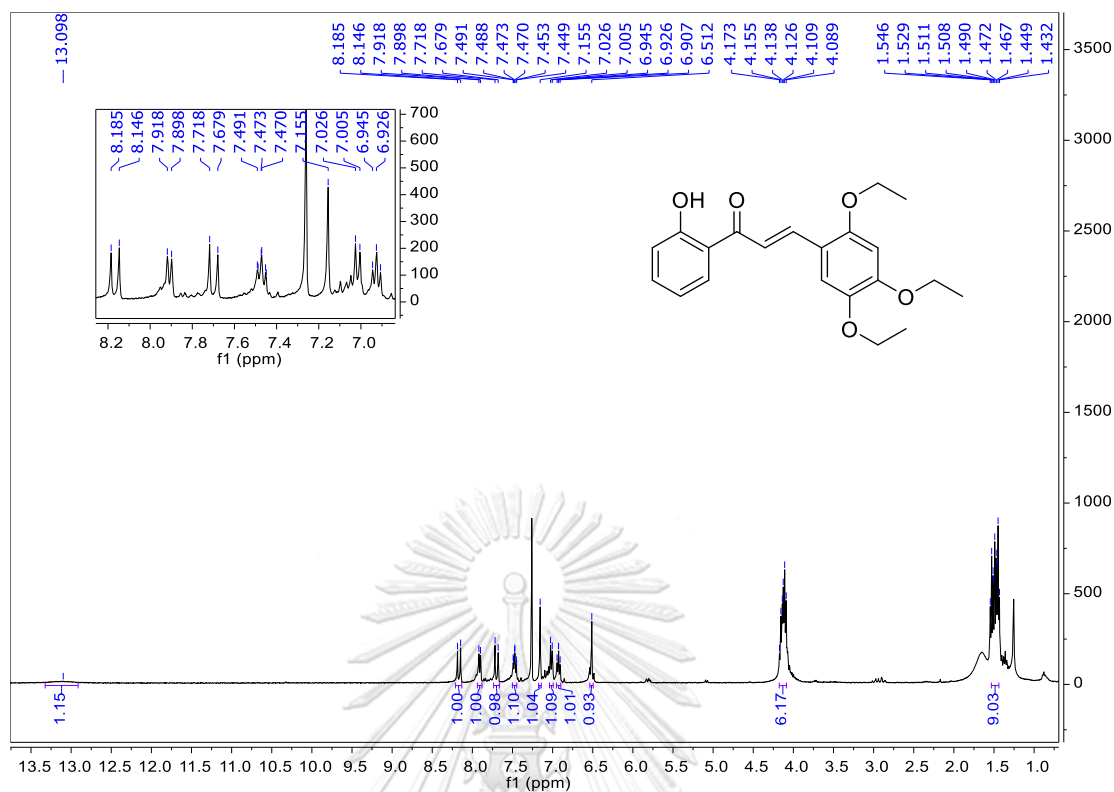


Figure A.101 The ^1H NMR spectrum (CDCl_3 , 400 MHz) of 102.

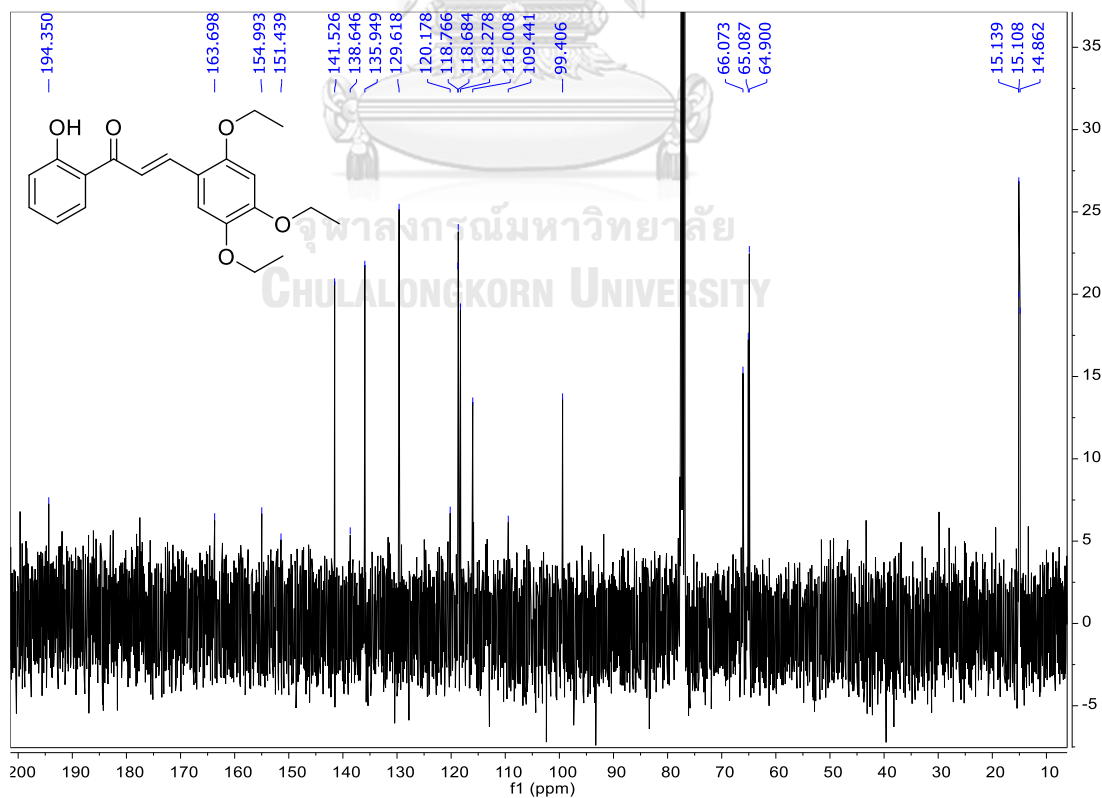


Figure A.102 The ^{13}C NMR spectrum (CDCl_3 , 100 MHz) of 102.

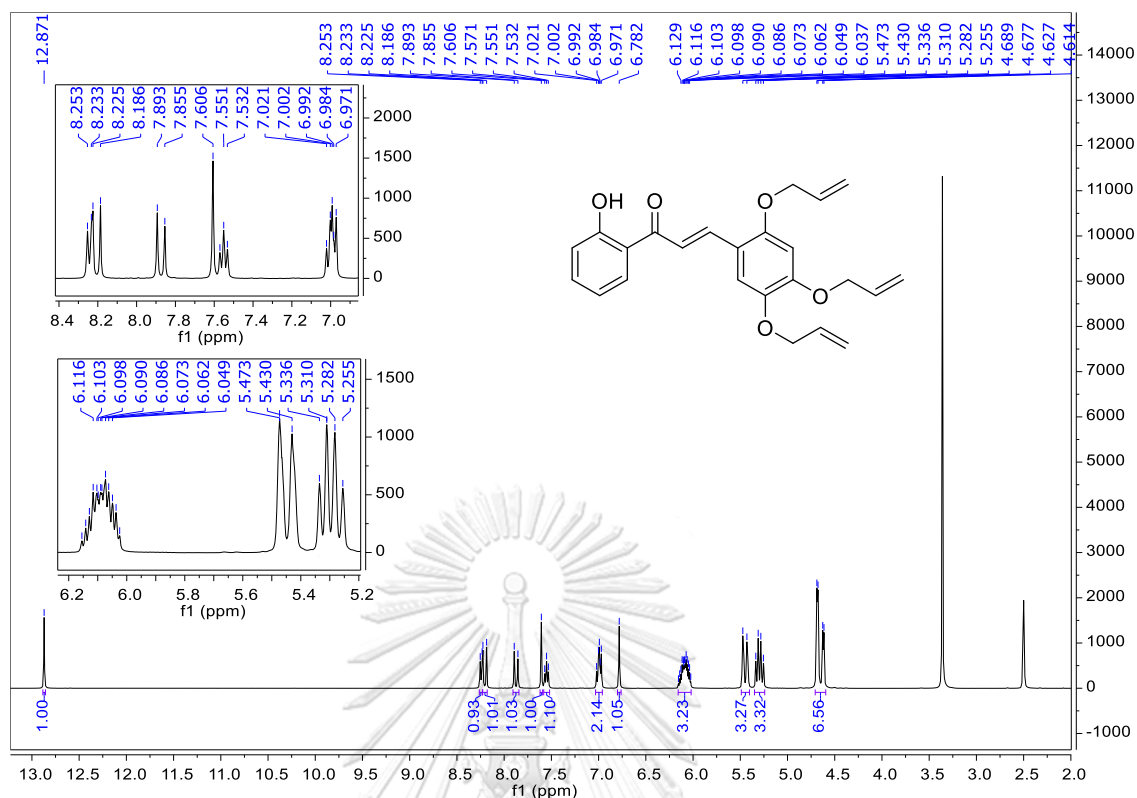


Figure A.103 The ^1H NMR spectrum (DMSO- d_6 , 400 MHz) of 103.

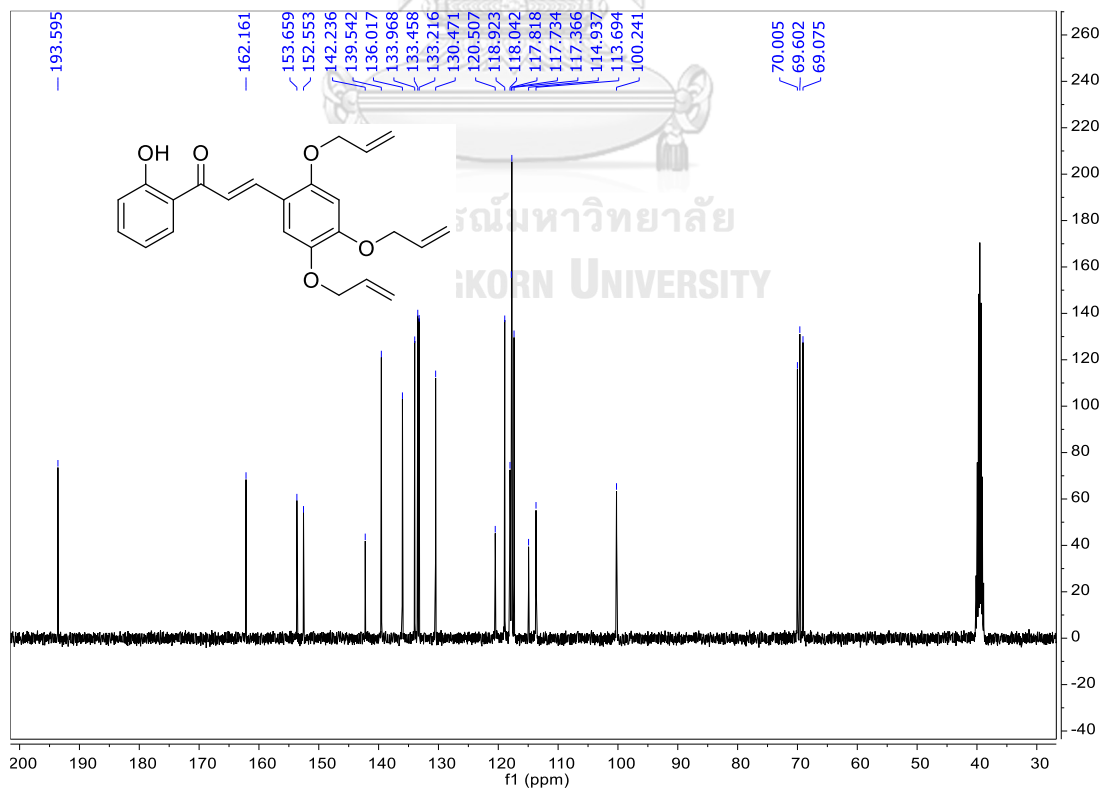


Figure A.104 The ^{13}C NMR spectrum (DMSO- d_6 , 100 MHz) of 103.

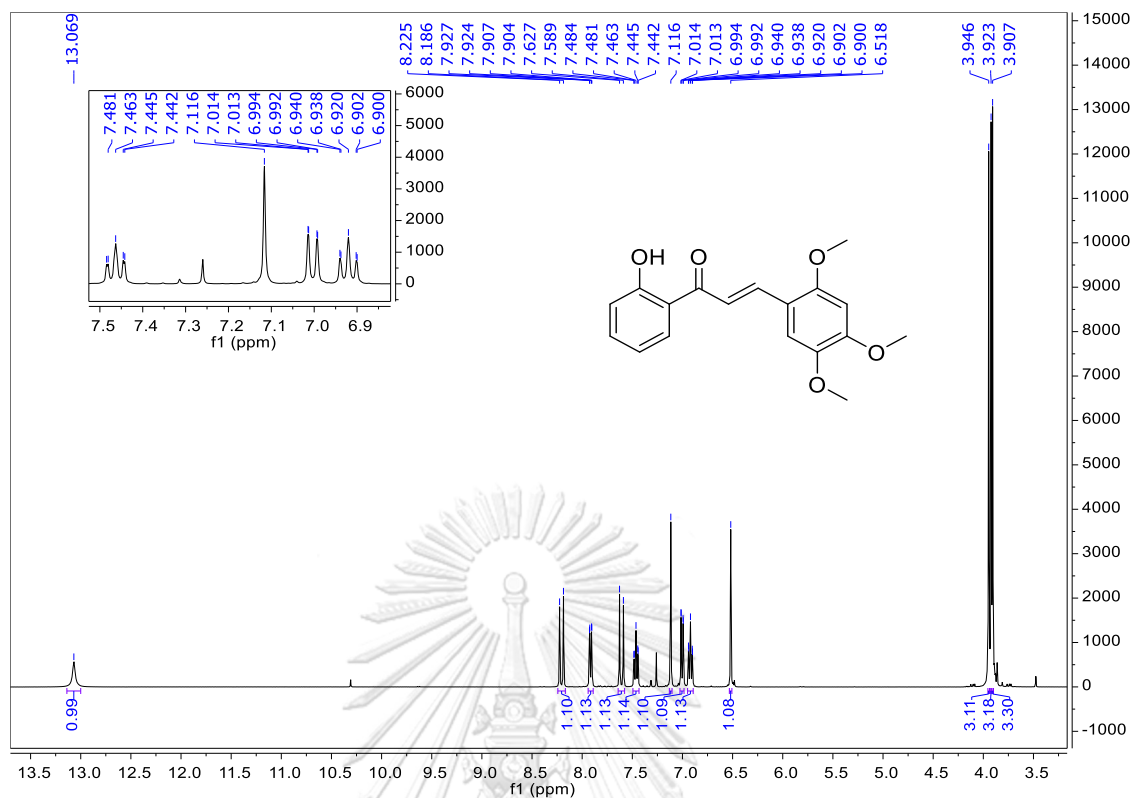


Figure A.105 The ¹H NMR spectrum (CDCl₃, 400 MHz) of 48.

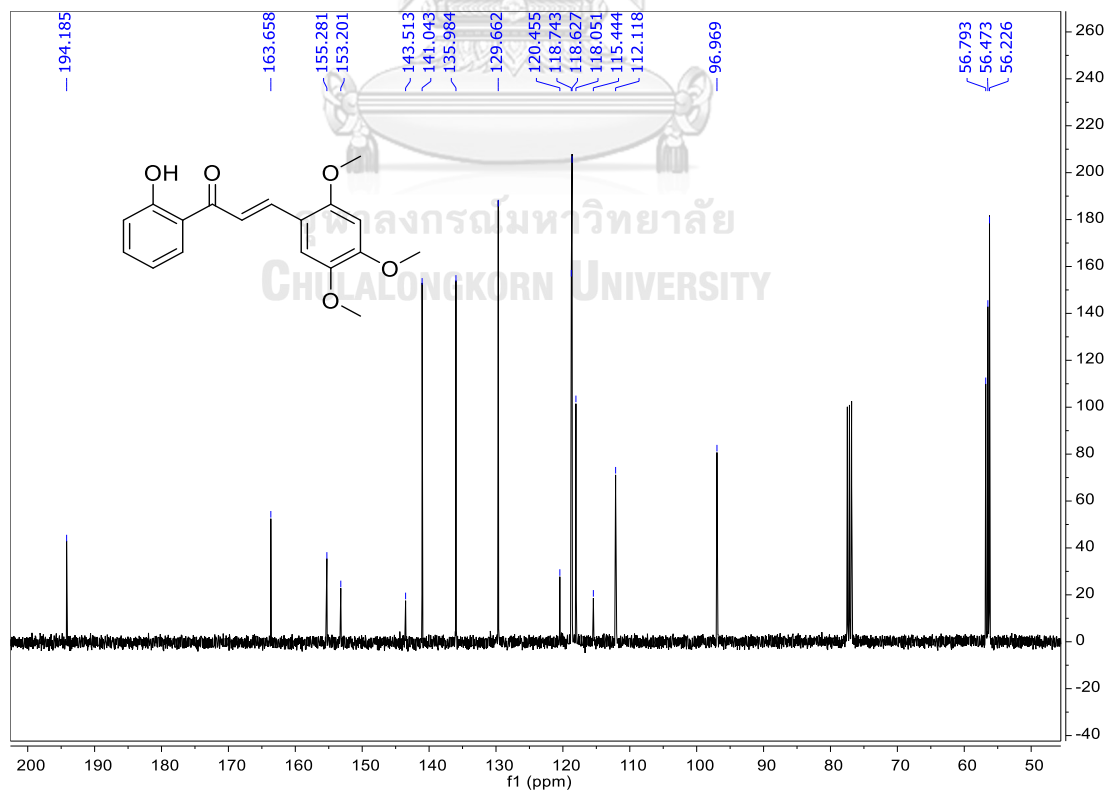


Figure A.106 The ¹³C NMR spectrum (CDCl₃, 100 MHz) of 48.

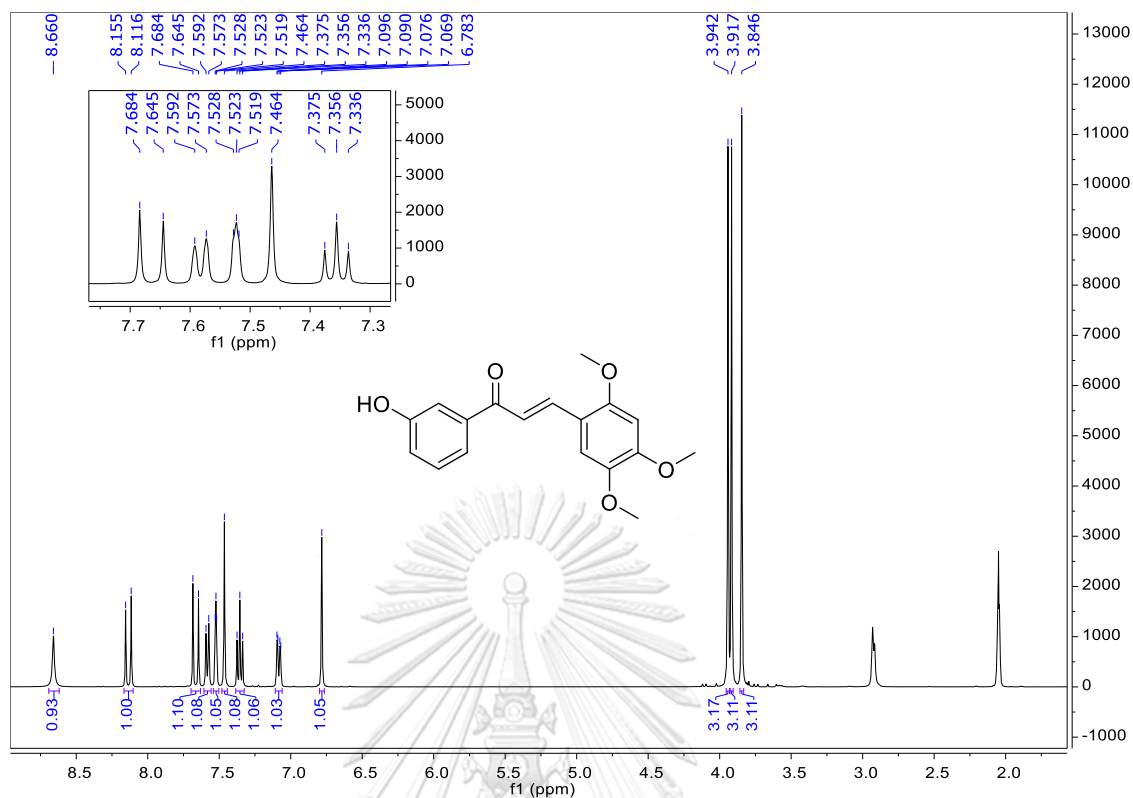


Figure A.107 The ^1H NMR spectrum (acetone- d_6 , 400 MHz) of 104.

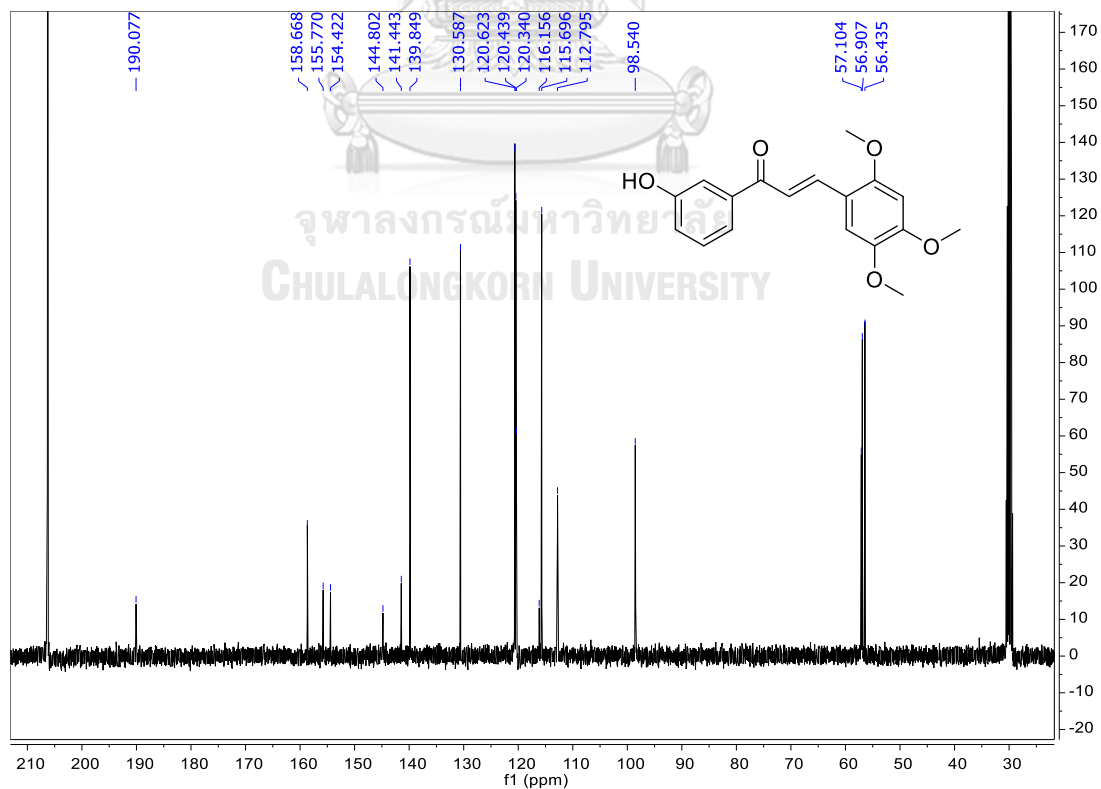


Figure A.108 The ^{13}C NMR spectrum (acetone- d_6 , 100 MHz) of 104.

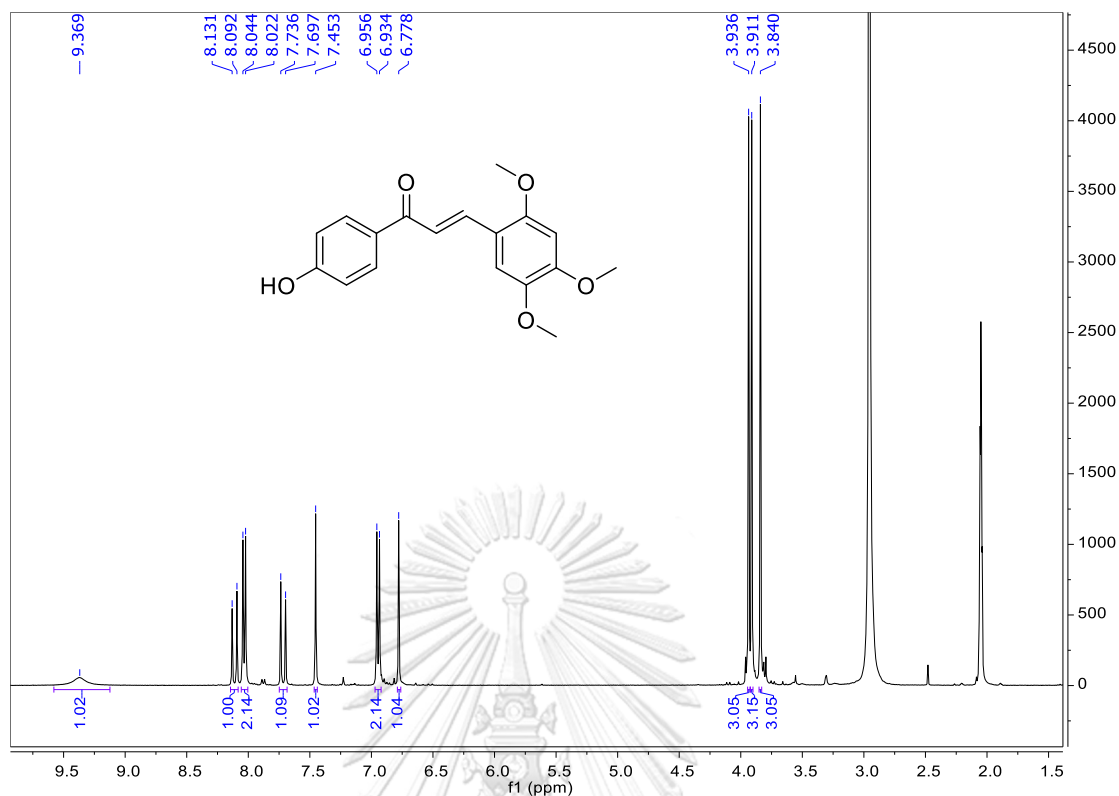


Figure A.109 The ^1H NMR spectrum (acetone- d_6 , 400 MHz) of **105**.

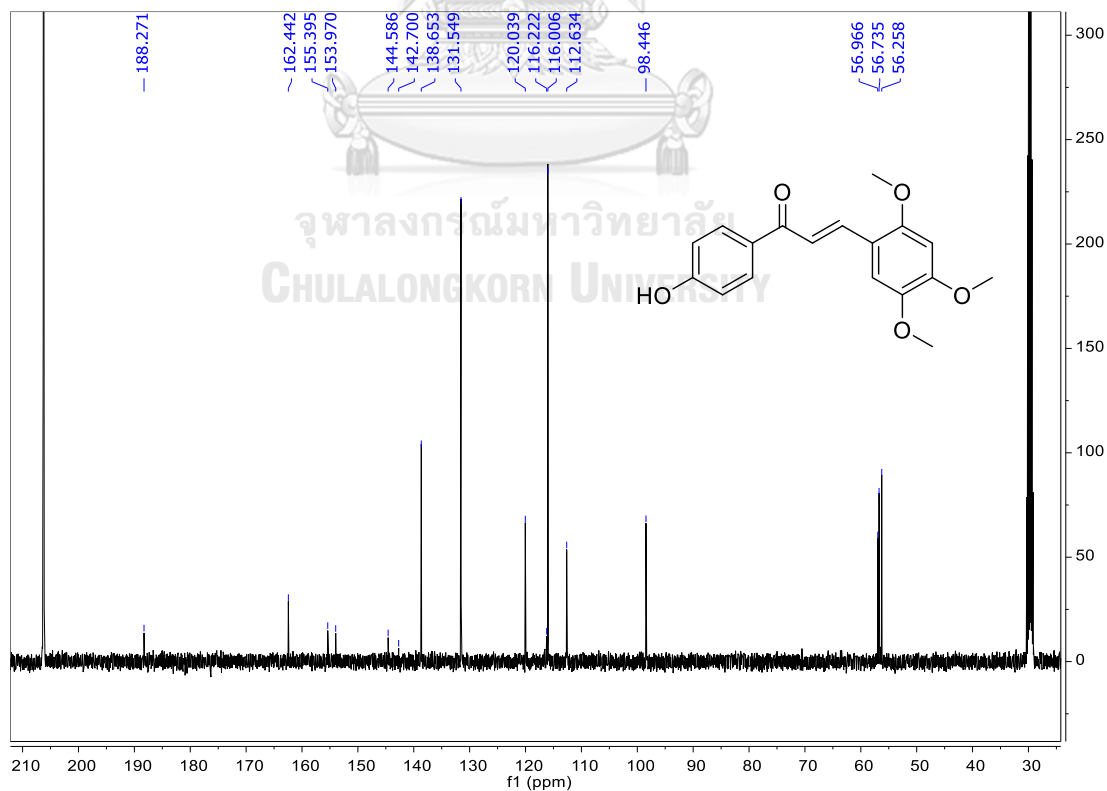


Figure A.110 The ^{13}C NMR spectrum (acetone- d_6 , 100 MHz) of **105**.

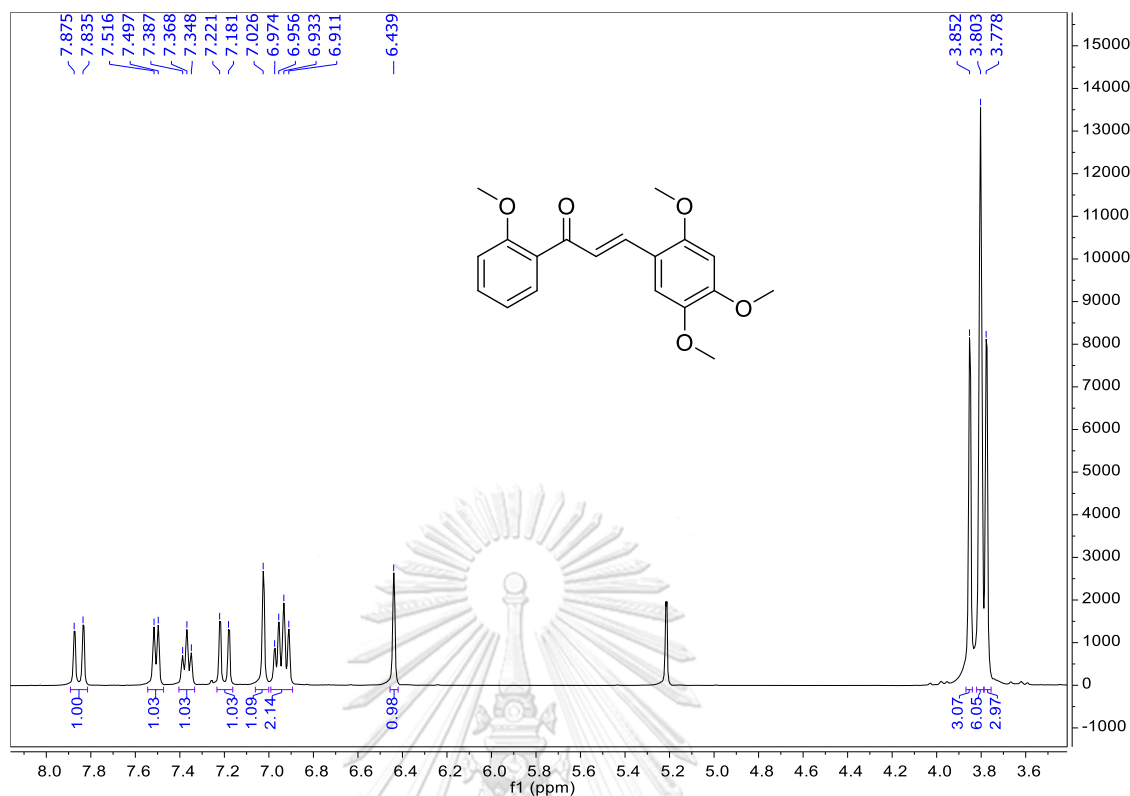


Figure A.111 The ^1H NMR spectrum (CDCl_3 , 400 MHz) of **106**.

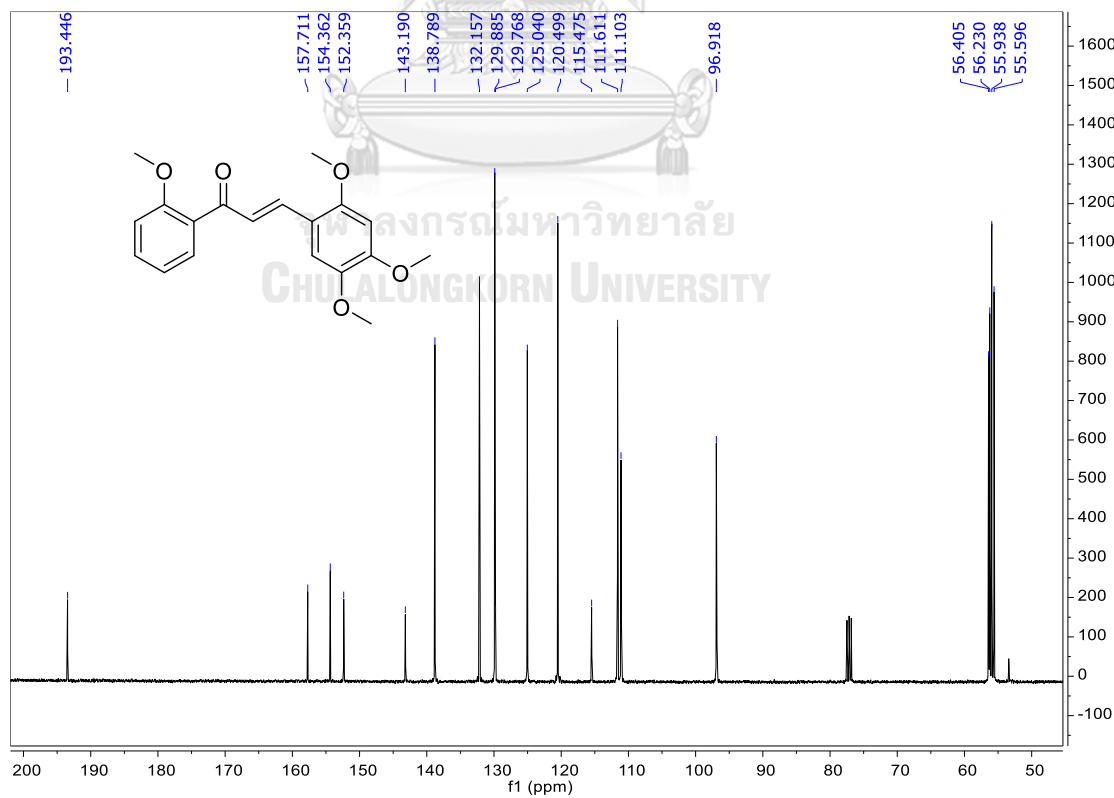


Figure A.112 The ^{13}C NMR spectrum (CDCl_3 , 100 MHz) of **106**.

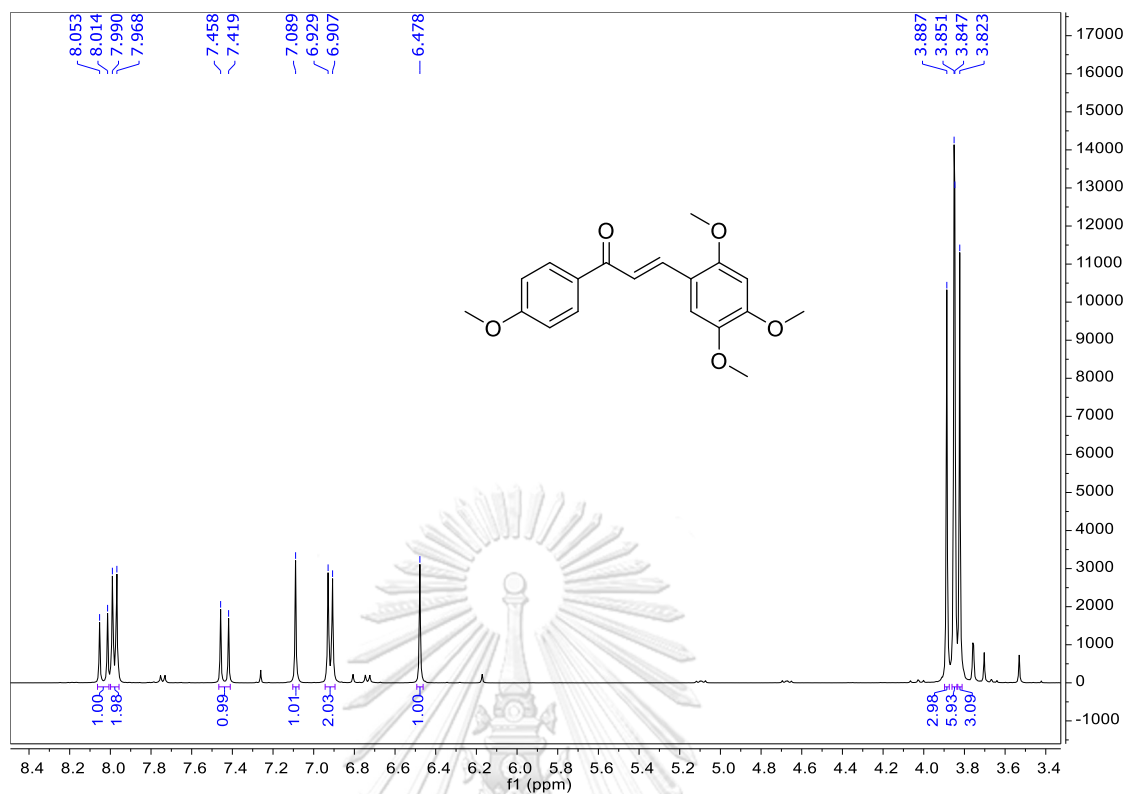


Figure A.113 The ^1H NMR spectrum (CDCl_3 , 400 MHz) of **108**.

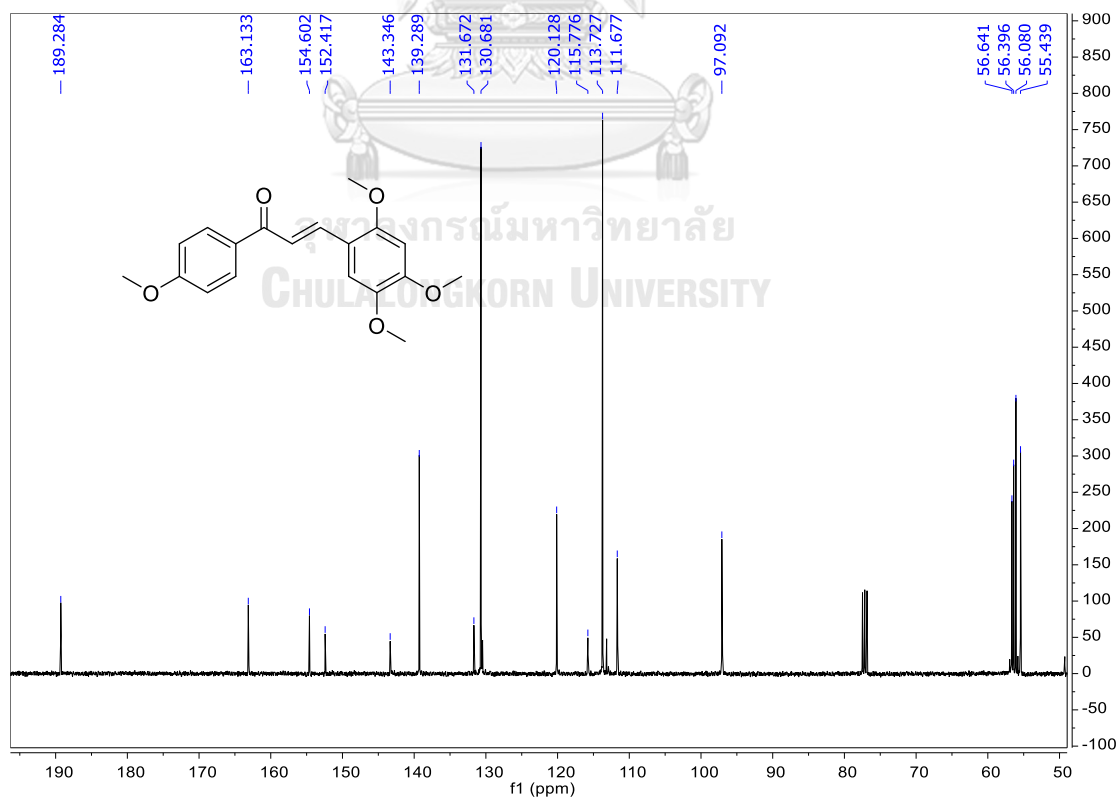


Figure A.114 The ^{13}C NMR spectrum (CDCl_3 , 100 MHz) of **108**.

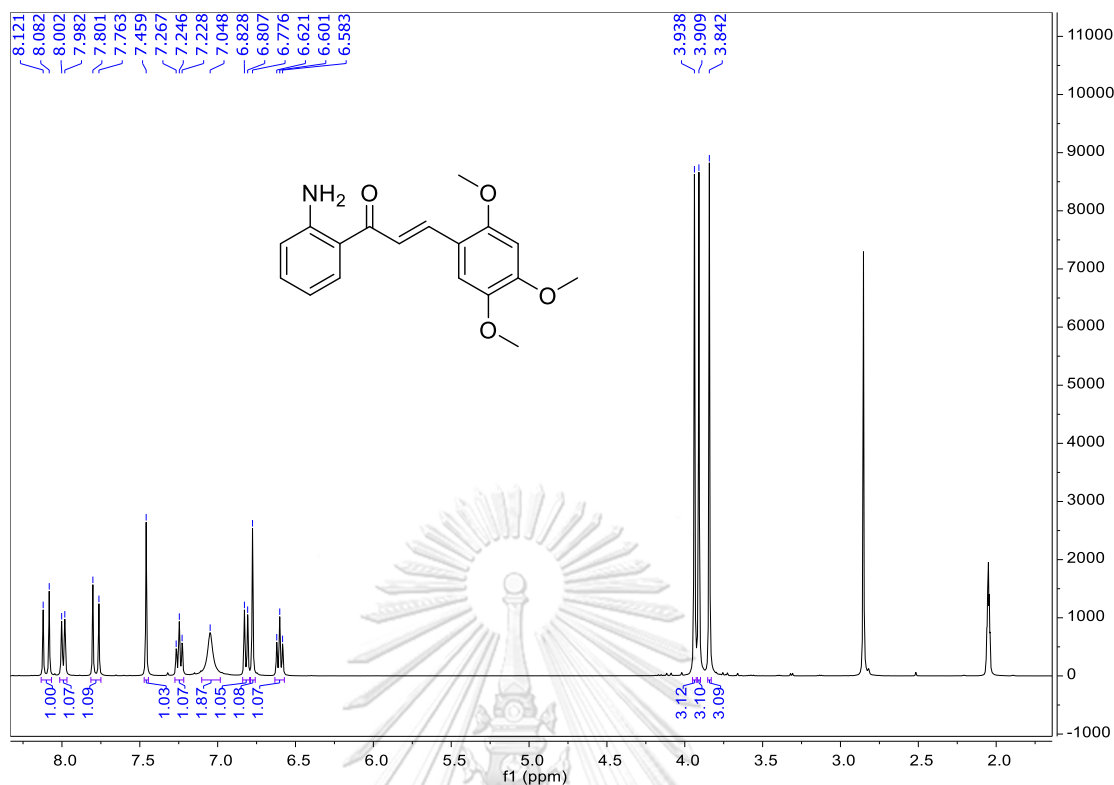


Figure A.115 The ^1H NMR spectrum (acetone- d_6 , 400 MHz) of 109.

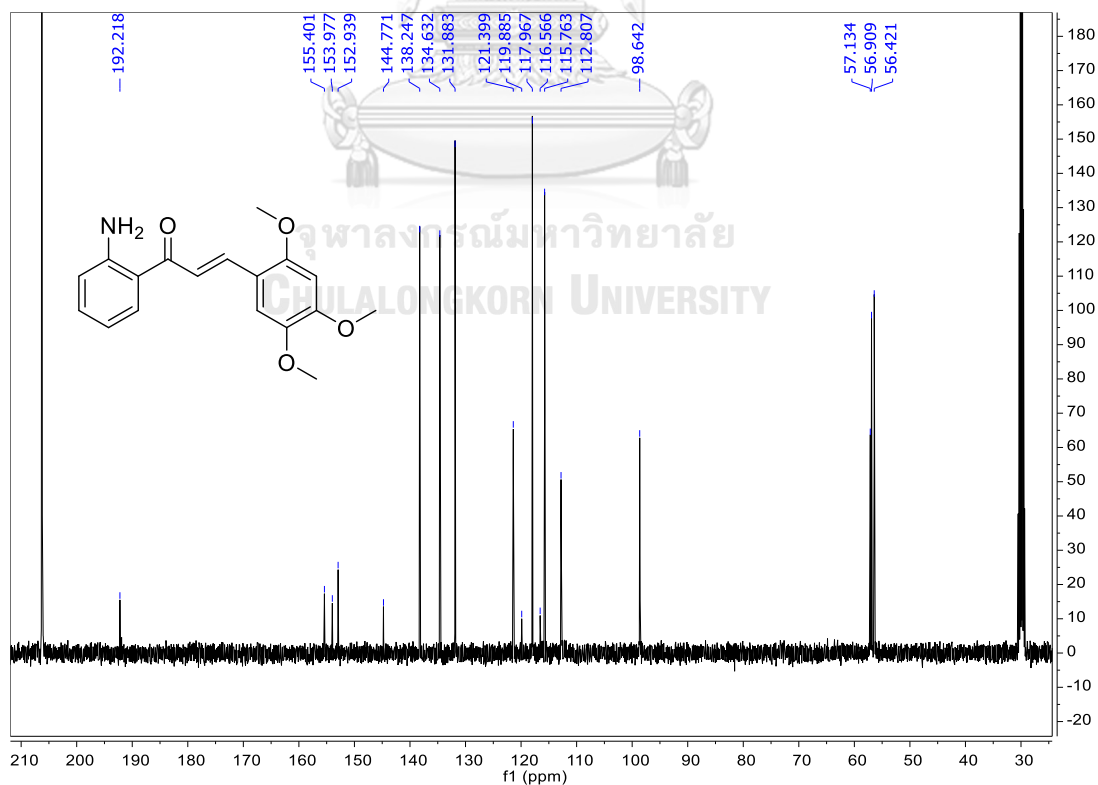


Figure A.116 The ^{13}C NMR spectrum (acetone- d_6 , 100 MHz) of 109.

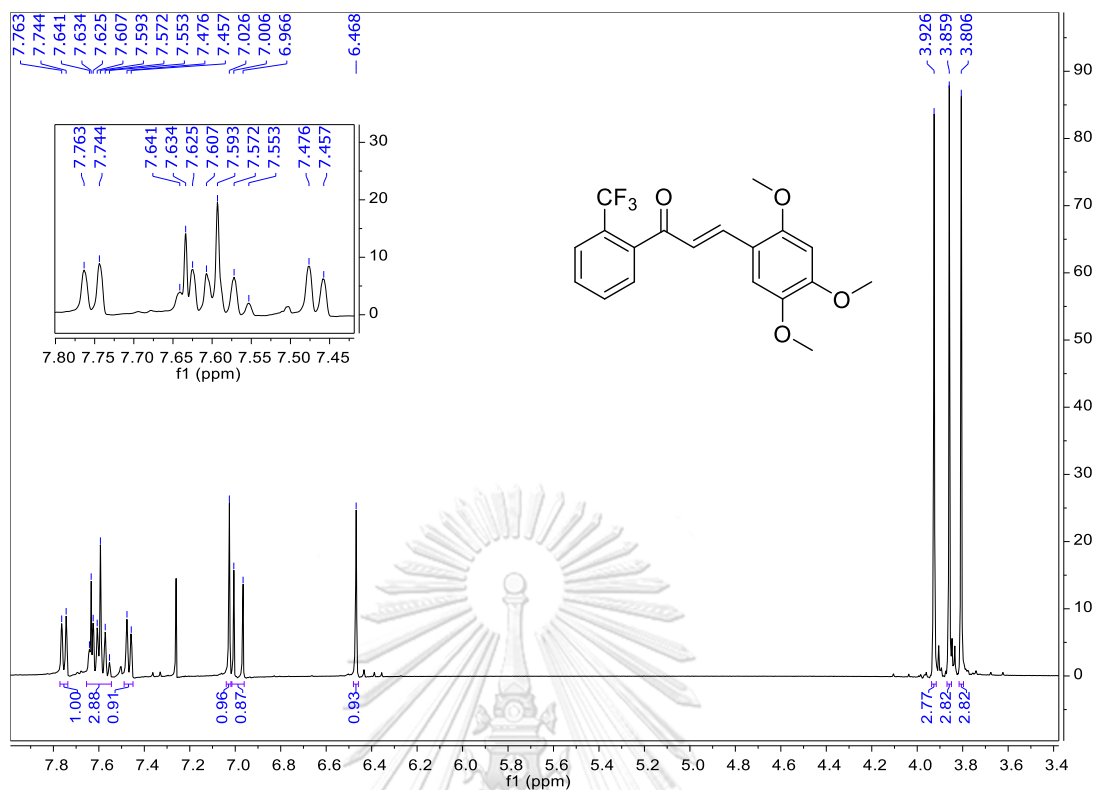


Figure A.117 The ^1H NMR spectrum (CDCl₃, 400 MHz) of 110.

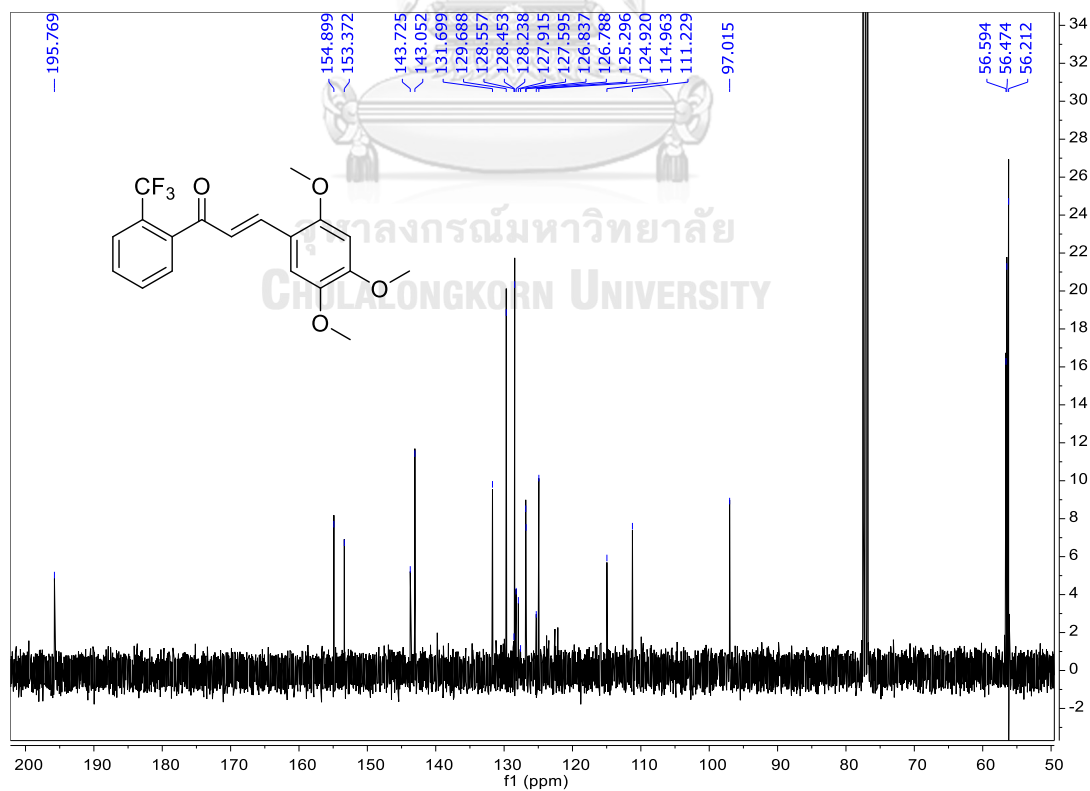


Figure A.118 The ^{13}C NMR spectrum (CDCl₃, 100 MHz) of 110.

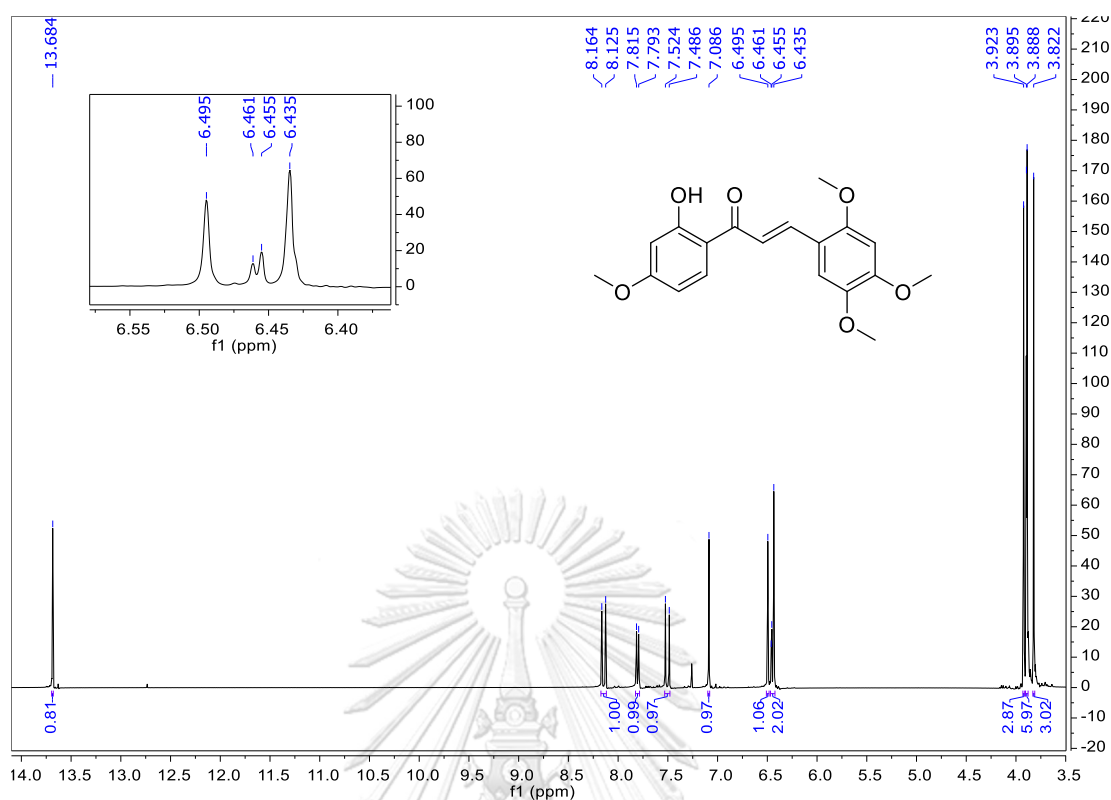


Figure A.119 The ^1H NMR spectrum (CDCl₃, 400 MHz) of **111**.

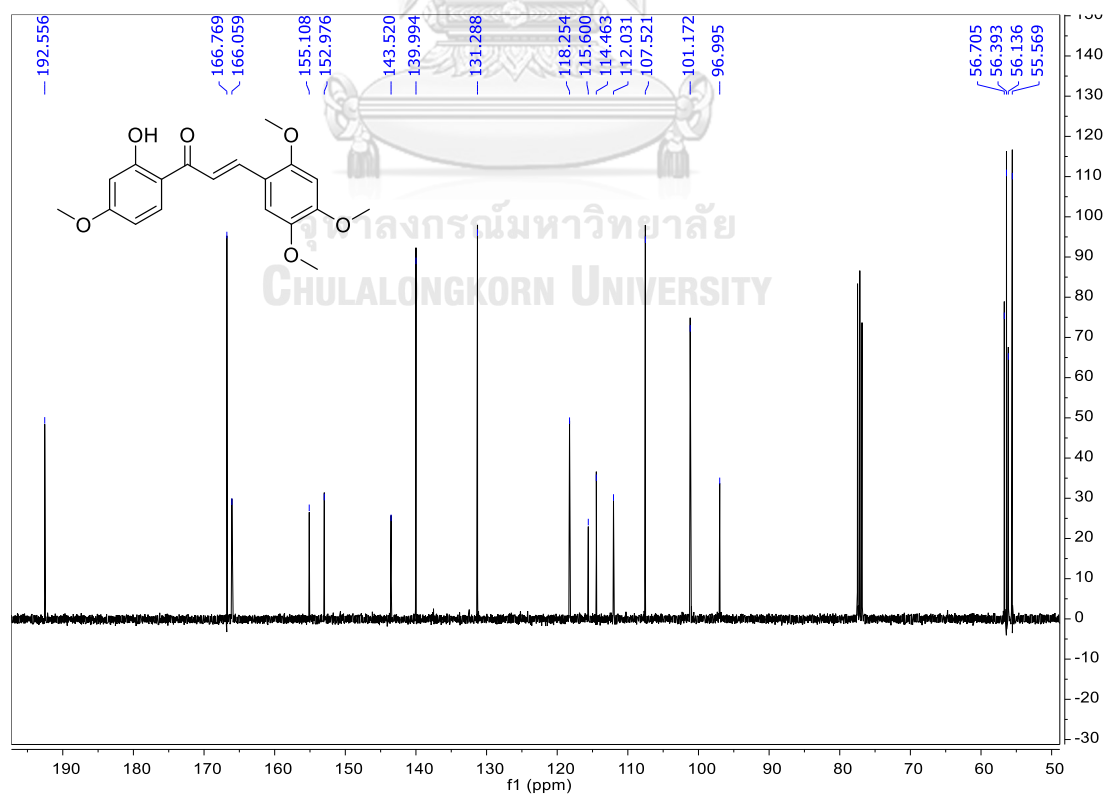


Figure A.120 The ^{13}C NMR spectrum (CDCl₃, 100 MHz) of **111**.

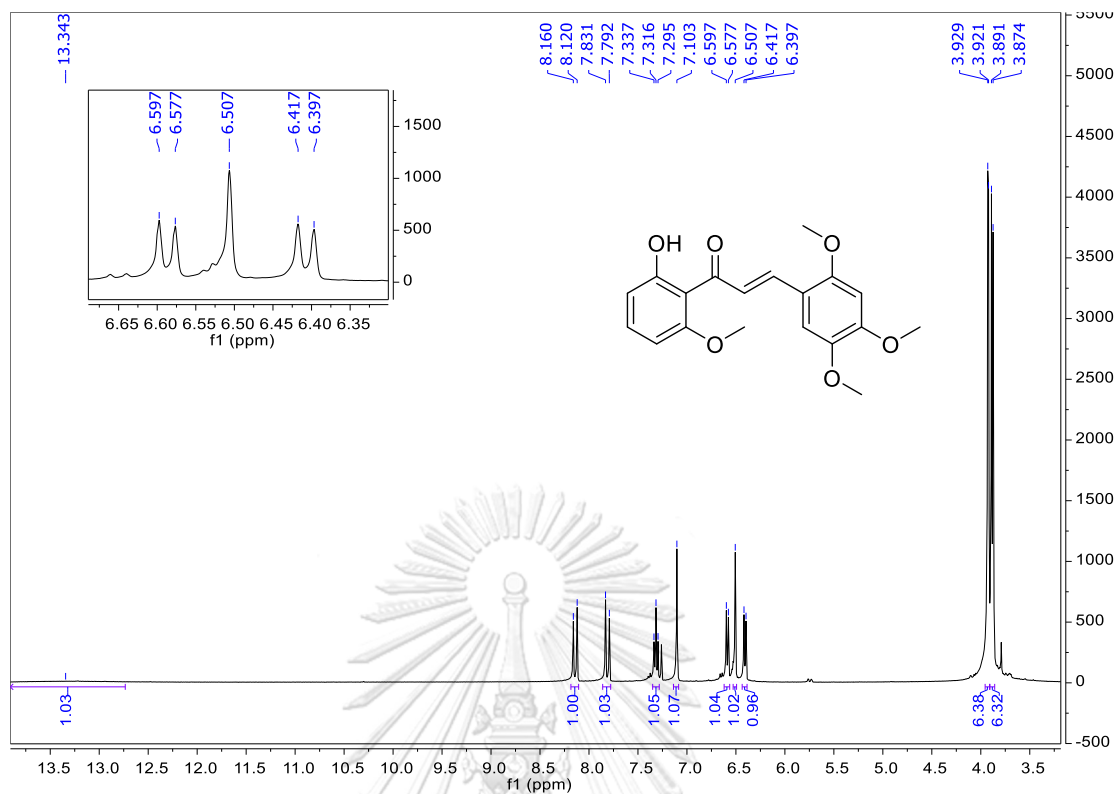


Figure A.121 The ^1H NMR spectrum (CDCl_3 , 400 MHz) of **112**.

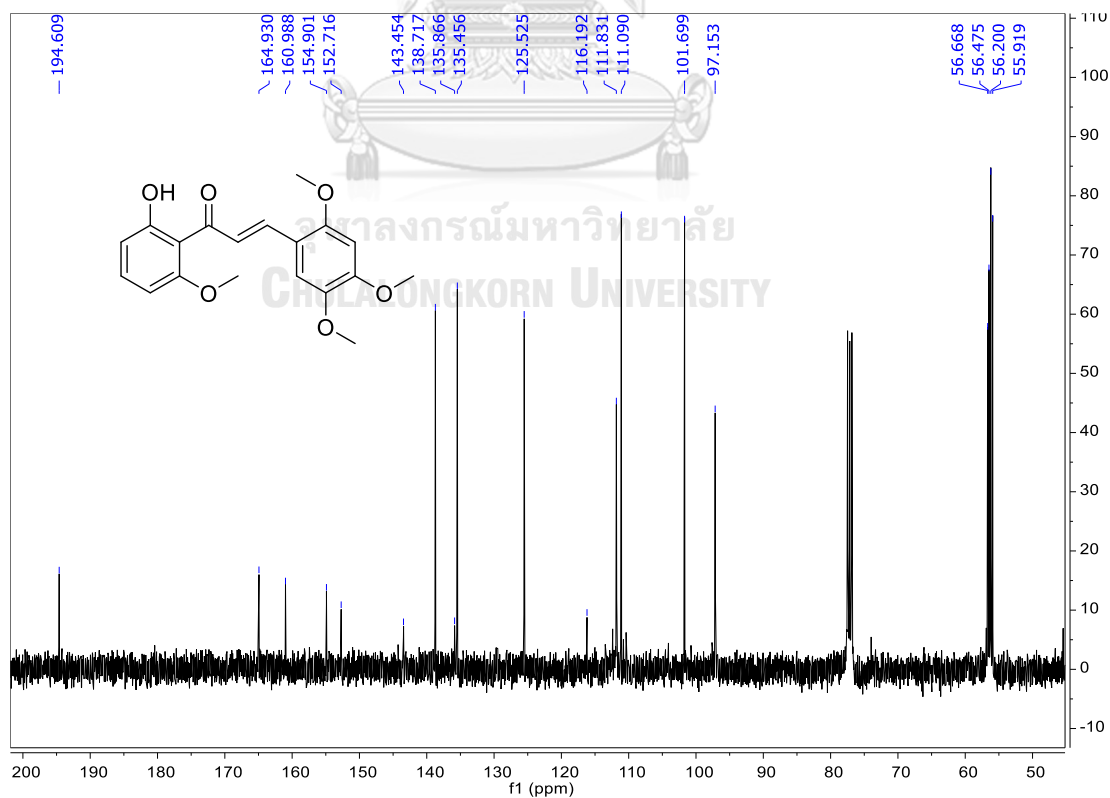


Figure A.122 The ^{13}C NMR spectrum (CDCl_3 , 100 MHz) of **112**.

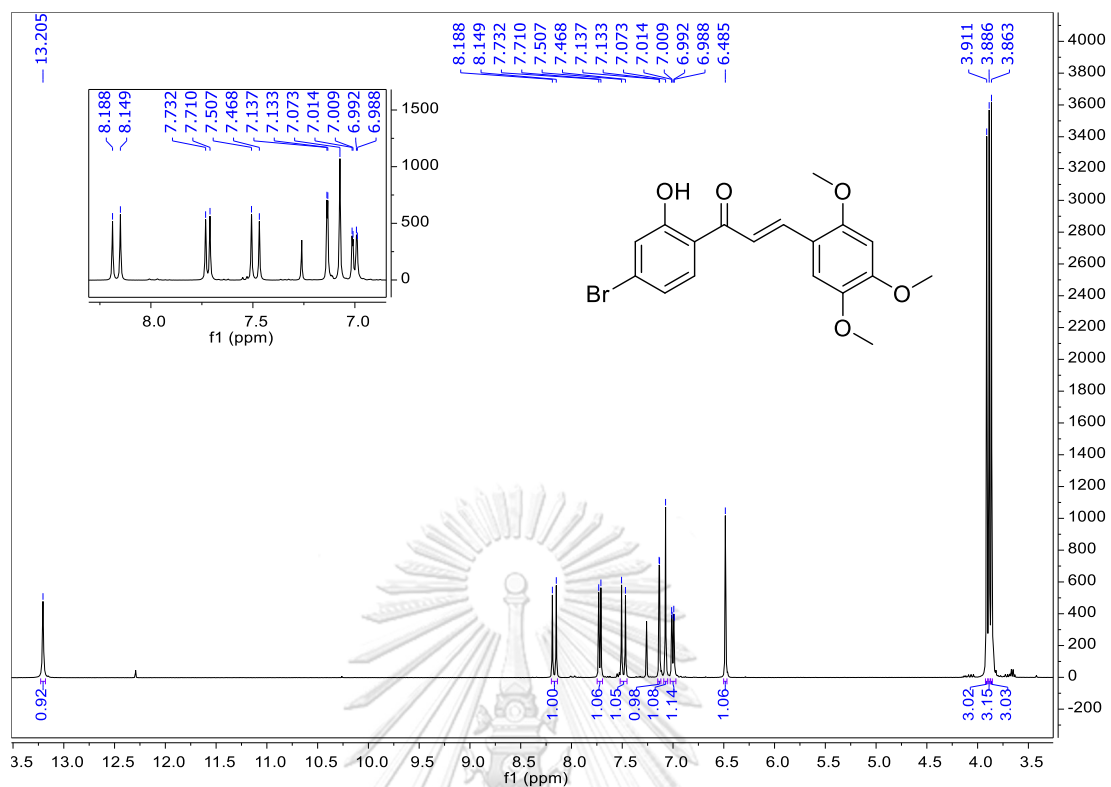


Figure A.123 The ^1H NMR spectrum (CDCl_3 , 400 MHz) of 113.

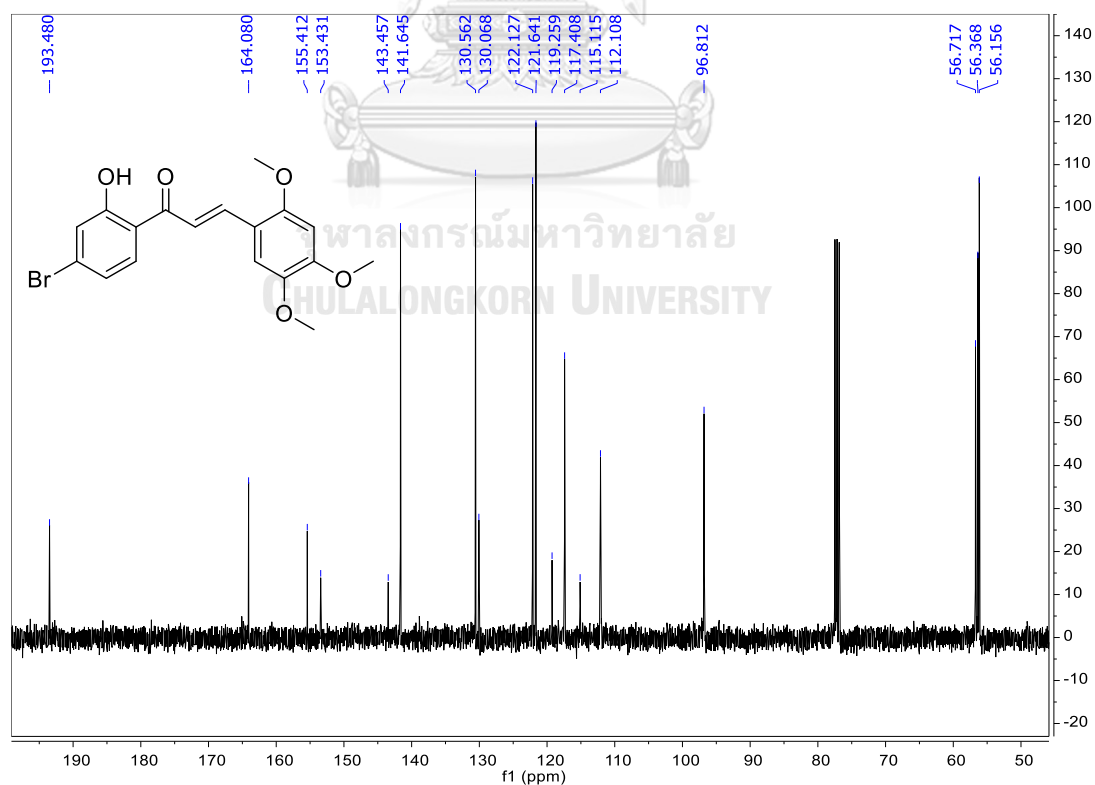


Figure A.124 The ^{13}C NMR spectrum (CDCl_3 , 100 MHz) of 113.

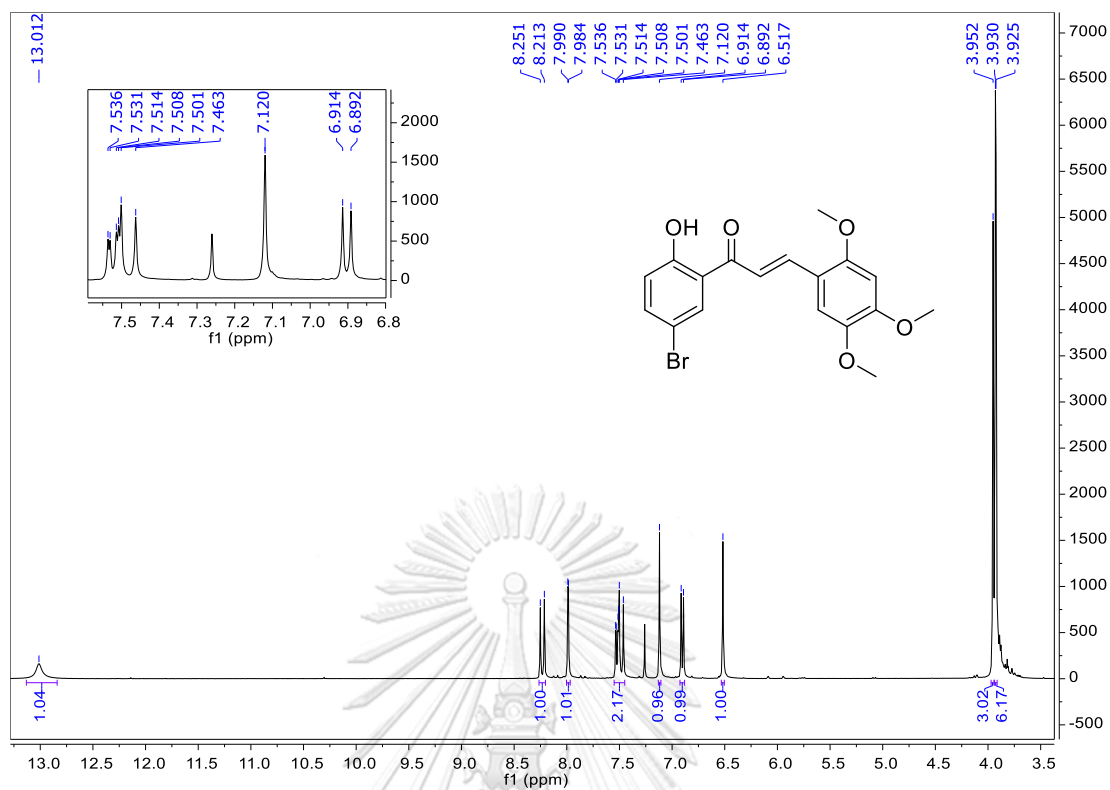


Figure A.125 The ¹H NMR spectrum (CDCl₃, 400 MHz) of **114**.

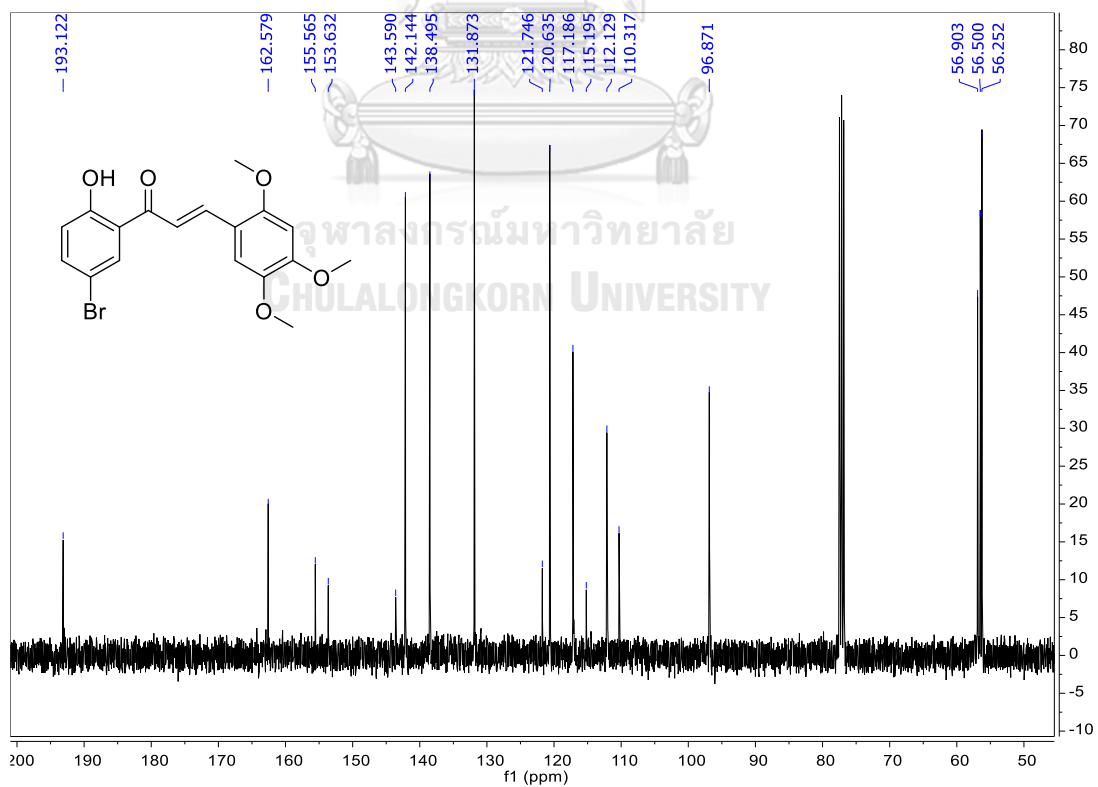


Figure A.126 The ¹³C NMR spectrum (CDCl₃, 100 MHz) of **114**.

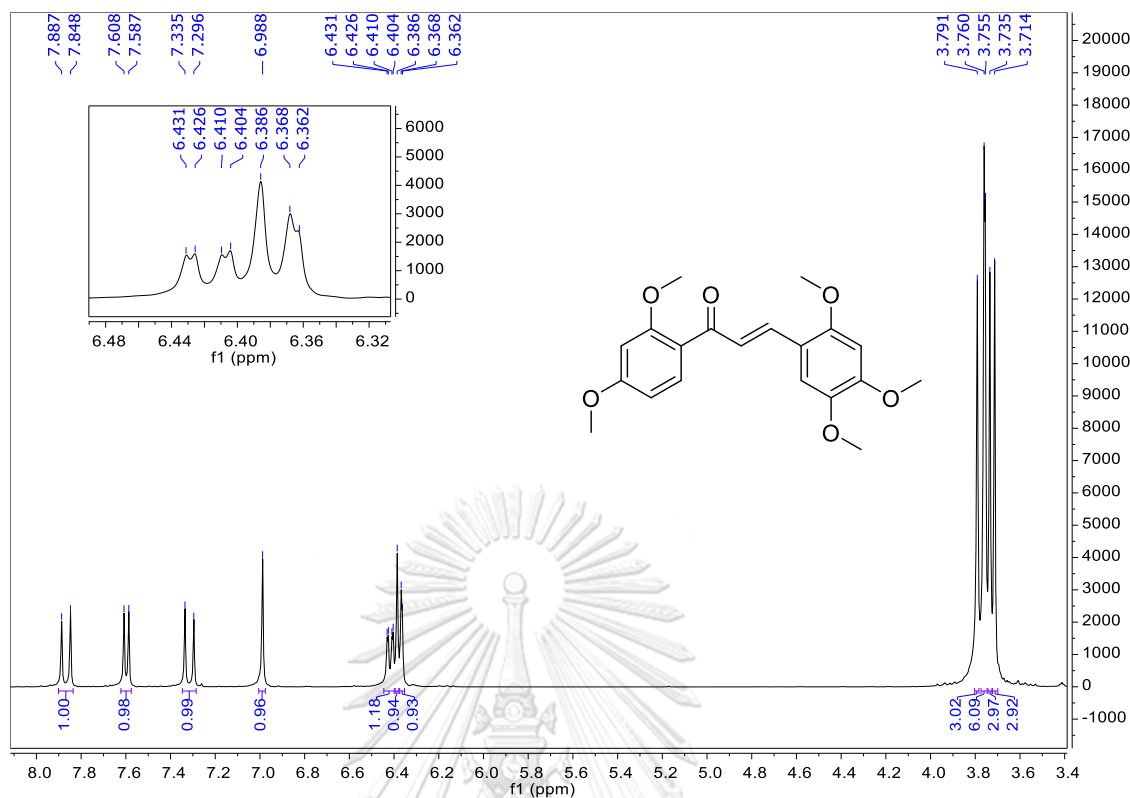


Figure A.127 The ^1H NMR spectrum (CDCl_3 , 400 MHz) of **115**.

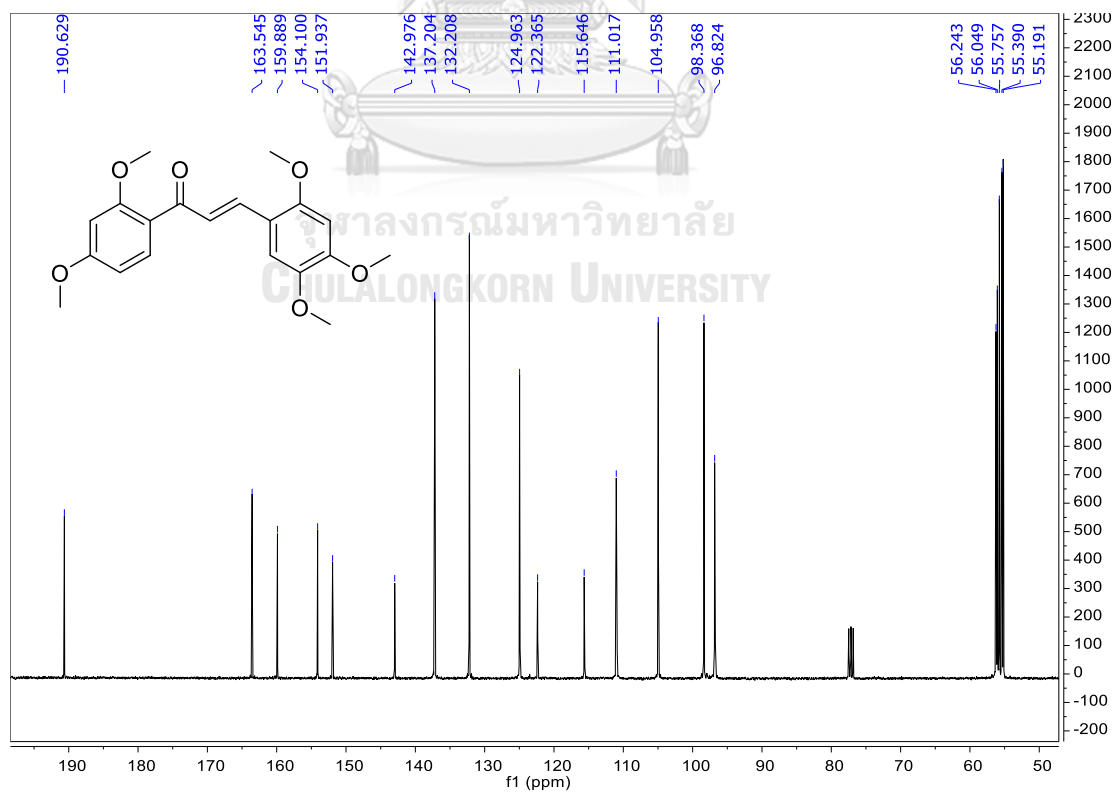


Figure A.128 The ^{13}C NMR spectrum (CDCl_3 , 100 MHz) of **115**.

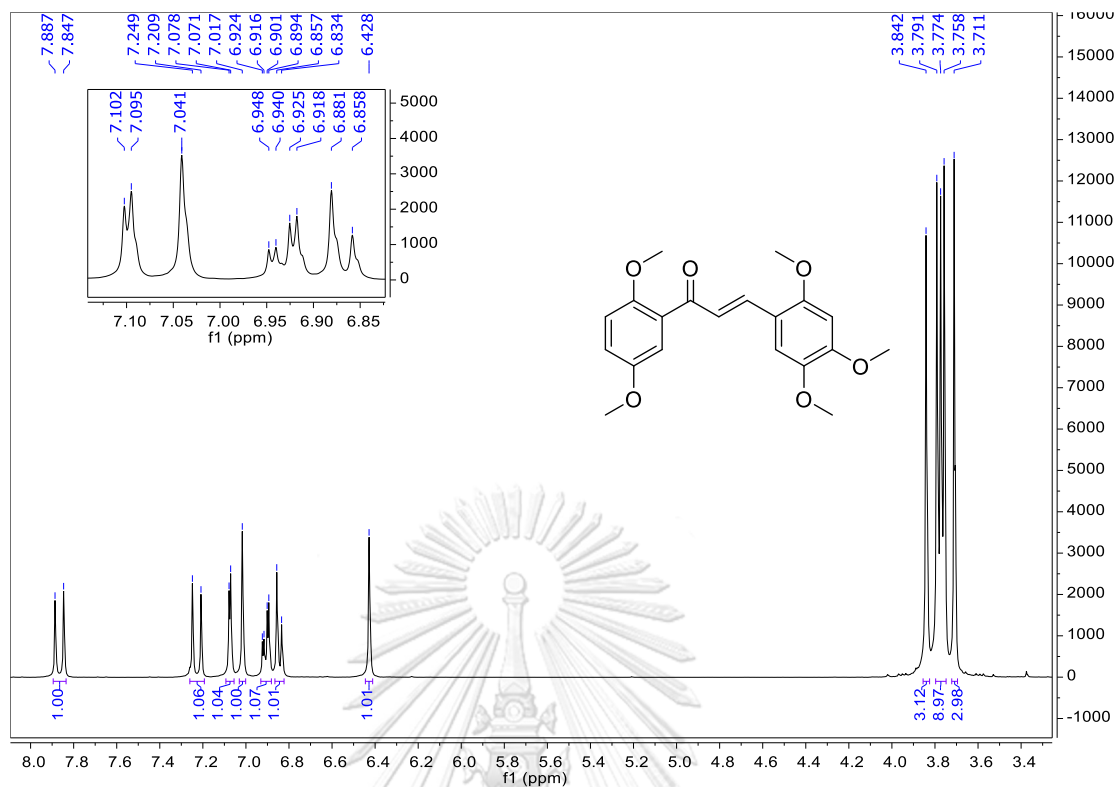


Figure A.129 The ^1H NMR spectrum (CDCl_3 , 400 MHz) of 116.

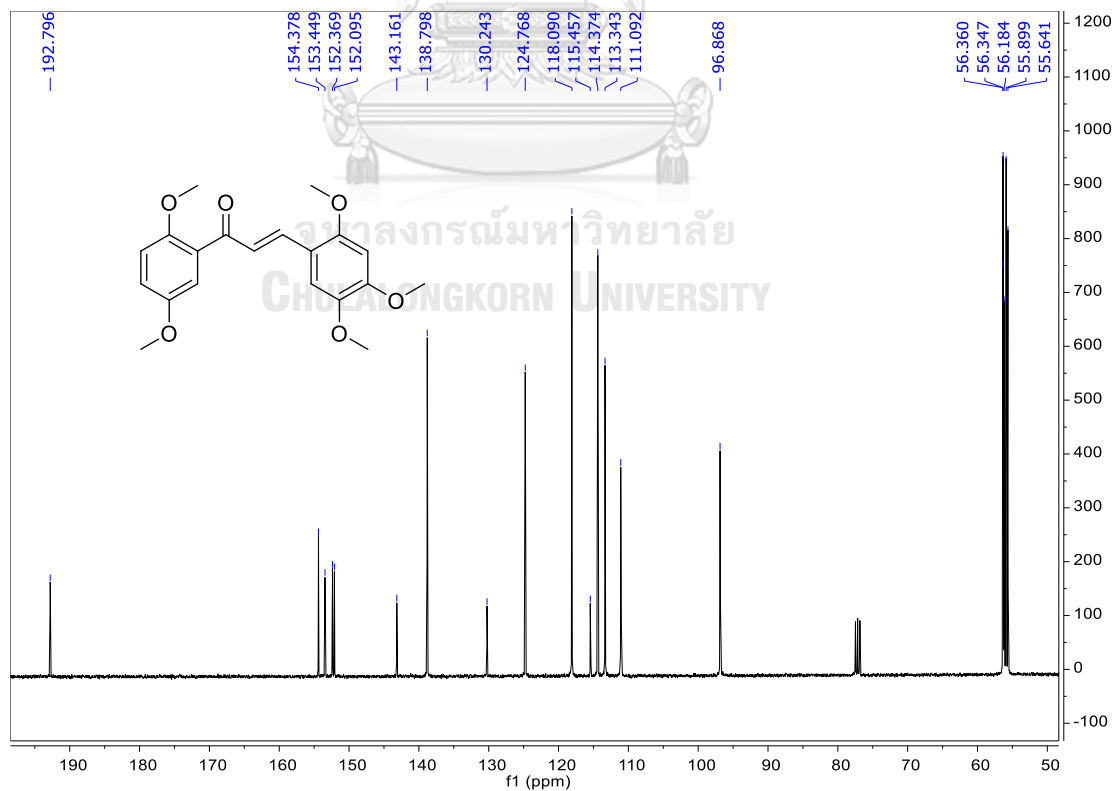


Figure A.130 The ^{13}C NMR spectrum (CDCl_3 , 100 MHz) of 116.

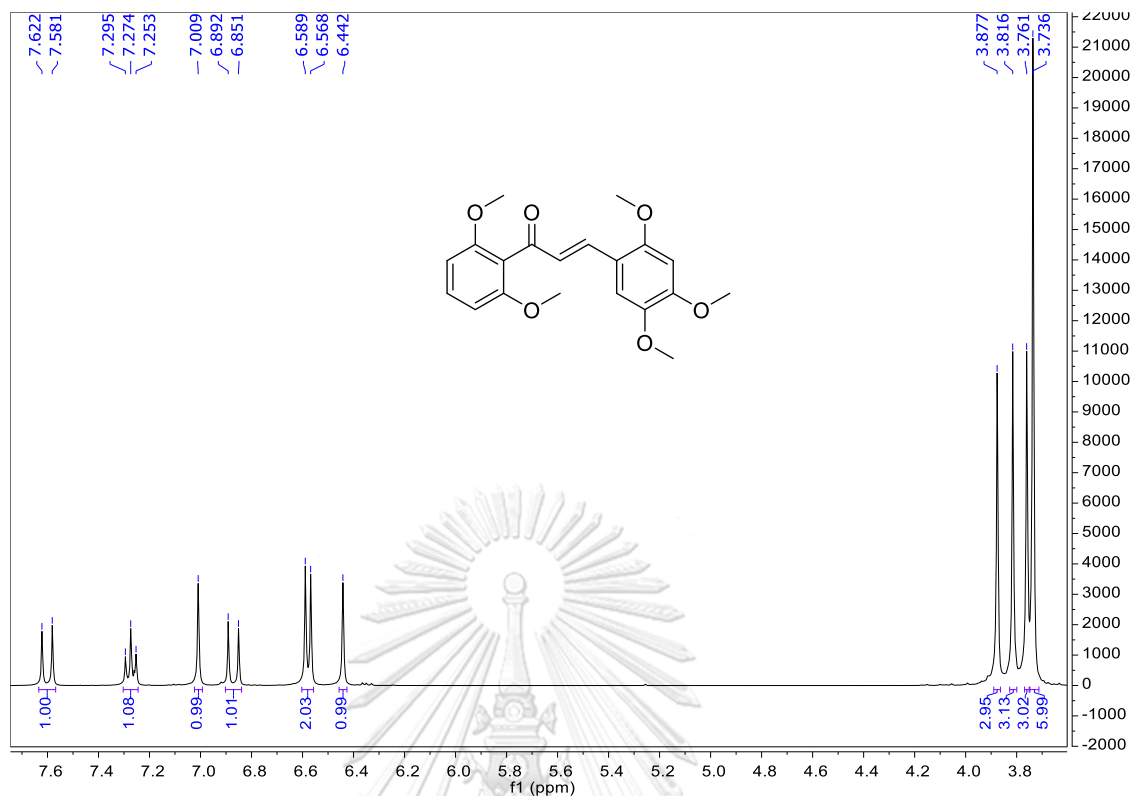


Figure A.131 The ^1H NMR spectrum (CDCl_3 , 400 MHz) of **117**.

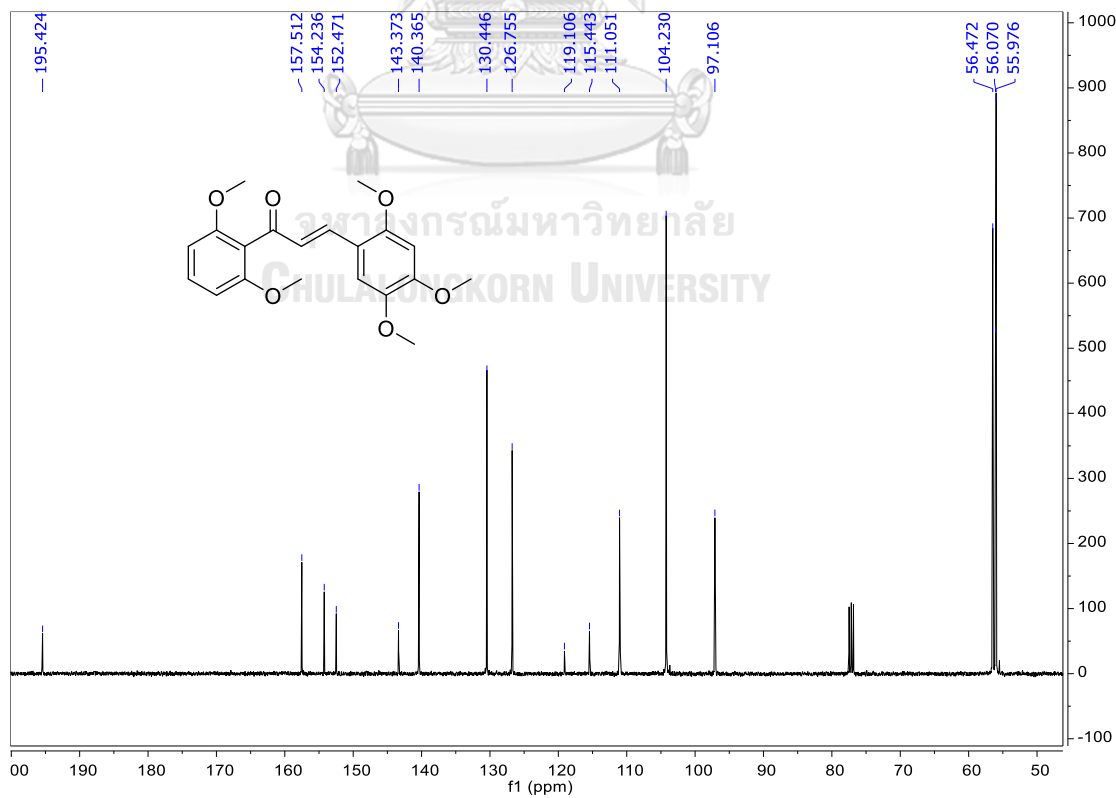


Figure A.132 The ^{13}C NMR spectrum (CDCl_3 , 100 MHz) of **117**.

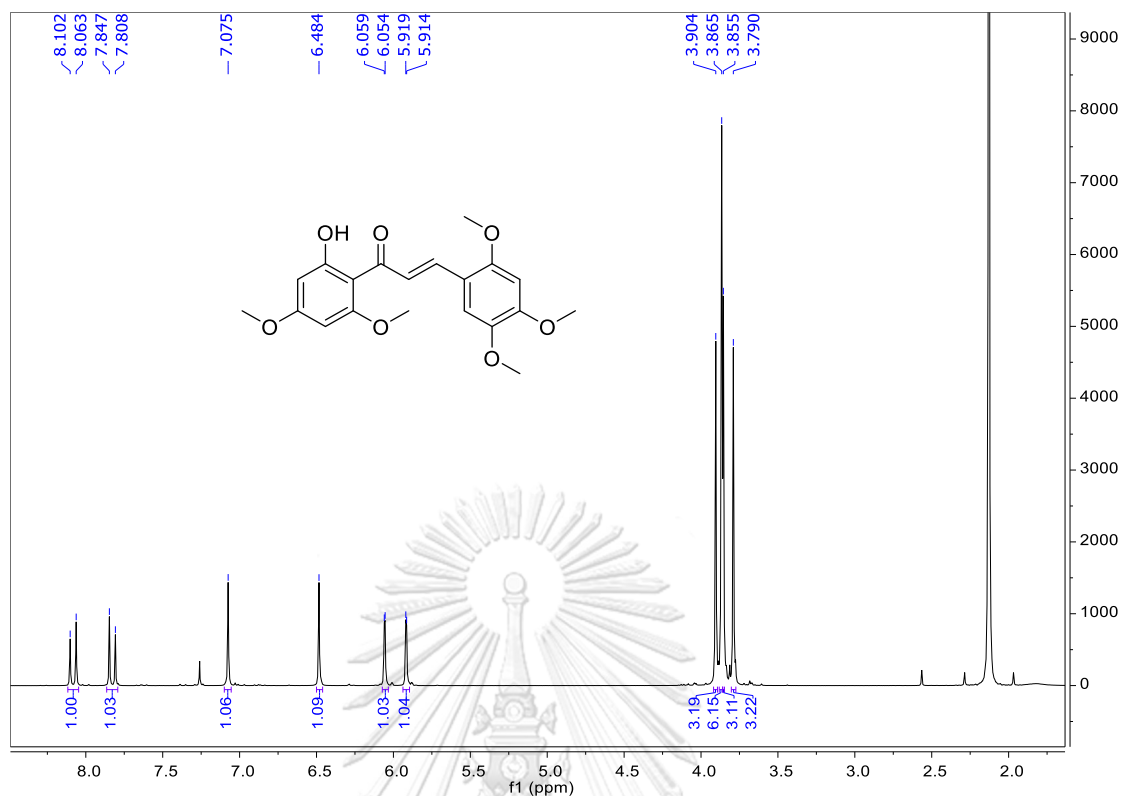


Figure A.133 The ^1H NMR spectrum (CDCl_3 , 400 MHz) of **118**.

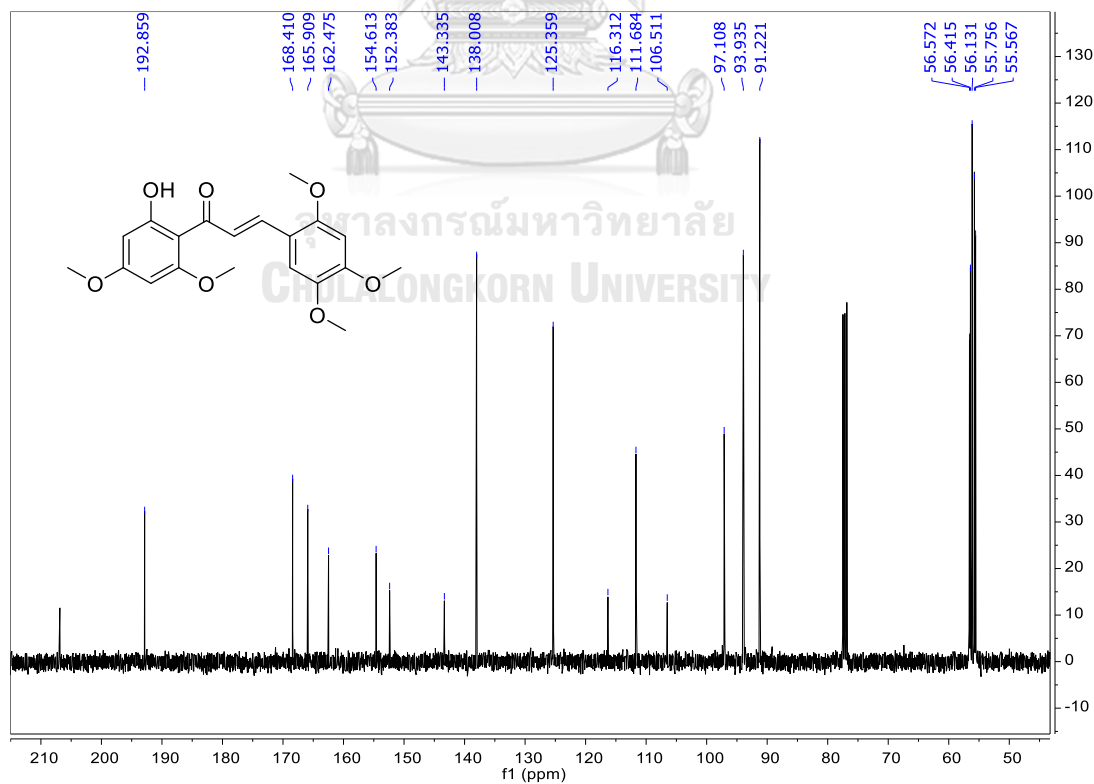


Figure A.134 The ^{13}C NMR spectrum (CDCl_3 , 100 MHz) of **118**.

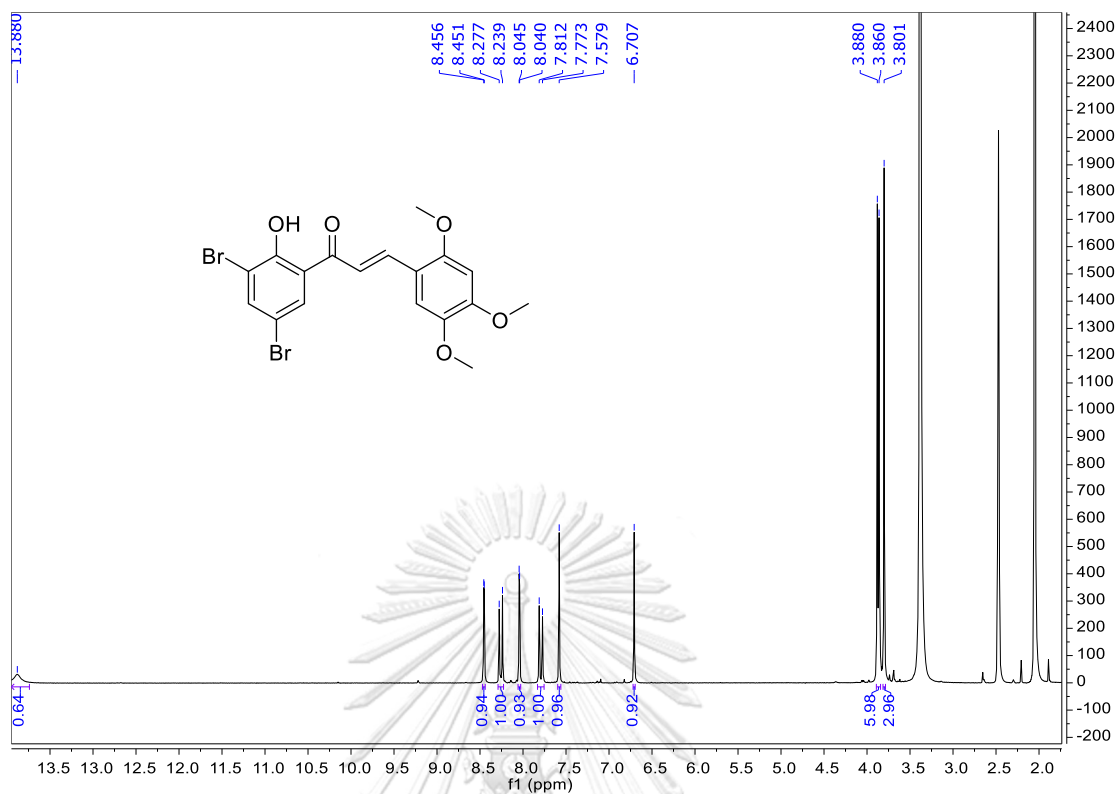


Figure A.135 The ^1H NMR spectrum (acetone- d_6 , 400 MHz) of **119**.

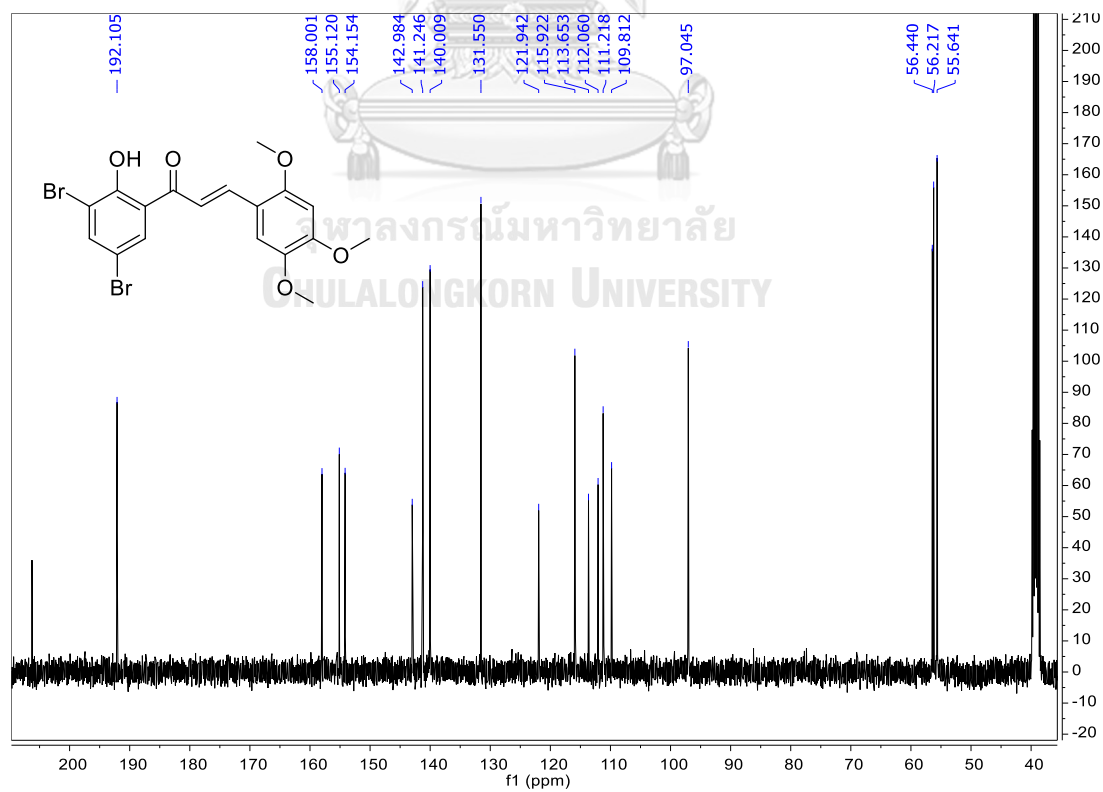


Figure A.136 The ^{13}C NMR spectrum (acetone- d_6 , 100 MHz) of **119**.

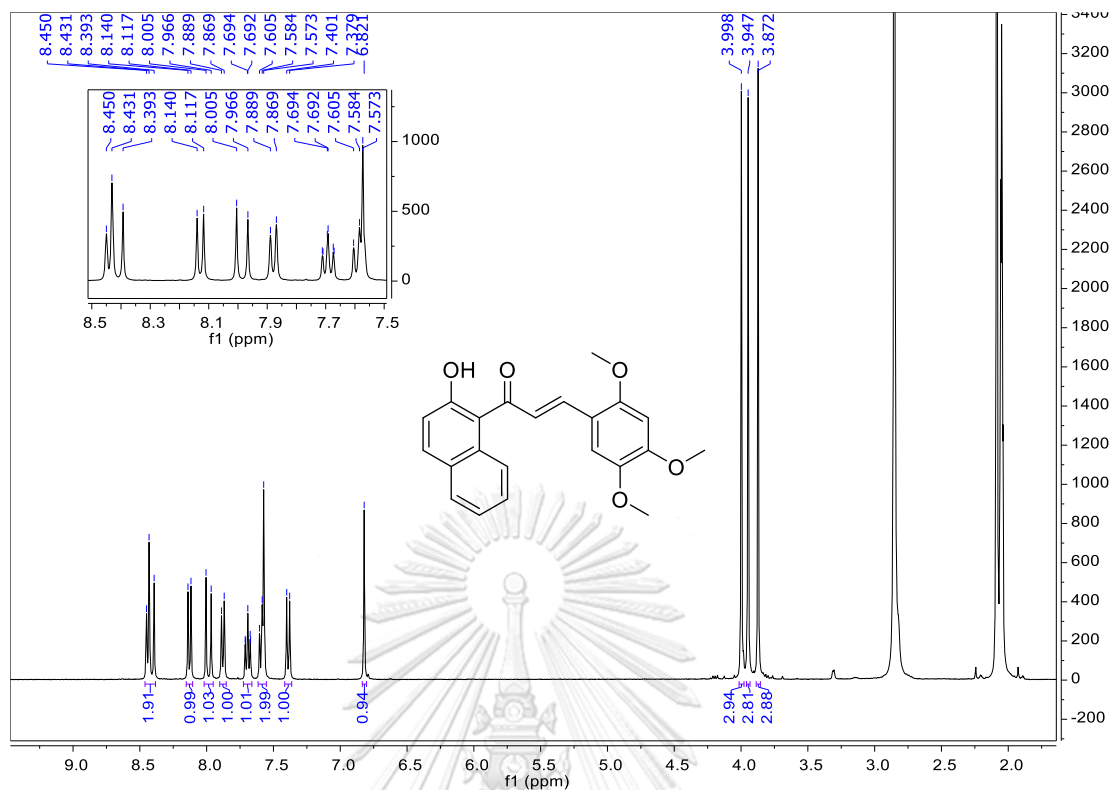


Figure A.137 The ^1H NMR spectrum (acetone- d_6 , 400 MHz) of 120.

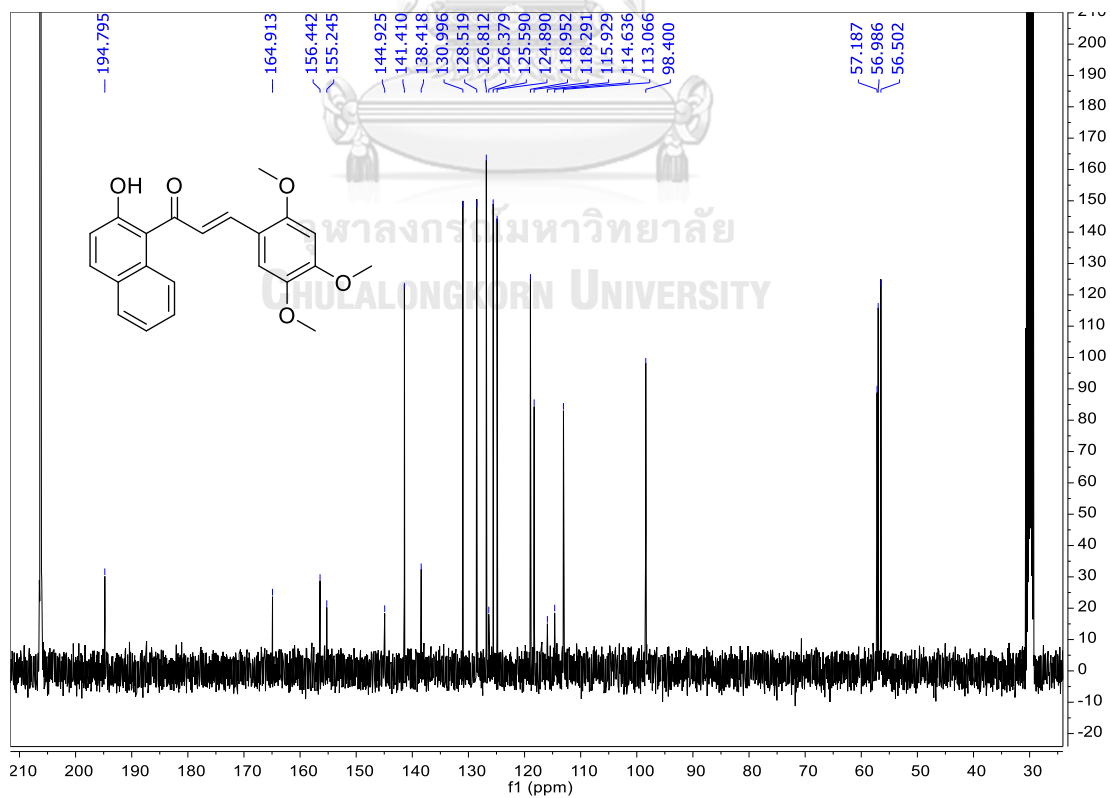


Figure A.138 The ^{13}C NMR spectrum (acetone- d_6 , 100 MHz) of 120.

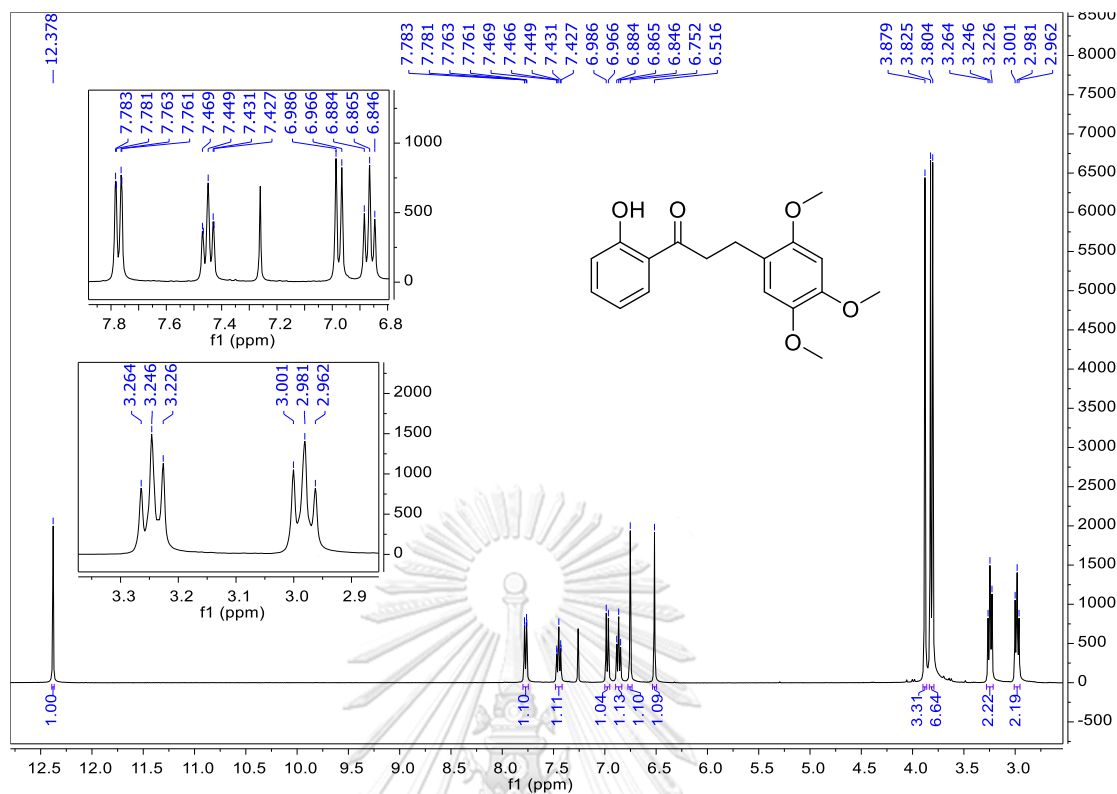


Figure A.139 The ^1H NMR spectrum (CDCl_3 , 400 MHz) of **121**.

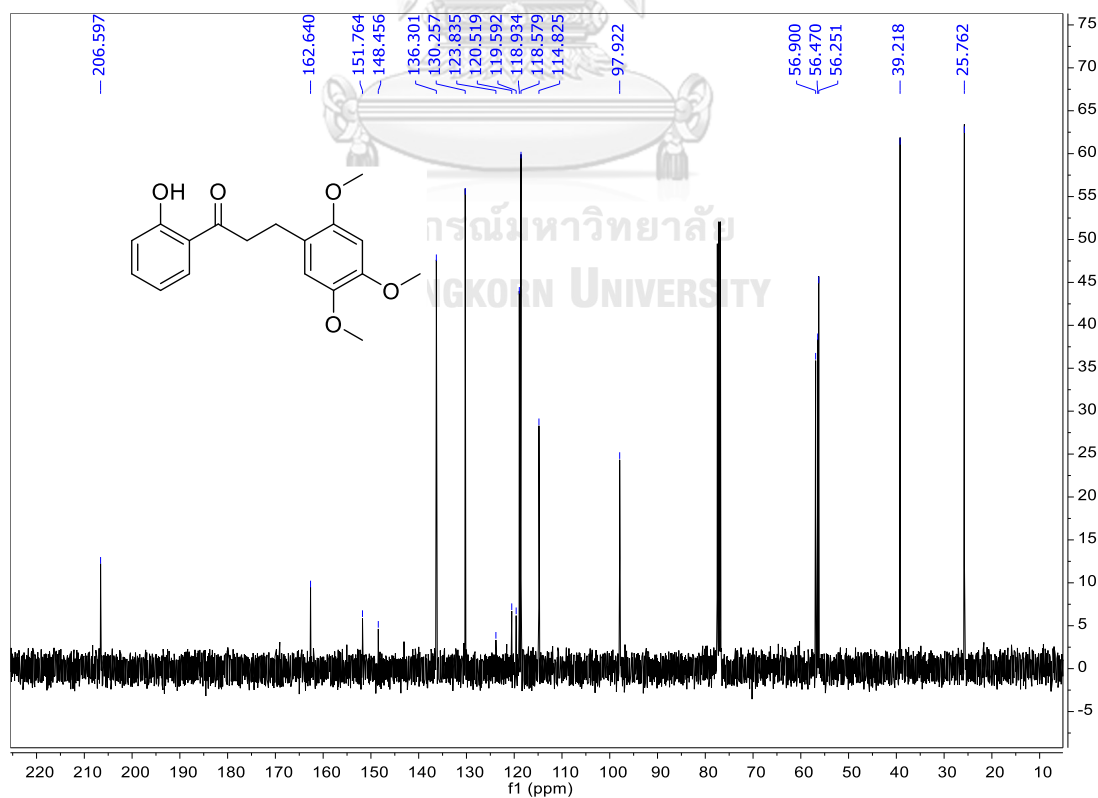


Figure A.140 The ^{13}C NMR spectrum (CDCl_3 , 100 MHz) of **121**.

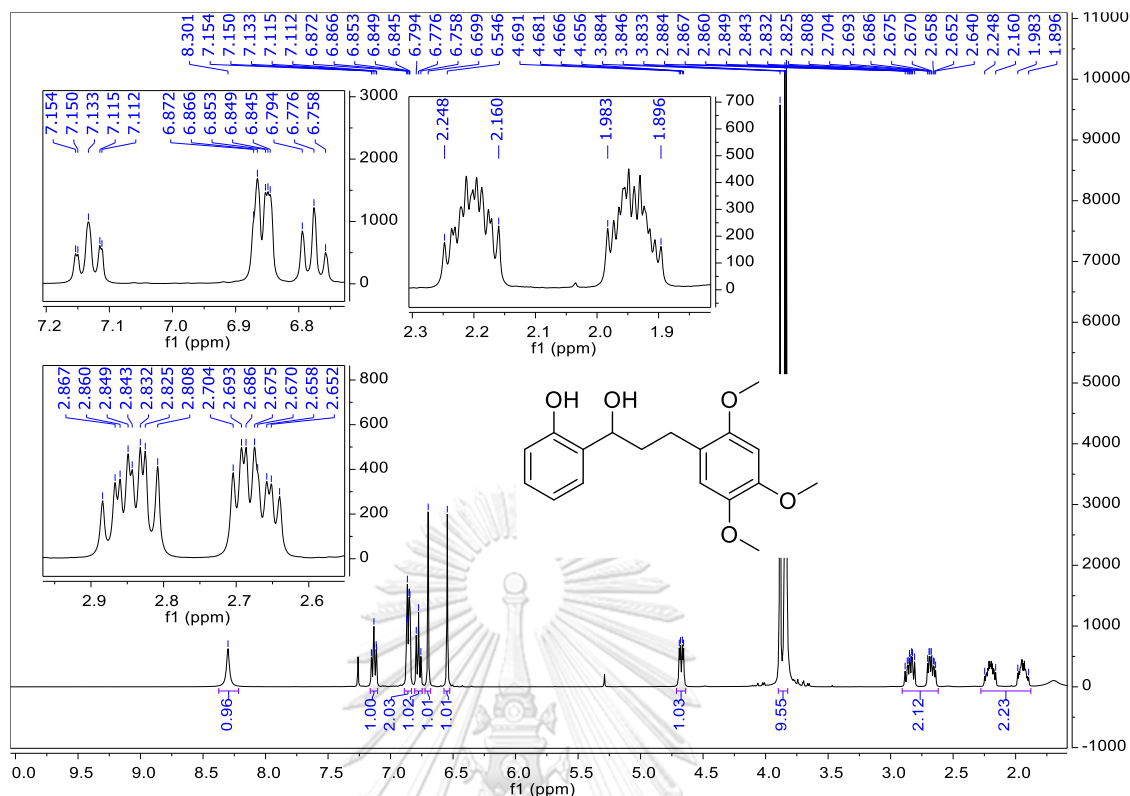


Figure A.141 The ^1H NMR spectrum (CDCl₃, 400 MHz) of 122.

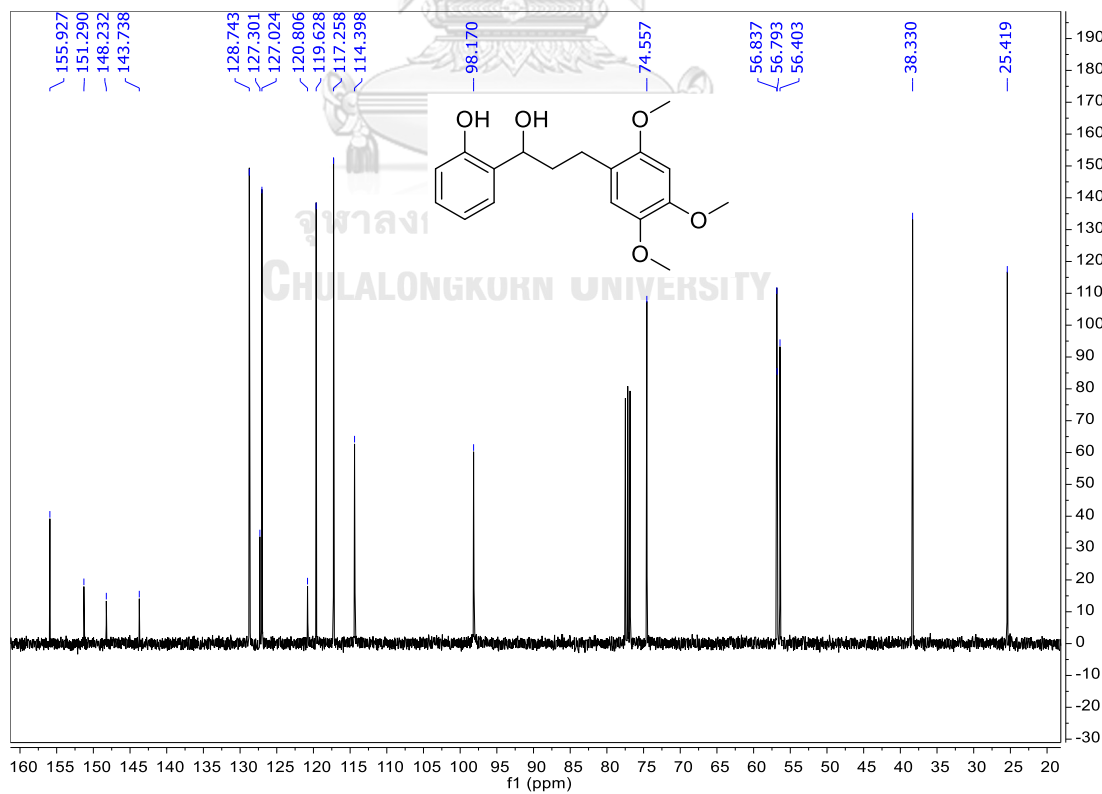


Figure A.142 The ^{13}C NMR spectrum (CDCl₃, 100 MHz) of 122.

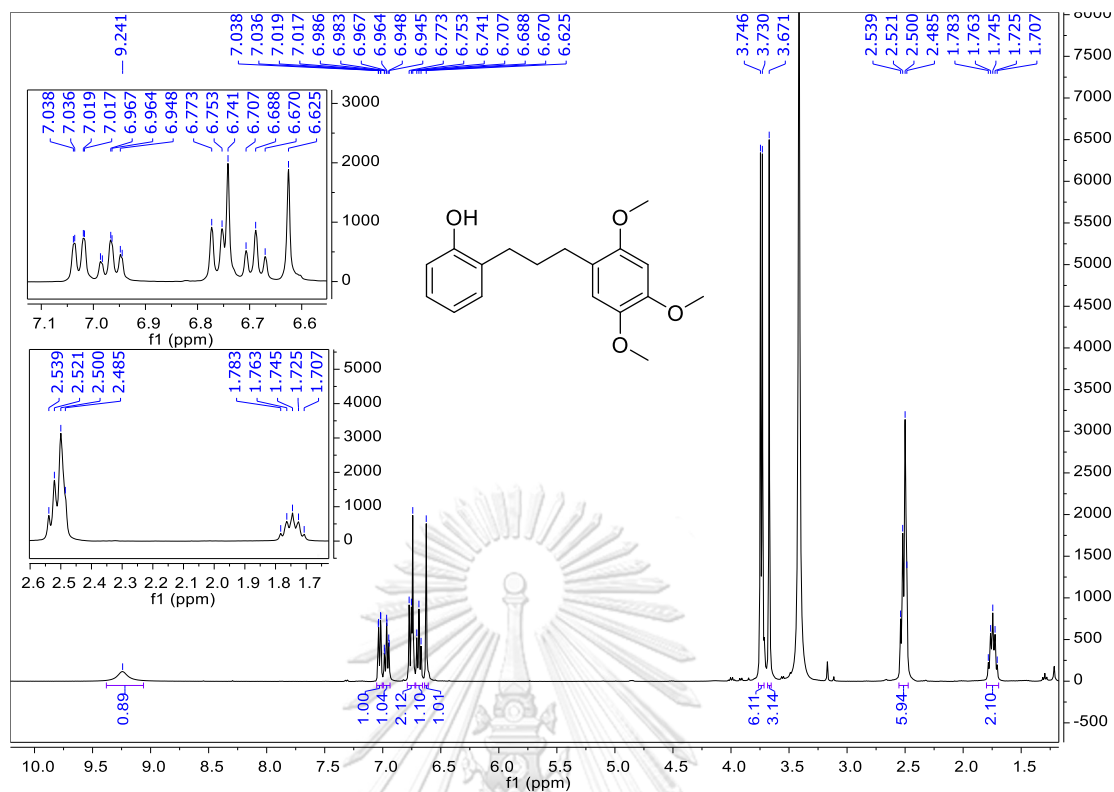


Figure A.143 The ^1H NMR spectrum (DMSO- d_6 , 400 MHz) of 123.

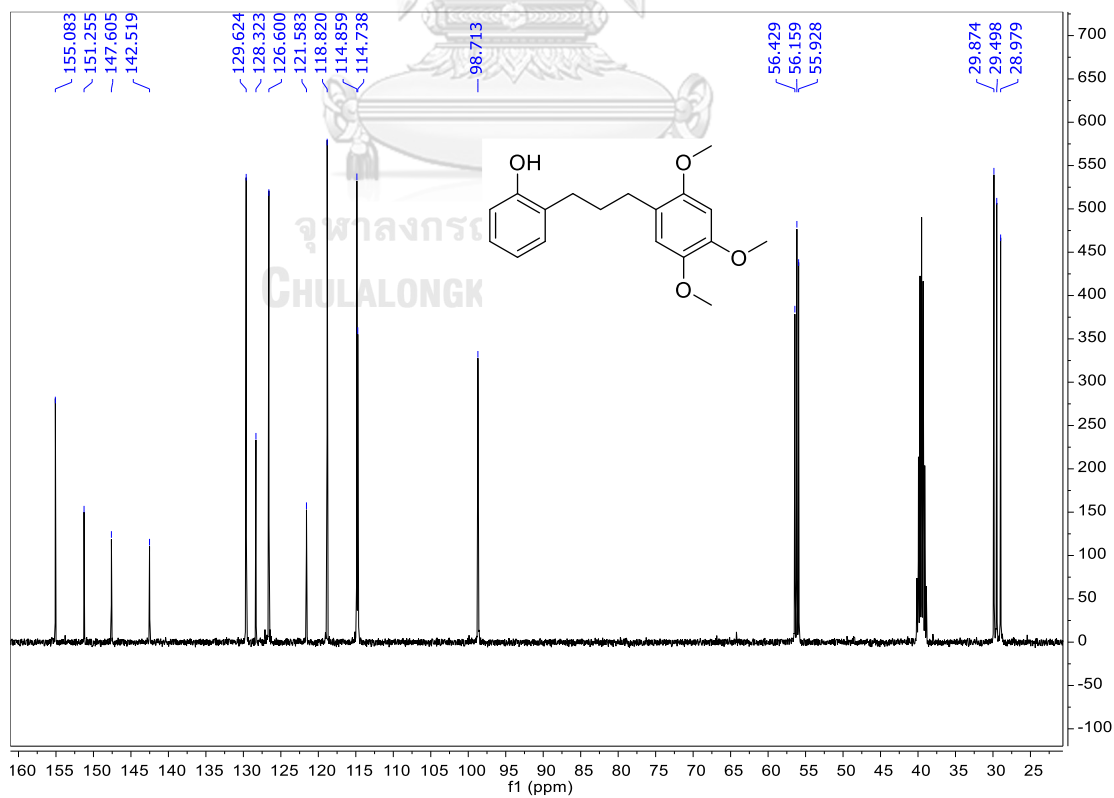


Figure A.144 The ^{13}C NMR spectrum (DMSO- d_6 , 100 MHz) of 123.

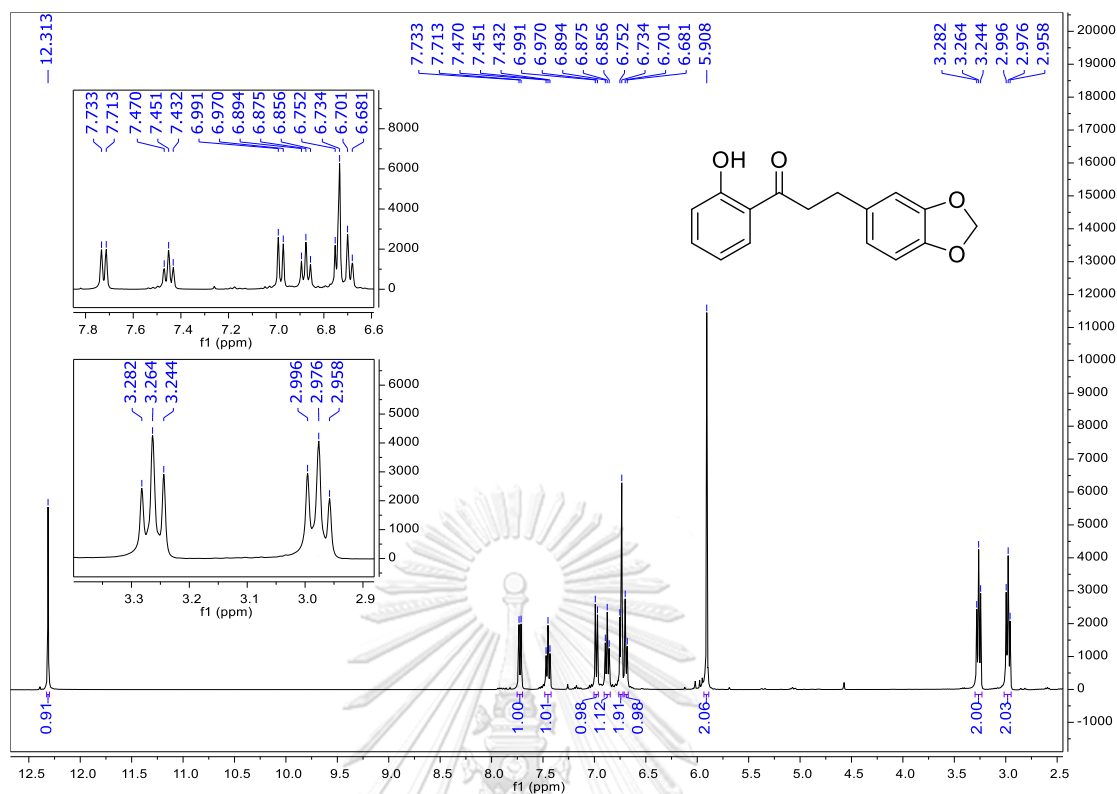


Figure A.145 The ^1H NMR spectrum (DMSO- d_6 , 400 MHz) of 124.

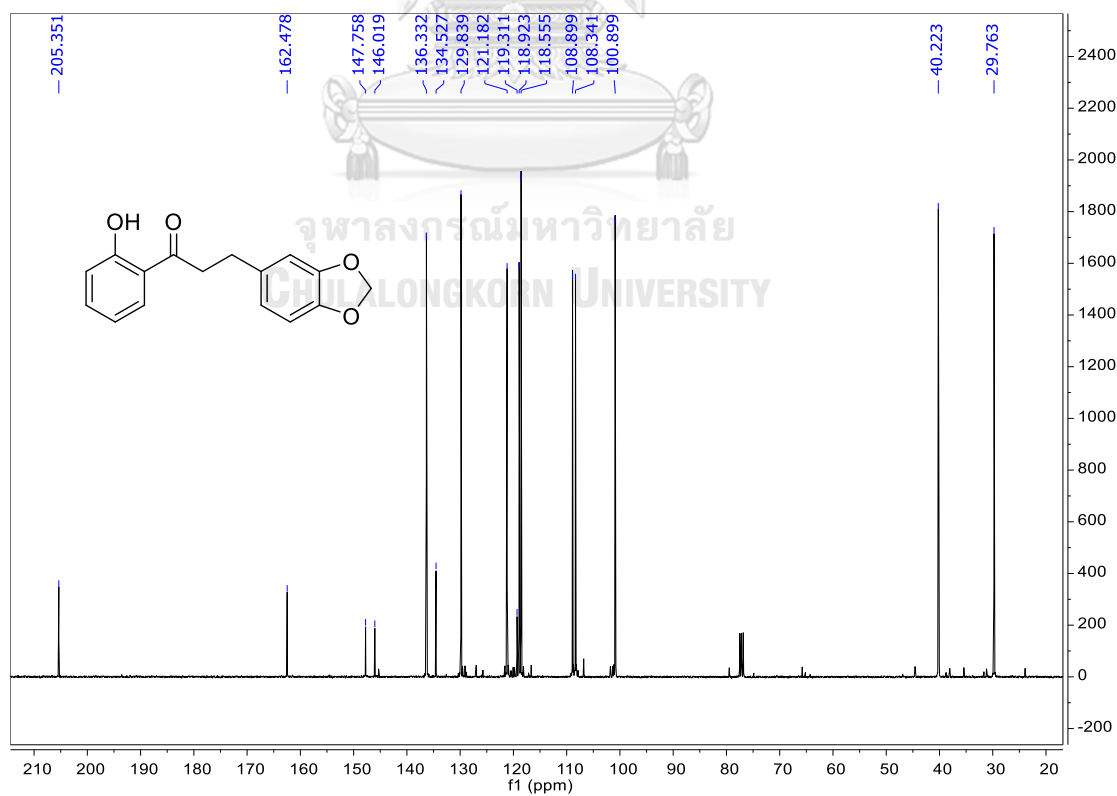


Figure A.146 The ^{13}C NMR spectrum (DMSO- d_6 , 100 MHz) of 124.

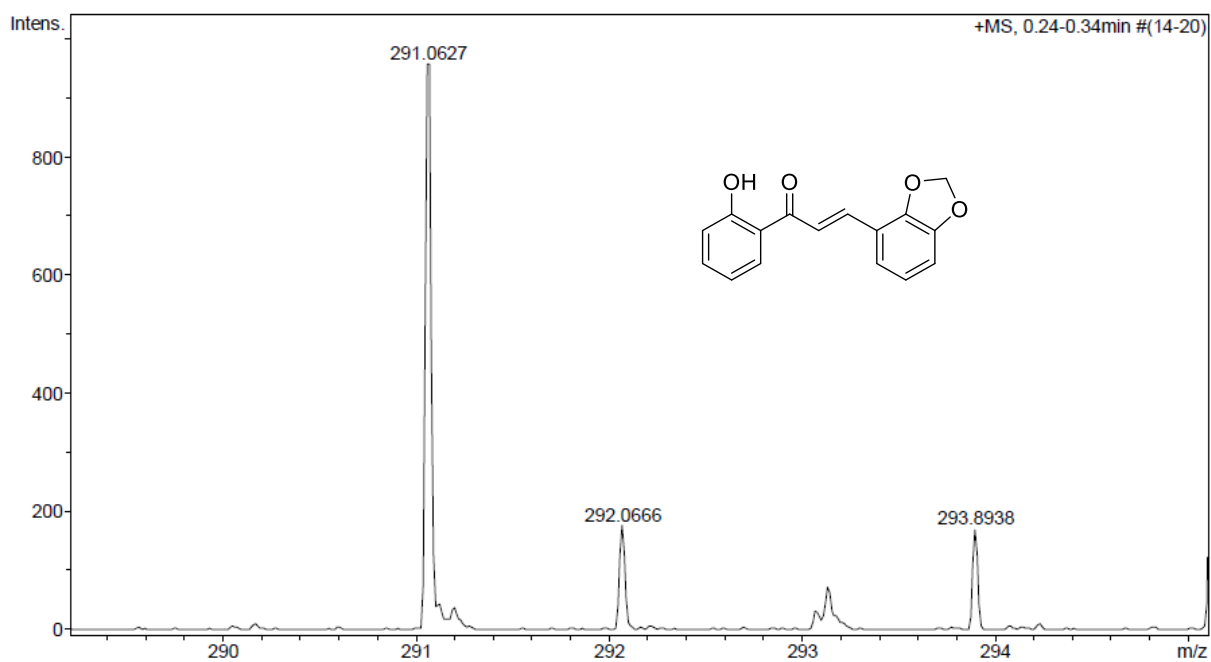


Figure A.147 The HR-ESI-MS of 59.

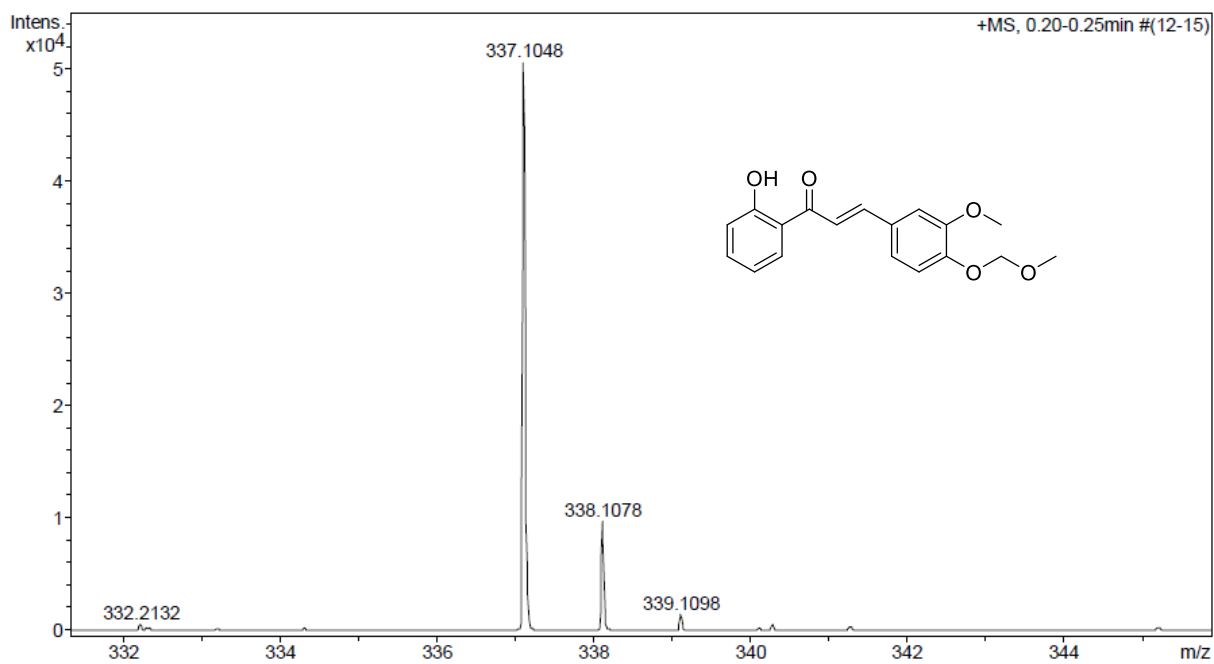


Figure A.148 The HR-ESI-MS of 74.

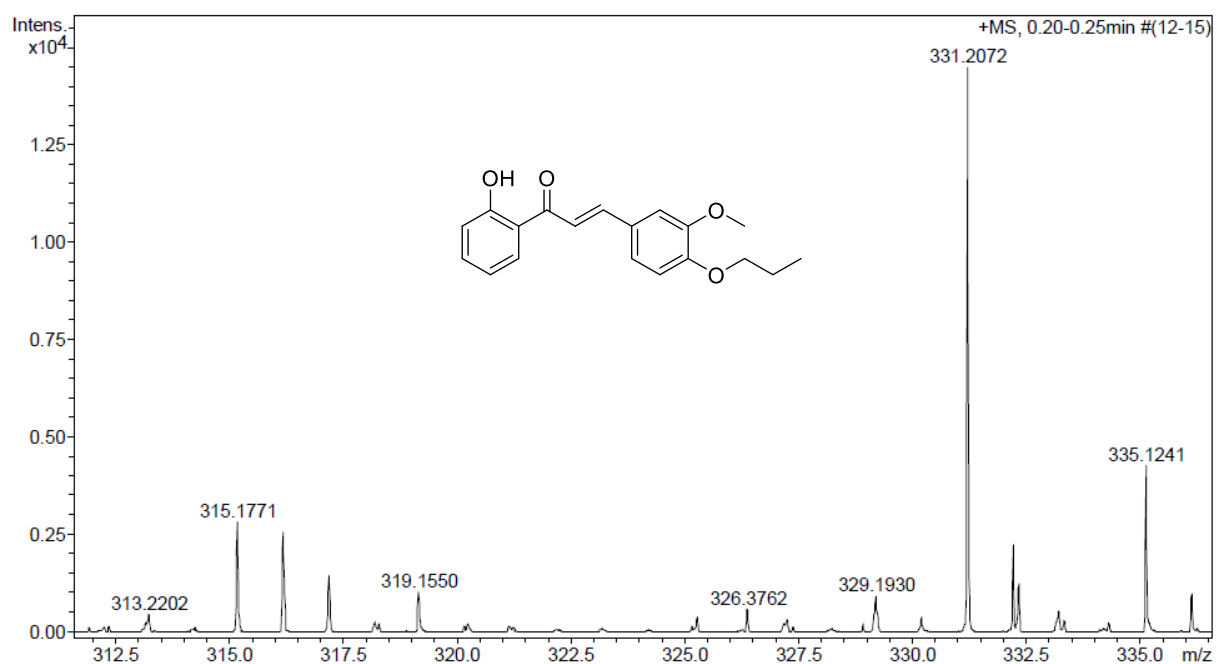


Figure A.149 The HR-ESI-MS of 89.

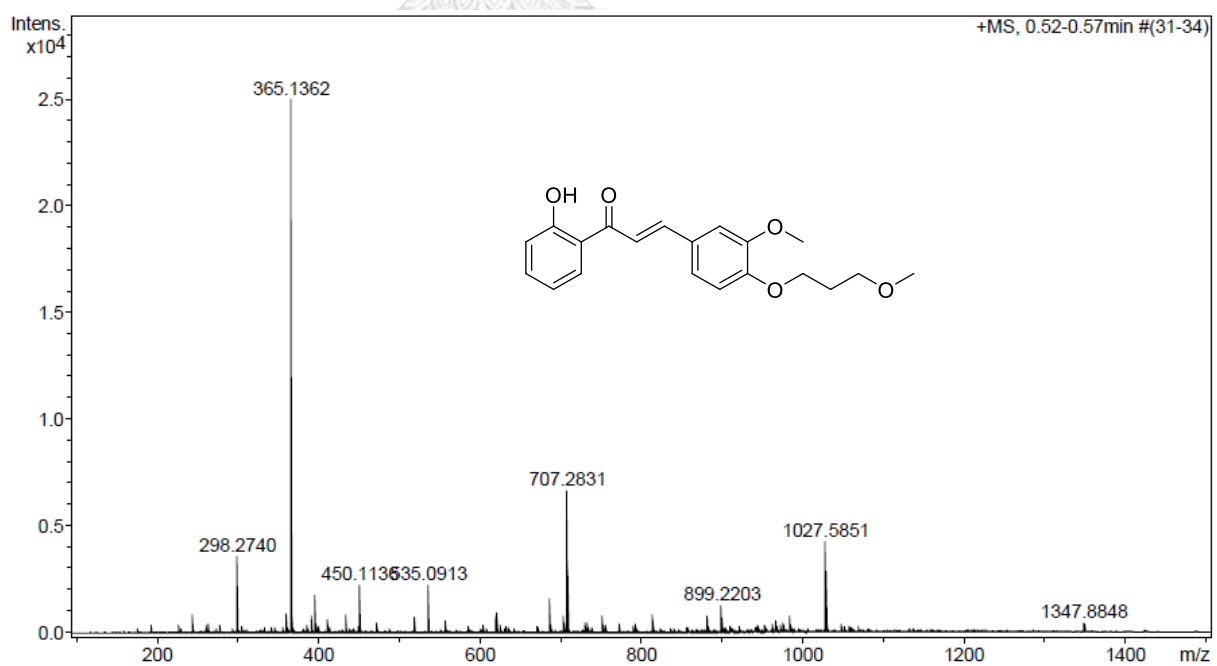
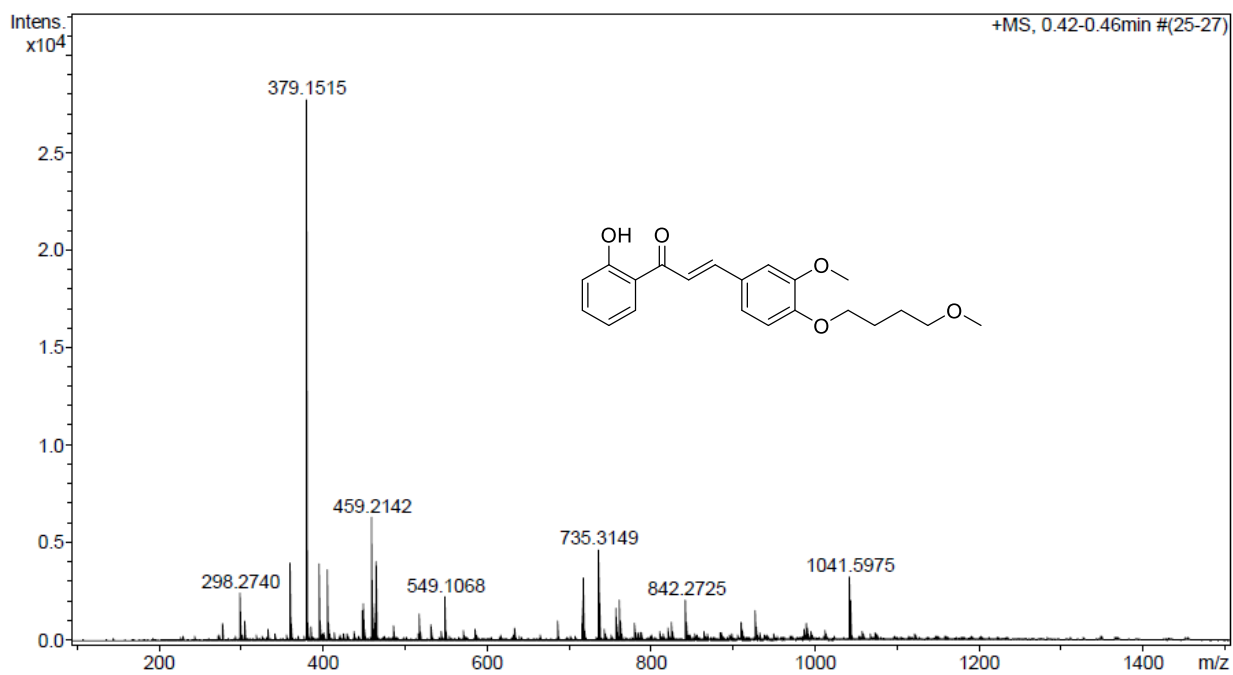
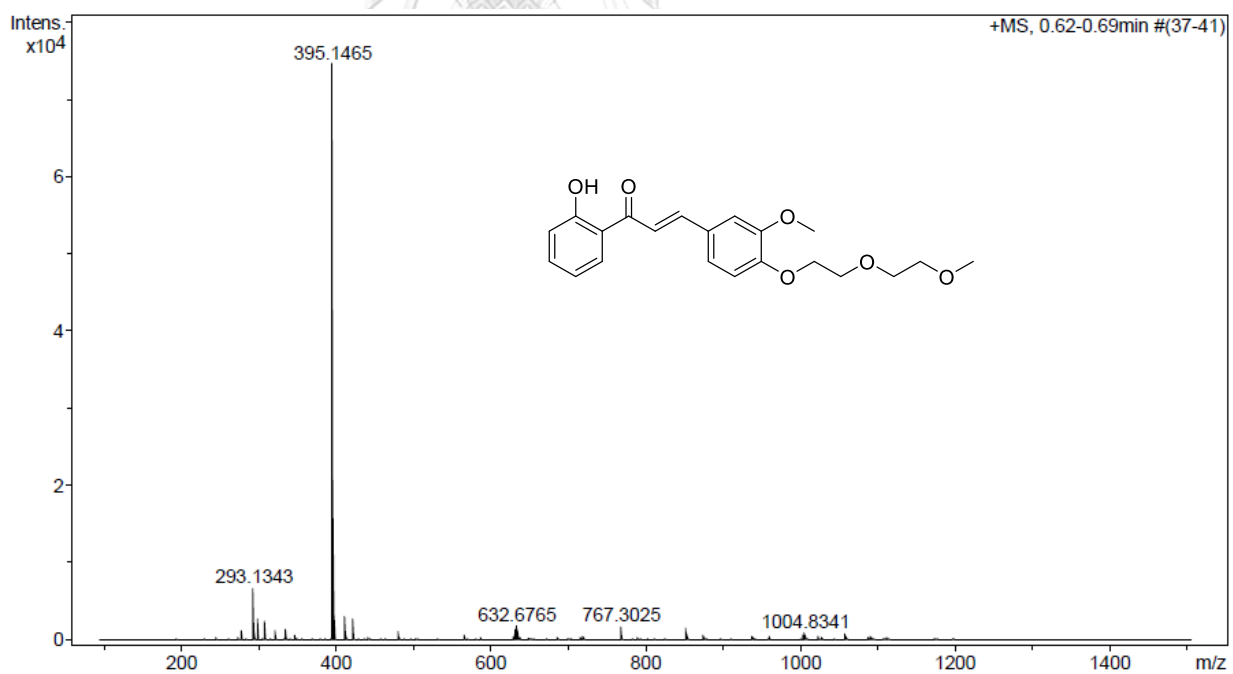
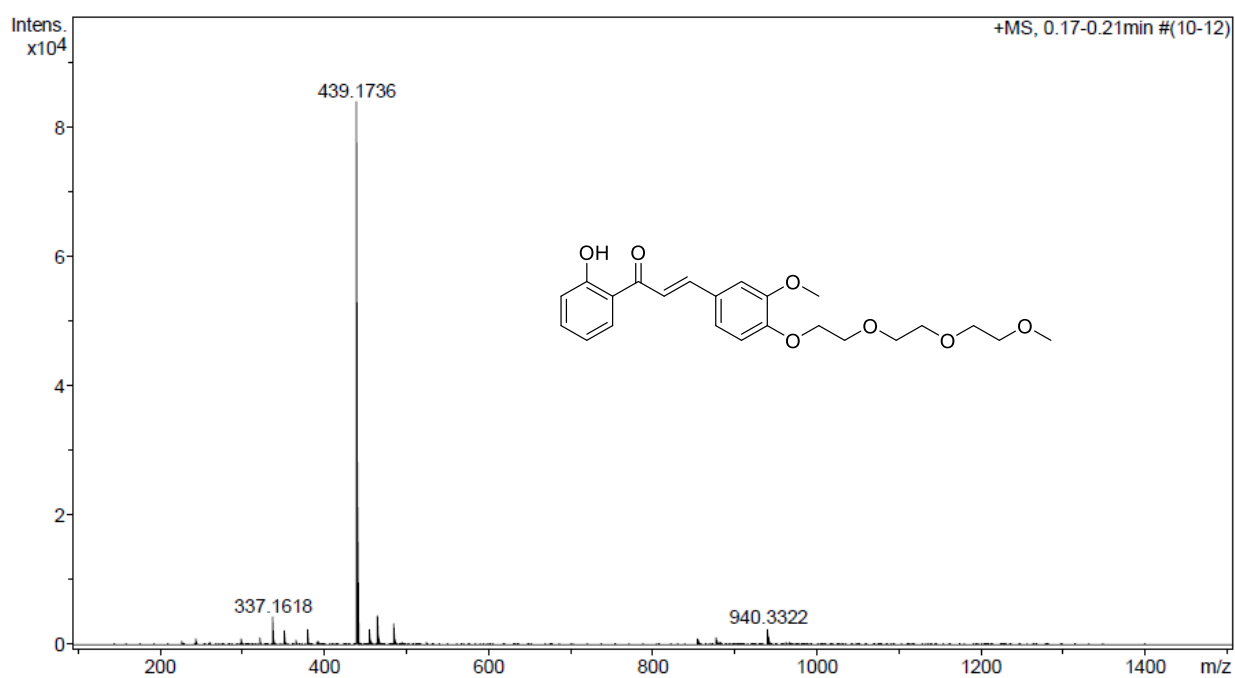
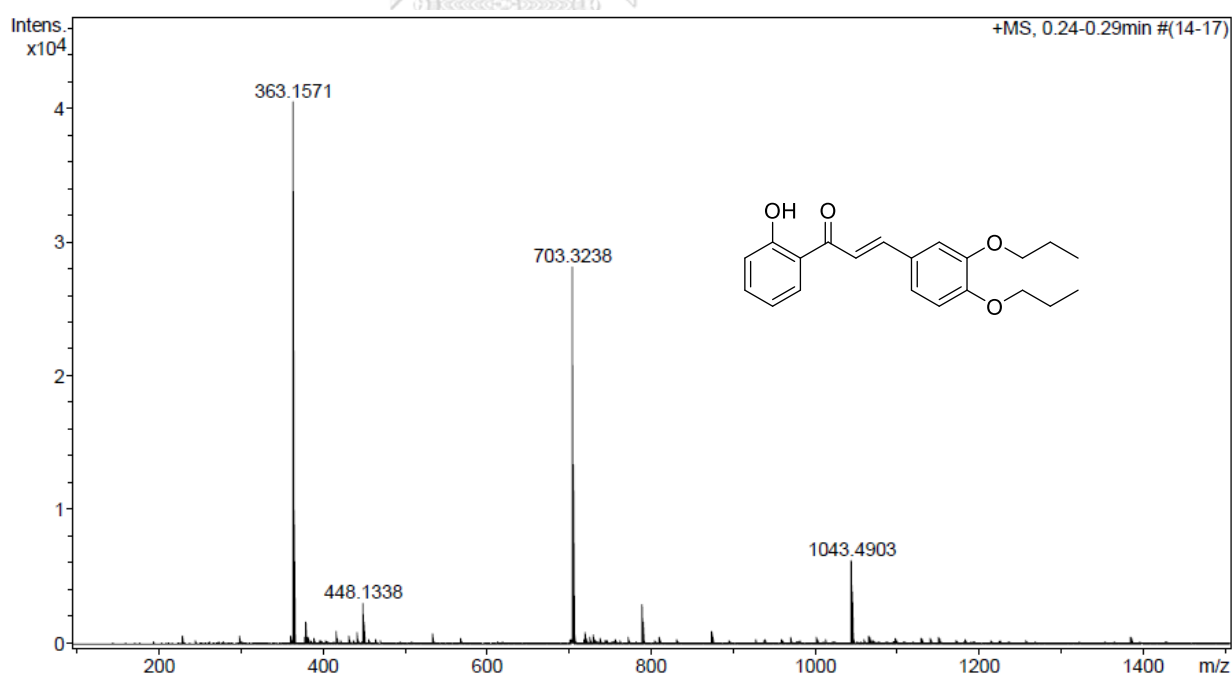
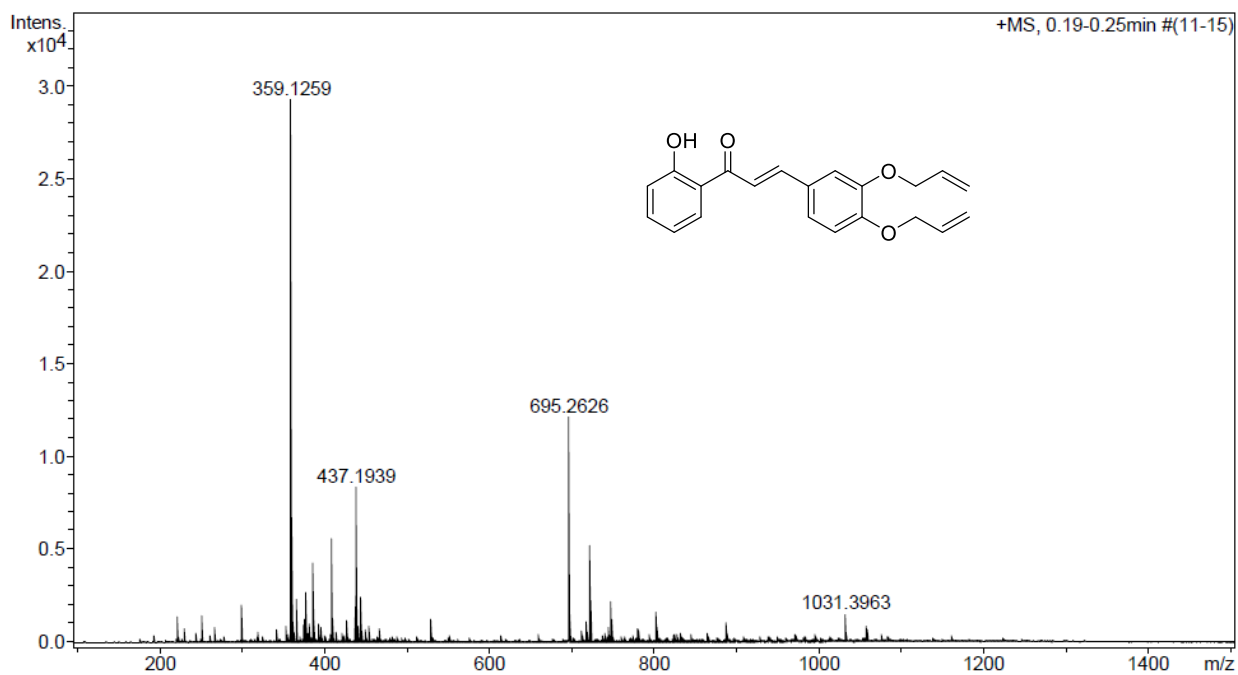
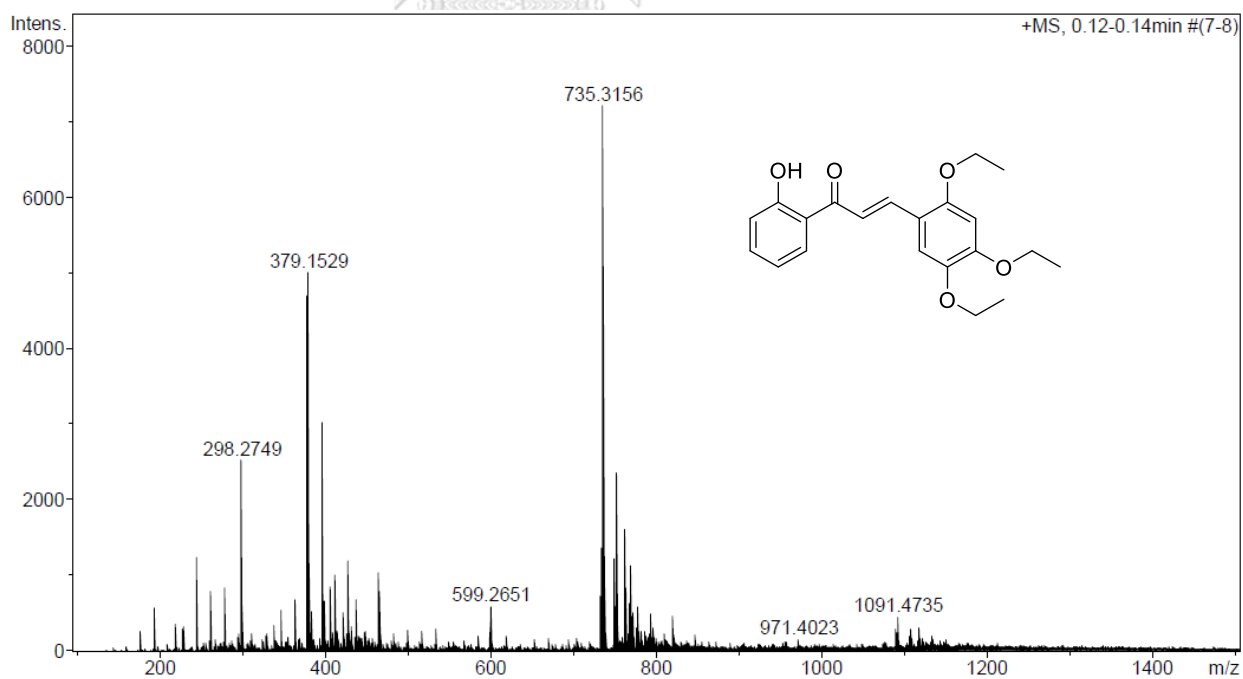
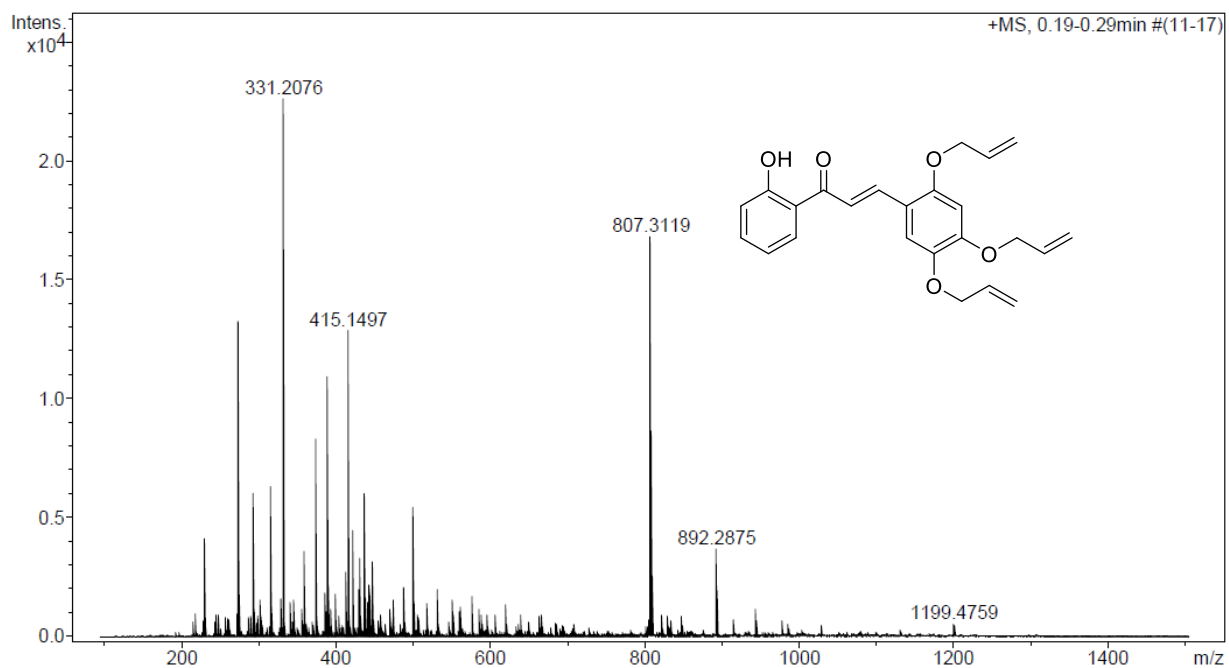
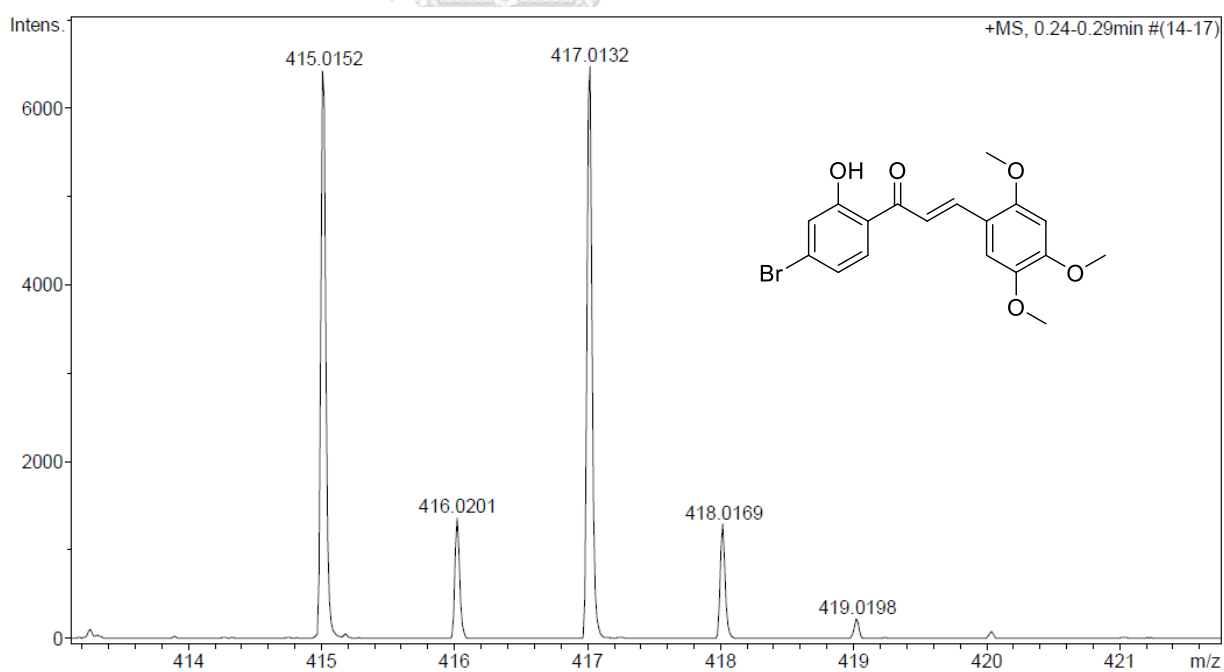


Figure A.150 The HR-ESI-MS of 92.

Figure A.151 The HR-ESI-MS of **93**.Figure A.152 The HR-ESI-MS of **94**.

Figure A.153 The HR-ESI-MS of **95**.Figure A.154 The HR-ESI-MS of **98**.

Figure A.155 The HR-ESI-MS of **99**.Figure A.156 The HR-ESI-MS of **102**.

Figure A.157 The HR-ESI-MS of **103**.Figure A.158 The HR-ESI-MS of **113**.

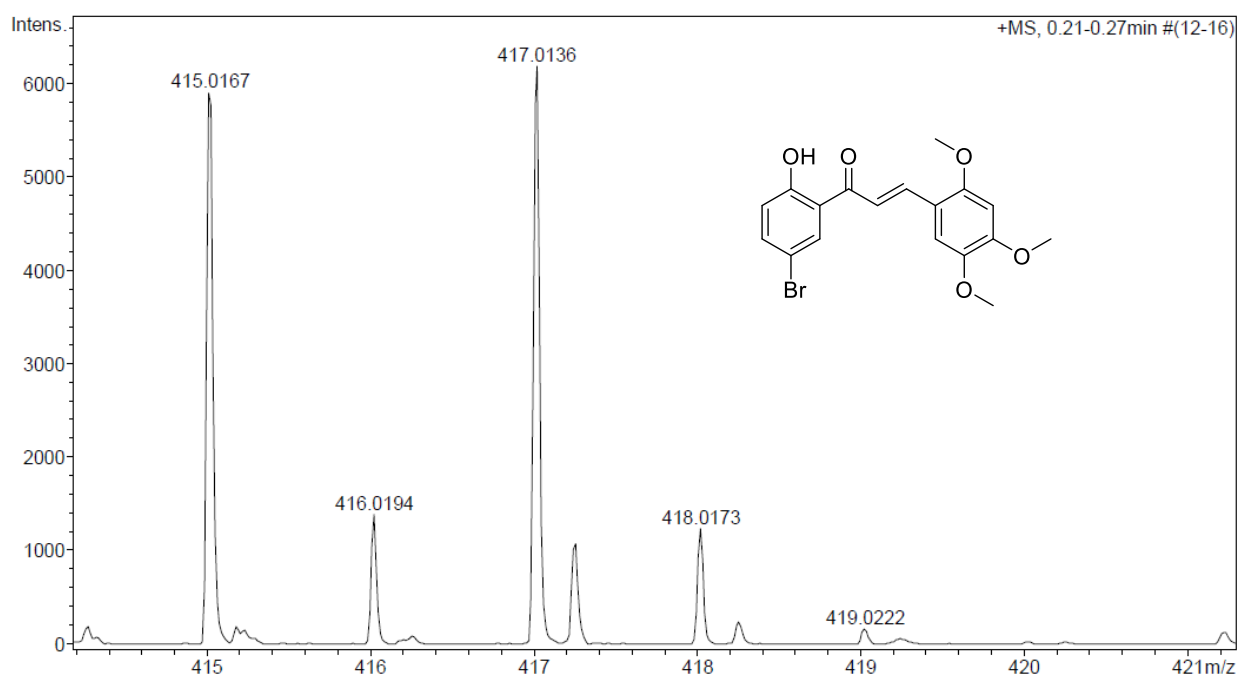


Figure A.159 The HR-ESI-MS of 114.

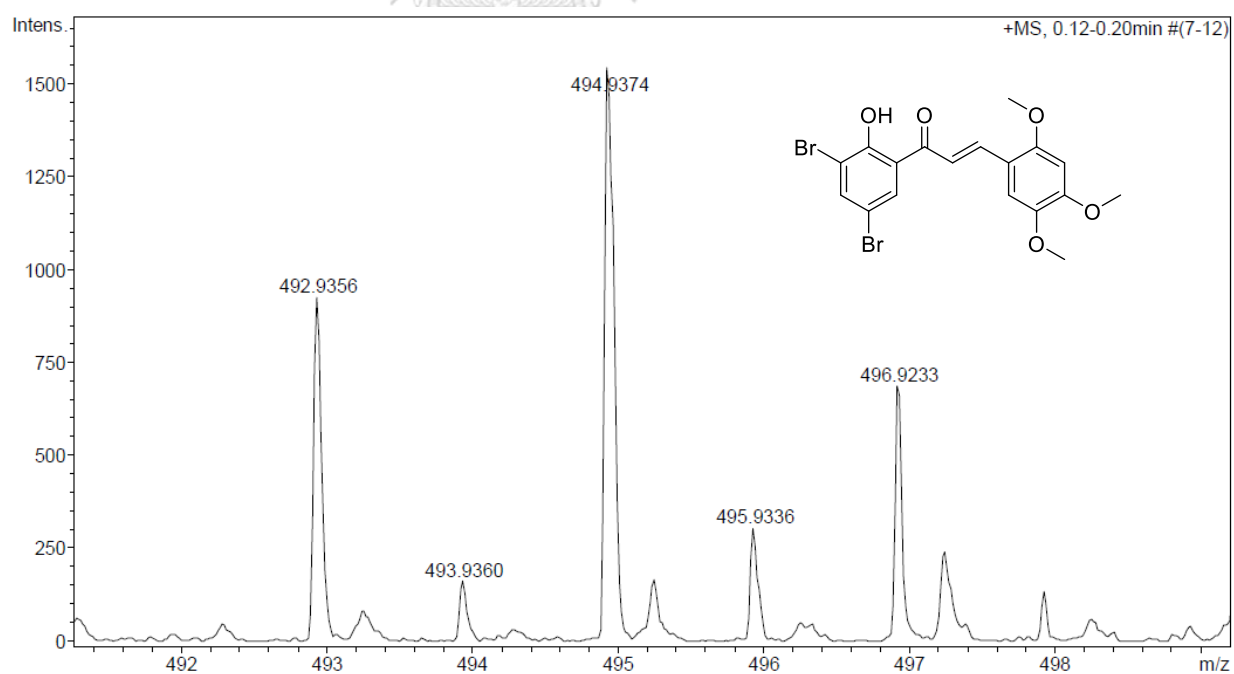
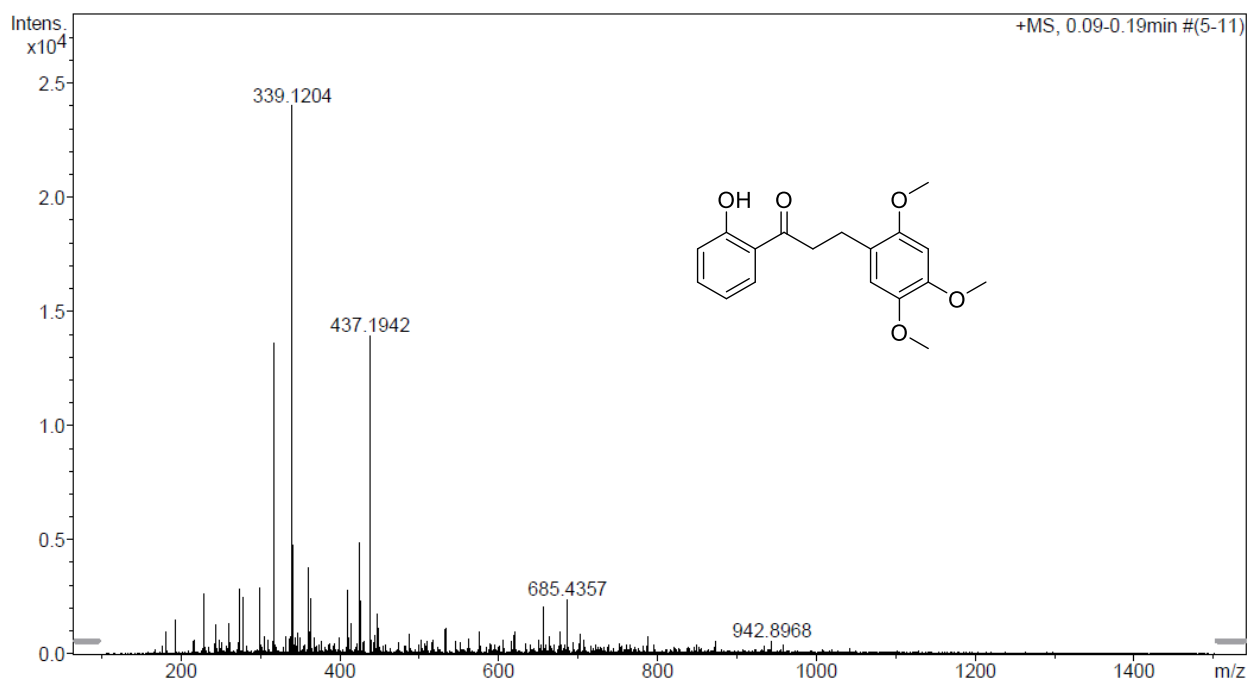
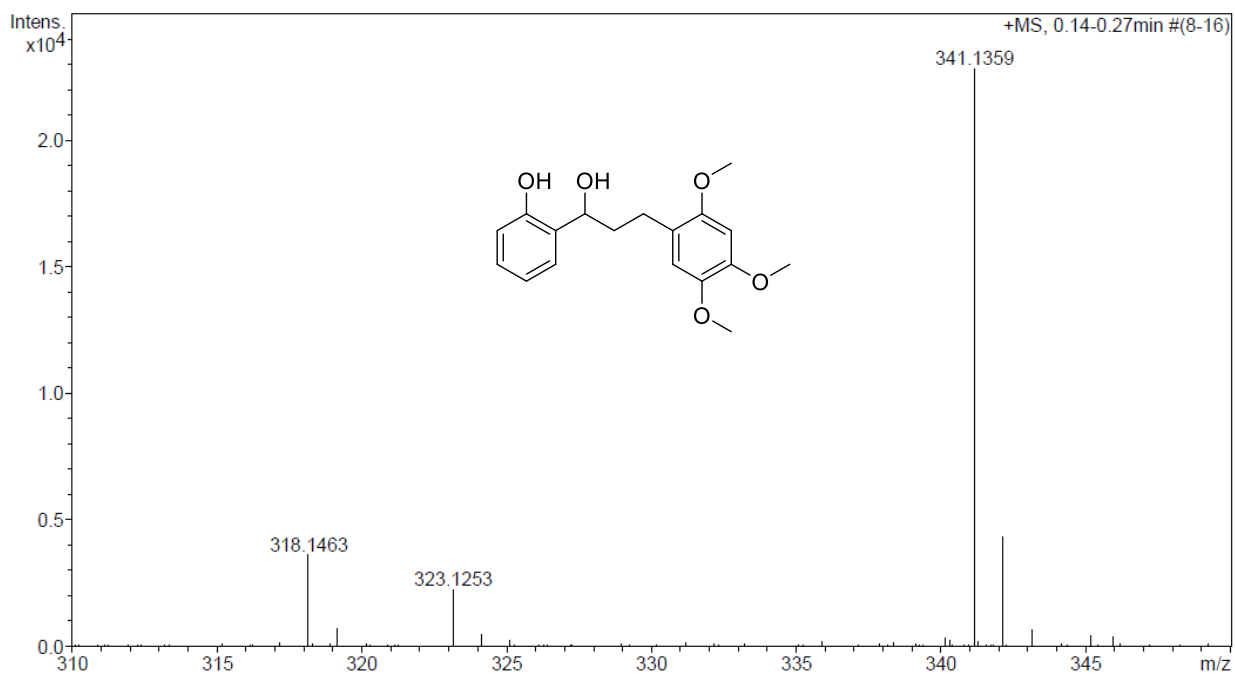


Figure A.160 The HR-ESI-MS of 119.

Figure A.161 The HR-ESI-MS of **121**.Figure A.162 The HR-ESI-MS of **122**.

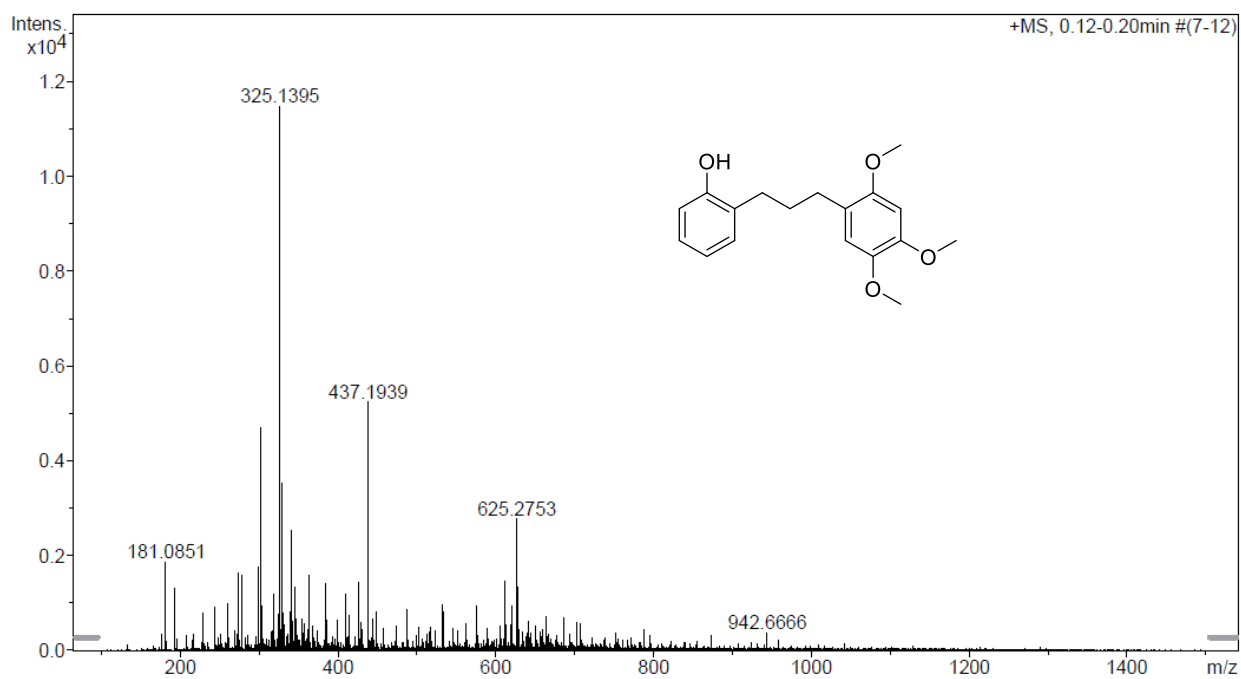


Figure A.163 The HR-ESI-MS of 123.

REFERENCES



จุฬาลงกรณ์มหาวิทยาลัย
CHULALONGKORN UNIVERSITY

1. Ayabe, S.; Uchiyama, H.; Aoki, T.; Akashi, T., Plant phenolics: phenylpropanoids. *Comprehensive Natural Products II* **2010**, 929-976.
2. Wu, J.; Li, J.; Cai, Y.; Pan, Y.; Ye, F.; Zhang, Y.; Zhao, Y.; Yang, S.; Li, X.; Liang, G., Evaluation and discovery of novel synthetic chalcone derivatives as anti-inflammatory agents. *J. Med. Chem.* **2011**, *54*, 8110-8123.
3. Israf, D. A.; Khaizurin, T. A.; Syahida, A.; Lajis, N. H.; Khozirah, S., Cardamonin inhibits COX and iNOS expression via inhibition of p65NF- κ B nuclear translocation and IK-B phosphorylation in RAW 264.7 macrophage cells. *Mol. Immunol.* **2007**, *44*, 673-679.
4. Srinivasan, B.; Johnson, T. E.; Lad, R.; Xing, C., Structure–activity relationship studies of chalcone leading to 3-hydroxy-4,3',4',5'-tetramethoxychalcone and its analogues as potent nuclear factor κ B inhibitors and their anticancer activities. *J. Med. Chem.* **2009**, *52*, 7228-7235.
5. Sugii, M.; Ohkita, M.; Taniguchi, M.; Baba, K.; Kawai, Y.; Tahara, C.; Takaoka, M.; Matsumura, Y., Xanthoangelol D isolated from the roots of *Angelica keiskei* inhibits endothelin-1 production through the suppression of nuclear factor κ B. *Biol. Pharm. Bull.* **2005**, *28*, 607-610.
6. Kim, H. D.; Li, H.; Han, E. Y.; Jeong, H. J.; Lee, J. H.; Ryu, J.-H., Modulation of inducible nitric oxide synthase expression in LPS-stimulated BV-2 microglia by prenylated chalcones from *Cullen corylifolium* (L.) Medik. through inhibition of I- κ B α degradation. *Molecules* **2018**, *23*, 109.
7. Orlikova, B.; Schnekenburger, M.; Zloh, M.; Golais, F.; Diederich, M.; Tasdemir, D., Natural chalcones as dual inhibitors of HDACs and NF- κ B. *Oncol. Rep.* **2012**, *28*, 797-805.
8. Baba, M.; Asano, R.; Takigami, I.; Takahashi, T.; Ohmura, M.; Okada, Y.; Sugimoto, H.; Arika, T.; Nishino, H.; Okuyama, T., Studies on cancer chemoprevention by traditional folk medicines XXV. Inhibitory effect of isoliquiritigenin on azoxymethane-induced murine colon aberrant crypt focus formation and carcinogenesis. *Biol. Pharm. Bull.* **2002**, *25*, 247-250.

9. Lahsasni, S. A.; Al Korbi, F. H.; Aljaber, N. A.-A., Synthesis, characterization and evaluation of antioxidant activities of some novel chalcones analogues. *Chem. Cent. J.* **2014**, *8*, 32.
10. Hsieh, C.-T.; Hsieh, T.-J.; El-Shazly, M.; Chuang, D.-W.; Tsai, Y.-H.; Yen, C.-T.; Wu, S.-F.; Wu, Y.-C.; Chang, F.-R., Synthesis of chalcone derivatives as potential anti-diabetic agents. *Bioorg. Med.* **2012**, *22*, 3912-3915.
11. Rozmer, Z.; Perjési, P., Naturally occurring chalcones and their biological activities. *Phytochemistry Rev* **2016**, *15*, 87-120.
12. Fang, S.-C.; Hsu, C.-L.; Yu, Y.-S.; Yen, G.-C., Cytotoxic effects of new geranyl chalcone derivatives isolated from the leaves of *Artocarpus communis* in SW 872 human liposarcoma cells. *J. Agr. Food Chem.* **2008**, *56*, 8859-8868.
13. Shankaraiah, N.; Nekkanti, S.; Brahma, U. R.; Kumar, N. P.; Deshpande, N.; Prasanna, D.; Senwar, K. R.; Lakshmi, U. J., Synthesis of different heterocycles-linked chalcone conjugates as cytotoxic agents and tubulin polymerization inhibitors. *Bioorg. Med. Chem* **2017**, *25*, 4805-4816.
14. Lim, A. K., Diabetic nephropathy—complications and treatment. *Int. J. Nephrol. Renovasc. Dis.* **2014**, *7*, 361.
15. Lal, M. A.; Young, K. W.; Andag, U., Targeting the podocyte to treat glomerular kidney disease. *Drug Discov. Today* **2015**, *20*, 1228-1234.
16. Anil Kumar, P.; Welsh, G. I.; Saleem, M. A.; Menon, R. K., Molecular and cellular events mediating glomerular podocyte dysfunction and depletion in diabetes mellitus. *Front. Endocrinol.* **2014**, *5*, 151.
17. Dronavalli, S.; Duka, I.; Bakris, G. L., The pathogenesis of diabetic nephropathy. *Nat. Rev. Endocrinol.* **2008**, *4*, 444.
18. Reidy, K.; Kang, H. M.; Hostetter, T.; Susztak, K., Molecular mechanisms of diabetic kidney disease. *J. Clin. Invest.* **2014**, *124*, 2333-2340.
19. Fineberg, D.; Jandeleit-Dahm, K. A.; Cooper, M. E., Diabetic nephropathy: diagnosis and treatment. *Nat. Rev. Endocrinol.* **2013**, *9*, 713.
20. Coward, R.; Fornoni, A., Insulin signaling: implications for podocyte biology in diabetic kidney disease. *Curr. Opin. Nephrol. Hypertens.* **2015**, *24*, 104.

21. Tejada, T.; Catanuto, P.; Ijaz, A.; Santos, J.; Xia, X.; Sanchez, P.; Sanabria, N.; Lenz, O.; Elliot, S.; Fornoni, A., Failure to phosphorylate AKT in podocytes from mice with early diabetic nephropathy promotes cell death. *Kidney Int.* **2008**, *73*, 1385-1393.
22. Welsh, G. I.; Hale, L. J.; Eremina, V.; Jeansson, M.; Maezawa, Y.; Lennon, R.; Pons, D. A.; Owen, R. J.; Satchell, S. C.; Miles, M. J., Insulin signaling to the glomerular podocyte is critical for normal kidney function. *Cell Metab.* **2010**, *12*, 329-340.
23. Susztak, K.; Raff, A. C.; Schiffer, M.; Böttinger, E. P., Glucose-induced reactive oxygen species cause apoptosis of podocytes and podocyte depletion at the onset of diabetic nephropathy. *Diabetes* **2006**, *55*, 225-233.
24. Wharram, B. L.; Goyal, M.; Wiggins, J. E.; Sanden, S. K.; Hussain, S.; Filipiak, W. E.; Saunders, T. L.; Dysko, R. C.; Kohno, K.; Holzman, L. B., Podocyte depletion causes glomerulosclerosis: Diphtheria toxin-induced podocyte depletion in rats expressing human diphtheria toxin receptor transgene. *J AM SOC NEPHROL.* **2005**, *16*, 2941-2952.
25. Artunc, F.; Schleicher, E.; Weigert, C.; Fritsche, A.; Stefan, N.; Haering, H.-U., The impact of insulin resistance on the kidney and vasculature. *Nat. Rev. Nephrol.* **2016**, *12*, 721.
26. Sanders, M. J.; Grondin, P. O.; Hegarty, B. D.; Snowden, M. A.; Carling, D., Investigating the mechanism for AMP activation of the AMP-activated protein kinase cascade. *Biochem. J.* **2007**, *403*, 139-148.
27. Suter, M.; Riek, U.; Tuerk, R.; Schlattner, U.; Wallimann, T.; Neumann, D., Dissecting the role of 5'-AMP for allosteric stimulation, activation, and deactivation of AMP-activated protein kinase. *J. Biol. Chem.* **2006**, *281*, 32207-32216.
28. Shaw, R. J.; Kosmatka, M.; Bardeesy, N.; Hurley, R. L.; Witters, L. A.; DePinho, R. A.; Cantley, L. C., The tumor suppressor LKB1 kinase directly activates AMP-activated kinase and regulates apoptosis in response to energy stress. *Proc. Natl. Acad. Sci.* **2004**, *101*, 3329-3335.

29. Woods, A.; Johnstone, S. R.; Dickerson, K.; Leiper, F. C.; Fryer, L. G.; Neumann, D.; Schlattner, U.; Wallimann, T.; Carlson, M.; Carling, D., LKB1 is the upstream kinase in the AMP-activated protein kinase cascade. *Curr. Biol.* **2003**, *13*, 2004-2008.
30. Hawley, S. A.; Pan, D. A.; Mustard, K. J.; Ross, L.; Bain, J.; Edelman, A. M.; Frenguelli, B. G.; Hardie, D. G., Calmodulin-dependent protein kinase kinase- β is an alternative upstream kinase for AMP-activated protein kinase. *Cell Metab.* **2005**, *2*, 9-19.
31. Hurley, R. L.; Anderson, K. A.; Franzone, J. M.; Kemp, B. E.; Means, A. R.; Witters, L. A., The Ca^{2+} /calmodulin-dependent protein kinase kinases are AMP-activated protein kinase kinases. *J BIOL CHEM.* **2005**, *280*, 29060-29066.
32. Woods, A.; Dickerson, K.; Heath, R.; Hong, S.-P.; Momcilovic, M.; Johnstone, S. R.; Carlson, M.; Carling, D., Ca^{2+} /calmodulin-dependent protein kinase kinase- β acts upstream of AMP-activated protein kinase in mammalian cells. *Cell Metab.* **2005**, *2*, 21-33.
33. Jeon, S.-M., Regulation and function of AMPK in physiology and diseases. *Exp. Mol. Med.* **2016**, *48*, e245.
34. Kim, J.; Yang, G.; Kim, Y.; Kim, J.; Ha, J., AMPK activators: mechanisms of action and physiological activities. *Exp. Mol. Med.* **2016**, *48*, e224.
35. Steinberg, G. R.; Carling, D., AMP-activated protein kinase: the current landscape for drug development. *Nat. Rev. Drug Discov.* **2019**, *18*, 527-551.
36. Marín-Aguilar, F.; Pavillard, L. E.; Giampieri, F.; Bullón, P.; Cordero, M. D., Adenosine monophosphate (AMP)-activated protein kinase: a new target for nutraceutical compounds. *Int. J. Mol.* **2017**, *18*, 288.
37. Ruderman, N. B.; Carling, D.; Prentki, M.; Cacicedo, J. M., AMPK, insulin resistance, and the metabolic syndrome. *J. Clin. Invest.* **2013**, *123*, 2764-2772.
38. Fujii, N.; Ho, R. C.; Manabe, Y.; Jessen, N.; Toyoda, T.; Holland, W. L.; Summers, S. A.; Hirshman, M. F.; Goodyear, L. J., Ablation of AMP-activated protein kinase $\alpha 2$ activity exacerbates insulin resistance induced by high-fat feeding of mice. *Diabetes* **2008**, *57*, 2958-2966.

39. Group, U. P. D. S., Effect of intensive blood-glucose control with metformin on complications in overweight patients with type 2 diabetes (UKPDS 34). *The Lancet* **1998**, *352*, 854-865.
40. Kim, Y.; Lim, J. H.; Kim, M. Y.; Kim, E. N.; Yoon, H. E.; Shin, S. J.; Choi, B. S.; Kim, Y.-S.; Chang, Y. S.; Park, C. W., The adiponectin receptor agonist AdipoRon ameliorates diabetic nephropathy in a model of type 2 diabetes. *J. AM. SOC. NEPHROL.* **2018**, *29*, 1108-1127.
41. Eid, A. A.; Ford, B. M.; Block, K.; Kasinath, B. S.; Gorin, Y.; Ghosh-Choudhury, G.; Barnes, J. L.; Abboud, H. E., AMP-activated protein kinase (AMPK) negatively regulates Nox4-dependent activation of p53 and epithelial cell apoptosis in diabetes. *J. Biol. Chem.* **2010**, *285*, 37503-37512.
42. Rogacka, D.; Audzeyenka, I.; Rychłowski, M.; Rachubik, P.; Szrejder, M.; Angielski, S.; Piwkowska, A., Metformin overcomes high glucose-induced insulin resistance of podocytes by pleiotropic effects on SIRT1 and AMPK. *BBA-MOL. BASIS DIS.* **2018**, *1864*, 115-125.
43. Piwkowska, A.; Rogacka, D.; Angielski, S.; Jankowski, M., Hydrogen peroxide induces activation of insulin signaling pathway via AMP-dependent kinase in podocytes. *Biochem. Biophys. Res.* **2012**, *428*, 167-172.
44. Kim, D.; Lee, J. E.; Jung, Y. J.; Lee, A. S.; Lee, S.; Park, S. K.; Kim, S. H.; Park, B.-H.; Kim, W.; Kang, K. P., Metformin decreases high-fat diet-induced renal injury by regulating the expression of adipokines and the renal AMP-activated protein kinase/acetyl-CoA carboxylase pathway in mice. *Int. J. Mol. Med.* **2013**, *32*, 1293-1302.
45. Guo, Z.; Zhao, Z., Effect of N-acetylcysteine on plasma adiponectin and renal adiponectin receptors in streptozotocin-induced diabetic rats. *Eur. J. Pharmacol.* **2007**, *558*, 208-213.
46. Gai, Z.; Wang, T.; Visentin, M.; Kullak-Ublick, G. A.; Fu, X.; Wang, Z., Lipid accumulation and chronic kidney disease. *Nutrients* **2019**, *11*, 722.
47. Patti, M.-E.; Corvera, S., The role of mitochondria in the pathogenesis of type 2 diabetes. *Endocr. Rev.* **2010**, *31*, 364-395.

48. Dugan, L. L.; You, Y.-H.; Ali, S. S.; Diamond-Stanic, M.; Miyamoto, S.; DeClevés, A.-E.; Andreyev, A.; Quach, T.; Ly, S.; Shekhtman, G., AMPK dysregulation promotes diabetes-related reduction of superoxide and mitochondrial function. *J. Clin. Invest.* **2013**, *123*, 4888-4899.
49. Rogacka, D.; Piwkowska, A.; Audzeyenka, I.; Angielski, S.; Jankowski, M., SIRT1-AMPK crosstalk is involved in high glucose-dependent impairment of insulin responsiveness in primary rat podocytes. *Exp. Cell Res.* **2016**, *349*, 328-338.
50. Quan, H. Y.; Kim, S. J.; Jo, H. K.; Kim, G. W.; Chung, S. H., Licochalcone A regulates hepatic lipid metabolism through activation of AMP-activated protein kinase. *Fitoterapia* **2013**, *86*, 208-216.
51. Zhang, T.; Yamamoto, N.; Ashida, H., Chalcones suppress fatty acid-induced lipid accumulation through a LKB1/AMPK signaling pathway in HepG2 cells. *FOOD FUNCT.* **2014**, *5*, 1134-1141.
52. Ohta, M.; Fujinami, A.; Kobayashi, N.; Amano, A.; Ishigami, A.; Tokuda, H.; Suzuki, N.; Ito, F.; Mori, T.; Sawada, M., Two chalcones, 4-hydroxyderricin and xanthoangelol, stimulate GLUT4-dependent glucose uptake through the LKB1/AMP-activated protein kinase signaling pathway in 3T3-L1 adipocytes. *Nutr. Res.* **2015**, *35*, 618-625.
53. Yibcharoenporn, C.; Chusuth, P.; Jakakul, C.; Rungrotmongkol, T.; Chavasiri, W.; Muanprasat, C., Discovery of a novel chalcone derivative inhibiting CFTR chloride channel via AMPK activation and its anti-diarrheal application. *J. Pharmacol. Sci.* **2019**, *140*, 273-283.
54. Reggelin, M.; Doerr, S., A modified low-cost preparation of chloromethyl methyl ether (MOM-Cl). *Synlett* **2004**, *2004*, 1117-1117.
55. Kim, B.-T.; Chun, J.-C.; Hwang, K.-J., Synthesis of dihydroxylated chalcone derivatives with diverse substitution patterns and their radical scavenging ability toward DPPH free radicals. *Bull. Korean Chem. Soc.* **2008**, *29*, 1125-1130.
56. Matsuda, T.; Okuda, A.; Watanabe, Y.; Miura, T.; Ozawa, H.; Tosaka, A.; Yamazaki, K.; Yamaguchi, Y.; Kurobuchi, S.; Koura, M.; Shibuya, K., Design and discovery of 2-oxochromene derivatives as liver X receptor β -selective agonists. *Bioorg. Med.* **2015**, *25*, 1274-1278.

57. Krohn, K.; Steingröver, K.; Rao, M. S., Isolation and synthesis of chalcones with different degrees of saturation. *Phytochemistry* **2002**, *61*, 931-936.
58. Saleem, M. A.; O'Hare, M. J.; Reiser, J.; Coward, R. J.; Inward, C. D.; Farren, T.; Xing, C. Y.; Ni, L.; Mathieson, P. W.; Mundel, P., A conditionally immortalized human podocyte cell line demonstrating nephrin and podocin expression. *J. AM. SOC. NEPHROL.* **2002**, *13*, 630-638.
59. Rao, Y. K.; Fang, S.-H.; Tzeng, Y.-M., Synthesis and biological evaluation of 3', 4', 5'-trimethoxychalcone analogues as inhibitors of nitric oxide production and tumor cell proliferation. *Bioorg. Med. Chem.* **2009**, *17*, 7909-7914.



VITA

NAME Duy Vu Nguyen

DATE OF BIRTH 09 October 1995

PLACE OF BIRTH Phan Thiet, Binh Thuan, Vietnam

INSTITUTIONS ATTENDED Department of Chemistry, University of Education, HCMC,
Viet Nam

HOME ADDRESS Diana Court, Phetchaburi soi 6, Phetchaburi Road,
Phetchaburi, Ratchathewi, Bangkok 10400, Thailand.

